ATOMIC MOTION, AMORPHOUS PHASE FORMATION AND NANOCRYSTALLIZATION STUDY IN LIQUID METALS AND THEIR ALLOYS

A Thesis Submitted to

The Maharaja Sayajirao University of Baroda

for the degree of

Doctor of Philosophy

in

Applied Physics

By

Ashmi Tarun Patel

Under the Guidance of

Prof. Arun Pratap

Condensed Matter Physics Laboratory

Applied Physics Department

Faculty of Technology & Engineering

The Maharaja Sayajirao University of Baroda

Vadodara – 390 001.

November 2012

Dedicated

To

My Beloved

Father

(Late Mr. Nandkumar G. Shah)

APPLIED PHYSICS DEPARTMENT

Telephone No.: 2434188
Fax: 2423898
No. PL/

Faculty of Technology & Engineering
The M. S .University of Baroda
Vadodara-390 001
INDIA

Date:

CERTIFICATE

This is to certify that the work presented in the thesis entitled "***Atomic Motion, Amorphous Phase Formation and Nanocrystallization Study of Liquid Metals and Their Alloys***" which is being submitted by ***Mrs. Ashmi Tarun Patel***, Applied Physics Department, Faculty of Technology & Engineering, The Maharaja Sayajirao University of Baroda for the degree of ***Doctor of Philosophy*** in ***Applied Physics*** has been carried out by her from May 2008 to November 2012 under my supervision and guidance. The matter presented in this thesis is original and has not been submitted for the award of any other degree or diploma.

Prof. Arun Pratap
Research Guide
Professor of Condensed Matter Physics
Applied Physics Department

Head
Applied Physics Department

Dean
Faculty of Technology & Engineering

ACKNOWLEDGMENTS

First and foremost, I pay my respect to our God Almighty without whom I could do nothing. I fell blessed to be a part of scientific research that reveals previously unknown aspects of His glorious creation. This piece of work will never be accomplished without His blessings, His power that work within me and also without the people behind my life for inspiring, guiding and accompanying me through thick and thin.

I am forever indebted to Professor Arun Pratap, my supervisor and teacher, for everything he has done to help me to reach where I am. His continuous support, encouragement and invaluable guidance from the initial level to the final level enabled me to develop an understanding of the subject. He showed me different paths to approach a research problem and the need to be persistent to accomplish any goal. He made me understand that patience and hard-work are two arms of a researcher. The joy and enthusiasm he has for research work is contagious and motivational for me at every step of my research work. Apart from the subject of my research, I learnt a lot from him which I am sure will be helpful in various stages of my life.

I express my deep sense of gratitude to Dr. Kirit N. Lad, my senior colleague, for his advice, invaluable help and support offered pleasantly during my research work.

I express my sincere thanks to Dr. T. Lilly Shanker Rao, my senior colleague, for her generous support during my research work.

My warm and loving thanks go to Heena, my best friend and colleague, for her motivational support and enthusiasm. I learnt many important things from her at starting stage of my research work.

I am truly thankful to Dr. D. R. Joshi, Head of Applied Physics Department, for his motivational support.

My sincere gratitude goes to every faculty and staff member of the Applied Physics Department who helped me lot in various ways.

The thesis would not have been possible without the confidence, endurance and support of my family. I thank my entire family for supporting me through this long journey. My parents have always been a source of inspiration and encouragement. I wish to thank my parents for their love, unconditional support and freedom to pursue my interests. It is my father's, Mr. Nandkumar G. Shah's, dream that I pursue Ph. D., and I tried to make it possible. He always showed me the correct path in my tough time. I pray to God, that today wherever he is, showers blessing on me. I can't express my feelings in mere words for my mother, Mrs. Jyotsna N. Shah. She is backbone of my patience and strength. I truly adore her for her loving nature and simplicity.

I devote my loving and warm thanks to Tarun, my husband, for his constant support, valuable ideas and patience. I admire him lot for his affection and trust in me. Without his love and support I could not able to complete my doctoral work.

My special thanks to Nishi, my daughter, whose arrival challenged yet, rejuvenated me. Her smiles and acts brightened my life.

I truly thank Ankit, my brother, for providing me lively atmosphere, assistance and strength whenever required. He is a big source of enthusiasm for me. My warm thanks to Sonal, my sister-in-law, who provides me all the assistance needed, like a little sister and very jolly atmosphere as well.

I sincerely thank my in-laws, Mr. Dinesh N. Patel, my father-in-law, and Mrs. Sharda D. Patel, my mother-in-law, for their perpetual support and understanding. It is their love and blessings, so that I can pursue and finish my research work.

I wish to express my sincere thanks to Mr. Piyush D. Patel, my brother-in-law, Rashmi bhabhi, my sister-in-law and Jigna di, my sister-in-law, for their valuable support and understanding. They always make me feel special for whatever I do.

I am very much thankful to Purvi, Prapti, Supriya and Sonal, my junior colleagues, for providing very lively atmosphere in the laboratory.

Last but not the least, I offer my regards and wishes to all those who supported me in any respect during the completion of my work.

Ashmi Tarun Patel

CONTENTS

List of Figures

Chapter 1

Chapter 2

Chapter 3

Chapter 4

Chapter 5

List of Tables

Chapter 2

Chapter 3

Chapter 4

Chapter 5

Chapter 6

List of Publications

• Papers published in international refereed journals

1. *Study of Kinetics of Glass Transition of Metallic Glasses*
   Ashmi T. Patel, Arun Pratap
   Journal of Thermal Analysis and Calorimetry, **110(2)**; 2012: 567-571

2. *Kinetics of Crystallization of $Zr_{52}Cu_{18}Ni_{14}Al_{10}Ti_6$ Metallic Glass*
   Ashmi T. Patel and Arun Pratap
   Journal of Thermal Analysis and Calorimetry, **107(1)**; 2012: 159-165

3. *Thermodynamics of $Zr_{52.5}Cu_{17.9}Ni_{14.6}Al_{10}Ti_5$ Bulk Metallic Glass forming Alloy*
   Ashmi T. Patel, Heena R. Shevde and Arun Pratap
   Journal of Thermal Analysis and Calorimetry, **107(1)**; 2012: 167-170

4. *Glass forming ability of Ca-based bulk metallic glasses*
   Ashmi T. Patel, Kirit N. Lad and Arun Pratap
   Latest Trends in Condensed Matter Physics: Experimental and Theoretical Aspects, Special Issue of Solid State Phenomena, **171**; 2011: 121-126

5. *Study of Thermodynamic Properties of $Pt_{57.3}Cu_{14.6}Ni_{5.3}P_{22.8}$ Bulk Metallic Glass*
   Ashmi T. Patel and Arun Pratap
   AIP Conference Proceedings, **1249**; 2010: 161-165

• Paper published in national refereed journal

1. *Thermodynamic study of Bulk Metallic Glass: $Zr_{57}Cu_{15.4}NI_{12.6}Al_{10}Nb_5$*
   Ashmi T. Patel, Heena R. Shevde, Arun Pratap
   Techno-Path, Journal of Sci. Engg. & Tech. Mgt., **3(1)**; 2011: 9-12

• Review Article published

1. *Crystallization Kinetics of Metallic Glasses*
   Arun Pratap & **Ashmi T. Patel**
   A book chapter in "Advances in Crystallization Processes" from InTech.
   Edited by Yitzhak Mastai, Section-2 Chapter 5; April 2012: 107-126.

• Paper presented at Conferences

1. *Thermodynamic Properties of $Pd_{77.5}Cu_6Si_{16.5}$ undercooled melt*
   Ashmi T. Patel and Arun Pratap
   54^{th} proceedings of the DAE Solid State Physics Symposium, 2009, Ed.
   A. K. Rajarajan, Alka B. Garg and G. P. Kothiyal, E-32, 501-502.

2. *Grain Size Limit of Nanocrystalline Materials obtained by Annealing Bulk Metallic Glasses*
   Arun Pratap, **Ashmi T. Patel**, Heena R. Shevde and Kirit N. Lad
   Proceedings of National Symposium on Materials and Processing – 2012,
   October 10-12, 2012, IT-21

• Other publication

1. *Kinetics of Crystallization of Co-based multi-component amorphous alloy*
   Heena Dhurandhar, **Ashmi T. Patel**, T. Lilly Shanker Rao, Kirit N. Lad and Arun Pratap
   Journal of ASTM International, **7(No. 10)**; 2010: 1-15

• Papers under consideration for publication

1. *Effect of addition of Al and Ag on Glass forming ability of Cu-Zr binary amorphous alloys*
   Ashmi T. Patel and Arun Pratap
   To be communicated to the Journal of Non-crystalline Solids (December'2012)

2. *Estimation of Gibbs free energy of crystallization of glass forming alloys*
   Arun Pratap, Heena Dhurandhar, **Ashmi T. Patel**, Kirit N. Lad and G. K. Dey
   To be communicated to the Journal of Alloys and Compounds (December'2012)

CHAPTER – 1

INTRODUCTION

This chapter introduces the metallic glass, the material of the future; whose different thermal properties and kinetics are studied in the present work. Historical background, from the first discovery of metallic glass to recent development, is discussed. Applications of metallic glass in different areas and technologies are also included.

1.1 Amorphous Alloys

There are three major states of matter: Solid, liquid and gaseous. In solid state, materials are classified into two categories: crystalline and amorphous.

Crystalline structure is generally regular structure; atoms in this structure are situated at a particular position and form a building block. These building blocks of crystalline solids are arranged in orderly, three-dimensional, periodic arrays.

In contrast to this, amorphous structure is random in nature. Atoms or molecules are not arranged in a definite pattern. The atoms or molecules of amorphous materials are arranged in the same manner as they are in liquid. An amorphous material is still solid, but the spatial arrangement of the atoms is nearly random.

All amorphous materials have their crystalline counterparts. An important aspect of this is that of the two structures, the crystalline form will generally be more stable. This is because the crystalline solid is at chemical equilibrium, whereas the amorphous form is not. Preparation of amorphous solid requires rapid cooling to avoid crystallization. The internal structure of materials is very much important from its properties point of view. The models of crystalline and amorphous structure are shown in Fig. 1.1. As the structure of the material varies, its behavior in different conditions also changes. Following are some basic differences between the amorphous and crystalline materials.

- Amorphous solids don’t have definite geometrical shape, whereas, crystalline solids have characteristic geometrical shape.

- Amorphous solids melt over a wide range of temperature. They don't have particular melting point. While crystalline solids have sharp melting point.

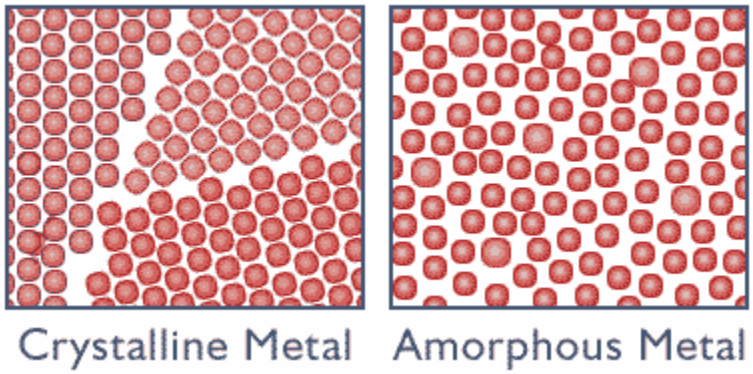

Fig. 1.1: Crystalline and amorphous structure
(Source: http://www.idfuel.com)

- Physical properties of amorphous solids are same in different direction i.e. amorphous solids are isotropic, whereas, in crystalline solids physical properties are different in different direction i.e. these solids are anisotropic.
- Amorphous solids are unsymmetrical. When crystalline solids are rotated about an axis, their appearance does not change. This shows that they are symmetrical.
- Amorphous solids don't break at fixed points; on the other hand, crystalline solids do break at fixed points/planes.

1.2 Metallic Glasses

All metals are generally considered crystalline in nature, possessing translational symmetry, i.e. their constituent atoms are arranged in a regular manner in 3-dimensions.

The search for new and advanced materials, with enhanced properties and characteristics, has been the major aim of materials scientists. From last few decades focus is on development of completely new materials. Significant improvements have

Fig. 1.2: Stronger than steel or titanium-and just as tough-a metallic glass rod before heating and molding (left); a molded metallic glass part (middle); the final product trimmed of excess material (right) (Credit: www.futurity.org)

been achieved in the mechanical, chemical and physical properties of materials by the addition of alloying elements, microstructural modification and by subjecting the materials to thermal, mechanical or thermo-mechanical processing methods. Completely new materials have also been synthesized, which include metallic glasses, nanocrystalline materials, high-temperature superconductors and quasicrystals etc. [1.1]

Any noncrystalline material means any solid material that does not posses crystallinity. A noncrystalline solid formed by continuous cooling from the liquid state is termed as “glass”. Whereas, a noncrystalline material obtained by any other process, e.g. vapor deposition or solid-state processing methods such as mechanical alloying, but not directly from the liquid state is known as an “amorphous material”.

When molten alloys are cooled rapidly, i.e. with very high cooling rates, metallic glasses are formed. Since these molten alloys are based on metals, these are referred as “glassy metals” or “metallic glasses” (Fig. 1.2). The amorphous nature of the liquid is preserved upon cooling to the solid state, hence amorphous metals can be further classified as “undercooled liquids” or more commonly “liquid metals”.

When cooling below the melting temperature T_m occur, molecular motion slows down. If the liquid is cooled sufficiently fast, crystallization can be avoided means molecules or atoms cannot adequately arrange in a periodic configuration in the available time allowed by the cooling rate [1.2]. The liquid’s structure therefore appears “frozen” on the time scale, and this “frozen-in liquid” is referred to as metallic glass or liquid metals.

1.2.1 History of Metallic Glass

During 1959-1960, at California Institute of Technology (CalTech) in Pasadena, Pol Duwez *et. al.* discovered the first metallic glass ($Au_{80}Si_{20}$). This molten metal or alloy is solidified with rapid solidification processing at rates of about 10^6 Ks^{-1} [1.3, 1.4].

Since the first discovery of a metallic glass in 1960, thousands of other metallic glasses of different compositions have been prepared as metallic glass till the date.

Whereas previous metallic glasses were prepared by cooling the melt at rates of 10^5-10^6 Ks^{-1}, the more recently developed alloys require cooling rates of only 1-100 Ks^{-1} or even less than that.

In 1969, Chen and Turnbull formed amorphous spheres of ternary Pd-M-Si (with M = Ag, Cu or Au) by quenching melts to room temperature at critical cooling rates of 10^2 Ks^{-1} to 10^3 Ks^{-1}, specifically $Pd_{77.5}Cu_6Si_{16.5}$ with a diameter of 0.5 mm [1.5].

The field of metallic glasses accelerated in the early 1970's and during the same period, Chen and collaborators used simple suction casting method and formed millimeter diameter rods of ternary Pd-Cu-Si alloys, the first bulk metallic glass at sufficiently low cooling rates in the range of 10^3 Ks^{-1} [1.6].

In the early 1980s, Turnbull's group produced glassy ingots of $Pd_{40}Ni_{40}P_{20}$ with a diameter of 5 mm using surface etching followed by heating and cooling cycles [1.7]. By processing in a boron oxide flux, they increased critical casting thickness to 1 cm at cooling rates in the 10 Ks^{-1} regions.

Since the 1980s, Akihisa Inoue of Tohoku University's Institute of Materials Research, and William L. Johnson of Caltech have discovered strongly glass forming multicomponent La-, Pd-, Fe-, Cu- and Ti-based alloys with large undercooling and low critical cooling rates of 1 KS^{-1} to 100 KS^{-1} [1.8]. These properties allow an increase in time before crystallization, enabling a greater critical casting thickness by conventional moldings [1.9]. A similar family of alloys, with the rare-earth metal partially replaced by the alkali earth metal Mg was also developed along with the parallel family of multi component Zr-based alloy [1.10].

An extended supercooled liquid region was achieved with a critical casting thickness of 15 mm for $Zr_{65}Al_{7.5}Ni_{10}Cu_{17.5}$. Caltech's Johnson and Peker developed a pentary alloy based on $Zr_{41.2}Ti_{13.8}Cu_{12.5}Ni_{10}Be_{22.5}$ in 1992 [1.11], as a part of a US Department of Energy and NASA funded project to develop new aerospace materials. Bulk metallic glass formation has been reported in various alloys based on Cu, Ti, Fe, Nd and Pr since 1988. But these alloys, fabricated with small supercooled regions and critical sizes for glass formation are generally smaller than that (3 mm) of Zr-based metallic alloys. However, taking attention back to Pd based alloys, large glass formation by water quenching using B_2O_3 flux has been reported in $Pd_{40}Cu_{30}Ni_{10}P_{20}$ alloy with diameter upto 72 mm [1.12], which is one of the largest size of bulk metallic glasses reported [1.13].

1.2.2 Bulk Metallic Glass

Fig. 1.3: Bulk metallic glass
(Source: http://en.wikipedia.org)

Metallic glasses with at least a section thickness of 1 mm are considered as "Bulk Metallic Glasses" (BMG). Before the development of BMG, shown in Fig. 1.3, materials there have been many limitations of using metallic glasses, mainly limitation of size and ability of work. The problem of limitation of size has been solved by discovery of bulk metallic glasses [1.14]. Bulk metallic alloy systems have three

minimum components; generally the number is much larger and that is why they are frequently referred as multicomponent alloy systems. They can be produced at slow cooling rates, typically 10^3 Ks^{-1} or less. BMG's exhibit large section thickness or diameters, a minimum of about 1mm & they possess a large supercooled liquid region, means the difference between the glass transition temperature T_g and crystallization temperature T_x, i.e. $\Delta T_x = T_x - T_g$ is large [1.1].

In general, the BMG's forming ability tends to increase as more components are added to the alloy. Greer [1.15] proposed 'confusion principle', which means that more number of components involved, the lower the chance that alloy can select viable crystal structures, and hence the greater the chance of glass formation [1.16]. Inoue summarized the results of glass formation in multicomponent alloys and proposed three empirical rules [1.17]:

- Multicomponent systems consisting of more than three elements.
- There should be a significant difference in atomic sizes with size ratios (>12%) among the three main constituent elements.
- And the three main constituent elements should have negative heats of mixing

The atomic configurations favor the glass formation in terms of thermodynamics, kinetics as well as the microstructure development [1.18].

Bulk metallic glasses naturally exhibit low driving force for crystallization in the supercooled liquid. The low driving force means less nucleation and therefore gives improved glass forming ability. Therefore, BMGs are novel class of materials, which exhibits unique mechanical, thermal, magnetic, electrical and corrosion properties.

1.3 Properties and Applications of Metallic Glasses

Metallic glasses are alloys that are tougher than any known pure metal. The amorphous internal structure that gives metallic glasses their remarkable properties consists of an assembly of small and large atoms packed as tightly together as possible [1.19]. The advantages of metallic glasses compared with conventional crystalline metals and alloys include high elasticity, superior strength (Fig. 1.4) and excellent wear and corrosion resistance, attributed to the lack of grain boundaries and crystal defects that usually lead to weakening of pure metal's strength. Principal areas for products of metallic glasses are sports and luxury goods, electronics, medical and defense.

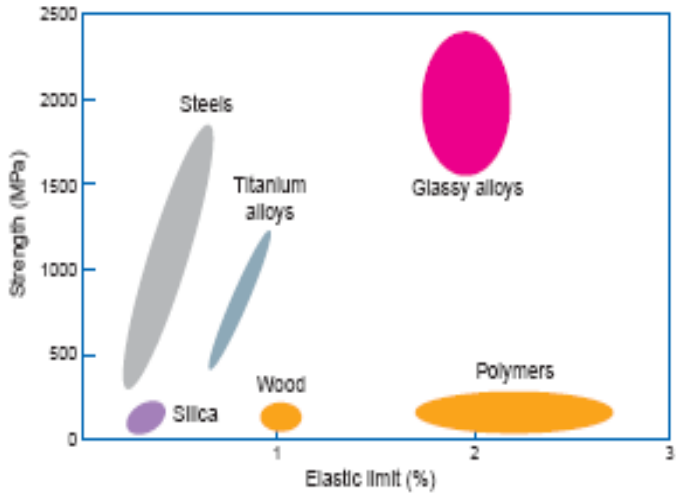

Fig. 1.4: Amorphous metallic alloys combine higher strength than crystalline metal alloys with the elasticity of polymers
(Source: www.its.caltech.edu/~vitreloy/development.htm)

Metallic Glasses are used to make Sports Equipment:

The first application of these glassy metals is found to be as golf club heads. Twice as hard and four times as elastic as Ti drivers, 99% of the impact energy from a BMG

head is transferred to the ball. Higher strength-to-weight ratio allows mass to be distributed differently, enabling various shapes and sizes of heads.

They are used to make frames of tennis rackets, which is shown in Fig. 1.5. The increased stiffness enhances energy return with 29% more power. Other potential applications in sporting goods include fishing equipment, hunting bows, guns, scuba gear, baseball bats, marine applications and bicycle frames [1.20].

Fig. 1.5: (a) A HEAD Radical tennis racket, (b) Golf clubs made of bulk metallic glass & (c) A base ball made up of metallic glass
(Source: (a) & (c) Liquidmetal Technologies
(b)http://www.ornl.gov/info/ornlreview/v38_1_05/article17.shtml)

Biomedical Applications:

Metallic glass has a high elasticity, superior strength, highly biocompatible, nonallergenic form, which is ideal for corrosion and wear resistant medical applications. They are used in knee-replacement devices, pacemaker casings, dental implants & ophthalmic scalpel blades [1.20]. Corrosion testing of BMGs has demonstrated that these materials have much better corrosion properties in

physiological solution compared to many common metallic biomaterials [1.21]. Recently, experiments have demonstrated that BMGs are, in general, nontoxic to cells and compatible with cell growth and tissue function [1.22-1.24].

When bones break, surgeons need screws and metal plates to fix the broken bones in place. These supports are usually made of stainless steel or titanium. Once the bones have healed, the metal parts have to be removed from the body via further surgery. In order to reduce the burden on patients, more recently, magnesium-zinc based BMGs

Fig. 1.6: (a) Biodegradable bone implants made of metallic glass, (b) Metallic glass hardware produced by Liquidmetal Technologies [Credit: (a) http://physicsworld.com (b) Liquidmetal Technologies].

have been developed for application as biodegradable and biocompatible bone implants (Fig. 1.6) [1.25].

Applications of BMGs in Nanotechnology and Micro Electro Mechanical Systems (MEMS):

Making use of the excellent thermal formability of BMGs, supercooled liquid fabrication provides an alternative and economic approach for the fabrication of

micro- and nano-sized metallic parts and surface patterns for MEMS and micro- and nano-machines. [1.16].

Pressure Sensors:

Due to the environmental issues, low energy consumption and safety point of view, miniaturized pressure sensors with high sensitivity is required in order to reduce toxic smoke and CO_2 gas from automobiles. The metallic glass alloys are highly promising for producing miniaturized diaphragms with high sensitivity and high pressure resistance due to their low Yong's modulus and high strength. The pressure sensors are constructed with a metallic diaphragm and deposited strain gauge as shown in Fig. 1.7-(a) [1.26-1.28].

Microgeared Motors:

Using metallic glasses, high-torque geared motor parts are fabricated with diameters <5 mm. Super-small geared motors of 1.5 and 2.4mm in diameter were developed from 2004 to 2006 [1.26, 1.27, 1.29-31]. This was achieved by utilizing the high strength of metallic glasses along with their ability to provide precision and surface flatness.

Using these BMG gear parts, micro-motors were constructed (Fig. 1.7-(b)). Super small and high-power geared motors with much longer lifetimes are expected to find applications in various kinds of micro-precision machines such as microsurgical instruments, microlathes and so on.

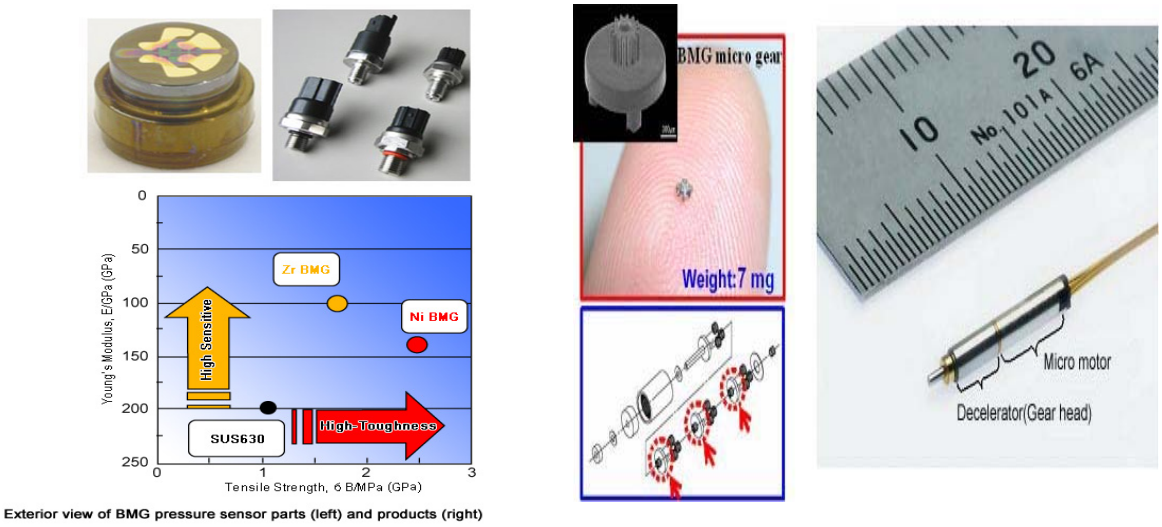

Fig. 1.7: (a) Metallic glass pressure sensors, (b) Micro-geared motor constructed by Ni-based glassy alloy
(Source: http://www.arcmg.imr.tohoku.ac.jp/en/topics/inoue.html)

Optical Components:

Metallic glasses are useful in fabrication of reflective optical components, optical mirrors because of excellent micro/nanoformability along with good mechanical properties exhibited by them. The diffraction gratings of 1 um interval are also fabricated on Pt-based BMG [1.32]. Fabrication of holograms with metallic glass is also possible. Compared with polymer holograms, metallic glass holograms are simpler to fabricate and do not require a reflection coating. Production of gapless microlens arrays is also another optical application of metallic glass [1.33].

Magnetic Properties and Applications:

The magnetic properties of the metallic glasses offer the greatest promise for commercial application. Amorphous metallic alloys do not exhibit magneto crystalline anisotropy. Ferrous (Fe) metallic glasses are among the most easily magnetized of all ferromagnetic material. Furthermore, resistance of metallic glasses

to current flow is generally higher than that of crystalline alloys. This helps to minimize eddy-current losses that occur due to rapid magnetization and demagnetization of material [1.18]. Magnetic metallic glasses are used to fabricate soft magnetic chock coils, transformer cores, magnetic sensors, soft magnetic high frequency power coils and magnetic iron core for high rotation speed motor [1.34].

Defense and Aerospace:

Due to their unique properties, many military components, like composite armor, missile components and aircraft fasteners, are being developed using BMGs by US Department of Defense (DOD) [1.35]. In future, W-reinforced BMG-composite armor-piercing projectiles can replace depleted uranium penetrators due to their similar density and self-sharpening behavior.

Catching Solar wind

Launched as part of NASA's Discovery Program, Genesis space craft is expected to capture solar wind particles and ions (high energy isotopes of nitrogen and oxygen) using circular passive collector arrays. Each array consists of hexagonal tiles coated with Zr-based BMG, which absorbs and retains noble gases He and Ne (Fig. 1.8-(b)). Once the collectors are back on Earth, sophisticated acid etching techniques are used and the surfaces of metallic glasses dissolve evenly, allowing the captured ions to be

Fig. 1.8: (a) Artist's impression of the Genesis spacecraft in collection mode, opened up to collect and store samples of solar wind particles. (b) Genesis' array, held by Andy Stone of the Jet Propulsion Laboratory, showing the collector materials. [(a) Courtesy of JPL; (b) Courtesy of NASA Johnson Space Center]

released in equal layers. This allows genesis to test proposals that the higher energy particles differ in composition from the solar wind [1.36, 1.37].

Jewelry Industry:

Fine jewelry industry is the latest one to grab BMGs due to their unique properties, which includes a metal surface that is both, exceptionally hard and scratch resistant; still it can be polished to high luster that is maintained over time [1.18].

Usage in Consumer Electronics:

Liquidmetal Technologies, US, is one of the first companies to utilize BMGs for commercial applications. It is working with design firm Ideo to create a vitreloy-encased laptop that rolls up like a piece of paper [1.20]. Being tough, metallic glasses are also lightweight and elastic. For this reason metallic glasses are used to make cell phone and watch cases (Omega watches use metallic glass to create designer pieces), outer shield of SanDisk USB memory stick (Fig. 1.9 & 1.10).

Fig. 1.9: (a) USB drive case and (b) Watch case made up of metallic glass
(Source: (a) http://allthatmatters.heber.org
(b) http://www.omegawatches.com/spirit/watchmaking/liquidmetal)

Promising research work going on worldwide on this amorphous metallic glasses, greatly improves the prospects for the discovery of new BMGs with impressive properties that will ensure practical manufacturing. In turn, it will open up new dimensions and set novel horizons in this fast growing technological world.

Fig. 1.10: (a) Mobile case made up of metallic glass (b) Metallic glass hardware produced by Liquidmetal Technologies and adopted in products manufactured by Motorola, Samsung and LG Electronics [Credit: Liquidmetal Technologies]

1.4 Glass Forming Ability & Thermodynamic Aspects

Glass forming ability is defined as the ability of a liquid to suppress crystallization, that is, crystal nucleation and growth, when cooling below the melting temperature (T_m). Crystal nucleation and growth both require a finite amount of time to proceed and if liquid metal is cooled from T_m to below glass transition temperature, T_g at sufficiently high rate, the liquid will freeze as a glass because nucleation and growth will be completely avoided. Many factors, such as atomic size mismatch, increased atomic packing density, contribute to the frustration of crystallization, leading to good glass formation. Besides consideration of the packing density, the improved glass forming ability of the multicomponent systems has also been nominally understood by the 'confusion principle' and Inoue's three empirical rules, which are already discussed in the previous section.

Knowledge of glass forming ability (GFA) of amorphous metallic alloys is very important from both theoretical and practical point of view. Thermodynamically, the knowledge of Gibbs free energy difference ΔG between the crystalline and corresponding amorphous phase, entropy difference ΔS and enthalpy difference ΔH plays an important role to investigate nucleation and growth phenomena and to predict glass forming ability (GFA). With the knowledge of the specific heat of the under cooled liquid, the thermodynamic functions can be determined. However, in most of the cases, the specific heat data of under cooled liquid is not available due to its metastable nature. In absence of specific heat data in under cooled region, the functional dependence of ΔG, ΔS and ΔH on under cooling are estimated

theoretically. Many expressions are available for ΔG calculations in literature [1.38-1.47]. All these expressions depend on some kind of assumption for temperature dependence of heat capacity.

ΔC_p defined as C_p^l - C_p^s is the difference in specific heats of the two phases. It is observed that ΔC_p shows linear and hyperbolic variation with temperature. So, in this study, linear and hyperbolic variations of ΔC_p are taken into consideration, which involves A & B coefficients for linear variation and C & D coefficients for hyperbolic variation. Using these variations of ΔC_p, equations for ΔG, ΔS and ΔH are derived and they are calculated for various glass forming systems like $Pd_{77.5}Cu_6Si_{16.5}$, $Pr_{55}Ni_{25}Al_{20}$, $Pt_{57.3}Cu_{14.6}Ni_{5.3}P_{22.8}$ and Zr-based liquid metals. The detailed formulation and the results for thermodynamic properties along with the comparison with the experimental results are given chapter-2 of thesis.

From the thermodynamic point of view, the Gibbs free energy difference, ΔG between the undercooled liquid and the corresponding crystalline state is driving force for crystallization. As a consequence, it is a good indicator for glass forming ability of metallic glasses. In chapter 2, the expressions are proposed to calculate ΔG, ΔS and ΔH using linear and hyperbolic variations of ΔC_p in the undercooled region for $Zr_{46}Cu_{46}Al_8$ and $Zr_{46}(Cu_{4.5/5.5}Ag_{1/5.5})_{46}Al_8$ bulk metallic glasses. Different GFA criteria are also evaluated for systems taken up in the study and effect of addition of Al and Ag in CuZr binary system is investigated.

Chapter 2 also includes, calculation of Gibbs free energy difference, ΔG as a function of temperature, using Lad *et al.* expression and other GFA parameters for different five Ca-based multicomponent metallic alloys.

1.5 Kinetics of Crystallization & Glass Transition:

The study of the thermally-activated phase transformations is of great significance in the field of materials science as the properties of materials change due to the change in the composition and/or microstructure. The properties of amorphous materials are usually different from their fully or partly crystalline counterparts. The bulk properties of the material are the manifestation of the atomic interactions and dynamics at the microscopic level. Since the amorphous state is thermodynamically unstable, the thermal stability of amorphous alloys is crucial from the application viewpoint. This makes the *thermo-analytical* study of the amorphous alloys an important field of research. The study of crystallization kinetics and kinetics of glass transition of amorphous alloys using thermo-analytical technique i.e. Differential Scanning Calorimetry (DSC) provides very useful information about the thermal stability. Crystallization kinetics and kinetics of glass transition are the ways to determine the activation energy and other kinetic parameters. Thus, we can predict glass forming ability and thermal stability of glassy alloy.

The kinetics of crystallization of Zr-based and Co-based metallic glasses has been investigated using DSC technique. Kinetic parameters, obtained from non-isothermal rate laws by both iso-kinetic and iso-conversional methods, are included in chapter 4.

Kinetics of Glass Transition of $Ti_{50}Cu_{20}Ni_{30}$ and $Fe_{67}Co_{18}B_{14}Si_1$ (2605CO) is also studied using DSC with continuous heating of the sample at various heating rates in chapter 5. The heating rate dependence of the glass transition temperature (T_g) is investigated. The activation energy (E) throughout the glass transition region was determined using Moynihan and Kissinger equations. The fragility index m is

calculated using activation energy determined by the above two methods for both the glassy alloys which included in the same chapter.

1.6 Nanocrystallization & Grain Size Limit

By controlling the crystallization of the BMG alloys, bulk nanocrystalline materials composites can also be obtained. Experimentally it is found that the smallest grain size is obtained when the glasses are annealed at a crystallization temperature which is nearly half of the melting temperature in metallic glasses. At this temperature the Gibbs free energy difference between the amorphous and crystalline state is maximum. In chapter 6, the minimum grain size is calculated for different metallic glasses by considering a simple thermodynamic relation that suggests a general thermodynamic lower limit of grain size of metallic nanocrystalline materials.

1.7 Objectives of The Thesis

The main objectives of the thesis are

- Derive an analytical expression for ΔG, ΔS and ΔH for metallic glasses which would give accurate values close to the experimental results and also would overcome the limitations of earlier existing expressions.
- Using DSC technique, study the kinetics of crystallization of Co-based metallic glass $Co_{66}Si_{12}B_{16}Fe_4Mo_2$, and Zr-based multicomponent metallic glass, $Zr_{52}Cu_{18}Ni_{14}Al_{10}Ti_6$ and to evaluate the kinetic parameters for these systems using different isokinetic and isoconversional methods.

- Study of another important phase transformation, i.e., kinetics of glass transition of ternary metallic glass $Ti_{50}Cu_{20}Ni_{30}$ and iron-based $Fe_{67}Co_{18}B_{14}Si_1$ (2605CO) amorphous liquid metal using two different methods and to determine activation energies.
- Determination of minimum grain size of nanocrystalline materials obtained by annealing bulk metallic glasses.

References

[1.1] C. Suryanarayana and A. Inoue, *Bulk metallic Glass*, Chapter **1**, CRC Press Taylor & Francis Group, 2011.

[1.2] P. Sharma and A. Inoue, *Handbook of Silicon based MEMS materials and technologies*, Chapter **27**, edited by V. Lindroos, M. Tilli, A. Lehto and T. Motooka, Elsevier, 2010.

[1.3] P. Duwez, R.H. Willens and W. Klement, *Nature* **187**; 1960: 869.

[1.4] P. Duwez, *Trans. ASM Q.* **60**; 1967: 607.

[1.5] H.S. Chen and D. Turnbull, *Acta Metall.* **17**; 1969: 1021.

[1.6] H.S. Chen, *Acta Metall.* **22**; 1974: pp. 1505.

[1.7] A.L. Drehman, A.L. Greer and D. Turnbull, *Appl. Phys. Lett.* **41**; 1982: pp. 716.

[1.8] A. Inoue, H. Yamaguchi and T. Zhang, *Mater. Trans., The Japan Institute of Metals* **31**; 1990: pp.104.

[1.9] A. Inoue, T. Nakamura, N. Nishiyama and T. Masumoto, *Mater. Trans., The Japan Institute of Metals* **33**; 1992: pp. 937.

[1.10] A. Inoue, T. Zhang and N. Nishiyama, *Mater. Trans., The Japan Institute of Metals* **34**; 1993: pp. 1234.

[1.11] A. Peker and W.L. Johnson, *App. Phys. Lett.* **63**; 1993: pp. 2342.

[1.12] A. Inoue, N. Nishiyama and Y. Matsuda, *Mater. Trans., The Japan Institute of Metals* **37(2)**; 1996: pp. 181.

[1.13] Z.P. Lu, *Glass Forming Ability and Glass Transition study of rare-Earth based Bulk Metallic Glasses*, Ph. D. Thesis, National University of Singapore; 2000.

[1.14] R. Nowosielski and R. Babilas, *J, Achiev. Mater. Manufacture. Engg.* **20(1-2)**; 2007: pp. 487.

[1.15] A.L. Greer, *Nature* **366**; 1993: pp. 303.

[1.16] M. Chen, *NPG Asia Mater.* **3**; 2011: pp. 82.

[1.17] A. Inoue, *Acta Mater.* **48**; 2000: pp. 279.

[1.18] B. Ramkrishna Rao, *DRDO Science Spectrum March*; 2009: pp. 212.

[1.19] http://www.nature.com/am/journal/2011/201109/full/am2011160a.html

[1.20] M. Telford, *Materials Today* March; 2004: pp. 36.

[1.21] M.L. Morrison et al, *J. Biomed. Mater. Res. A* **74A**; 2005: pp. 430.

[1.22] S. Buzzi et al, *Intermetallics* **14**; 2006: pp. 729.

[1.23] J. Schrores, G. Kumar, T.M. Hodges, S. Chen and T.R. Kyriakides, *JOM* **61**; 2009: pp. 21.

[1.24] M.D. Demetriou et al, *JOM* **62**; 2010: pp. 83.

[1.25] B. Zberg, P.J. Uggowitzer and J.F. Loffler, *Nature Mater.* **8**; 2009: pp. 887.

[1.26] A. Inoue and N. Nishiyama, *MRS Bull.* **32**; 2007: pp. 651.

[1.27] A. Inoue, *Proc. Jpn. Acad. Ser. B-Phys. Biol. Sci.* **81**; 2005: pp. 172.

[1.28] N. Nishiyama and A. Inoue, *J. Non-Cryst. Solids* **353**; 2007: pp. 3615.

[1.29] M. Ishida, H. Takeda, N. Nishiyama, K. Kita, Y. Shimizu, Y. Saotome and A. Inoue, *Mater. Sci. Eng. A* **449-451**; 2007: pp. 149.

[1.30] http://www. imr.tohoku.ac.jp/eng/information/results/2004.html.

[1.31] http://www.imr.tohoku.ac.jp/eng/information/results/2006.html.

[1.32] Y. Saotome, Y. Fukuda, I. Yamguchi and A. Inoue, *J. Alloy. Compd.* **434-435**; 2007: pp. 97.

[1.33] C.T. Pan, T.T. Wu, Y.C. Chang, J.C. Huang and J. Micromech, *Microeng.* **18**; 2008: pp. 025010.

[1.34] A. Inoue, X.M. Wang and W. Zhang, *Rev. Adv. Mater. Sci.* **18**; 2008: pp. 1.

[1.35] http://www.liquidmetal.com/applications

[1.36] W.H. Wang et al, *Mater. Sci. Eng. R* **44**; 2004: 45.

[1.37] http://genesismission.jlp.nasa.gov

[1.38] D. Turnbull, *J. Appl. Phys.* **21**; 1950: pp. 1022.

[1.39] J.D. Hoffman, *J. Chem. Phys*. **29**; 1958: pp 1992.

[1.40] D.R.H. Jones and G.A. Chadwick, *Phil. Mag.* **24**; 1971: pp. 995.

[1.41] C.V. Thompson and F. Spaepen, *Acta Metall.*, **27**; 1979: pp. 1855.

[1.42] H.B.Singh and A. Holz, *Solid State Commun.*, **45**; 1983: pp. 985.

[1.43] K.S. Dubey and P. Ramchandrarao, *Acta Metall.* **32**; 1984: pp. 91.

[1.44] L. Battezzati and E. Garrone, *Z. Metallkunde* **75**; 1984: pp. 305.

[1.45] K.N.Lad, Arun Pratap and K.G. Raval, *J. Mater. Sci. Lett.* **21**; 2002: pp. 1419.

[1.46] K. Mondal, U.K. Chatterjee and B.S. Murthy, *Appl. Phys. Lett.* **83**; 2003: pp. 671.

[1.47] K.N. Lad, K.G.Raval and Arun Pratap, *J. Non-Cryst. Solids* **334 & 335**; 2004: pp. 259.

CHAPTER – 2

THERMODYNAMIC PROPERTIES OF METALLIC GLASSES

This chapter gives the novel expressions for the Gibbs free energy difference between the amorphous phase and the corresponding crystalline state (ΔG). The present expressions have been derived assuming the linear and hyperbolic variations of specific heat difference ΔC_p, without any logarithmic approximations, which is applicable over wide undercooled region. Results, based on the calculations from present expressions, show that the ΔG values obtained for a variety of bulk glass forming alloys are in excellent agreement with experimental values. Expressions for ΔS and ΔH are also derived using the proposed ΔG expressions. Values of ΔS and ΔH, calculated from present equations, are also give quite good results with the experimental data.

2.1 Introduction

It is known that any metallic glass, rapidly cooled below its melting temperature, T_m, will not get sufficient time to arrange it's atoms in a regular periodic fashion. Therefore, all the metallic glasses are not in a thermodynamically stable state. From physics point of view, glasses are in excited state, and at any given temperature if sufficient time is provided, they will relax and eventually transform to the crystalline ground state. The thermodynamic principles can also be used when the system under consideration is an undercooled liquid. It is well known that metallic liquids can be significantly undercooled for extended periods of time avoiding crystallization from occurring [2.1].

The properties in the highly undercooled liquid state which have not been accessible for metallic materials so far include temperature dependent thermodynamic properties such as specific heat, entropy, enthalpy and Gibbs free energy.

2.2 Thermodynamic Stability of Metallic Glasses

If metallic glasses are annealed at high enough temperatures, they will crystallize, indicating that they are in metastable phases [2.2]. When a liquid cools, it will take the equilibrium state, minimizing its free energy. The thermodynamic stability of a system at constant temperature and pressure is determined by its Gibbs free energy, G, defined as

$$G = H - TS \tag{2.1}$$

where, H is the enthalpy, T is absolute temperature and S is the entropy.

Thermodynamically, a system will be in equilibrium state, that is, it will not transform into any other phase under the given conditions of temperature & pressure, if it has attains the lowest possible value of the Gibbs free energy. The above equation says that a system at any temperature can be most stable either by increasing the entropy or decreasing the enthalpy or both. Metallic crystalline solids have the strongest atomic bonding and therefore lowest enthalpy, *H*. Consequently, solids are most stable phases at low temperatures. On the other hand, the atomic vibration frequency increases with increasing temperature and consequently, the entropy, *S* is high at higher temperatures. Hence, the product of temperature and entropy increases and therefore the value of *–TS* term dominate at elevated temperatures. Because of this reason, phases with more freedom of atomic movement, that is, liquids and gases, become more stable at elevated temperatures [2.3].

2.2.1 Thermodynamic Properties: Gibbs Free Energy Difference, ΔG, Entropy Difference, ΔS & Enthalpy Difference, ΔH

From the above concepts, one can say that, a metallic glass becomes more "stable" when the Gibbs free energy of the amorphous phase is lower than that of the competing crystalline counter phase. In other words, the system becomes stable when the change in Gibbs free energy, ΔG $(= G_{glass} - G_{crystal})$ becomes minimum. The mathematical equation is given by

$$\Delta G = \Delta H - T\Delta S \tag{2.2}$$

where,

the Δ symbol represents the change in these quantities between the final and initial states

ΔH and ΔS represents the enthalpy difference and entropy difference respectively.

The system becomes stable when the value of ΔG is the lowest. A minimum value of ΔG can be obtained either by decreasing the value of ΔH or increasing the value of ΔS or both. Since entropy is nothing but a disorder in a system, means a measure of the different ways in which the constituent atoms can be arranged and obviously, this value will increase with increasing number of components in the amorphous alloy system. Thus, even if ΔH remains constant, the free energy will be lower because of the increment in entropy, when the system is multicomponent alloy system. But, the value of ΔH will not remain constant because of the chemical interaction between the different constituent elements.

The free energy of the system can also be decreased, at a constant temperature, in case of low chemical potential due to low enthalpy, and large interfacial energy between the liquid and solid phases. Since it is difficult to control these parameters in an alloy system, the simplest way to decrease the free energy would be to increase ΔS by having a large number of components in the alloy system.

Increase in ΔS also results in an increase in the degree of dense random packing of atoms, due to that ΔH decreases and consequently solid-liquid interfacial energy increases [2.1].

Thus, Gibbs free energy difference, ΔG, the difference of free energy between amorphous metallic alloy and its crystalline counterpart, entropy difference, ΔS and enthalpy difference, ΔH are important parameters in order to know the thermal stability of metallic glass.

2.2.2 Crystal Nucleation and Growth

Both solidification and melting of metals occur by nucleation and growth. However, in the case of cooling a liquid, the process of nucleation is much more difficult than it is in the case of melting. When the liquid alloy is undercooled below its glass transition temperature, nucleation will never occur and the undercooled liquid becomes a metallic glass and it is in a metastable state. The difference in Gibbs free energy, ΔG between the undercooled liquid and the crystal is the driving force for crystallization . Therefore, all metallic glasses will crystallize if heated to sufficiently high temperatures. In order to understand the importance of ΔG in the nucleation theory, it would be useful to consider the factors that can influence nucleation. Upon nucleation of crystals, the system's free energy changes as a result of the presence of the nuclei. If spherical shape for the nuclei is assumed, the free energy associated with an undercooled liquid nucleating a crystal by homogeneous nucleation is defined as

$$\Delta G = 4\pi r^2 \sigma - \frac{4\pi}{3} r^3 \Delta G_v \tag{2.3}$$

where, r is the radius of the nuclei, σ is the interfacial surface energy, and ΔG_v is the free energy difference between the crystal and the amorphous liquid per unit volume. The critical nuclei and free energy maximum are given by

$$r_c = \frac{2\sigma}{\Delta G_v} \tag{2.4}$$

$$\Delta G_c = \frac{16\pi}{3}\left(\frac{\sigma^3}{\Delta G_v^2}\right) \tag{2.5}$$

The steady state homogeneous nucleation rate is defined as,

$$I_v = \frac{A}{\eta}\exp\left(-\frac{16\pi\sigma^3}{3k_B T\Delta G_c^2}\right) \tag{2.6}$$

where A is a constant, η is viscosity, and k_B is the Boltzmann constant. The viscosity is defined as $\eta(T) = \eta_0 \exp\left(\frac{DT_0}{T - T_0}\right)$, where D is the diffusivity. Crystal growth rate can be defined as

$$u = \frac{k_B}{3\pi l^2 \eta}\left[1 - \exp\left(-\frac{n\Delta G_c}{k_B T}\right)\right] \tag{2.7}$$

where l is the average atomic diameter, n is the average atomic volume and ΔG_c, or ΔG in the present context, is the free energy difference between liquid and crystal phases and it is a function of temperature T. Thus, the classical nucleation theory suggests that the nucleation rate exponentially depends on Gibbs free energy difference, ΔG [2.4, 2.5]. The Gibbs free energy difference, ΔG, between undercooled melt and corresponding crystalline solid, acts as the driving force for crystallization.

In an amorphous alloy system, lower value of ΔG indicates less driving force of crystallization, which enhances stability of metallic supercooled liquid and leads to better glass forming ability. Thus, ΔG gives a qualitative measure of the stability of the glass compared to the crystalline state.

2.3 Expressions for Calculation of Thermodynamic Parameters

Knowledge of the thermodynamic properties i.e., Gibbs free energy difference ΔG, entropy difference ΔS, enthalpy difference ΔH and specific heat difference ΔC_p, plays an important role to find out the glass forming ability and thermal stability of metallic amorphous alloys. The Gibbs free energy difference gives a qualitative measure of the stability of the glass compared to the crystalline state as discussed in the earlier (section 2.2.1).

The equation for the Gibbs free energy difference between the liquid and crystalline phases is given by

$$\Delta G = \Delta H - T\Delta S$$

where

$$\Delta H = \Delta H_m - \int_T^{T_m} \Delta C_p dT \tag{2.8}$$

$$\Delta S = \Delta S_m - \int_T^{T_m} \Delta C_p \frac{dT}{T} \tag{2.9}$$

where, T_m is the melting temperature, ΔS_m is the entropy difference at melting temperature and ΔH_m is the enthalpy difference at melting temperature. They are related to each other by the following relation:

$$\Delta S_m = \frac{\Delta H_m}{T_m} \tag{2.10}$$

ΔC_p, defined as $C_p^l - C_p^x$, is the difference in specific heats of the liquid and corresponding crystalline phases of metallic alloy.

Hence, the expression for ΔG becomes

$$\Delta G = \frac{\Delta H_m \Delta T}{T_m} - \int_T^{T_m} \Delta C_p dT + T \int_T^{T_m} \Delta C_p \frac{dT}{T} \tag{2.11}$$

Thus, experimental ΔG values can be calculated with the help of above Eq. (2.11), if the experimental specific heat data is available for the undercooled and the crystal phases of a material. However, metallic liquids are generally not stable over an extended temperature range in the supercooled liquid, making it difficult to determine the specific heat capacity; one has to switch to suitable expression of ΔC_p that effectively represents the temperature dependence of ΔC_p. Hence, considering the values of ΔC_p, the correct evaluation of ΔG is possible.

Several models [2.6-2.15, 2.23] of varying degrees of complexity are available in literature for the determination of ΔG on undercooling. All these analytical expressions consider some kind of assumption for the temperature dependence of the heat capacity.

Analytical equation for ΔG proposed by Turnbull [2.6] assumed $\Delta C_p = 0$. Very often ΔC_p is non-zero, therefore the expression given by Turnbull shows very large deviation.

Most of other expressions use ΔC_p = constant assumption, which work quite well in most of the bulk glass forming alloys. Since it is observed that, in these kinds of glassy alloys, the specific heat of undercooled liquid C_p^l does not vary much with temperature. Hence, $\Delta C_p = C_p^l - C_p^x$ remains nearly constant throughout the entire undercooled region.

However, in many glass forming amorphous alloys which possess exceptionally high glass forming ability (GFA), the ΔC_p = constant assumption does not work at all. In such systems, ΔC_p increases considerably with undercooling. The linear and hyperbolic variations of specific heat capacity with temperature are the most common options available to estimate ΔG in the undercooled region. The two types of variation of ΔC_p with temperature are represented as

$$\Delta C_p = AT + B \qquad \text{(a)}$$

$$\Delta C_p = \frac{C}{T} + D \qquad \text{(b)}$$

which involves coefficients A & B for linear trend and C & D for hyperbolic trend. These four coefficients are easily evaluated with the help of ΔC_p^m and T_K, where ΔC_p^m is specific heat difference at melting temperature and T_K is Kauzmann temperature also known as isentropic temperature because at T_K the entropy difference, ΔS becomes zero.

2.3.1 Equations for ΔG assuming Linear and Hyperbolic Variations of ΔC_p with Temperature

All the expressions available in literature give good results for few glass forming alloys, but due to the approximations involved none of the expression is found to have excellent agreement with the experimental data upto large undercooled region. Therefore, it is quite clear that in order to achieve accurate values of ΔG, taking care of large undercooled region; one has to consider an appropriate variation of ΔC_p with temperature.

Considering the most common linear variation which is given by

$$\Delta C_p = AT + B \tag{2.12}$$

where, A and B are constants. Inserting this Eq. (2.12) in Eq. (2.11) of ΔG can be simplified to

$$\Delta G = \frac{\Delta H_m \Delta T}{T_m} - \frac{1}{2} A\left(\Delta T\right)^2 + B\left(T \ln \frac{T_m}{T} - \Delta T \right) \tag{2.13}$$

where the undercooling $\Delta T = T_m - T$.

Instead of linear variation, some systems may follow the hyperbolic trend for ΔC_p, which is given by

$$\Delta C_p = \frac{C}{T} + D \tag{2.14}$$

Again C and D are constants. Substituting ΔC_p from the above equation in Eq. (2.11), on simplification one can get the following expression

$$\Delta G = \frac{\Delta H_m \Delta T}{T_m} + \ln\frac{T_m}{T}(DT - C) - \Delta T\left(D - \frac{C}{T_m}\right) \tag{2.15}$$

There are four unknown constant A & B and C & D involved in the ΔG expressions (2.13) for linear variation and (2.15) for hyperbolic trend respectively. These unknown constants are dependent on the composition of the alloy. The researchers so far have found it difficult to obtain the values of unknown constants A & B in case of linear variation and C & D for hyperbolic dependence of ΔC_p on T. The difficulty arises due to the limitation of availability of ΔC_p only at one temperature i.e. at melting temperature T_m denoted by ΔC_p^m. Since there are two unknowns in both linear and hyperbolic case, one needs another expression for evaluation of the constants. This has been simply done by deriving an expression for ΔS from that of ΔG given by Eqs. (2.13) and (2.15) using the following relation

$$\Delta S = -\frac{\partial \Delta G}{\partial T} \tag{2.16}$$

In case of linear dependence of ΔC_p on T, one gets the following expression for ΔS through above Eq. (2.16)

$$\Delta S = \frac{\Delta H_m}{T_m} - A\Delta T - B\ln\frac{T_m}{T} \tag{2.17}$$

Utilizing the condition that ΔS becomes zero at isentropic temperature, T_K also known as Kauzmann temperature one easily gets the values of unknown constants A and B in terms of known experimental parameters

$$A = \frac{\frac{\Delta H_m}{T_m} - \Delta C_p^m \ln \frac{T_m}{T_K}}{T_m - T_K - T_m \ln \frac{T_m}{T_K}} \tag{2.18}$$

and

$$B = \Delta C_p^m - A T_m \tag{2.19}$$

Similarly, the expression for ΔS in case of hyperbolic dependence of ΔC_p on T obtained from Eq. (2.16) by partially differentiating the Eq. (2.15) provides

$$\Delta S = \frac{\Delta H_m}{T_m} - D \ln \frac{T_m}{T} - C\left(\frac{T_m - T}{T_m T}\right) \tag{2.20}$$

One gets the expressions for constants C and D from above equation after solving it for $\Delta S = 0$ at Kauzmann temperature, $T = T_K$

$$C = \frac{\Delta H_m - T_m \Delta C_p^m \ln \frac{T_m}{T_K}}{\frac{T_m - T_K}{T_K} - \ln \frac{T_m}{T_K}} \tag{2.21}$$

and

$$D = \Delta C_p^m - \frac{C}{T_m} \tag{2.22}$$

Either of the Eqs., (2.13) and (2.15) can be used to evaluate ΔG in the entire undercooled region, when the constants A & B for linear nature and C & D for hyperbolic trend are known through Eqs. (2.18) & (2.19) and (2.21) & (2.22), respectively. With the knowledge of these four constants entropy difference, ΔS is also determined using Eq. (2.17) for linear variation and Eq. (2.20) for hyperbolic

variation. Finally, to calculate the values of enthalpy difference, ΔH one can utilize the ΔG and ΔS values derived from the above Eqs., and inserting them into Eq. (2.2).

2.4 Results and Discussions

The coefficients A & B and C & D required for evaluation of thermodynamic properties, i.e., ΔG, ΔS and ΔH assuming linear and hyperbolic variations respectively have been calculated using Eqs. (2.18) & (2.19) and (2.21) & (2.22). Parameters used for determination of these constants are given in Table-1. These constants, in turn, have been incorporated in the expressions of thermodynamic properties, which are evaluated for different five metallic glasses, considering linear and hyperbolic variation of specific heat difference ΔC_p^m.

2.4.1 Gibbs Free Energy Difference, Entropy Difference and Enthalpy Difference for Pr-based, Pd-based and Pt-based Bulk Metallic Glass Forming Alloys

First bulk metallic glass forming system namely $Pr_{55}Ni_{25}Al_{20}$ has been taken up in the present study. This system is interesting due to its strong liquid side [2.16]. In this case, the value of Kauzmann temperature, T_K has been taken from the plot of the entropy difference, ΔS, since heating rate dependent T_g and T_x data are not available for evaluation of T_K. For $Pr_{55}Ni_{25}Al_{20,}$ the plots using linear and hyperbolic variation of ΔC_p fall quite close to the experimental points for ΔG. In fact, the linear and hyperbolic experimental points are almost coinciding with each other. Other results are also shown in the Fig. 2.1, where the results obtained through Dubey and

Ramchandrarao [2.11] and Thomson and Speapen [2.9] approaches underestimate on one side, while on the other side, hyperbolic expression [2.17] for ΔC_p overestimates mainly in the large undercooled region. The entropy difference ΔS, calculated using Eqs. (2.17) and (2.20) for linear and hyperbolic variation respectively, are shown in Fig. 2.2 with the experimental data. The plots clearly show that the calculated values fall very close and show similar variation as the experimental data in the entire undercooled region. Since, the earlier approaches show much large deviation for ΔG, the values for ΔS are not shown using those approaches. Similarly, Fig. 2.3 shows ΔH values which are calculated using Eq. (2.2) for both linear and hyperbolic variation of ΔC_p. The experimental values for ΔH are also shown in the figure and it can be seen that the calculated values lie quite close to the experimental one.

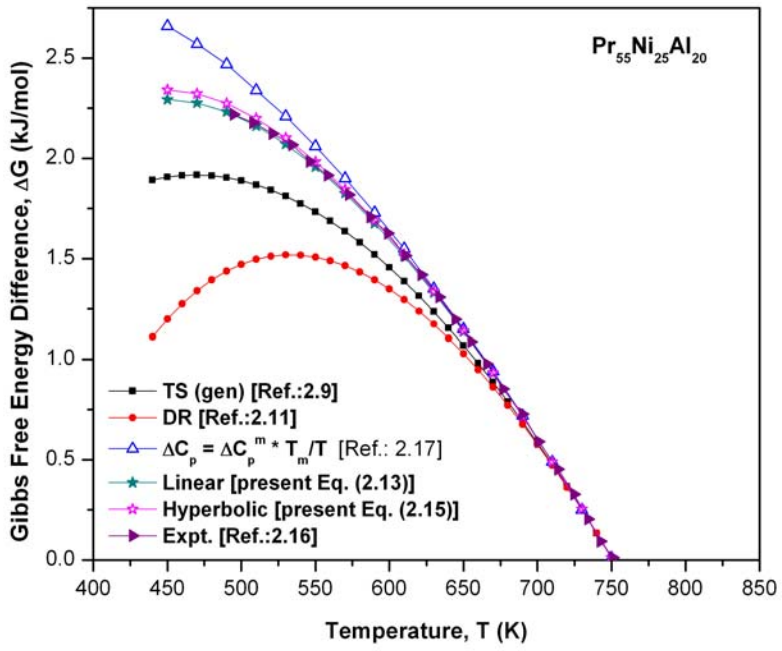

Fig. 2.1: Gibbs free energy difference, ΔG as a function of temperature for $Pr_{55}Ni_{25}Al_{20}$

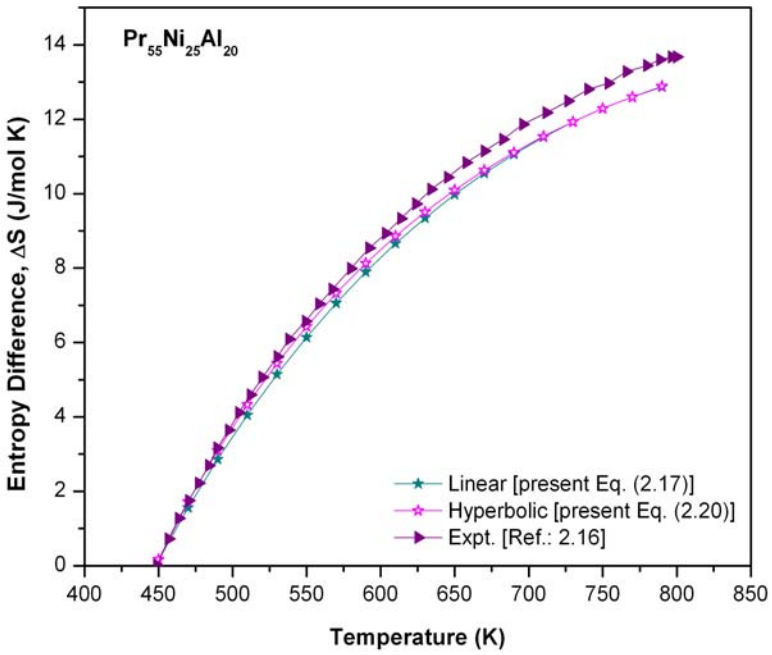

Fig. 2.2: Entropy difference, ΔS as a function of temperature for $Pr_{55}Ni_{25}Al_{20}$

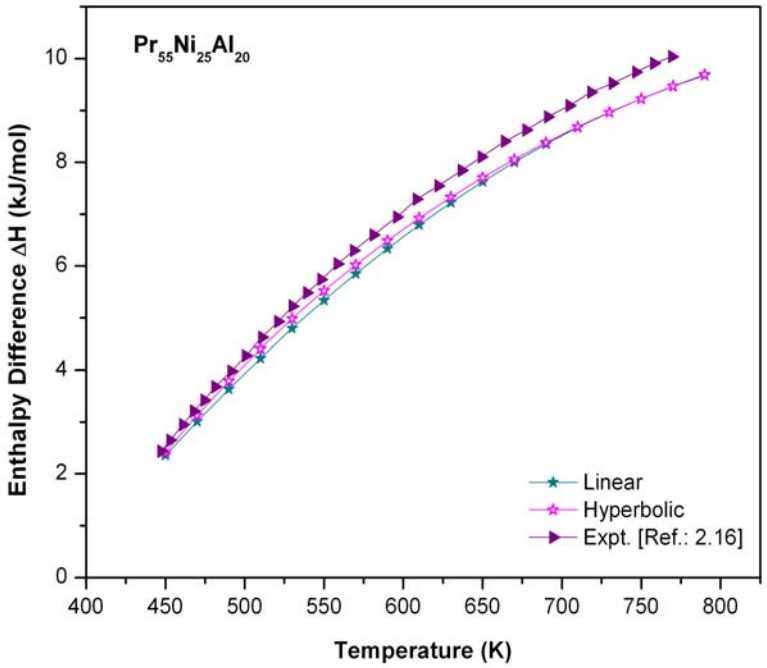

Fig. 2.3: Enthalpy difference, ΔH as a function of temperature for $Pr_{55}Ni_{25}Al_{20}$

Although $Pd_{77.5}Cu_6Si_{16.5}$ was the first bulk metallic glass [2.18], data on this alloy are incomplete and controversial [2.19]. For this BMG, the difference in specific heat capacity between liquid and crystalline phase, is determined using linear and hyperbolic variations as a function of temperature and compared with the experimental data as shown in Fig. 2.4. In the Fig. 2.5, the Gibbs free energy difference, ΔG as a function of temperature, is calculated for different ΔG expressions available. Similarly, the enthalpy difference, ΔH as a function of temperature is calculated and shown in Fig. 2.7. But, unfortunately, the experimental data for these two thermodynamic properties are not available. Fig. 2.6 shows the entropy difference between liquid and crystal, ΔS as a function of the temperature. The entropy of the undercooled liquid decreases with increasing undercooling until it reaches the entropy of the crystal at the Kauzmann temperature, T_K. The existence of an undercooled liquid below this temperature would violate thermodynamic rules, also called the Kauzmann paradox. Therefore, T_K will be the lower boundary for the glass transition from thermodynamic aspects. Here we have taken Kauzmann temperature T_K = 560 K [2.19]. It is obvious from the excellent agreement of the curves in Fig. 2.6 with the experimentally obtained ΔS that these linear and hyperbolic assumptions of ΔC_p variation are quite close to the actual situation. Further, assumption of constant ΔC_p may not work well for systems with excellent and enhanced glass forming ability (GFA) like the bulk metallic glasses.

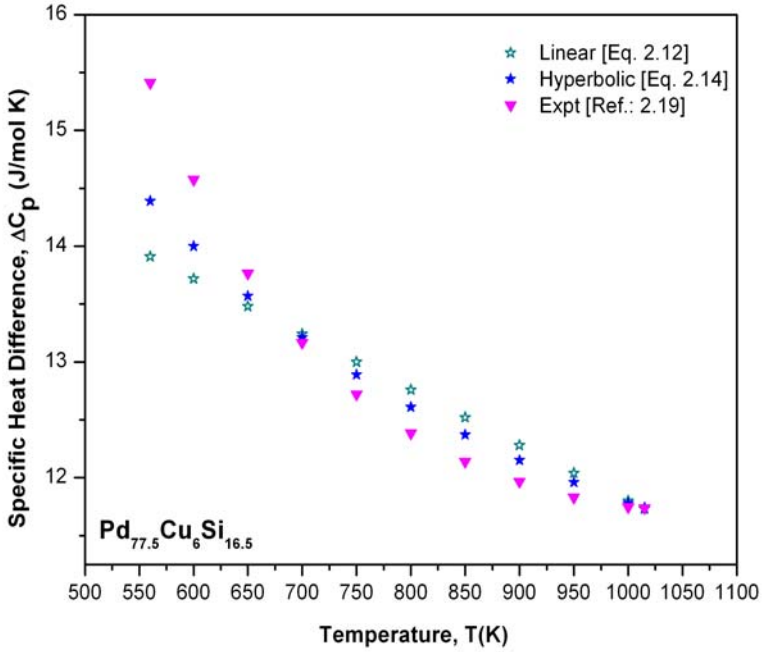

Fig. 2.4: Specific heat difference, ΔC_p as a function of temperature for $Pd_{77.5}Cu_6Si_{16.5}$

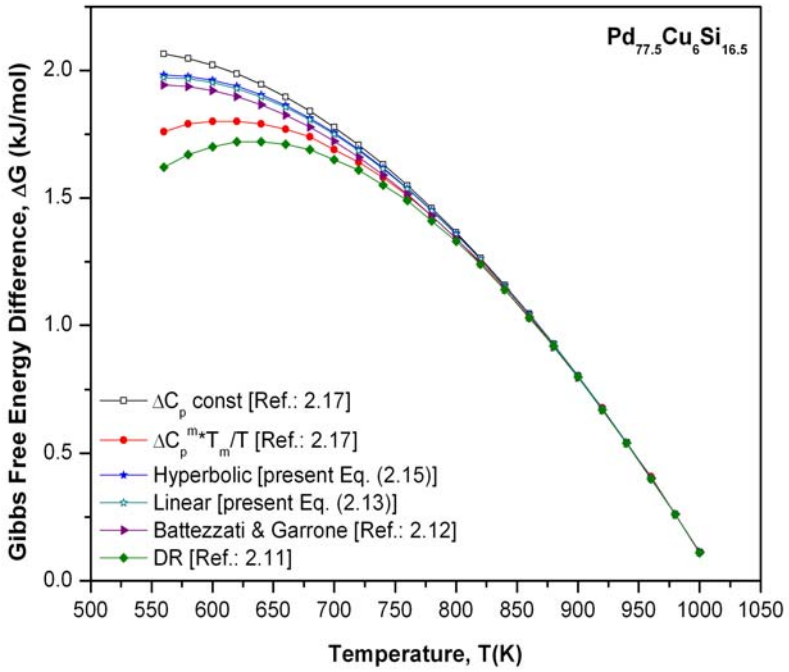

Fig. 2.5: Gibbs free energy difference, ΔG as a function of temperature for $Pd_{77.5}Cu_6Si_{16.5}$

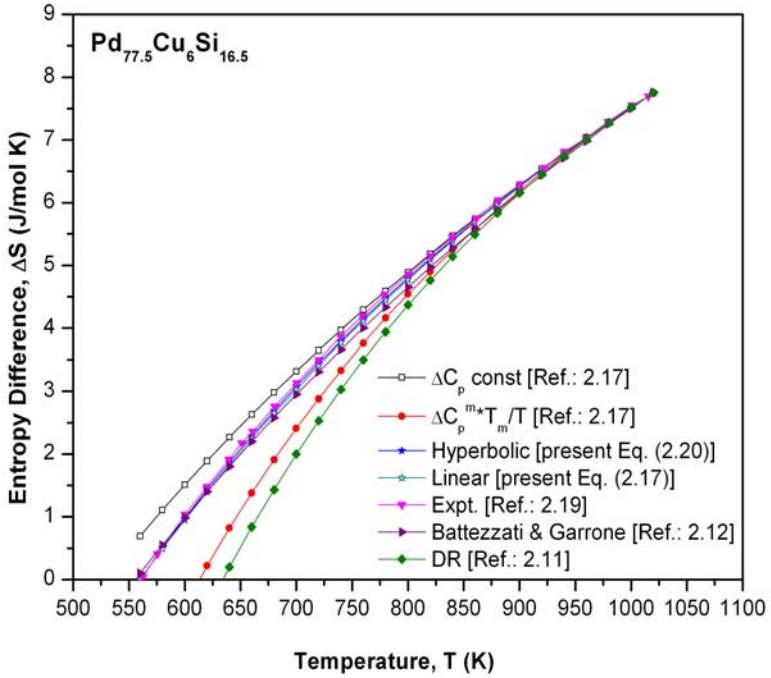

Fig. 2.6: Entropy difference, ΔS as a function of temperature for $Pd_{77.5}Cu_6Si_{16.5}$

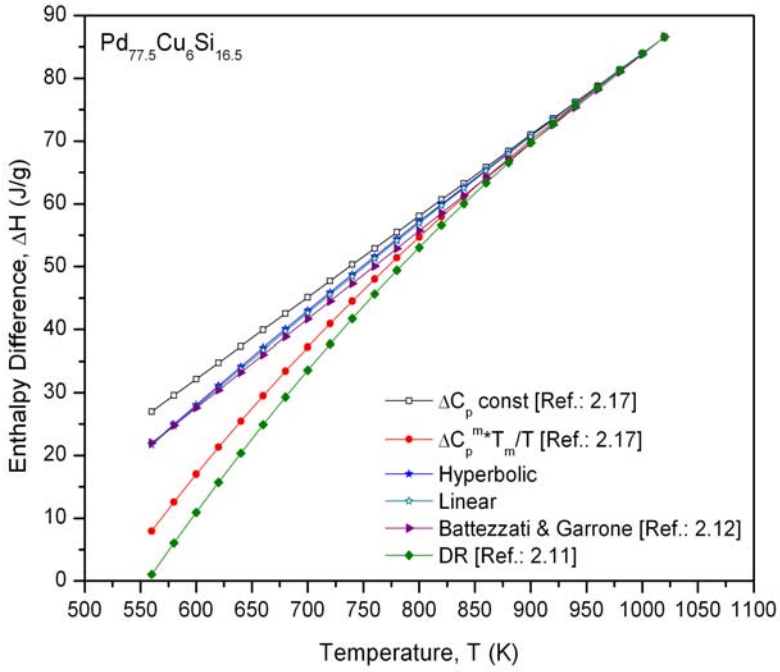

Fig. 2.7: Enthalpy difference, ΔH as a function of temperature for $Pd_{77.5}Cu_6Si_{16.5}$

The $Pt_{57.3}Cu_{14.6}Ni_{5.3}P_{22.8}$ alloy has been developed, with a critical cooling rate of the order of ~20 K/s. Its low liquidus temperature and large supercooled region expresses remarkable processing advantages over conventional platinum alloys [2.20]. For this metallic glass also, the difference in specific heat capacity between liquid and crystalline phase, is determined using linear and hyperbolic variations as a function of temperature and compared with the experimental data as shown in Fig. 2.8. Fig. 2.9 shows the Gibbs free energy difference, ΔG between undercooled liquid and corresponding crystalline solid as a function of temperature. Values of ΔG calculated using Linear and hyperbolic variations of heat capacity from Eqs. (2.13) and (2.15) are shown along with results obtained through other theoretical approaches and the experimental data. One can see that they are in excellent agreement with each other and also with the experimental points. The results obtained through other theoretical approaches, on the other hand, show large deviation (except TS-1) [2.9] in almost entire temperature range. The ΔG values evaluated using Lad-1 & Lad-2 equation [2.13, 2.15] fall much below the experimental data while that using S&H equation [2.10] overestimate ΔG, even though, ΔG plot evaluated using TS-1 equation [2.9] is close to the experimental data. The closeness of our results with the experimental data in comparison to other theoretical curves may be attributed to the fact that all the earlier workers have assumed constancy of ΔC_p and have not considered it as a variable with respect to temperature in the entire undercooled region.

The entropy difference ΔS for $Pt_{57.3}Cu_{14.6}Ni_{5.3}P_{22.8}$ system calculated from Eqs. (2.17) and (2.20) is shown in Fig. 2.10. The results from the other approaches [2.10, 2.13 and 2.15] are not shown because of their large deviation from the experimental ΔG

values as seen from Fig. 2.9. The calculated values show similar variation as seen for the experimental data. Once ΔG and ΔS values are known one can evaluate values of enthalpy difference, ΔH using Eq. (2.2). The results obtained for ΔH for $Pt_{57.3}Cu_{14.6}Ni_{5.3}P_{22.8}$, using both linear and hyperbolic variation of ΔC_p are plotted in Fig. 2.11. The experimental values of ΔH are also shown in the figure and it can be seen that the calculated values lie quiet close to the experimental values.

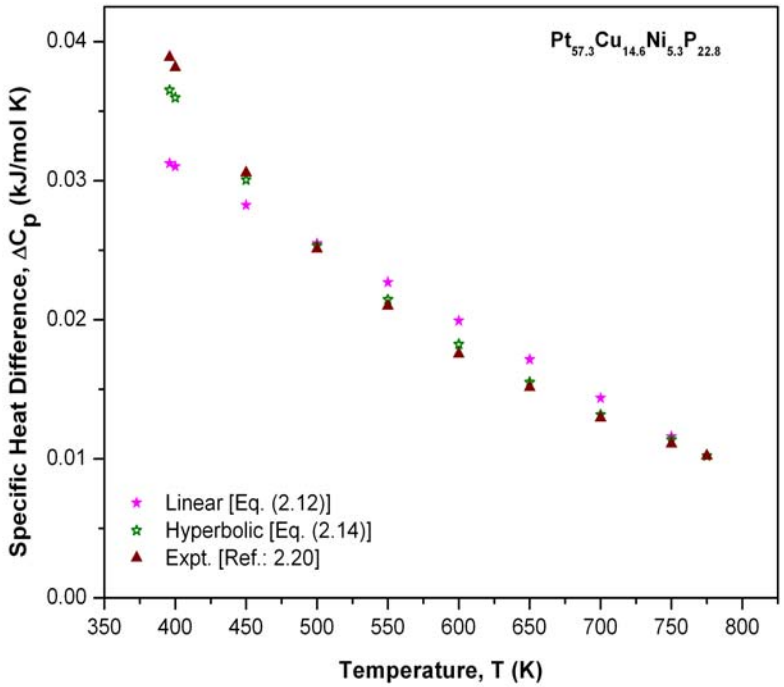

Fig. 2.8: Specific heat difference, ΔC_p as a function of temperature for $Pt_{57.3}Cu_{14.6}Ni_{5.3}P_{22.8}$

Table 2.1 Parameters used for calculations

SYSTEM	T_m (K)	T_K (K)	ΔH_m (kJ/mol)	ΔC_p^m (J/mol-K)	Reference
$Pr_{55}Ni_{25}Al_{20}$	751	448	9.24	12.57	2.16
$Pd_{77.5}Cu_6Si_{16.5}$	1015	560	7.81	11.74	2.19
$Pt_{57.3}Cu_{14.6}Ni_{5.3}P_{22.8}$	775	396	11.4	10.22	2.5

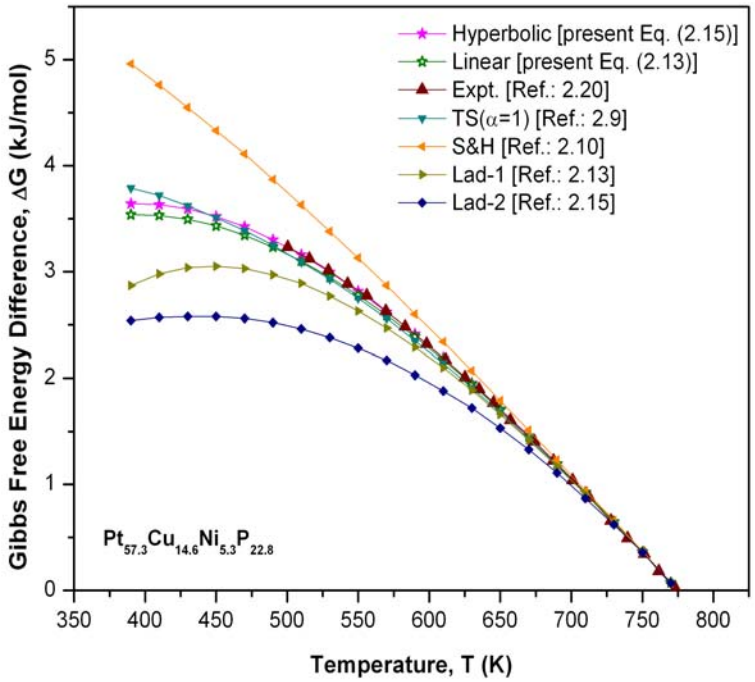

Fig. 2.9: Gibbs free energy difference, ΔG as a function of temperature for $Pt_{57.3}Cu_{14.6}Ni_{5.3}P_{22.8}$

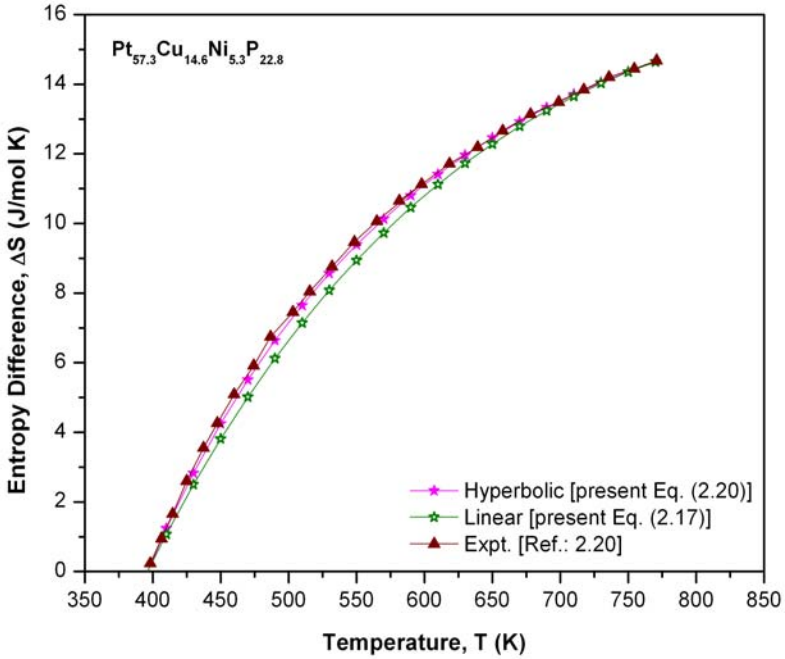

Fig. 2.10: Entropy difference, ΔS as a function of temperature for $Pt_{57.3}Cu_{14.6}Ni_{5.3}P_{22.8}$

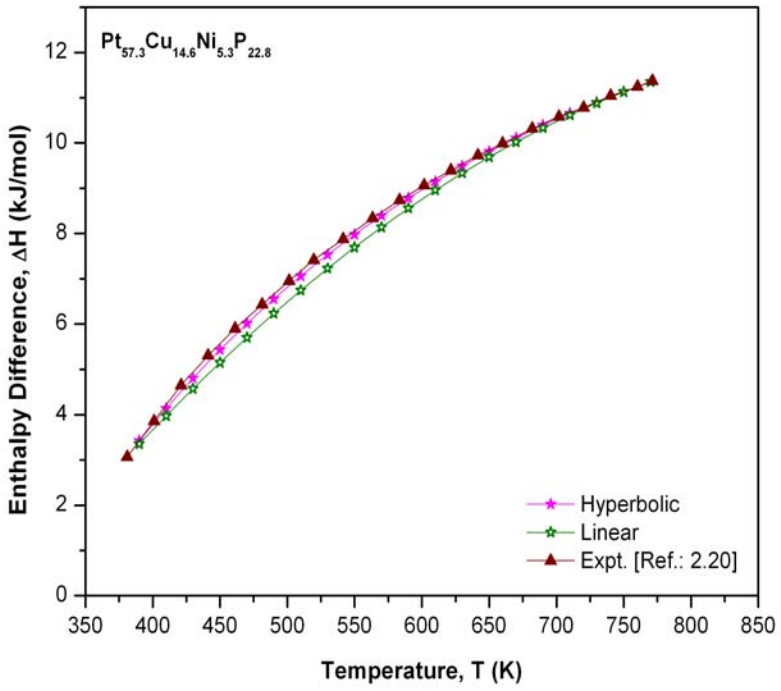

Fig. 2.11: Enthalpy difference, ΔH as a function of temperature for $Pt_{57.3}Cu_{14.6}Ni_{5.3}P_{22.8}$

2.4.2 Gibbs Free Energy Difference, Entropy Difference and Enthalpy Difference for Two Zr-based Bulk Metallic Glass Forming Alloys

In the present study, the thermodynamic behavior of $Zr_{57}Cu_{15.4}Ni_{12.6}Al_{10}Nb_5$ bulk metallic glass have been investigated, by evaluating ΔG in the entire temperature range from T_m to T_K. This multicomponent system is among the best non-beryllium containing glasses making it easier to process and handle [2.21]. Fig. 2.12 shows the Gibbs free energy difference between undercooled liquid and corresponding crystalline solid for $Zr_{57}Cu_{15.4}Ni_{12.6}Al_{10}Nb_5$ bulk metallic glass.

It is obvious from the figure that plots of ΔG estimated using linear and hyperbolic variations of ΔC_p almost coincide with the experimental points in the entire

undercooled region and hence are in excellent agreement with the experiment. Only two other expressions proposed by Dubey and Ramachandrarao [2.11] and Lad et al. [2.13] provide results somewhat close to the experimental data. However, even these two curves show variation in large undercooled region. All other theoretical formulations overestimate ΔG. Since ΔG is the driving force for crystallization, its accurate evaluation is important from the view point of alloy design for various applications. The entropy difference, ΔS between the undercooled liquid and corresponding crystalline solid has been obtained from the derivative of the plotted ΔG using Eqs. (2.13) and (2.15) and the same have been shown in Fig. 2.13 along with experimental results of Glade et al. It can be seen from the figure that the present approach accounts for accurate ΔS values in the entire temperature range and is matching excellently with the experimental points. Calculations using other theoretical expressions have not been shown as they are expected to show large variation from experiment. This has already been indicated in the ΔG plot and ΔS have been derived using the derivative of ΔG only. ΔH, shown in Fig. 2.14 the enthalpy difference between undercooled liquid and corresponding crystalline solid has been also evaluated from the known values of ΔG and ΔS using Eq. (2.2). The difference in the enthalpy between the liquid and the crystalline states at the glass transition, should in principle, provide the amount of enthalpy frozen into the liquid at T_g. Parameters used for calculations are given in Table 2.2 for both the systems.

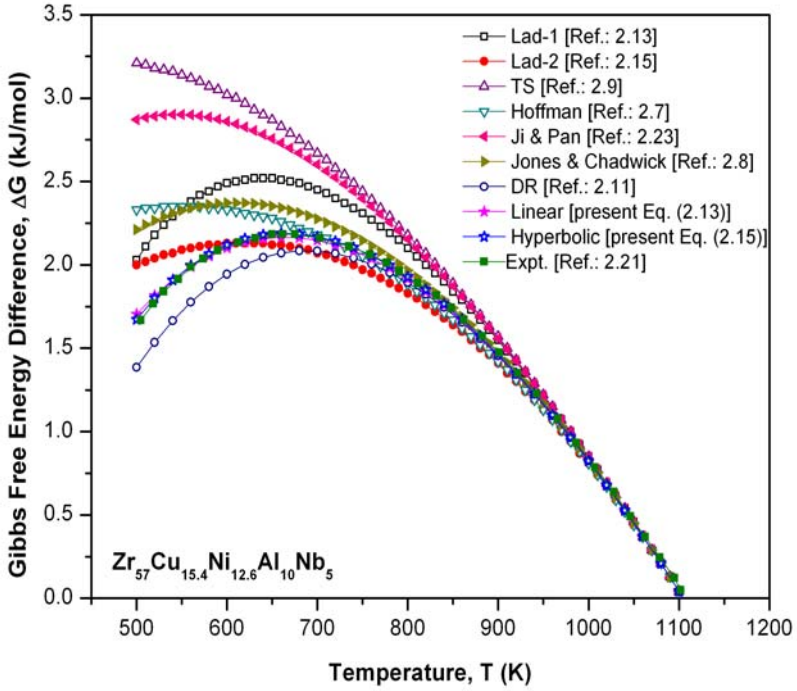

Fig. 2.12: Gibbs free energy difference, ΔG as a function of temperature for $Zr_{57}Cu_{15.4}Ni_{12.6}Al_{10}Nb_5$

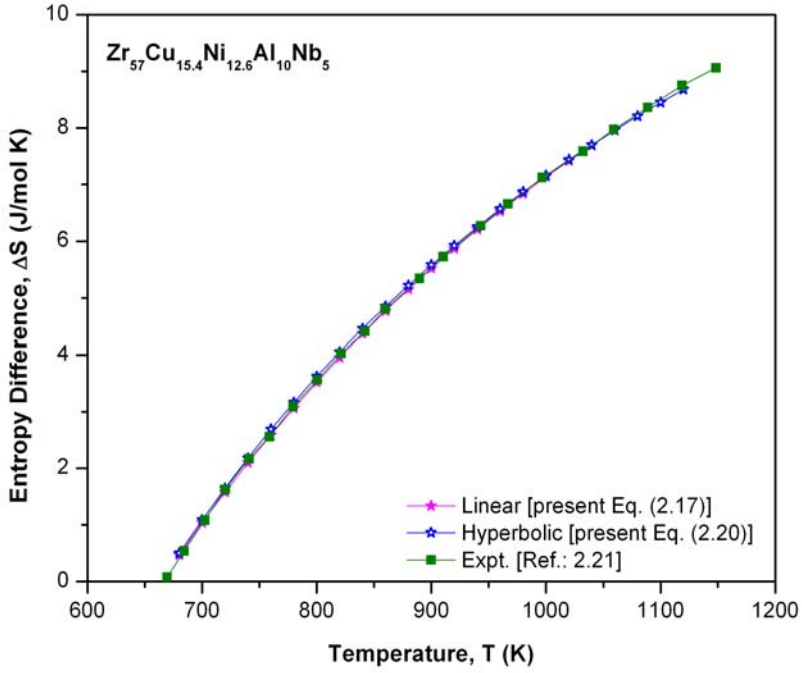

Fig. 2.13: Entropy difference, ΔS as a function of temperature for $Zr_{57}Cu_{15.4}Ni_{12.6}Al_{10}Nb_5$

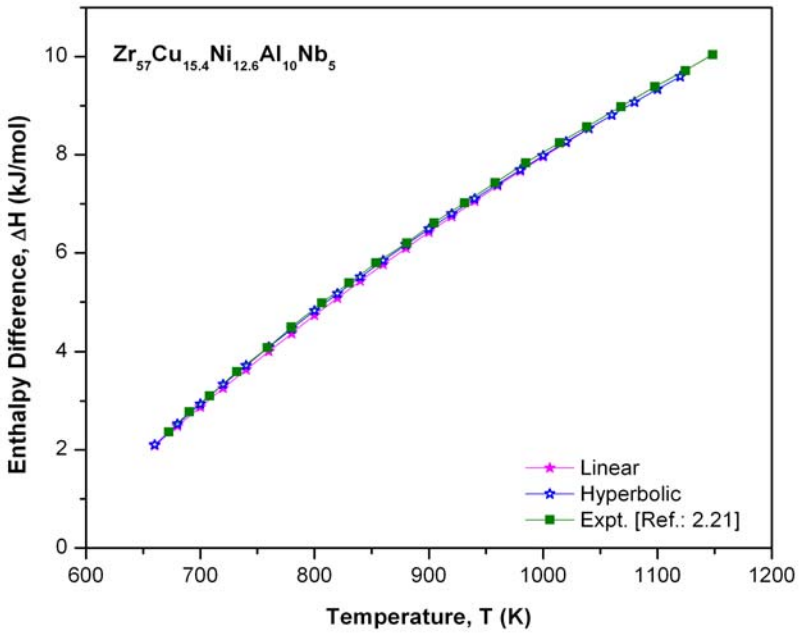

Fig. 2.14: Enthalpy difference, ΔH as a function of temperature for $Zr_{57}Cu_{15.4}Ni_{12.6}Al_{10}Nb_5$

Similarly, the thermodynamic behavior of $Zr_{52.5}Cu_{17.9}Ni_{14.6}Al_{10}Ti_5$ bulk metallic glass, have been studied by calculating ΔG in the entire temperature range from T_m to T_K. This amorphous mulitcomponent alloy is also one of the best nonberyllium containing glasses. Fig.2.15 shows the Gibbs free energy difference between undercooled liquid and corresponding crystalline solid for $Zr_{52.5}Cu_{17.9}Ni_{14.6}Al_{10}Ti_5$. It is obvious from the figure that plots of ΔG estimated using linear and hyperbolic variation of ΔC_p almost coincide with the experimental points in the entire undercooled region and hence are in excellent agreement with the experiment. Surprisingly, expression given by Lad et al. [2.13] abbreviated as Lad-1 provides results somewhat closer to the experimental ones, even though ΔC_p = constant assumption has been taken in this approach. Other expressions given by various workers either underestimate or overestimate ΔG particularly in large undercooled

region. The entropy difference, ΔS between the undercooled liquid and corresponding crystalline solid has been obtained from the derivative of the plotted ΔG and the same has been shown in Fig. 2.16 along with experimental results of Glade et al. [2.21]. It can be seen from the figure that the present approach accounts for accurate ΔS values in the entire temperature range and is matching excellently with the experimental points. Calculations using other theoretical expressions have not been shown as they are expected to show large variation from experiment. ΔH, the enthalpy difference between undercooled liquid and corresponding crystalline solid has been also evaluated from the known values of ΔG and ΔS using Eq. (2.2) as shown in Fig. 2.17. The difference in the enthalpy between the liquid and the crystalline states at the glass transition, should in principle, provide the amount of enthalpy frozen into the liquid at T_g. The changing thermodynamics between the phases has also been recently investigated [2.22].

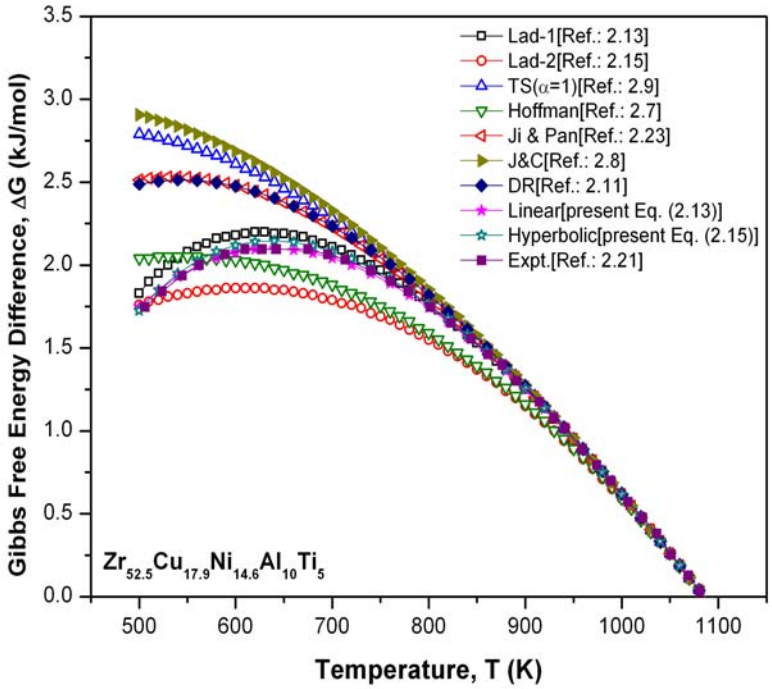

Fig. 2.15: Gibbs free energy difference, ΔG as a function of temperature for $Zr_{52.5}Cu_{17.9}Ni_{14.6}Al_{10}Ti_5$

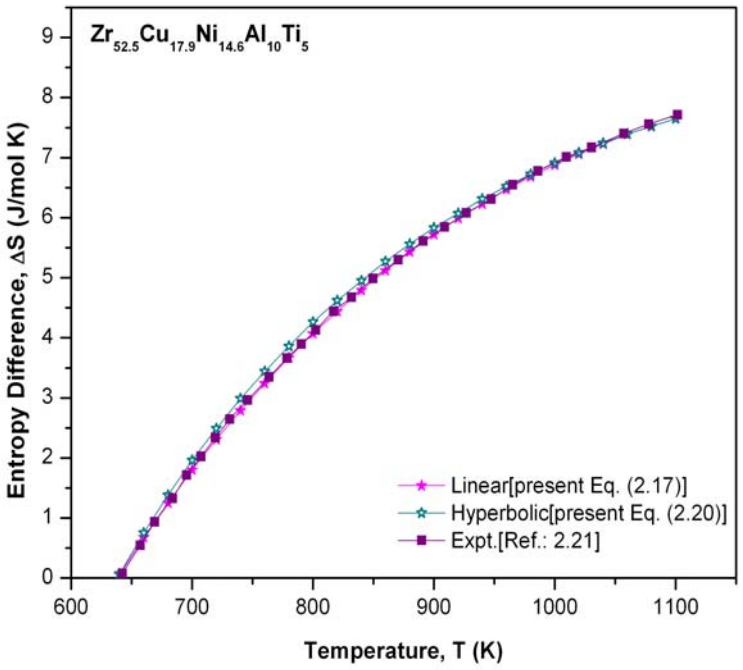

Fig. 2.16: Entropy difference, ΔS as a function of temperature for $Zr_{52.5}Cu_{17.9}Ni_{14.6}Al_{10}Ti_5$

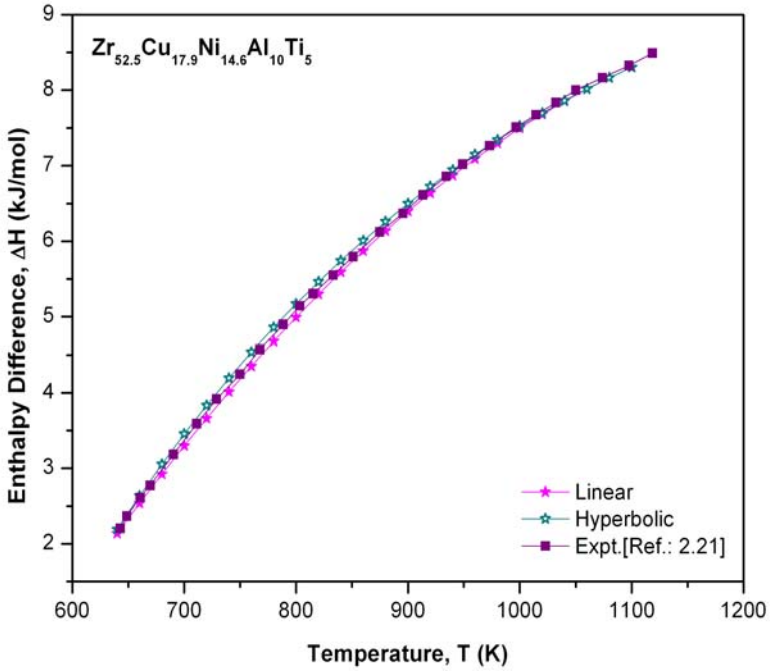

Fig. 2.17: Enthalpy difference, ΔH as a function of temperature for $Zr_{52.5}Cu_{17.9}Ni_{14.6}Al_{10}Ti_5$

Table 2.2 Parameters used for calculations

SYSTEM	T_m (K)	T_K (K)	ΔH_m (kJ/mol)	ΔC_p^m (J/mol-K)	Reference
$Zr_{57}Cu_{15.4}Ni_{12.6}Al_{10}Nb_5$	1105	664	9.4	12.87	2.21
$Zr_{52.5}Cu_{17.9}Ni_{14.6}Al_{10}Ti_5$	1085	638	8.2	7.02	2.21

2.5 Conclusions

It is important to consider an appropriate variation of ΔC_p with temperature while deriving an analytical expression for ΔG for bulk metallic glass forming alloys. Various earlier expressions, available to calculate ΔG, involve mainly two kinds of assumptions.

(1) Temperature dependence of specific heat capacity, ΔC_p is assumed to be linear. Due to non-availability of the experimental ΔC_p data in the undercooled region, most of the workers have assumed ΔC_p = constant in this region.

(2) Approximating the logarithmic term in the ΔG expression considering small degree of undercooling $T (=T_m - T)$.

These approximations in the expression for ΔG make it insensitive to the nature of the variation of ΔC_p in the undercooled region and also limit its validity upto small undercooling (ΔT).

Considering these limitations, two novel expressions for ΔG, depending on the type of ΔC_p variation (linear and hyperbolic), are derived.

The theoretical formulations used in this work, using linear and hyperbolic variations of ΔC_p, offer quite excellent results for thermodynamic parameters ΔG, ΔS *and* ΔH in the entire undercooled region of different bulk metallic glass forming alloys considered in present work.

All the BMG systems thermodynamic parameters, determined using linear and hyperbolic expression of ΔC_p, show almost one to one correspondence with their experimental data. The experimental data of ΔG & ΔH for $Pd_{77.5}Cu_6Si_{16.5}$ BMG are not available, but the values of ΔS evaluated using linear and hyperbolic expression shows excellent agreement with the experimental one. Therefore, one can conclude that values calculated of ΔG & ΔH from linear and hyperbolic variation, will also provide excellent results, if the experimental data are available.

The results assuming ΔC_p to be constant with temperature do show large variation and cannot be applied for the metallic glasses taken in this study. Therefore, to find out accurate values of thermodynamic properties one has to take into account variation of heat capacity difference, ΔC_p with temperature as considered here. As the ΔG is a signature of driving force for crystallization, accurate evaluation of it is very important as its value is an indicator of GFA of bulk metallic glass forming alloys.

References

[2.1] C. Suryanarayana & A. Inoue, *Bulk metallic Glass*, Chapter **1**, CRC Press Taylor & Francis Group, 2011.

[2.2] D. C. Hofmann, Designing Bulk Metallic Glass Matrix Composites with High Toughness and Tensile Ductility, Ph. D. Thesis, California Institute of Technology, 2009.

[2.3] D.R. Gaskell, *Introduction to the Thermodynamics of Materials*, 5th edition New York: Taylor & Fransis Group, LLC.

[2.4] R.K. Wunderlich and H. Fecht, *Mater. Trans.* **42**; 2001: pp. 565.

[2.5] B.A. Legg, J. Schrores and R. Busch, *Acta Mater.* **55**; 2007: pp. 1109.

[2.6] D. Turnbull, *J. Appl. Phys*. **21**;1950: pp. 1022.

[2.7] J.D. Hoffman, *J. Chem. Phys* **29**; 1958: pp. 1992.

[2.8] D.R.H. Jones and G.A. Chadwick, *Phil. Mag*. **24**; 1971: pp. 995.

[2.9] C.V. Thompson and F. Spaepen, *Acta Metall*., **27**; 1979: pp. 1855.

[2.10] H.B. Singh and A. Holz, *Solid State Commun*., **45**; 1983: pp. 985.

[2.11] K.S. Dubey and P. Ramchandrarao, *Acta Metall.* **32**; 1984: pp. 91.

[2.12] L. Battezzati and E. Garrone, *Z. Metallkunde* **75**; 1984: pp. 305.

[2.13] K.N. Lad, Arun Pratap and K.G. Raval, *J. Mater. Sci. Lett.* **21**; 2002: pp. 1419

[2.14] K. Mondal, U.K. Chatterjee and B.S. Murthy, *Appl. Phys. Lett.* **83**; 2003: pp. 671.

[2.15] K.N. Lad, K.G. Raval and Arun Pratap, *J. Non-Cryst. Solids* **334 & 335**; 2004: pp. 259.

[2.16] Q.G. Meng, S.G. Zang, J.G. Li, and X.F. Bian, J. of Alloys and Compounds 431; 2008: pp. 191.

[2.17] H. Dhurandhar, T.L.S. Rao, K.N. Lad and Arun Pratap, *Phil. Mag. Lett.* **88**; 2008: pp. 239.

[2.18] H.S. Chen, *Acta Metall.* **22**; 1974: pp. 1505.

[2.19] G. Fiore, L. Battezzati, *J. Alloy. and Comp.* Article in Press.

[2.20] B.A. Legg, J. Schroers and R. Busch, *Acta Mater.* **55**; 2007: pp. 1109.

[2.21] S.C. Glade, R. Busch, D.S. Lee and W.L. Johnson, *J. App. Phys.* **87, No. 10**; 2000: pp. 7242.

[2.22] B. Wunderlich, *J. Therm. Anal. Calorim.* **102**; 2010: pp. 413.

[2.23] X. Ji and Y. Pan, *J. Non-Cryst. Solids* **353**; 2007: pp. 2443.

CHAPTER – 3

GLASS FORMING ABILITY OF BULK METALLIC GLASSES

Till now, it was difficult to find out that which ΔG expression is best suitable for the bulk metallic glasses. Now, one can know a priori whether the ΔC_p is constant or varying linearly or hyperbolically with temperature. Hence, according to the nature of variation of ΔC_p, appropriate ΔG equation could be chosen for theoretical investigations. Also, the effect of addition of Al and Ag in CuZr binary system is discussed.

Glass forming ability of bulk metallic glasses is an important parameter from both theoretical and practical point of view. Different GFA criteria are calculated for various bulk metallic glasses. Based on the results, it is crystal clear that ΔG is the best criterion to estimate the GFA of any metallic glassy systems.

3.1 Introduction

To produce metallic glasses in a reasonable and reliable way; also their production in large quantities and to increase reproducibility, it is essential to know the basic reasons about glass formation from the liquid melts.

The ability of a liquid metallic alloy to transform into the metallic glassy state is referred as the glass forming ability (GFA). The excellent glass forming ability of the new alloys has been generally attributed to the increased atomic packing density in the multicomponent system, as there are more atoms of the correct size to fill empty space in the randomly packed glass structure. This seems to be true as the total energy of alloys with directionless metallic bonding depends on the packing density; denser packing leads to lower energy and thereby higher stability [3.1]. Besides considering the packing density; the improved glass forming ability of the multicomponent systems has also been understood by the 'confusion principle', i.e., the more elements involved, the lower the chance that the alloy can select viable crystal structure, and therefore greater the chance of good glass formation [3.2].

Since the discovery of metallic glasses, so many empirical rules on good metallic glass formation have been suggested by the factors such as atomic size, electron density, interatomic bonding and other structural features [3.3]. Even if these empirical rules work for certain alloys, they, many a times, fail for other glasses. After studying large number of alloys which have excellent glass forming ability, Inoue suggested a more comprehensive set of empirical rules for excellent glass formation [3.4]: alloys should be multicomponent systems consisting of more than

three elements, there should be significant atomic size mismatch (ratio >12%) among the three main constituent elements, and the three main components should have negative heat of mixing.

Due to non-availability of the experimental ΔC_p data in the undercooled region, most of the workers have assumed ΔC_p= constant in this region. ΔC_p= constant is supposed to work well for binary glass forming systems and therefore this assumption has been taken in the present work for $Cu_{46}Zr_{54}$ and $Cu_{54}Zr_{46}$ alloys. However, even minor addition of elements, like Al and Ag, in the binary systems is reported to enhance the GFA quite considerably. Therefore, $Zr_{46}Cu_{46}Al_8$ and $Zr_{46}(Cu_{4.5/5.5}Ag_{1/5.5})_{46}Al_8$ having excellent improved GFA exhibit appreciable increase (variation) in ΔC_p with increased undercooling. To take care of that variation and to incorporate the same, linear and hyperbolic variations of ΔC_p have been assumed.

3.2 Expression of ΔG, Considering the ΔC_p Variation

Knowledge of the thermodynamic properties i.e, Gibbs free energy difference (ΔG), entropy difference (ΔS), enthalpy difference (ΔH) and specific heat difference (ΔC_p), plays an important role in order to find out the glass forming ability and thermal stability of metallic amorphous alloys. The Gibbs free energy difference gives a qualitative measure of the stability of the glass compared to the crystalline state.

To evaluate ΔG, the values of ΔS and ΔH are required with the variation in temperature. And to calculate those two, the knowledge of the specific heat difference ΔC_p is required as equations are given in chapter 2.

ΔC_p, defined as $C_p^l - C_p^x$, is the difference in specific heats of the liquid and corresponding crystalline phases of metallic alloy. Therefore, experimental ΔG can be calculated using Eq. (2.1), (2.8) & (2.9), if the experimental specific heat data is available for the undercooled and the crystal phases of a material. However, due to the metastable nature of amorphous metallic materials experimental ΔC_p data is unavailable; therefore one has to switch to suitable expression of ΔC_p that adequately represents the temperature dependence of ΔC_p.

Up till now no such method was available from which one can find out a priori whether the nature of ΔC_p is constant or varying. This could be possible if one had the estimate of Kauzmann temperature T_K and the other two parameters viz. ΔC_p^m at melting temperature T_m.

Assuming ΔC_p to be constant in the undercooled region, and taking $\Delta S = 0$, one can find that at $T = T_K$,

$$\Delta C_p = \alpha \frac{\Delta H_m}{T_m} \tag{3.1}$$

where, $$\alpha = \frac{1}{\ln T_m / T_K} \tag{3.2}$$

Treating ΔC_p to be constant, one can take the value of $\Delta C_p = \Delta C_p^m$, the corresponding value at the melting point and rewriting the Eq. (3.1) for α,

$$\alpha = \frac{\Delta C_p^m T_m}{\Delta H_m} \tag{3.3}$$

Here, considering the value of α obtained using Eq. (3.2) as α_1 and that derived through Eq. (3.3) as α_2 one can get two values of α which are given in Table 3.1 for the present Zr-based two systems.

Table 3.1 Values of α_1 and α_2

System	α_1	α_2
$Zr_{46}Cu_{46}Al_8$	2.01	1.64
$Zr_{46}(Cu_{4.5/5.5}Ag_{1/5.5})_{46}Al_8$	2.17	1.65

For a particular metallic glass if these values are nearly equal then ΔC_p can be taken as constant for that particular system and if two α values are different then ΔC_p is not constant and it is varying with temperature in the undercooled region for that system. From the Table 3.1 one can see that for the last two systems taken up in the present study, α values are not coming same, therefore, ΔC_p is a function of temperature.

So in the present case, for $Zr_{46}Cu_{46}Al_8$ and $Zr_{46}(Cu_{4.5/5.5}Ag_{1/5.5})_{46}Al_8$ systems, we have opted for two different linear and hyperbolic variations of ΔC_p, which involve A & B coefficients for linear variation and C & D coefficients for hyperbolic variation. These coefficients can be evaluated with the knowledge of ΔC_p^m and T_K, where ΔC_p^m is specific heat difference at melting temperature and T_K is Kauzmann temperature where entropy difference, $\Delta S = 0$. Considering these two types of ΔC_p variations, linear and hyperbolic as discussed in chapter - 2, expressions for ΔG are derived.

3.3 Different Glass Forming Ability (GFA) Parameters

As the accurate prediction of the glass forming ability of amorphous metallic systems is very much important from theoretical and practical point of view, so many GFA parameters such as γ parameter (GFA indicator), critical cooling rate (R_c), reduced glass transition temperature (T_{rg}), deep eutectics, Gibbs free energy difference (ΔG) have been put forward [3.5] for the evaluation of GFA. The most extensively used GFA criteria are the reduced glass transition temperature, T_{rg}, the parameter, γ and the supercooled liquid range, ΔT_x [3.6-3.8]. Actually, quite a large number of good glass forming systems obey these criteria barring few exceptions [3.9, 3.10]. Recently, Suo et al [3.11] have proposed a new criterion for the evaluation of GFA of Ca-based BMGs. This approach combines the liquid phase stability, resistance to crystallization and the glass transition enthalpy.

ΔG has played an important role in predicting the glass forming ability of multicomponent metallic alloys. Lesser the value of ΔG, easier is the formation of BMGs. Study of ΔG in large undercooled region is very interesting to gauge the GFA of metallic alloys.

3.4 Results & Discussions

3.4.1 Effect of Addition of Al and Ag on Glass Forming Ability in Cu-Zr Binary Alloys

Gibbs free energy difference, ΔG is the driving force for the crystallization and therefore, a good glass former is expected to have a small thermodynamic driving force [3.12]. For a high glass forming ability, thermodynamically lower ΔG is expected to stabilize the undercooled melt against crystallization.

Cu-Zr binary systems are of special interest because they posses excellent GFA, good mechanical property, lower cost and also have wide glass-forming range. For $Cu_{46}Zr_{54}$ and $Cu_{54}Zr_{46}$ BMGs, ΔG is evaluated using expressions of Lad-1, Lad-2, ΔC_p constant, and Thompson and Speapen ($\alpha = 1$) [3.13-3.16] as shown in Fig. 3.1 and Fig. 3.2 respectively. Since the data for specific heat difference ΔC_p in the undercooled region is not available, calculations from the present Eqs. (2.13) and (2.15) are not possible, which are derived from linear and hyperbolic variation of ΔC_p with temperature respectively. Further, values of Kauzmann temperature, T_K for these two binary systems are also not available. Therefore, the temperatures at peak values of ΔG obtained from the expression of Lad-I, are taken as Kauzmann temperature (where ΔS=0) for the respective systems, which are listed in Table 3.2. Taking these T_K values into account, the α values for both systems have been found out. Since the experimental values for the specific heat difference are not available, ΔC_p is assumed to be constant for both binary systems. As ΔC_p is taken to be constant, the values of

α_1 and α_2 become same for a given system. Therefore, taking $\alpha_1 = \alpha_2 = \alpha$, and substituting it in Eq. (3.3), ΔC_p^m are calculated for both binary systems, which are given in Table 3.2. Due to this, α value is not shown for them in Table 3.1.

Table 3.2 Parameters used for calculations

System	T_g (K)	T_x (K)	T_m (K)	T_l (K)	T_K (K)
$Cu_{46}Zr_{54}$	696 [3.5]	746 [3.22]	1198.6 [3.5]	1201 [3.22]	680
$Cu_{54}Zr_{46}$	694 [3.5]	745 [3.23]	1195.7 [3.5]	1184 [3.23]	690
$Zr_{46}Cu_{46}Al_8$	715 [3.17]	771 [3.17]	979 [3.17]	1163 [3.17]	596 [3.17]
$Zr_{46}(Cu_{4.5/5.5}Ag_{1/5.5})_{46}Al_8$	703 [3.17]	775 [3.17]	1063 [3.17]	1126 [3.17]	671 [3.17]

Table 3.2 Continues……

System	ΔH_m (kJ/mol)	ΔC_p^m (J/mol-K)	ΔS_m (J/mol-K)
$Cu_{46}Zr_{54}$	17.43	25.65	14.54
$Cu_{54}Zr_{46}$	14.09	21.42	11.78
$Zr_{46}Cu_{46}Al_8$	8.03 [3.17]	13.49 [3.17]	8.20 [3.17]
$Zr_{46}(Cu_{4.5/5.5}Ag_{1/5.5})_{46}Al_8$	7.10 [3.17]	11.06 [3.17]	6.68 [3.17]

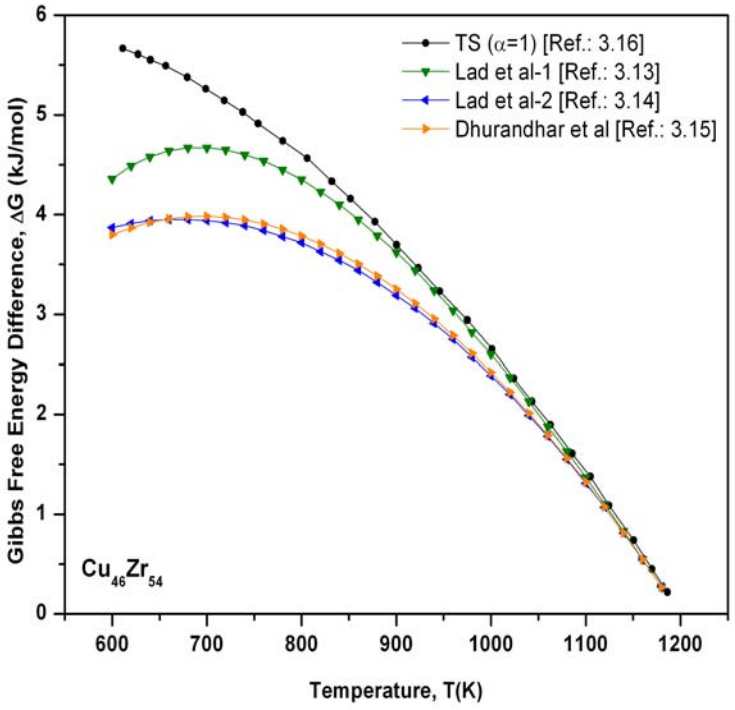

Fig. 3.1: Gibbs free energy difference, ΔG as a function of temperature for $Cu_{46}Zr_{54}$

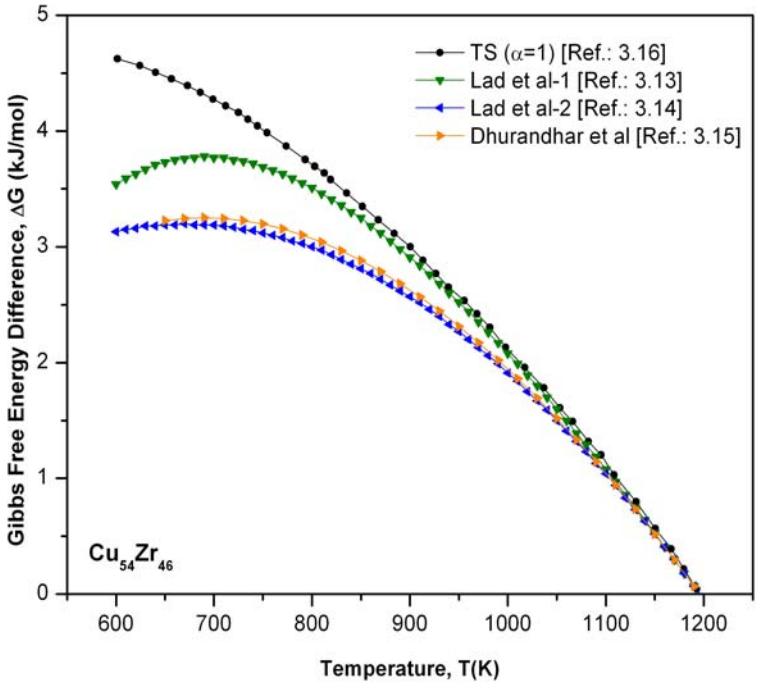

Fig. 3.2: Gibbs free energy difference, ΔG as a function of temperature for $Cu_{54}Zr_{46}$

Adding aluminum in this binary system, a new BMG $Zr_{46}Cu_{46}Al_8$ is fabricated [3.17]. Its Gibbs free energy difference, ΔG is calculated using Eqs. (2.13) and (2.15) and compared with the experimental data [3.17]. The coefficients A, B, C & D are required to calculate Gibbs free energy difference ΔG and entropy difference ΔS considering linear and hyperbolic variation of ΔC_p with temperature. These coefficients can be evaluated using Eqs. (2.18), (2.19), (2.21) & (2.22), and required parameters for calculation of them are listed in Table 3.2.

It can be seen from Fig. 3.3 that the results obtained from linear and hyperbolic Eqs. coincide with each other and they also lie very close to the experimental values. The results obtained through other theoretical approaches except Lad-2 [3.14] show large variation. Though ΔG values obtained from Lad-2 considering ΔC_p constant also fall close to the experimental data, other expressions treating ΔC_p constant [3.13, 3.15, 3.16, 3.18, 3.19] overestimate ΔG mainly in the large undercooled region.

The entropy difference ΔS for $Zr_{46}Cu_{46}Al_8$ system calculated using Eqs. (2.17) and (2.20), and the experimental results are shown in Fig. 3.4. From the given plots it is clearly noted that the calculated values fall very close and show similar variation as the experimental data in the whole undercooled region. The results from the other approaches are not shown because of their large deviation from the experimental ΔG values as seen from Fig. 3.3. Consequently, it is expected that ΔS will also show large deviation. Using Eq. (2.2), one can evaluate the enthalpy difference ΔH, if ΔG and ΔS values are known. Fig. 3.5 shows ΔH values which are calculated using Eq. (2.2) for both linear and hyperbolic variation of ΔC_p. The experimental values for ΔH are also

shown in the figure and it can be seen that the calculated values lie quite close to the experimental data.

Fixing the Al content and on the substitution of small amount of silver replacing Cu, one can get $Zr_{46}(Cu_{4.5/5.5}Ag_{1/5.5})_{46}Al_8$ BMG. For $Zr_{46}(Cu_{4.5/5.5}Ag_{1/5.5})_{46}Al_8$ plots for ΔG of linear and hyperbolic variation of ΔC_p gives results shown in Fig. 3.6, which are in excellent agreement with the experimental data and appear superimposed on each other. Other results are also shown in Fig. 3.6, where the results obtained through Lad-2 [3.14] and Dubey and Ramchandrarao [3.19] show slight variation with the experimental data, while others show very large overestimation.

In Fig. 3.7 the ΔS for the $Zr_{46}(Cu_{4.5/5.5}Ag_{1/5.5})_{46}Al_8$ system is calculated using Eqs. (2.17) and (2.20). The calculated values show excellent match with the experimental one and also follows the similar variation. Again, earlier approaches show large deviation for ΔG, and hence the values for ΔS are not evaluated using those approaches.

Fig. 3.8 shows ΔH values which are calculated usin g ΔG equation through both linear and hyperbolic variation of ΔC_p. One can see that the calculated values are almost coinciding with the experiment as shown in figure.

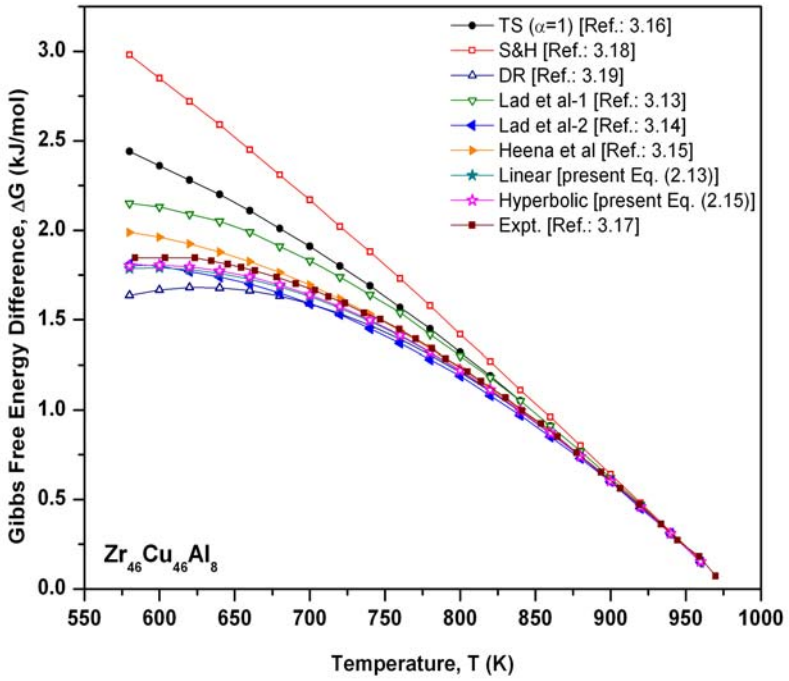

Fig. 3.3: Gibbs free energy difference, ΔG as a function of temperature for $Zr_{46}Cu_{46}Al_8$

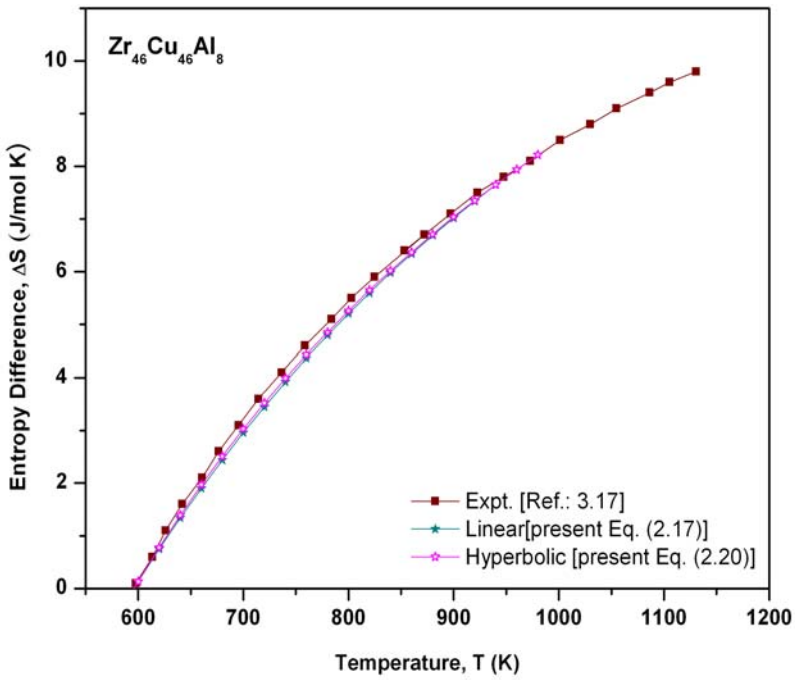

Fig. 3.4: Entropy difference, ΔS as a function of temperature for $Zr_{46}Cu_{46}Al_8$

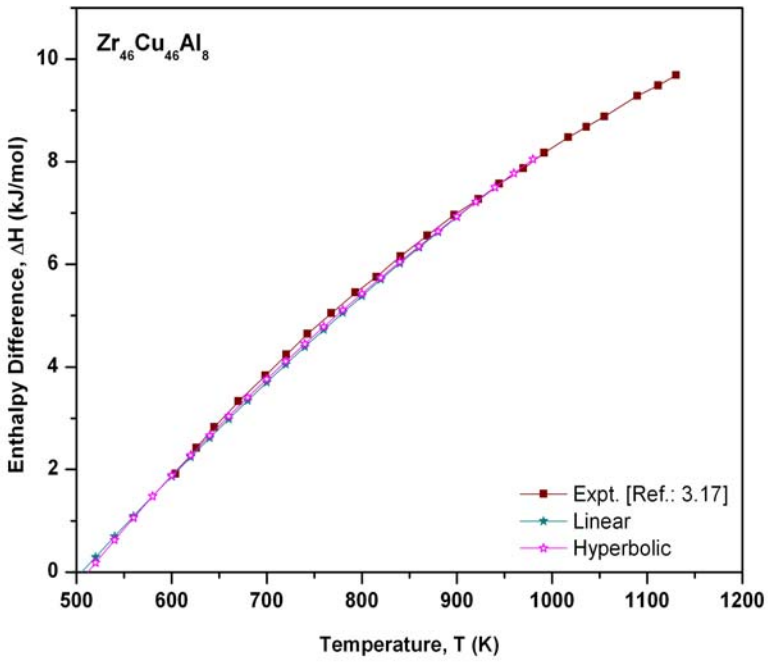

Fig. 3.5: Enthalpy difference, ΔH as a function of temperature for $Zr_{46}Cu_{46}Al_8$

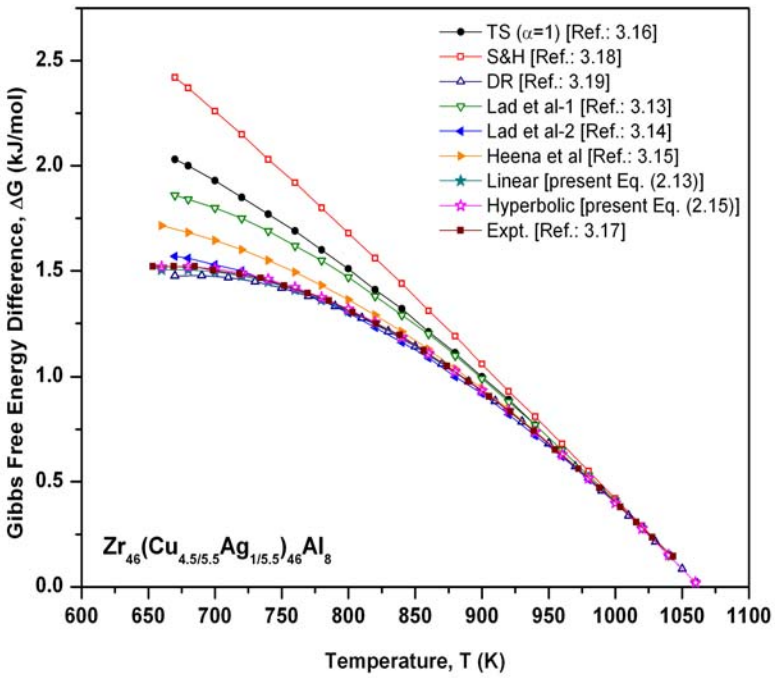

Fig. 3.6: Gibbs free energy difference, ΔG as a function of temperature for $Zr_{46}(Cu_{4.5/5.5}Ag_{1/5.5})_{46}Al_8$

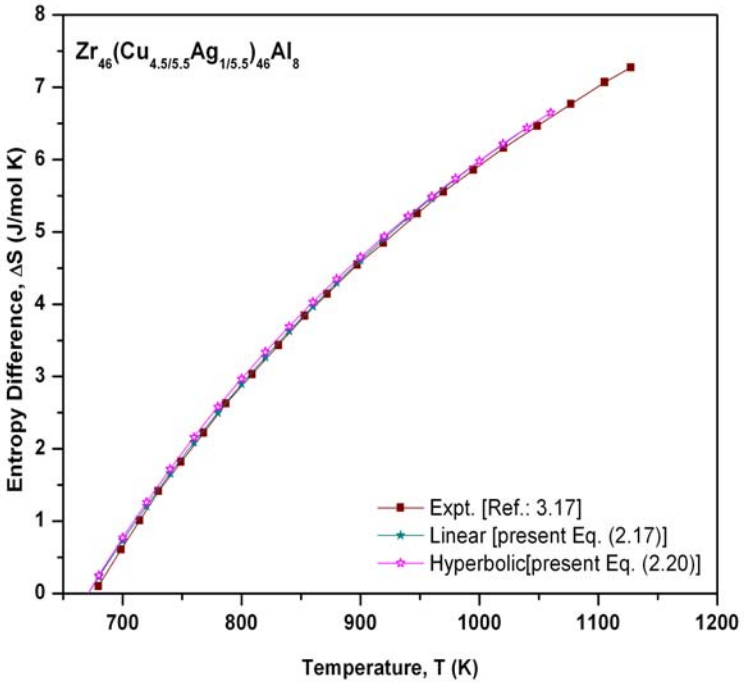

Fig. 3.7: Entropy difference, ΔS as a function of temperature for $Zr_{46}(Cu_{4.5/5.5}Ag_{1/5.5})_{46}Al_8$

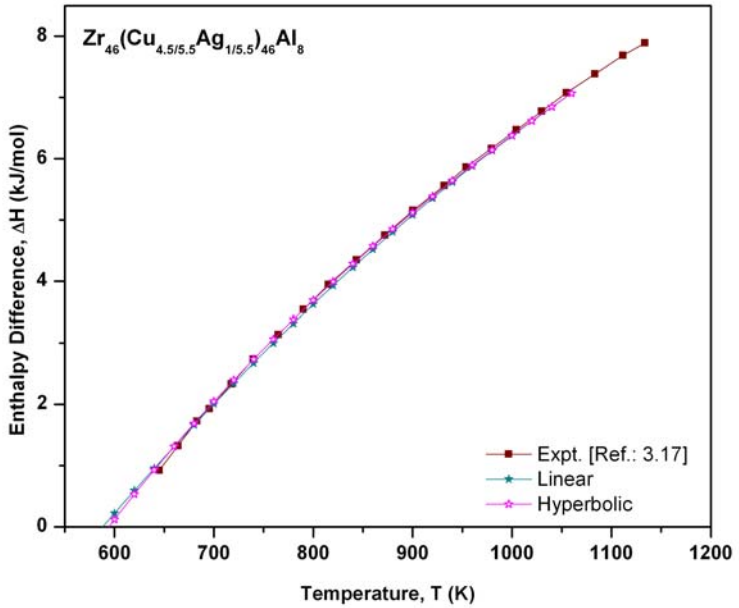

Fig. 3.8: Enthalpy difference, ΔH as a function of temperature for $Zr_{46}(Cu_{4.5/5.5}Ag_{1/5.5})_{46}Al_8$

3.4.2 Calculation of Different GFA Parameters

The prime requirement for the formation of amorphous phase from a liquid state is essentially suppression of competing nucleation and growth of the crystalline phases in the supercooled region. Turnbull [3.6] divulged a ratio widely adapted as reduced glass transition temperature, T_{rg}; a ratio between glass transition temperature T_g and liquidus temperature T_l of an alloy, often used as a criterion to determine the GFA of an alloy.

There are so many different criteria also available in literature [3.20, 3.21] for the estimation of GFA, such as $\delta(=T_K/T_m)$, $T_{rg}(=T_g/T_l)$, $\Delta C_p^m/\Delta S_m$, $\gamma_m(=2T_x - T_g/T_l)$, $\gamma(=T_x/T_g+T_l)$ and T_x/T_l. These criteria are mainly based on melting temperature (T_m), Kauzmann temperature (T_K), crystallization temperature (T_x), glass transition temperature (T_g), liquidus Temperature (T_l), specific heat difference (ΔC_p^m) and entropy difference (ΔS_m).

Two Zr-based and five Ca-based BMGs are taken up in this present work. For five Ca-based BMGs, ΔG has been evaluated through Lad et al-2 [3.14] expression and the plots for five compositions of this amorphous alloy system are shown in Fig. 3.9. Different GFA criteria are calculated for them and they are compiled in Table 3.3, 3.4-(a) & 3.4-(b).

It can be seen from the evaluated parameters given in Table 3.4-(a) that different GFA criteria laid down by different workers do not show any systematic variation in the glass forming tendency at various compositions of these Ca-based ternary alloys. The parameters namely T_{rg} , γ_m and γ are almost constant with values of 0.6, 0.7 and 0.4

respectively and even T_x/T_l does not vary appreciably. Only recently proposed parameter Q by Suo et al [3.11] seems to be a sensitive parameter showing variation with change in composition. However, it may be noted that the evaluation of Q essentially requires the knowledge of crystalline enthalpy ΔE. Another interesting point may be observed from the expression of Q that this parameter also indicated the inverse relation of GFA with ΔH_m. As ΔH_m decreases, glass forming tendency increases. This can be seen from Table 3.4-(b).

The ΔG values at Kauzmann temperature of respective systems are also listed with different GFA criteria. Thermodynamically, smaller Gibbs free energy difference ΔG, is expected to stabilize the undercooled melt against crystallization. Basically, ΔG is the driving force for crystallization and as a result, it is a reliable indicator for GFA.

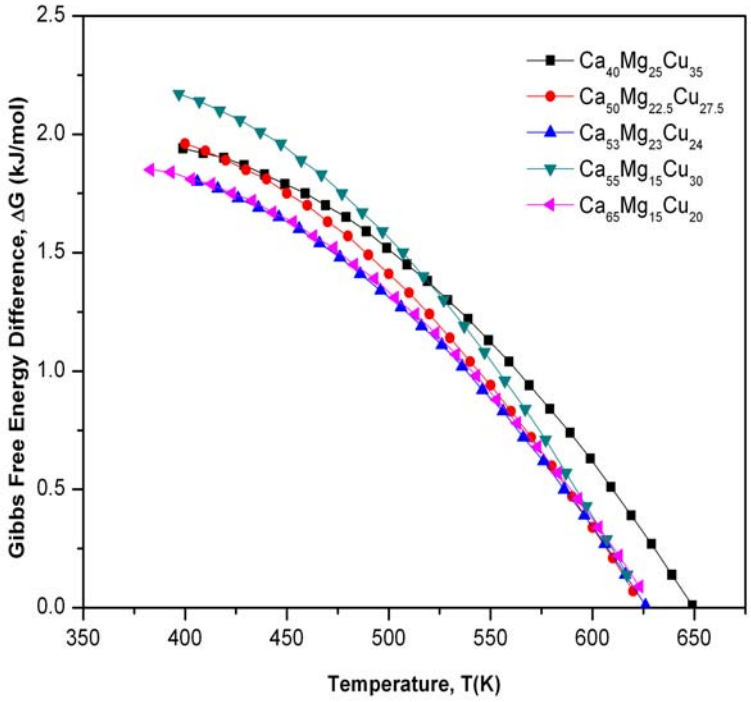

Fig. 3.9: ΔG as a function of temperature for different Ca-based BMGs

Table 3.3 Different GFA Criteria

System	$\delta = \frac{T_K}{T_m}$	$T_{rg} = \frac{T_g}{T_l}$	$\gamma_m = \frac{(2T_x - T_g)}{T_l}$	$\gamma = \frac{T_x}{T_g + T_l}$
$Cu_{46}Zr_{54}$	0.567	0.579	0.662	0.393
$Cu_{54}Zr_{46}$	0.577	0.586	0.672	0.397
$Zr_{46}Cu_{46}Al_8$	0.609	0.615	0.711	0.410
$Zr_{46}(Cu_{4.5/5.5}Ag_{1/5.5})_{46}Al_8$	0.631	0.624	0.752	0.424

Table 3.3 Continues……..

System	$\frac{T_x}{T_l}$	$\frac{\Delta C_p^m}{\Delta S_m}$	*ΔG at T_K (kJ/mol)*
$Cu_{46}Zr_{54}$	0.621	1.764	3.96
$Cu_{54}Zr_{46}$	0.629	1.819	3.19
$Zr_{46}Cu_{46}Al_8$	0.663	1.642	1.80
$Zr_{46}(Cu_{4.5/5.5}Ag_{1/5.5})_{46}Al_8$	0.688	1.655	1.51

Table 3.4(a) Different GFA Criteria for different Ca-based BMGs

System	$T_{rg} = \frac{T_g}{T_l}$	$\gamma_m = \frac{(2T_x - T_g)}{T_l}$	$\gamma = \frac{T_x}{T_g + T_l}$
$Ca_{53}Mg_{23}Cu_{24}$	0.62	0.72	0.41
$Ca_{65}Mg_{15}Cu_{20}$	0.56	0.64	0.38
$Ca_{40}Mg_{25}Cu_{35}$	0.59	0.69	0.40
$Ca_{50}Mg_{22.5}Cu_{27.5}$	0.60	0.73	0.41
$Ca_{55}Mg_{15}Cu_{30}$	0.56	0.67	0.39

Table 3.4(a) Continues…….

System	$\frac{T_x}{T_l}$	$Q=\left(\left(T_g+T_x\right)/T_l\right)\left(\Delta E/\Delta H_m\right)$ Ref. [3.11]
$Ca_{53}Mg_{23}Cu_{24}$	0.67	0.886
$Ca_{65}Mg_{15}Cu_{20}$	0.60	0.683
$Ca_{40}Mg_{25}Cu_{35}$	0.64	0.558
$Ca_{50}Mg_{22.5}Cu_{27.5}$	0.67	0.916
$Ca_{55}Mg_{15}Cu_{30}$	0.62	0.744

Table 3.4(b) *ΔG (T_g)* as an indicator of glass forming ability parameter

System	T_g (K) [16]	T_x (K) [16]	T_m (K) [16]	T_l (K) [16]	ΔH_m [kJ/mol] [16]	$\Delta G\ (T_g)$ [kJ/mol]	$\Delta G(T_g)/\Delta H_m$
$Ca_{53}Mg_{23}Cu_{24}$	406	439	627	655	8.25	1.8	0.218
$Ca_{65}Mg_{15}Cu_{20}$	383	409	630	682	8.27	1.85	0.223
$Ca_{40}Mg_{25}Cu_{35}$	399	436	650	680	8.69	1.94	0.223
$Ca_{50}Mg_{22.5}Cu_{27.5}$	400	442	625	663	8.94	1.96	0.219
$Ca_{55}Mg_{15}Cu_{30}$	397	437	626	706	9.85	2.17	0.220

3.5 Conclusions

In the past, it was difficult to find out that which ΔG expression is best suitable for the BMG. Now, one can know a priori whether the ΔC_p is constant or varying with temperature as explained in the chapter. Therefore, according to the nature of variation of ΔC_p, appropriate ΔG expression could be chosen for theoretical calculations.

For Cu-Zr binary systems no experimental data is available for thermodynamic quantities such as ΔG, ΔS & ΔH. However, plots for ΔG, calculated from Turnbull and Thompson & Speapen expressions are available [3.5]. Therefore, it is worthwhile to calculate ΔG from the present equations, but experimental data of ΔC_p is unavailable. Hence, values of ΔG are calculated for Cu-Zr binary systems, from expressions proposed by Lad et al.-1 [3.13], Lad et al.-2 [3.14] and Dhurandhar et al. [3.15], shown in Fig. 3.1 and Fig. 3.2. All three expressions are based on the assumption that ΔC_p is constant and it works well for the binary systems taken up in the present study. In these plots one can see the closeness of Lad et al.-2 [3.14] and Dhurandhar et al. [3.15] curves. It is due to the fact that in the Lad et al-2 expression the Taylor series expansion has been taken up to second term to approximate logarithmic term, while in the Dhurandhar et al. equation the logarithmic term has not been approximated. Calculations for entropy difference, ΔS and enthalpy difference, ΔH are not done due to the lack of experimental data.

The equations proposed in the present work for ΔG considering linear and hyperbolic variation of specific heat capacity ΔC_p with temperature provides quite accurate

results for Cu-Zr based multicomponent amorphous alloys namely $Zr_{46}Cu_{46}Al_8$ and $Zr_{46}(Cu_{4.5/5.5}Ag_{1/5.5})_{46}Al_8$, in the entire undercooled region. Values of Gibbs free energy difference ΔG, entropy difference ΔS and enthalpy difference ΔH evaluated from linear and hyperbolic variation of ΔC_p lie very close to the experimental data.

The potential substitution of Zr by Al with atomic size intermediate between that of Cu and Zr atoms causes decrease in melting point and increase of atomic packing, consequently, GFA enhances in comparison to that of the binary alloys.

GFA could be increased when Cu is partially replaced by Ag in the $Zr_{46}Cu_{46}Al_8$ alloy. Enhancement of GFA may be attributed to the overall increase of GFA parameters viz. $\delta(=T_K/T_m)$, T_{rg}, γ_m, γ and T_x/T_l, even though individual parameters T_l, T_x, T_g, and T_K may decrease or increase. These GFA indicators increase with Ag addition consistently. Only $\Delta C_p^m/\Delta S_m$, a GFA indicator decreases with Ag addition similar in behavior to that of ΔG. In alloy with reduced melting temperature, the liquid phase is more stabilized with respect to the competing crystalline phases during solidification due to significant increase of viscosity. This allows an increase in the atomic packing density. In fact, the origin of the excellent GFA is attributed to denser local atomic packing and the smaller difference in Gibbs free energy between amorphous and crystalline phases of $Zr_{46}(Cu_{4.5/5.5}Ag_{1/5.5})_{46}Al_8$.

Gibbs Free Energy Difference, ΔG ⟶ The Best GFA Criteria

According to ΔG equations of Lad-2 and Dhurandhar et al, ΔG value for $Cu_{46}Zr_{54}$ BMG is ~3.96 kJ/mol and for $Cu_{54}Zr_{46}$ it is ~3.19 kJ/mol as shown in Fig. 1 and Fig.

2 at their respective Kauzmann temperatures. Now on the addition of aluminum in Cu-Zr binary system, one can get $Zr_{46}Cu_{46}Al_8$ BMG, and its ΔG value decreases drastically to ~1.80 kJ/mol at its Kauzmann temperature which is also known as isentropic temperature. As the value of ΔG decreases, GFA increases. Thus, increase of Al concentration significantly affects the glass forming ability (GFA) of the alloy system. On the addition of small amount of aluminum in the CuZr binary system, $Zr_{46}Cu_{46}Al_8$ BMG has been formulated, which has very low ΔG value and hence high GFA. Fixing the Al content, we then examined the effect of (Cu, Ag) content on the thermodynamic properties and GFA. It is noted that, substitution of even a very small amount of Ag reduces the value of ΔG (~1.51 kJ/mol) at T_K further, which enhances the GFA of $Zr_{46}(Cu_{4.5/5.5}Ag_{1/5.5})_{46}Al_8$ BMG.

Considering different GFA criteria and looking to the Table 3.3, one can see the appreciable change in ΔG values as we go from binary to ternary and ternary to quaternary system. Addition of very small amount of Al and Ag gives almost half (or even less than that) of the ΔG value as compared to that of the binary system. Other GFA parameters do not show significant change in their values as shown by Gibbs free energy difference, ΔG as we go from binary to ternary and quaternary system.

For Ca-based ternary alloy with five different composition, the GFA is evaluated in the entire undercooled region and could see a clear cut trend in increase of GFA with decreasing ΔG values at T_g of the respective alloys. This is quite logical as the lower value of ΔG is a signature of lower driving force for crystallization. Thus, $Ca_{53}Mg_{23}Cu_{24}$ appears to have highest glass forming tendency having lowest ΔG

value of ~1.8 kJ/mol at T_g and $Ca_{55}Mg_{15}Cu_{30}$ having high value (~2.17 kJ/mol) of ΔG at T_g.

Based on the results obtained, one can say that ΔG is an important parameter and its theoretical estimation provides quite a fair idea about the GFA of multi-component alloys. Hence, the Gibbs free energy difference, ΔG which is the driving force for crystallization is the best criterion in order to distinctly estimate the GFA of any amorphous metallic system.

References

[3.1] M. Chen, *NPG Asia Mater.* **3**; 2011: pp. 82.

[3.2] A.L. Greer, *Nature* **366**; 1993: pp. 303.

[3.3] I. Gutzow, D. Kashciev and I. Avramov, *J. Non-Cryst. Solids* **73**; 1985: pp. 477

[3.4] A. Inoue, *Acta Mater.* **48**; 2000: pp. 279

[3.5] L. Ge, X. Hui, E.R. Wang, G.L. Chen, R. Arroyave and Z.K. Liu, *Intermetallics* **16**; 2008: pp. 27.

[3.6] D. Turnbull, *Contem. Phys.* **10**; 1969: pp. 473.

[3.7] A. Inoue, T. Zhang and T. Masumoto, *J. Non-Cryst. Solids* **473**; 1993: pp. 156.

[3.8] O.N. Senkov and J.M. Scott, *Scripta Mater.* **50**; 2004: pp. 449.

[3.9] A. Takeuchi and A. Inoue, *Mater. Sci. Engg. A* **304-306**; 2009: pp. 446.

[3.10] Z.P. Lu and C.T. Liu, *Acta Mater.* **50**; 2002: pp. 3501.

[3.11] Z.Y. Suo, K.Q. Qiu, Q.F. Li, J.H. You, Y.L. Ren and Z.Q. Hu, *Mater. Sci. Engg. A* 528; 2010: pp. 429.

[3.12] G.J. Fan, J.F. Loffler, R.K. Wunderlich and H.J. Fecht, *Acta Mater.* **52**; 2004: pp. 667.

[3.13] K.N. Lad, A. Pratap and K.G. Raval, *J. Mater. Sci. Lett.* **21**; 2002: pp. 1419.

[3.14] K.N. Lad, K.G. Raval and A. Pratap, *J. Non-Cryst. Solids* **334&335**; 2004: pp. 259.

[3.15] H. Dhurandhar, T.L.S. Rao, K.N. Lad and A. Pratap, *Phil. Mag. Lett.* **88**; 2008: pp. 239.

[3.16] C.V. Thompson and F. Spaepen, *Acta Metall.* **27**; 1979: pp. 1855.

[3.17] Q.K. Jiang, X.D. Wang, X.P. Nie, G.Q. Zhang, H. Ma, H.J. Fecht, J. Bendnarcik, H. Franz, Y.G. Liu, Q.P. Cao and J.Z. Jiang, *Acta Mater.* **56**; 2008: pp. 1785.

[3.18] H.B. Singh and A. Holz, *Solid State Commun.* **45**; 1983: pp. 985.

[3.19] K.S. Dubey and P. Ramchandrarao, *Acta Metall.* **32**; 1984: pp. 91.

[3.20] R.K. Mishra and K.S. Dubey, *J. Non-Cryst. Solids* **355**; 2009: pp. 2199.

[3.21] S. Guo, Z.P. Lu and C.T. Liu, *Intermetallics* **18**; 2010: pp. 883.

[3.22] J. Xiu-lin and P. Ye, *Trans. Nonferrous Metals Soc. China* **19**; 2009: pp.1271.

[3.23] D.V. Louzguine-Luzgin, G. Xie, W. Zhang and A. Inoue, *Mater. Sci. Engg. A* **465**; 2007: pp. 146.

CHAPTER – 4

CRYSTALLIZATION KINETICS OF METALLIC GLASSES

The study of thermally-activated phase transformation is of great significance in the field of materials science. The kinetics of crystallization process of amorphous materials can be studied with the help of different thermo-analytical techniques. The metallic glasses, which are kinetically metastable, can be transformed into crystalline state by both isothermal and non-isothermal methods. The study of this phase transformation and hence the thermal stability of metallic glasses is important from application view point. In the present chapter, crystallization kinetics of two metallic glasses namely, $Co_{66}Si_{12}B_{16}Fe_4Mo_2$ and $Zr_{52}Cu_{18}Ni_{14}Al_{10}Ti_6$ is studied under non-isothermal conditions using DSC. The Activation energy (E), Avrami exponent (n) and Pre exponential factor (k_0) are evaluated using different isokinetic as well as isoconversional approaches, and relative importance of these two methods is discussed.

4.1 Introduction

The study of the thermally-activated phase transformations is of great significance in the field of materials science as the properties of materials change due to the change in the composition and/or microstructure. The properties of fully or partly crystalline materials are usually different from their amorphous counterparts. From the view point of a materials scientist, the crystallization of amorphous or non-crystalline materials involves the nucleation and growth processes. The processes driven by nucleation and growth have attracted a lot of interest for tailoring technological applications. For example, the re-crystallization of the deformed metals, controlling the nucleation and growth of islands on terraces in order to get large scale arrays of nanostructures in the manufacturing of thin-film transistors [4.1]. Thus, the knowledge of the kinetics of crystallization would help to attain products with the required crystallized fraction and microstructure (e.g. nanocrystalline or quasicrystalline) or to avoid the degradation of materials at high processing (& operating) temperatures.

The kinetics of the crystallization process can be studied with the help of thermo-analytical techniques namely, differential scanning calorimetry (DSC) and differential thermal analyzer (DTA). The DSC/DTA experiments can be carried out in isothermal as well as non-isothermal (linear heating) conditions [4.2-4.6]. Efforts made by the researchers in this field so far, to analyze the data obtained from DSC and hence to determine the kinetic parameters of the crystallization processes (say, activation energy, rate constant etc.), raise two important issues: (i) the selection of the mode of

experiment (isothermal or non-isothermal) and, (ii) the choice of a sound method for the analysis of the experimental data. However, we are more concerned with the later issue due to the fact that several methods for the kinetic analysis are available in the literature. These methods are generally based on either the isokinetic hypothesis or the isoconversional principle and they can be accordingly categorized as: (1) isokinetic methods where the transformation mechanism is assumed to be the same throughout the temperature/time range of interest and, the kinetic parameters are assumed to be constant with respect to time and temperature; (2) isoconversional methods, which are generally used for non-isothermal analysis, assume that the reaction (transformation) rate at a constant extent of conversion (degree of transformation) is only a function of temperature [4.7, 4.8]. The kinetic parameters, in this case, are considered to be dependent on the degree of transformation at different temperature and time. The use of isoconversional methods is widespread in the physical chemistry for the determination of the kinetics of the thermally activated solid-state reactions. The physicochemical changes during an exothermic or endothermic event in DSC (or DTA) are complex and involve multi-step (serial or parallel) processes occurring simultaneously at different rates. Therefore, the activation energies for such processes can logically not be same and it may vary with the degree of conversion. This is contrary to the isokinetic view assuming all the constituents of the material to react simultaneously at the same rate. The activation energy, in the isokinetic case, is thus constant and independent of the degree of conversion. A strong difference of opinion persists among the researchers in the field of thermal analysis about the concept of variable activation energy [4.9, 4.10]. In the

metallurgical branch of materials science, most of the thermal phase transformations (like crystallization, recovery) are morphological and are considered to be governed by the nucleation and growth processes. The transformation mechanisms in these processes are also complex e.g. interface-controlled, diffusion-controlled growth. Notwithstanding this, the kinetic analysis of the transformation process like crystallization is done according to isokinetic hypothesis. The isoconversional methods are scarcely used for the study of the crystallization kinetics of metallic glasses.

In order to understand the relative importance of the two types of methods, a case study of the crystallization kinetics of $Co_{66}Si_{12}B_{16}Fe_4Mo_2$ and $Zr_{52}Cu_{18}Ni_{14}Al_{10}Ti_6$ metallic glasses is taken up in the present work.

4.2 Theory of Phase Transformation

To study the phase transformation, which involves nucleation and growth, many methods are developed. Most of the methods depend on the transformation rate equation given by Kolmogorov, Johnson, Mehl and Avrami [4.11-4.15], popularly known as KJMA equation, basically derived from experiments carried out under isothermal conditions. The KJMA rate equation is given by

$$\frac{d\alpha}{dt} = nk(1-\alpha)[-\ln(1-\alpha)]^{(n-1)/n} \tag{4.1}$$

where, α → degree of transformation at a given time t,

n → Avrami (growth) exponent

k → the rate constant

The Arrhenius form of the rate constant is given by

$$k(T) = k_0 \exp\left(-\frac{E}{RT}\right) \tag{4.2}$$

where, k_0 → pre-exponential factor

E → activation energy, and

R → universal gas constant

KJMA rate equation is based on some important assumptions and it has been suggested that the KJMA kinetic equation is accurate for reactions with linear growth subject to several conditions [4.16].

The isoconversional methods are also known as model-free methods. Therefore, the kinetic analysis using these methods is more deterministic and gives reliable values of activation energy E, which depends on degree of transformation, α. However, only activation energy will not give a complete picture of crystallization kinetics. The microstructural information (e.g. dimensionality of the growth) of the precipitating phase during the transformation is also very important for understanding the whole kinetics of crystallization. Microstructural information would be known to us when we take the isokinetic methods into account. Therefore, the complementary use of both the methods is more useful for understanding the kinetics of crystallization.

Differential Scanning Calorimetry (DSC) has become a convenient and widely used tool for studying the kinetics of phase transformations. The volume fraction (x) of the sample transformed in crystalline phase during the crystallization event has been

obtained from the DSC curve as a function of temperature (T). The volume fraction of precipitated crystal can be obtained from the DSC curve by using

$$x = S / S_0$$

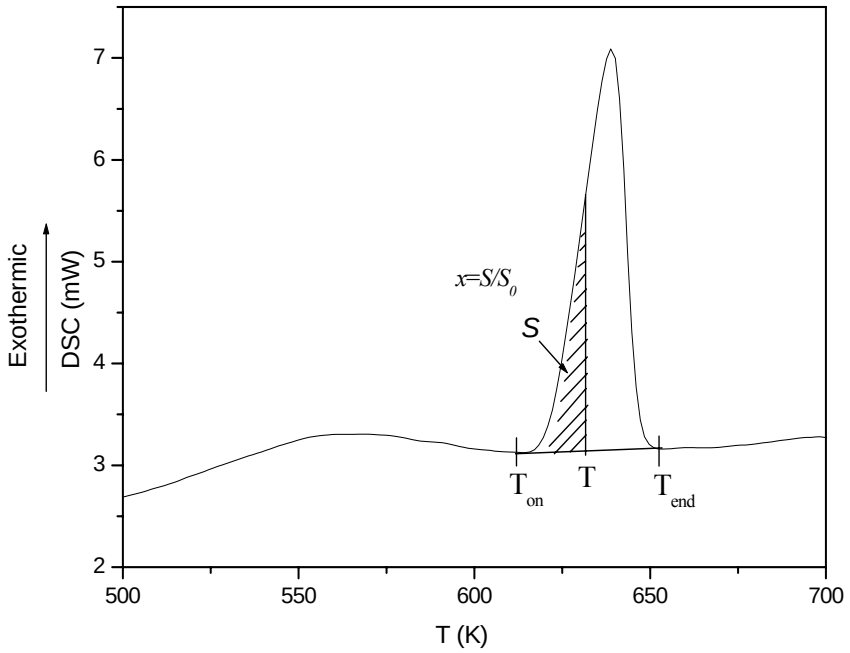

Where S_0 is the total area under the crystallization curve i.e. the area under the curve between the temperature at the onset of crystallization T_{on} and the end-set temperature T_{end} when the crystallization is completed. S is the area at any temperature T between T_{on} and T_{end} at which the fractional crystallization is required to be known.

There are three important modes of crystallization involving nucleation and growth processes, depending on the composition of a particular alloy: primary crystallization, polymorphous crystallization and eutectic crystallization [4.17]. In primary crystallization the primary phase of the alloy constituents crystallizes first. The

dispersed primary crystallized phase coexists with the amorphous matrix and may serve as the nucleation site for secondary or tertiary crystallization. In Fe-based alloys α-Fe crystallizes first, which is a kind of primary crystallization. Polymorphous crystallization is a transition of the amorphous phase to a crystalline one without any change in the composition of that phase. There is no concentration difference across the reaction front because the concentration does not change. Eutectic crystallization is simultaneous crystallization of two crystalline phases by a discontinuous reaction. This reaction takes longer than polymorphous crystallization to proceed because the two components have to separate by diffusion into two separate phases within the crystallized region [4.18].

4.3 Experimental Study using DSC Technique

The crystallization kinetics can be studied with the help of thermo-analytical techniques e.g. differential scanning calorimetry (DSC) and differential thermal analyzer (DTA). These DSC/DTA experiments can be carried out in isothermal as well as non-isothermal environment. The Differential Scanning Calorimetry (DSC) is very much important experimental method to obtain the kinetic behavior of metallic glasses in the field of thermal analysis [4.19-4.21]. The Differential Scanning Calorimeter is used in the present work for collecting the required data for kinetic analysis. The heat flux type of DSC (DSC-50, Shimadzu, Japan) is utilized. The DSC scans were recorded by a thermal analyzer (TA-50 WSI, Shimadzu, Japan) interfaced to a computer. The detection sensitivity of the instrument is ~10 μW. The phase

transformations and other essential physical quantities were obtained from the thermograms with the help of software, provided with the equipment. In DSC-50, the exothermic events are displayed by the upside shift of the baseline.

The metallic glass samples of $Co_{66}Si_{12}B_{16}Fe_4Mo_2$ (VITROVAC 6025) were in the form of sheet. The samples were prepared by melt spinning technique. The as-quenched samples were cut into small pieces and crimped in aluminum pans and heated in DSC for different heating rates of 4, 6, 8 and 10^oC/min.

Specimens of amorphous $Zr_{52}Cu_{18}Ni_{14}Al_{10}Ti_6$ alloy were prepared by a melt spinning technique. The samples of the metallic glass (5-6 mg) under consideration and the reference material α-Al_2O_3 were crimped in aluminum pans and loaded in the DSC cell. The linear heating experiments were carried out on the as-quenched samples at four different linear heating rates (5, 10, 15 and 20^oC/min.) in DSC from room temperature to 823 K in air.

4.4 Different Methods of Analysis to Study Kinetics of Crystallization

A multitude of methods for the kinetic analysis are available in the literature to determine the kinetic parameters of the crystallization processes. These methods are generally based on either the isokinetic hypothesis or the isoconversional principle and they can be accordingly categorized as:

(1) Isokinetic methods

(2) Isoconversional methods

4.4.1 Isoconversional Analysis

The isoconversional methods require the knowledge of temperatures $T_\alpha(\beta)$ at which an equivalent stage of reaction occurs for various heating rates. The equivalent stage is defined as the stage at which a fixed amount is transformed or at which a fixed fraction, α of the total amount is transformed [4.22]. These methods are broadly classified as linear and non-linear isoconversional methods. The linear methods can be further classified into integral and differential methods. The linear integral isoconversional methods [4.23-4.29] depend on the approximation of the temperature integral and require the data on $T_\alpha(\beta)$. The differential isoconversional methods depend on the rate of transformation at $T_\alpha(\beta)$ and the data on $T_\alpha(\beta)$ [4.30-4.32]. Vyazovkin [4.33] introduced a non-linear isoconversional method to increase the accuracy of evaluating the activation energy. The isoconversional methods are based on the basic kinetic equation [4.34]

$$\frac{d\alpha}{dT} = \frac{1}{\beta}k(T)f(\alpha) = \frac{A}{\beta}\exp\left(-\frac{E}{RT}\right)f(\alpha) \tag{4.3}$$

where $k(T)$ is the rate constant, β is the heating rate, α is the conversion fraction and $f(\alpha)$ is the reaction model which in case of KJMA formalism gives the Eq. (4.1). Eq. (4.3) can also be expressed in the integral form as

$$g(\alpha) = \int_0^\alpha [f(\alpha)]^{-1} d\alpha = \frac{A}{\beta}\int_0^T \exp\left(-\frac{E}{RT}\right)dT \tag{4.4}$$

As mentioned earlier, exact solution of the temperature integral is not available and various approximations made for this has resulted into different methods. We have

selected a few most commonly used methods. The accuracy of various isoconversional methods and, the experimental and analytical errors associated with these methods are discussed in detail by Starink [4.35]. Roura and Farjas [4.36] have proposed an analytical solution for the Kissinger equation. Rotaru and Gosa [4.37] describe their recently developed software that implements a number of known techniques such as various isoconversional methods, a method of invariant kinetic parameters, master plots methods, etc. Cai and Chen [4.38] have proposed a new numerical routine for a linear integral isoconversional method that allows one to obtain accurate values of the activation energy in the cases when the latter varies strongly with the extent of conversion. Criado et al. [4.39] provide a critical overview of isoconversional methods, putting the focus on establishing whether the observed variations in the activation energy are real or apparent [4.40].

4.4.1.1 Linear Integral Isoconversional Methods

[a] *Ozawa-Flynn-Wall (OFW) method*

In this method [4.24-4.27] the temperature integral in Eq. (4.4) is simplified by using the Doyle's approximation [4.41-4.43] and hence we obtain the following equation:

$$\ln \beta = -1.0516 \frac{E(\alpha)}{RT_{\alpha}} + const \qquad (4.5)$$

The factor 1.0516 is a correction factor. The plot of $ln\beta$ vs $1000/T_{\alpha}$ gives the slope $-1.0516\,E(\alpha)/R$ from which the activation energy has been evaluated. At $T_{\alpha} = T_p$ (peak temperature), above equation reduces to Ozawa method and the value of E is also determined.

[b] *Kissinger-Akahira-Sunose (KAS) method*

Kissinger, Akahira and Sunose used the approximation given by Coats & Redfern [4.44] to evaluate the integral in the rate Eq. (4.4). KAS method is based on the expression

$$\ln\left(\frac{\beta}{T^2}\right) = \ln\left(\frac{AR}{Eg(\alpha)}\right) - \frac{E}{RT} \tag{4.6}$$

The activation energy can be evaluated from the slope of plot $ln(\beta/T^2)$ vs $1000/T$ for constant conversion, α. The discussion given ahead describes some of the methods available in the literature which are basically special cases of the KAS Eq. (4.6).

i) Kissinger method: This well-known method assumes that the reaction rate is maximum at the peak temperature (T_p). This assumption also implies a constant degree of conversion (α) at T_p. The equation used by Kissinger is

$$\ln\left(\frac{\beta}{T_p^2}\right) = -\frac{E}{RT_p} + \ln\left(\frac{AR}{E}\right) \tag{4.7}$$

A plot of $ln(\beta/T_p^2)$ vs $1000/T_p$ gives an approximate straight line and the activation energy E can be calculated using the slope.

ii) Augis & Bennett's method: This method was suggested by Augis and Bennett [4.25] and is an extension of Kissinger method showing its applicability to heterogeneous reaction described by Avrami expression. Apart from the peak crystallization temperature it also incorporates the onset temperature of crystallization,

T_o and it is supposed to be a very accurate method of determining E through the equation

$$\ln\left(\frac{\beta}{\left(T_p - T_o\right)}\right) = -\frac{E}{RT_p} + \ln A \tag{4.8}$$

where T_p and T_o are the peak and the onset temperatures of crystallization respectively. The values of E is obtained from the plot $(ln(\beta/(T_p-T_o))$ vs $1000/T_p$.

Further,

$$n = 2.5\frac{T_p^2}{\Delta T\left(\frac{E}{R}\right)} \tag{4.9}$$

where ΔT is the full width at half maximum of the DSC curve. n can be derived using Eq. (4.9).

iii) Boswell method: Boswell [4.26] has found a limitation in the Augis & Bennett method that if $\frac{T_p - T_o}{T_p} \approx 1$,

then Augis & Bennett gives crude results. Boswell method determines the activation energy at peak temperature using the following equation

$$\ln\left(\frac{\beta}{T_p}\right) = -\frac{E}{RT_p} + const \tag{4.10}$$

4.4.1.2 Linear Differential Isoconversional Method

[a] *Friedman method*

The method suggested by Friedman [4.31] sometimes known as transformation rate-isoconversional method, utilizes the differential of the transformed fraction and hence it is called differential isoconversional method. Substituting value of *k(T)* in Eq. (4.3) and taking logarithm, Friedman derived a linear differential isoconversional expression as

$$\ln\left(\frac{d\alpha}{dt}\right)_{\alpha} = \ln\beta\left(\frac{d\alpha}{dT}\right)_{\alpha} = \ln\left(A\,f(\alpha)\right) - \frac{E_{\alpha}}{RT_{\alpha}} \tag{4.11}$$

by taking logarithm on both sides of Eq.(4.3). For a constant α, the plot of $\ln\left(\beta\frac{d\alpha}{dT}\right) vs \left(\frac{1}{T}\right)$ should be a straight line whose slope gives us the value of *E*.

Since this method does not take any mathematical approximation for the temperature integral, it is considered to give accurate estimate of *E*. Thus the method does not require any assumption on *f(α)*, i.e. it is a so-called model-free method. However, being a differential method, its accuracy is limited by the signal noise [4.45].

[b] *Gao and Wang method*

A method suggested by Gao and Wang [4.32] is a special case of the Friedman method. This method uses the following expression to determine the activation energy.

$$\ln\left(\beta\frac{d\alpha}{dT_p}\right) = -\frac{E}{RT_p} + const \tag{4.12}$$

$$K_p = \frac{\beta E}{RT_p^2} \tag{4.13}$$

where,

$$K_p = A\exp\left(\frac{-E}{RT_p}\right) and \left(\frac{d\alpha}{dt}\right)_p = 0.37nK_p$$

4.4.2 Isokinetic Methods

The isokinetic methods of kinetic analysis depend on the reaction model and hence are also called as model fitting methods. These methods rely on the isokinetic hypotheses to separate the kinetics of the transformation from its dependence on temperature. Different isokinetic methods are described below;

[a] *Matusita and Sakka method*

Matusita and Sakkka [4.46] suggested the following equation specifically for the non-isothermal data

$$\ln[-\ln(1-\alpha)] = -n\ln\beta - \frac{mE}{RT} + Const \tag{4.14}$$

where *m* is an integer which depends on the dimensionality of the crystal and the Avarami exponent *n* depends on the nucleation process. For a constant temperature, the plot of ln[-ln(1-α)] versus lnβ gives a straight line and the slope gives the value of

n. The plot of ln[-ln(1-α)] versus 1/T at constant heating rate should be a straight line and the value of mE is obtained from the slope.

[b] *Modified Kissinger method*

The modified Kissinger equation [4.47] given below can be utilized to derive the activation energy (*E*).

$$\ln\left(\frac{\beta^n}{T_p^2}\right) = -\frac{mE}{RT_p} + Const \tag{4.15}$$

Where *E* is the activation energy for crystallization, T_p is the peak temperature, *R* is the universal gas constant and *m* is known as the dimensionality of growth. In order to derive *E* from this equation, one must know the value of *n*. The *n* value can be obtained from the slope of the plot of ln[-ln(1-α)] Vs. lnβ at constant temperature. In order to evaluate *E*, the values of *n* are substituted in Eq. (4.15). Then plots of $\ln\left(\frac{\beta^n}{T_p^2}\right)$ Vs. $\frac{1}{T_p}$ give the values of activation energy *E*.

4.5 Results & Discussions

4.5.1 Crystallization Kinetics of $Co_{66}Si_{12}B_{16}Fe_4Mo_2$ Metallic Glass

Magnetic amorphous alloys have excellent soft magnetic properties such as low coercivity and low hysteresis loss and high permeability and high saturation magnetization. Hence, they are widely used in antitheft security system, magnetic recording heads, magnetic sensors, large transformers and electronic devices [4.48-

4.51]. The Co-based metallic glasses exhibit a very attractive combination of soft magnetic properties [4.52]. The nano-crystalline state has also been obtained from Co-based amorphous precursors [4.53, 4.54]. From recent reports, it is clear that Co-based metallic glass is suitable for its use in magnetic sensors [4.55].

The DSC thermograms at four different heating rates are shown in Fig. 4.1. The thermograms show three-stage crystallization. The first crystallization peak is evaluated for heating rates 4, 6, 8 and 10 K/min. Glass transition becomes clear as we go for the higher heating rates, but the third crystallization peak becomes less prominent as we go to the higher heating rates. The onset and endset of first crystallization exotherms exhibit different levels of heat flow i.e. the crystallization ends at slightly higher level followed by the second and third crystallization peak. This difference of the level indicates that the phases at the start of crystallization and at the end of it are not same. The analysis of DSC data to evaluate the kinetic parameters can be obtained from non-isothermal rate laws by both isokinetic, also known as model fitting methods, and isoconversional methods.

Fig. 4.2 shows the graphical representation of the volume fraction transformed (α) as a function of temperature (T) for different heating rates. The sigmoid plot exhibits the bulk crystallization and excludes the chance of surface crystallization. During the stage “a” nucleation occurs at various points in the bulk of the sample. The stage “b” shows the growth of nuclei with increased rate of reaction as the surface area of nucleation increases. The slowing down stage “c” shows the decrease in surface area as a result of nuclei coalescing.

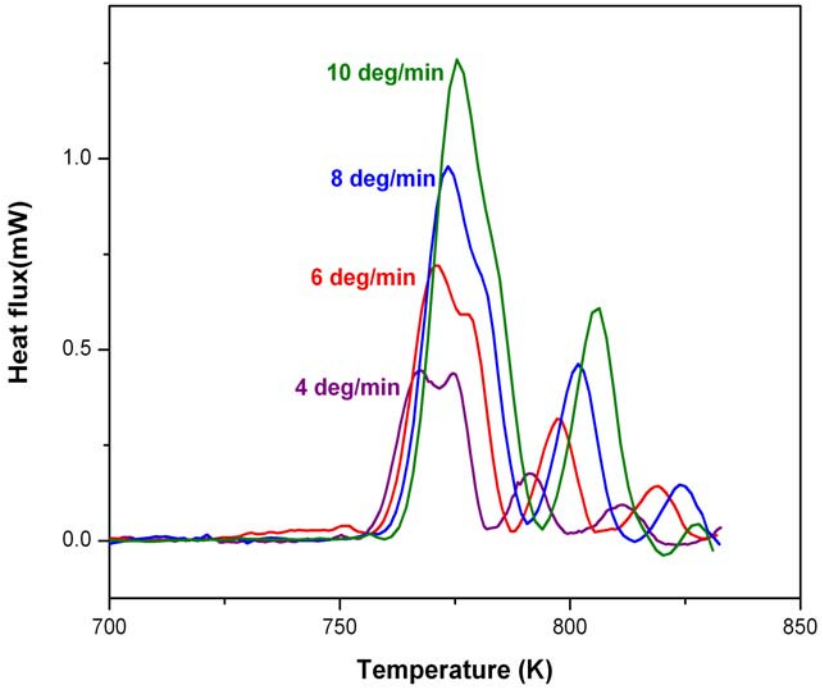

Fig. 4.1: DSC thermograms of the metallic glass $Co_{66}Si_{12}B_{16}Fe_4Mo_2$ at different heating rates

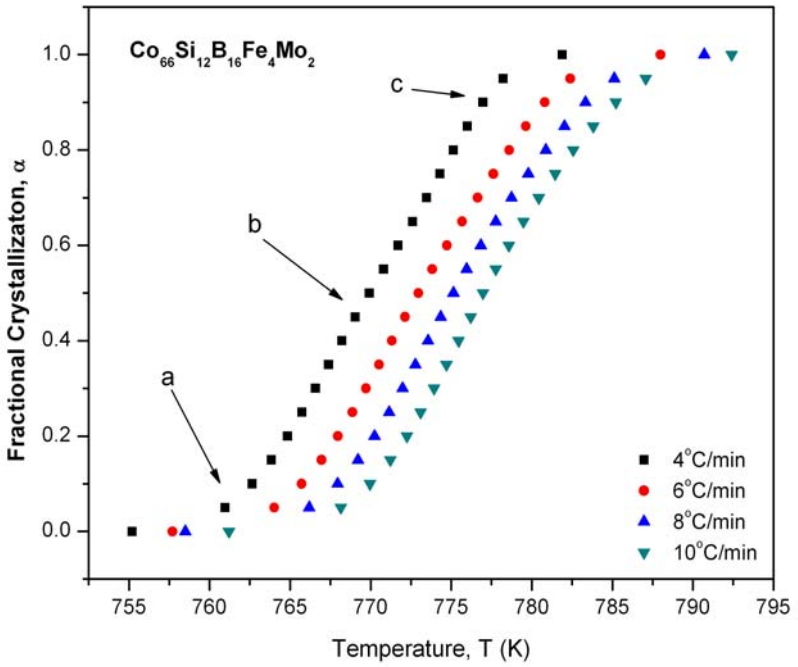

Fig. 4.2: Fractional crystallization as a function of temperature at various heating rates for $Co_{66}Si_{12}B_{16}Fe_4Mo_2$ metallic glass

4.5.1.1 Linear Integral Isoconversional Methods

Using the linear integral isoconversional methods given by OFW and KAS the activation energy at different extent of conversion (fractional crystallization) have been evaluated (Table 4.3). Figures 4.3 & 4.4 show the plots for OFW [Eq. (4.5)] and KAS [Eq. (4.6)] methods for a = 0.2, 0.4, 0.6 and 0.8. The E values obtained from both the methods decreases initially then increases and becomes maximum at 0.6 and afterwards again decreases.

The Kissinger method assumes that the reaction rate is maximum at the peak temperature (T_p) (Table 4.1). This assumption implies a constant degree of conversion (α_p) at T_p. This method is grouped as a special case of KAS isoconversional method. Referring to Eq. (4.7) a plot of $ln(\beta/T_p^2)$ Vs. $1000/T_p$ (Fig. 4.5) gives an approximate straight line with the slope (E/R) and the intercept $ln(AR/E)$. A single value of E is obtained at $T = T_p$ from the Ozawa plot [Eq. (4.5)] of $ln\beta$ Vs. $1000/T_p$ as in Fig. 4.6. The so obtained activation energy from both Kissinger and Ozawa methods are 553kJ/mol and 546 kJ/mol respectively (Table 4.2).

Table 4.1 Peak temperature, T_p and onset temperature, T_o for four different heating rates for $Co_{66}Si_{12}B_{16}Fe_4Mo_2$

Heating rates β (°C/min)	***T_p (K)***	***T_o (K)***
4	767.4	755.2
6	770.6	757.7
8	773.5	758.5
10	775.4	761.2

Using Eq. (4.10) for Boswell method, from the slope of the graph $\ln(\beta/T_p)$ *Vs.* $1000/T_p$ (Fig. 4.7) the value of *E* is determined as 443 kJ/mol. The Augis and Bennett method [Eq.(4.8)] uses the peak crystallization temperature and onset crystallization temperature (Table 4.1) to evaluate *E* and *A*. The plot of $\ln(\beta/T_p - T_o)$ Vs. $1000/T_p$ (Fig. 4.8) gives the values of *E* as 532 kJ/mol.

Table 4.2 Activation energy (E) derived using various methods for $Co_{66}Si_{12}B_{16}Fe_4Mo_2$

Methods	***Activation Energy E (kJ/mol)***
Kissinger	553 ± 2
Ozawa	546 ± 2
Augis & Bennett	532 ± 2
Boswell	443 ± 7

Table 4.3 Local Activation energy (E) at different conversion for different methods

α	**E (kJ/mol)**		
	KAS	**OFW**	**Friedman**
0.1	602 ± 2	584 ± 2	555 ± 1
0.2	597 ± 1	580 ± 1	626 ± 1
0.3	603 ± 1	586 ± 2	648 ± 1
0.4	615 ± 1	597 ± 1	687 ± 1
0.5	635 ± 1	616 ± 1	725 ± 1
0.6	654 ± 1	634 ± 1	702 ± 3
0.7	648 ± 1	629 ± 1	522 ± 5
0.8	606 ± 1	589 ± 1	398 ± 5
0.9	549 ± 1	534 ± 1	318 ± 2

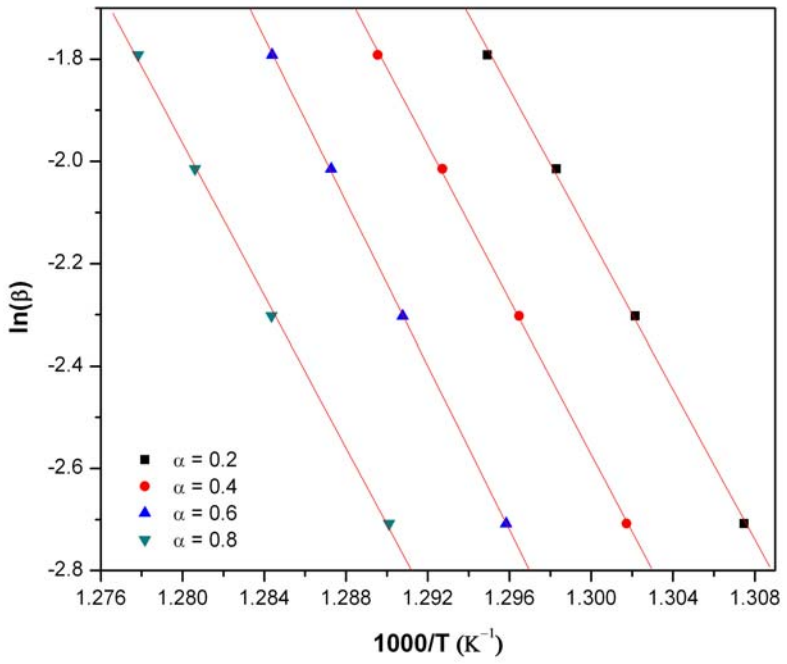

Fig. 4.3: OFW plots for $Co_{66}Si_{12}B_{16}Fe_4Mo_2$

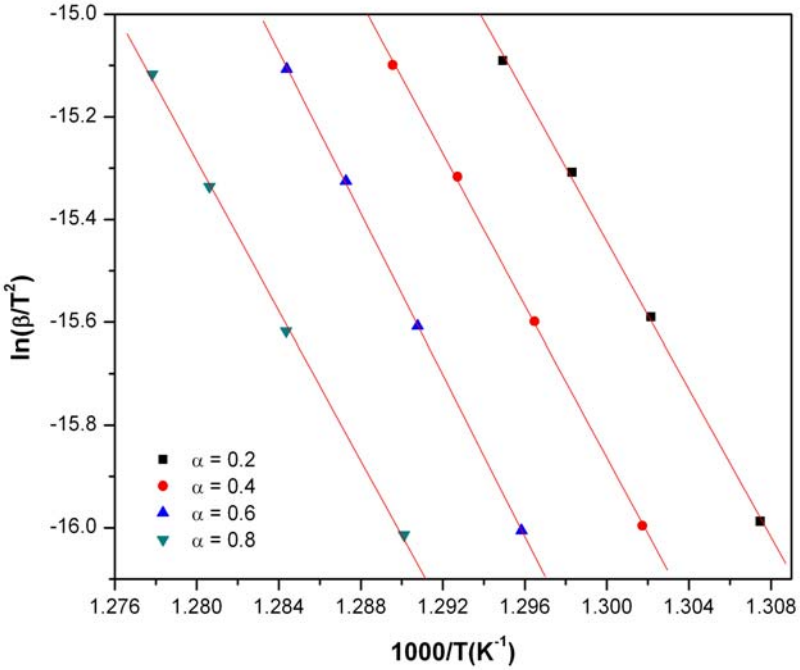

Fig. 4.4: KAS plots for $Co_{66}Si_{12}B_{16}Fe_4Mo_2$

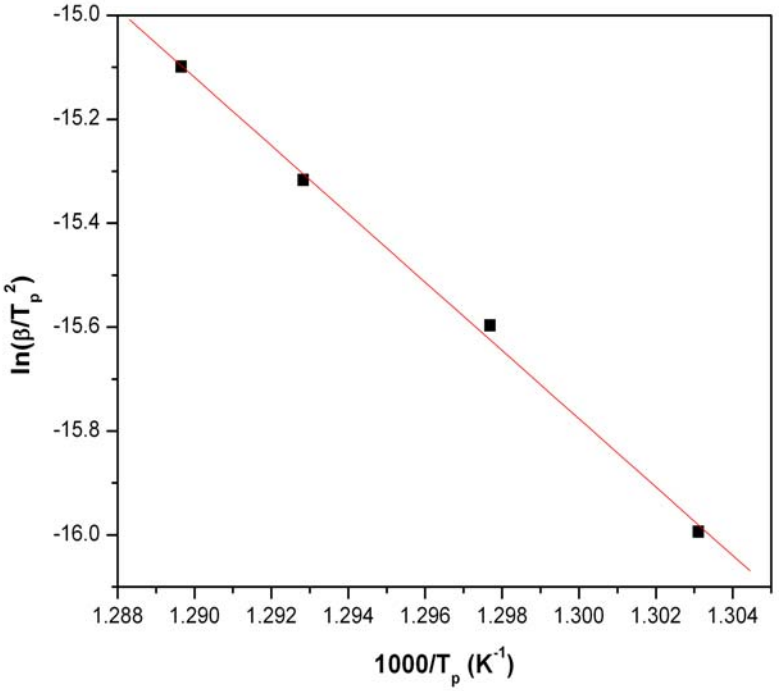

Fig. 4.5: Kissinger plot for $Co_{66}Si_{12}B_{16}Fe_4Mo_2$

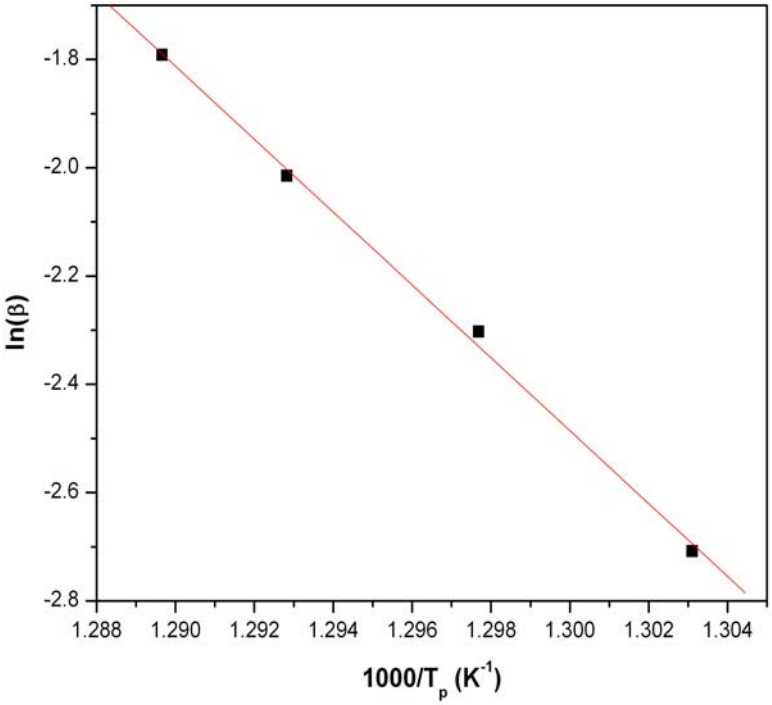

Fig. 4.6: Ozawa plot for $Co_{66}Si_{12}B_{16}Fe_4Mo_2$

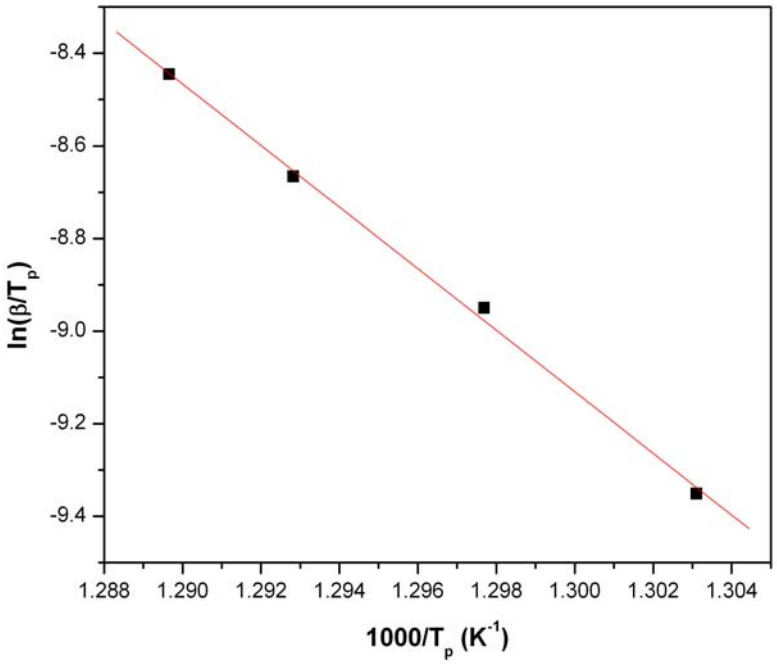

Fig. 4.7: Boswell plot for $Co_{66}Si_{12}B_{16}Fe_4Mo_2$

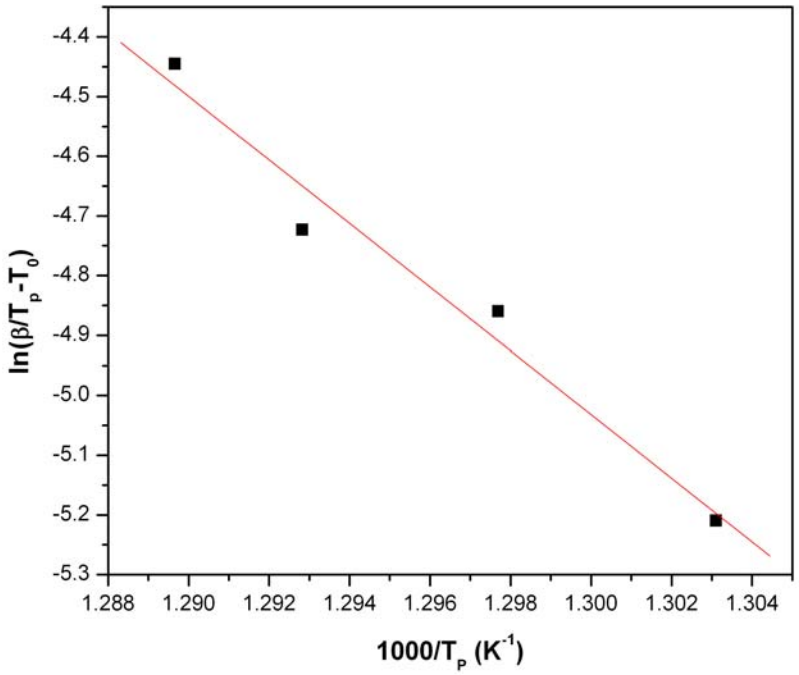

Fig. 4.8: Augis & Bennett plot for $Co_{66}Si_{12}B_{16}Fe_4Mo_2$

4.5.1.2 Linear Differential Isoconversional Method

From Friedman's Eq. (4.11), the plot of $\ln\left(\beta\frac{d\alpha}{dT}\right)$ Vs. *1000/T* gives various *E* values at different α (Fig. 4.10-(a) & (b)). These values are shown in Table 4.3. From the table it is evident that the *E* values increase in the interval 0.1 - 0.5 and then decreases from 0.6. The decrement in *E* is drastic from 0.6 - 0.9.

The enumerated vales of *E* of all the isoconversional methods is graphically represented in Fig. 4.9.

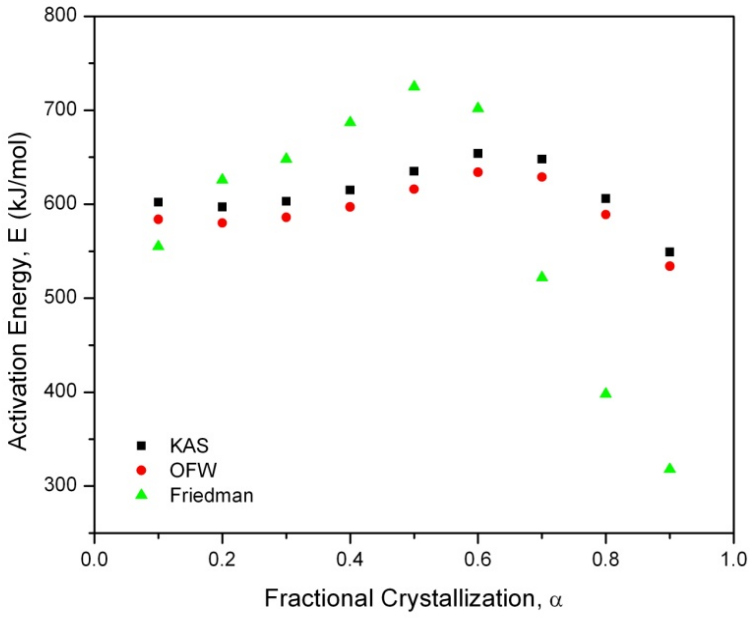

Fig. 4.9: Dependence of E on α from different methods for $Co_{66}Si_{12}B_{16}Fe_4Mo_2$

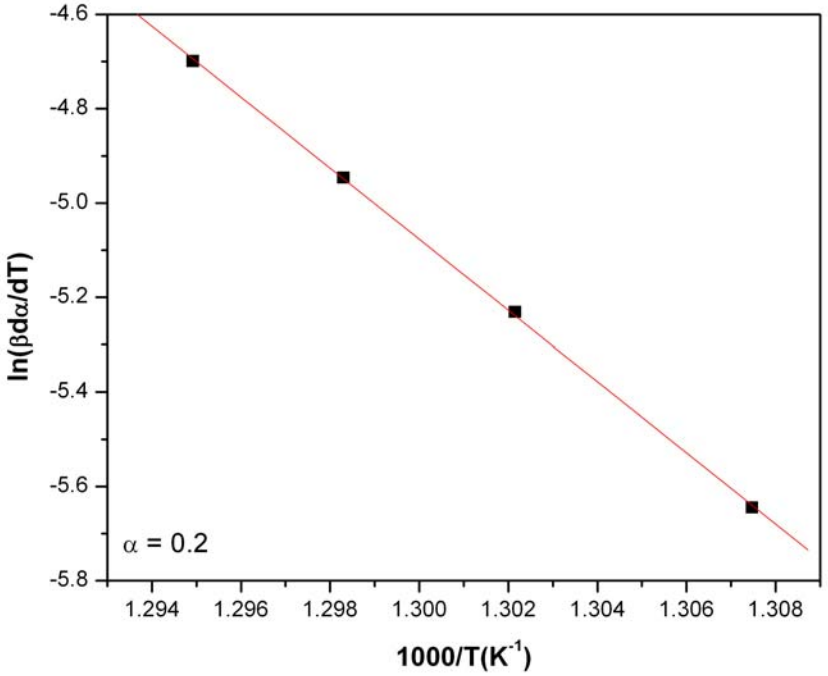

Fig. 4.10-(a): Friedman plot for $Co_{66}Si_{12}B_{16}Fe_4Mo_2$, for α = 0.2

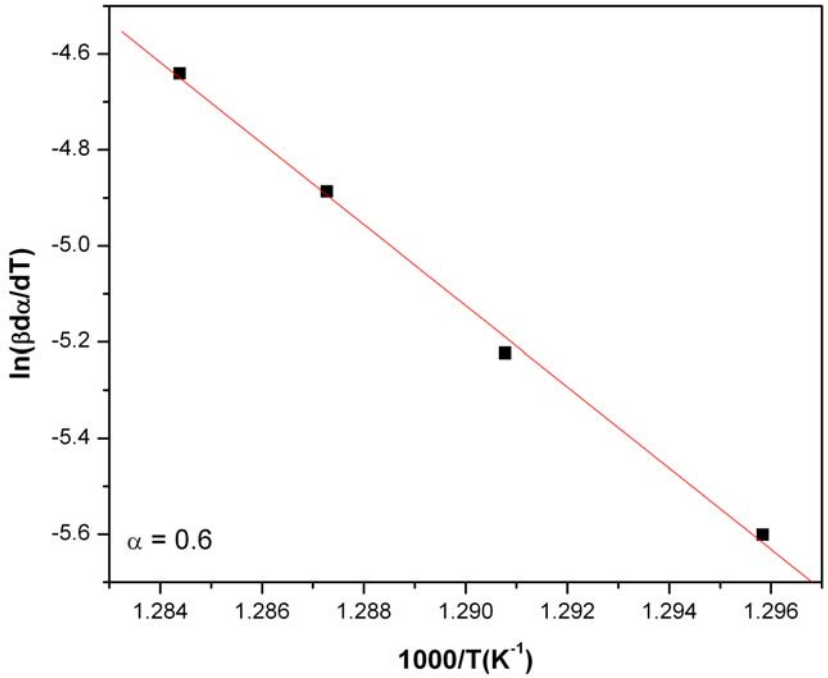

Fig. 4.10-(b): Friedman plot for $Co_{66}Si_{12}B_{16}Fe_4Mo_2$, for α = 0.4

4.5.1.3 Isokinetic Methods

For a constant temperature, the plot of *ln[-ln(1-α)]* versus *lnβ* gives a straight line (Fig.4.11-(a)) and the slope gives the value of *n*, which come out to be $n = 1.33$ and $n = 1.36$ for temperatures $T = 775$ K and $T = 778$ K respectively. The plot of *ln[-ln(1-α)]* versus *1/T* at constant heating rate gives straight line and the value of *mE* is obtained from the slope (Fig.4.11-(b)).

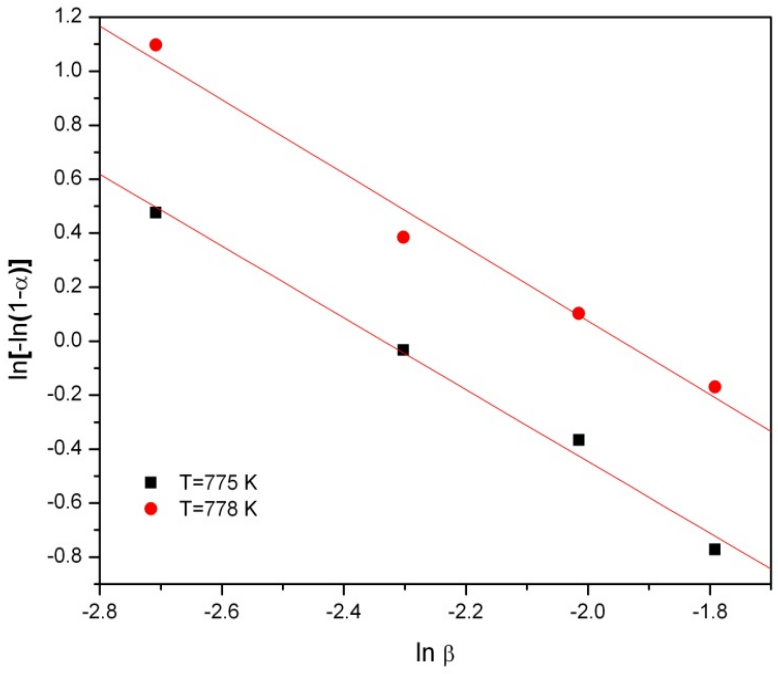

Fig. 4.11-(a): Matusita & Sakka plot of ln[-ln(1- α)] Vs. lnβ for T = 775 K & T = 778 K.

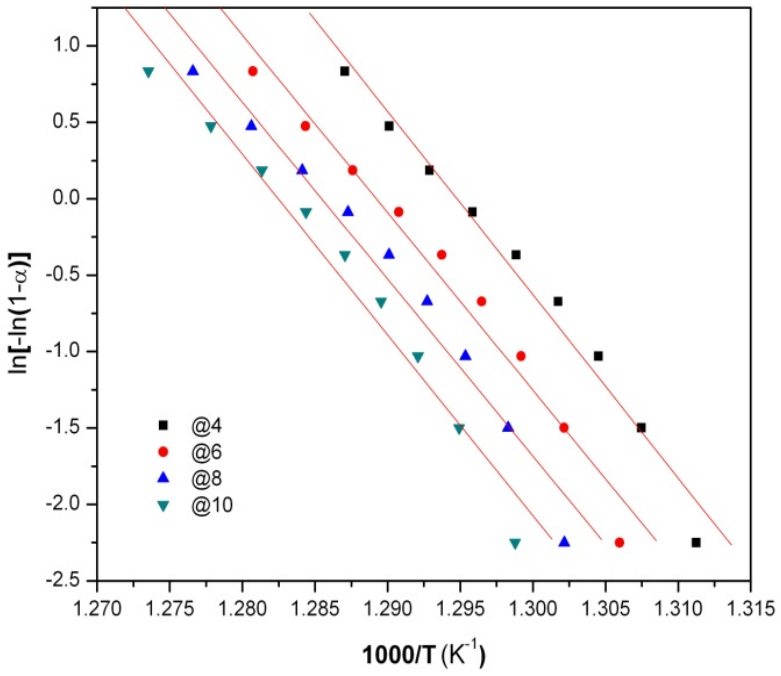

Fig. 4.11-(b): Matusita & Sakka plot of ln[-ln(1- α)] Vs. lnβ for different heating rates

The modified Kissinger equation Eq. (4.16) is utilized to derive the activation energy at peak temperature. In this equation, *m* is known as the dimensionality of growth and here $m = n$. In order to derive *E* from this equation, one must know the value of *n*. The *n* value can be obtained from the slope of the plot of $ln[-ln(1-\alpha)]$ Vs. $ln\beta$ at constant temperature. In order to evaluate *E*, the values of *n* are substituted in Eq. (4.16). Then plots of $\ln\left(\frac{\beta^n}{T_p^2}\right)$ Vs. $\frac{1}{T_p}$ (Fig. 4.12) gives the values of activation energy *E*, and the average *E* obtained is 549.80 kJ/mol.

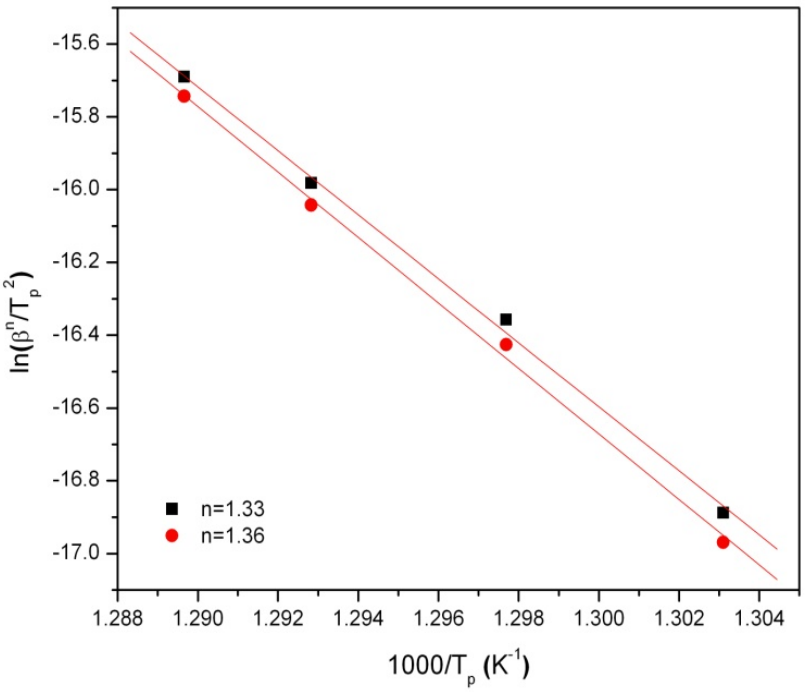

Fig. 4.12: Modified Kissinger plot for n = 1.33 and n = 1.36

A general trend of decrease in the values of n with increasing heating rate can be observed. Such trend has been also seen by Matusita and Sakka (Matusita & Sakka, 1979) and in other Fe-based (Raval et al., 2005) metallic glasses.

Table 4.4 Values of Avrami exponent (n)

Heating rate	*Matusita & Sakka*
4	*1.81*
6	*1.76*
8	*1.75*
10	*1.79*

4.5.2 Crystallization Kinetics of $Zr_{52}Cu_{18}Ni_{14}Al_{10}Ti_6$ Metallic Glass

In the present work, the kinetics of the crystallization of $Zr_{52}Cu_{18}Ni_{14}Al_{10}Ti_6$ glass forming alloy have been studied, which is among the best nonberyllium containing glasses, making them easier to process and to handle [4.56].

The DSC thermograms at four different heating rates (5, 10, 15, 20 deg/min) are shown in Fig. 4.13. The thermograms show three-stage crystallization process. The peak height of these steps varies with the heating rate. At lower heating rates, first peak is much distinct and diminishes as we go for higher heating rates and last peak visibility increases with increasing heating rate. Second peak is not much prominent in the 5, 10 and 15 deg/min heating rates. In the present paper, the first peak is taken into consideration for the kinetic analysis. Glass transition temperature is not very evident in all four thermograms. The analysis of DSC data to evaluate the kinetic parameters can be obtained from non-isothermal rate laws by both isokinetic (model fitting) and isoconversional (model independent) methods.

The plots of α Vs. T for different heating rates are shown in Fig. 4.14. The graphical representation of the volume fraction transformed (α) as a function of temperature (T) show the typical sigmoidal curves, which exhibit the bulk crystallization and exclude the chance of surface crystallization. During stage 1 nucleation occurs at various points in the bulk of the sample and bulk crystallization becomes dominant. The stage 2 shows the growth of nuclei with increased rate of reaction as the surface area of nucleation increases. The slowing down stage 3 shows the decrease in surface area as a result of nuclei coalescing.

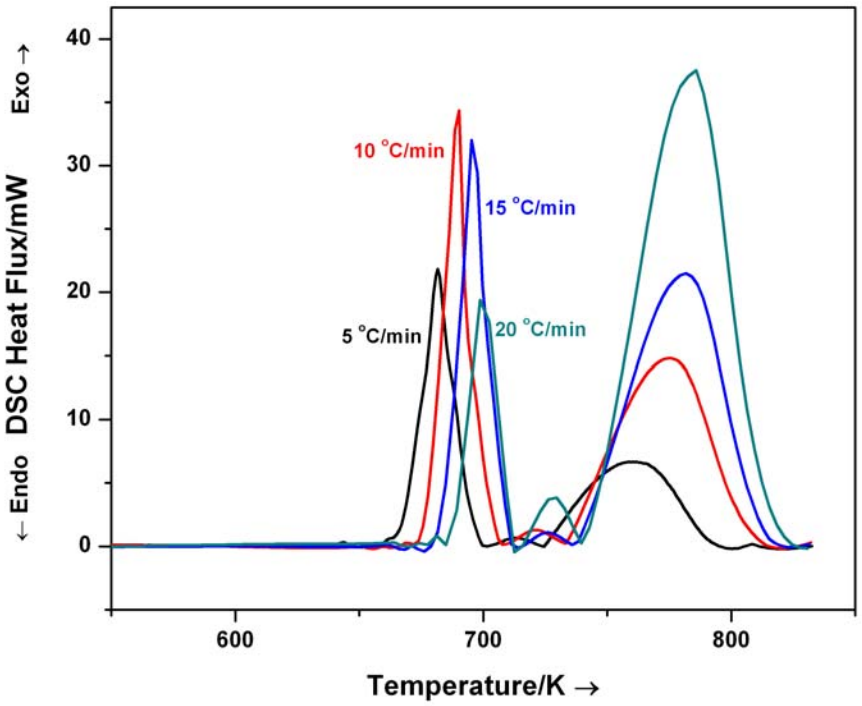

Fig. 4.13: DSC thermograms of the metallic glass $Zr_{52}Cu_{18}Ni_{14}Al_{10}Ti_6$ at different heating rates

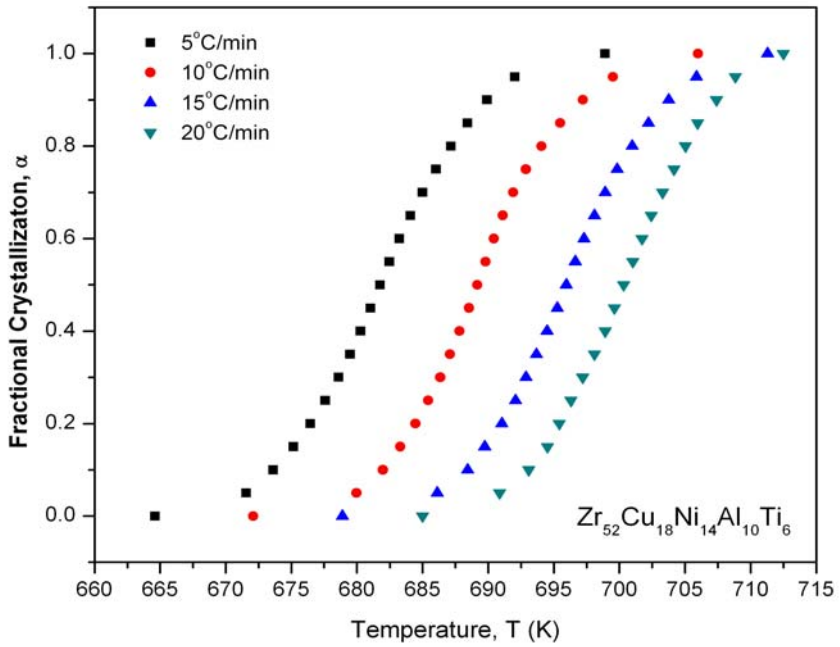

Fig. 4.14: Fractional crystallization as a function of temperature at various heating rates for $Zr_{52}Cu_{18}Ni_{14}Al_{10}Ti_6$ metallic glass

4.5.2.1 Linear Integral Isoconversional Methods

The values of local activation energy at particular α value are calculated using the OFW [Eq.(4.5)]and KAS [Eq.(4.6)] methods. The plots are shown in Figs. 4.15 and 4.16 and the values of E are listed in Table 4.7. It is observed that the activation energy continuously increases as α changes from 0.1 to 0.9, in case of both the methods.

Table 4.5 Peak temperature, T_p and onset temperature, T_o for four different heating rates for $Zr_{52}Cu_{18}Ni_{14}Al_{10}Ti_6$

Heating rates β (^{o}C/min)	***T_p (K)***	***T_o (K)***
4	681.7	664.6
6	689.9	672.1
8	696.6	678.9
10	702	685

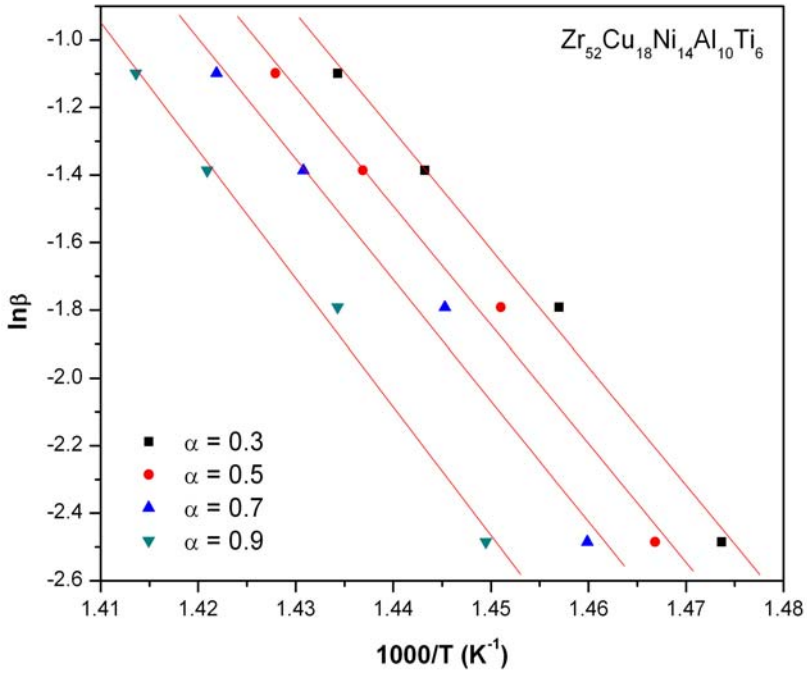

Fig. 4.15: OFW plots for $Zr_{52}Cu_{18}Ni_{14}Al_{10}Ti_6$

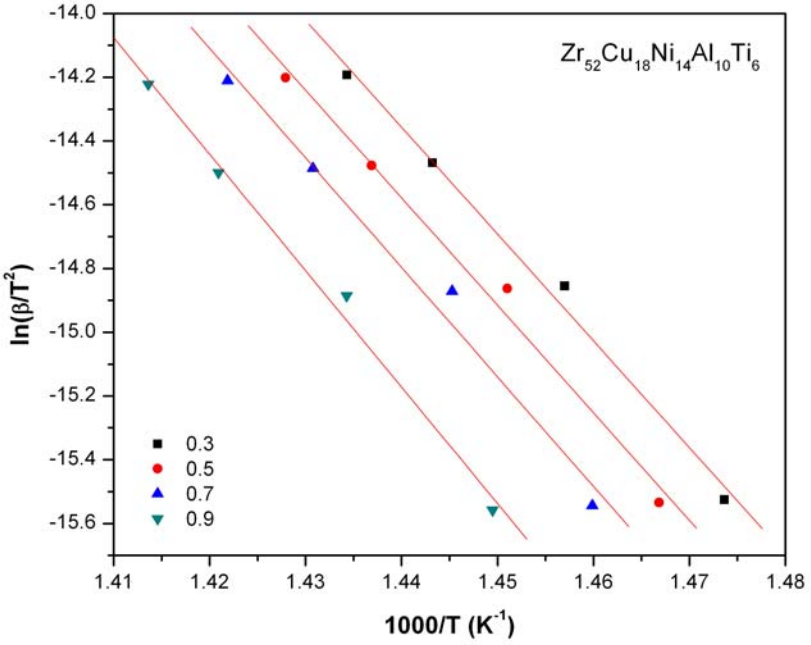

Fig. 4.16: KAS plots for $Zr_{52}Cu_{18}Ni_{14}Al_{10}Ti_6$

The shift in the crystallization peak with increasing heating rate is used to obtain the activation energy from Kissinger and Ozawa methods. Figs 4.17 and 4.18 show the Kissinger and Ozawa plots and the calculated *E* values are 260 and 258 kJ/mol respectively. The pre exponential factor calculated from Kissinger method is 4.26 x 10^{17}. In Bosewell method, $\ln\frac{\beta}{T_p} vs \frac{1}{T_p}$ is plotted (Fig. 4.19) and *E* value determined is given in Table 4.6. The Augis and Bennett plot [Eq.(4.8)] of $(ln(\beta/(T_p-T_o))$ versus $1000/T_p$ (Fig. 4.20) gives the values of *E* as 272 kJ/mol. The values of peak temperatures (T_p) and onset temperatures (T_o) are given in Table 4.5.

Table 4.6 Activation energy (E) derived using various methods for $Zr_{52}Cu_{18}Ni_{14}Al_{10}Ti_6$

Method	**E (kJ/mol)**	k_0 **(s^{-1})**
Kissinger	260 ± 2	4.86×10^{17}
Ozawa	258 ± 2	–
Augis & Bennett	272 ± 1	3.33×10^{18}
Boswell	256 ± 2	–
Gao & Wang	278 ± 3	-

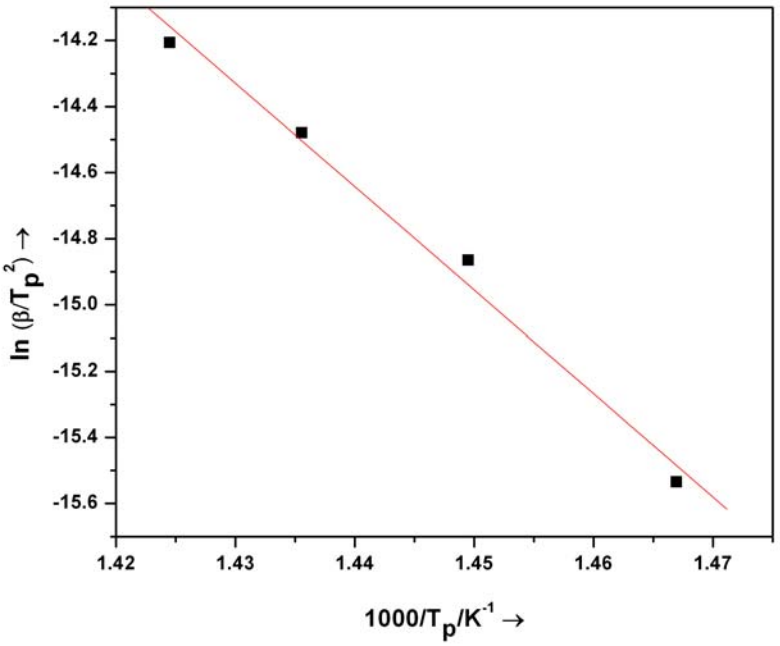

Fig. 4.17: Kissinger plot for $Zr_{52}Cu_{18}Ni_{14}Al_{10}Ti_6$

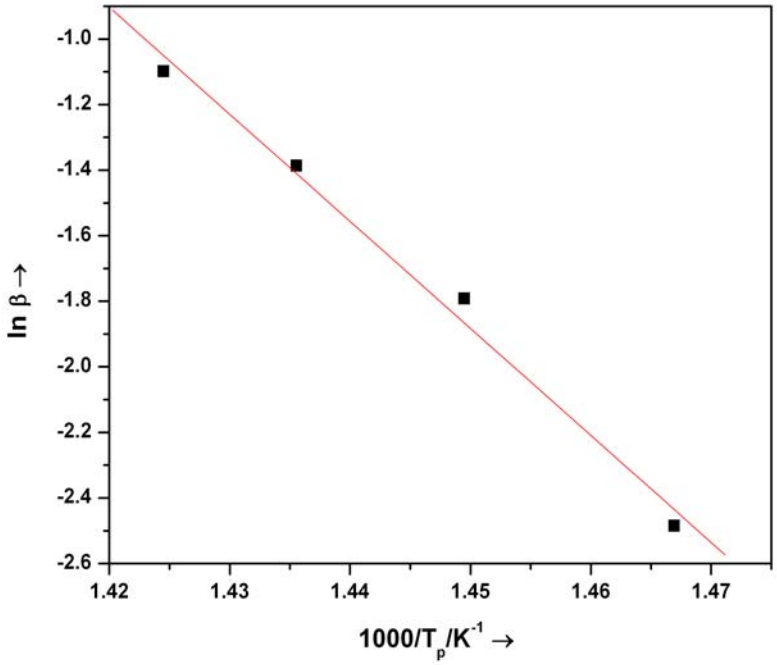

Fig. 4.18: Ozawa plot for $Zr_{52}Cu_{18}Ni_{14}Al_{10}Ti_6$

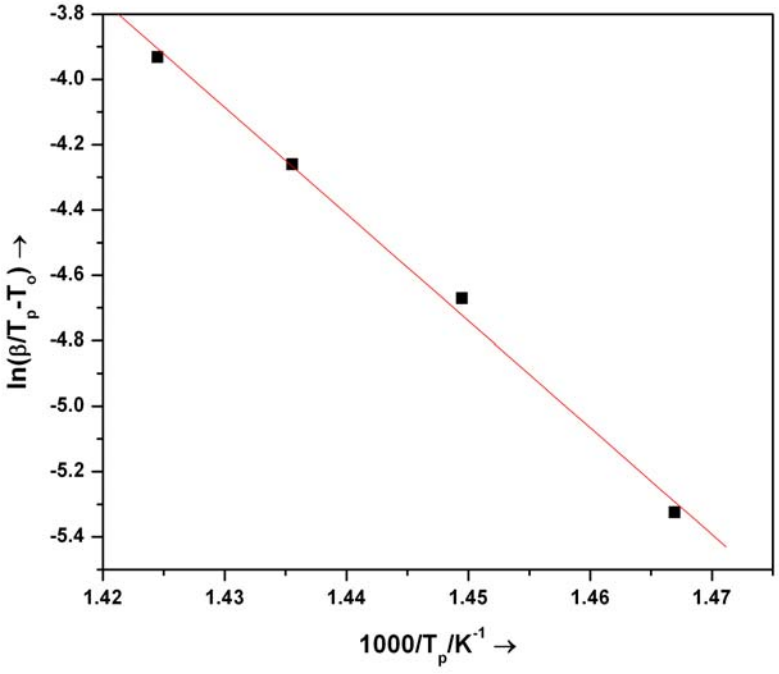

Fig. 4.19: Augis & Bennett plot for $Zr_{52}Cu_{18}Ni_{14}Al_{10}Ti_6$

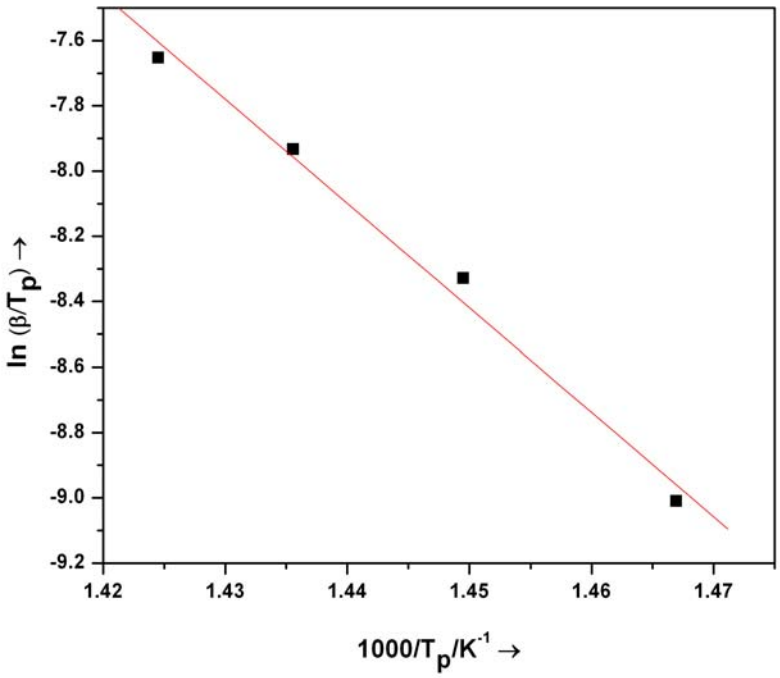

Fig. 4.20: Boswell plot for $Zr_{52}Cu_{18}Ni_{14}Al_{10}Ti_6$

4.5.2.2 Linear Differential Isoconversional Methods

According to the method suggested by Friedman [Eq.(4.11)] for a constant α, the graph of $\ln\left(\beta\frac{d\alpha}{dT}\right)_\alpha \; vs \left(\frac{1}{T_\alpha}\right)$ (Fig.4.21-(a) & (b)) is plotted, for the non-isothermal data obtained from thermograms recorded at several heating rates 5, 10, 15 and 20 deg/min^{-1}. The values of E calculated from the slope of these plots show random variation as α varies from 0.1 to 0.9 (Table 4.7).

The activation energy obtained from the Gao and Wang plot of $\ln\left(\beta\frac{d\alpha}{dT}\right)_p \; vs \frac{1}{T_p}$ (Fig. 4.22) is given in Table 4.6. This method gives a single value of E like Kissinger, Boswell etc., at the peak crystallization temperature. The deduced value of E = 278 kJ/mol, which is similar to other obtained values.

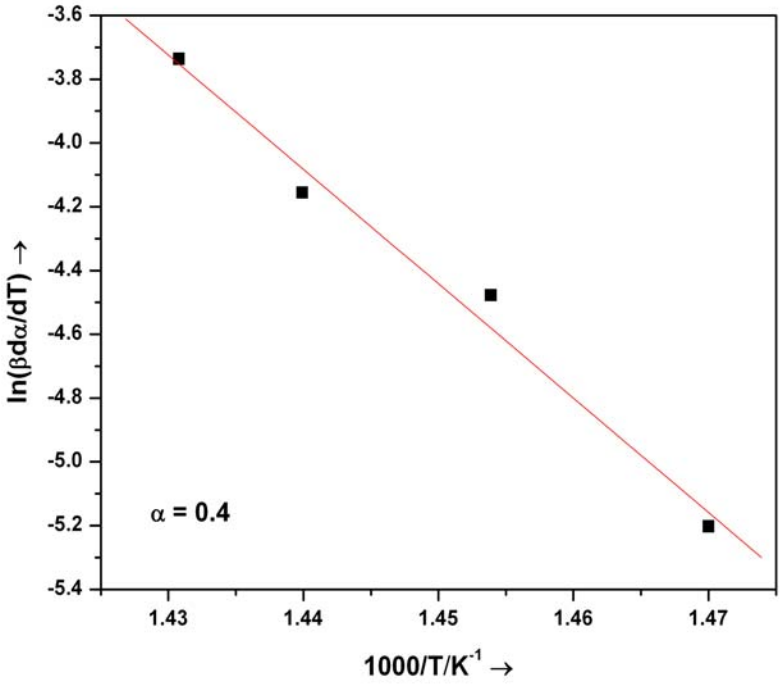

Fig. 4.21-(a): Friedman plot for $Zr_{52}Cu_{18}Ni_{14}Al_{10}Ti_6$, for α = 0.4

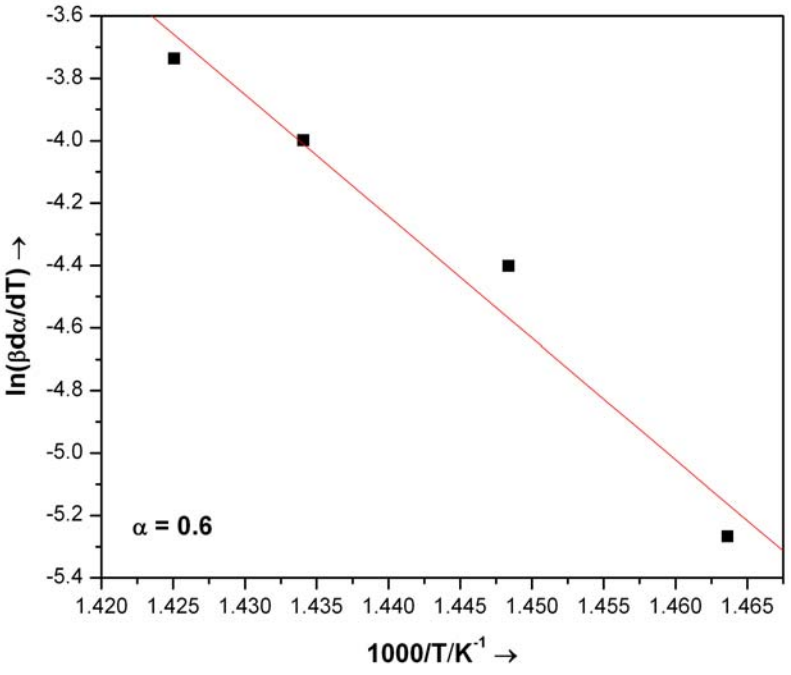

Fig. 4.21-(b): Friedman plot for $Zr_{52}Cu_{18}Ni_{14}Al_{10}Ti_6$, for $\alpha = 0.6$

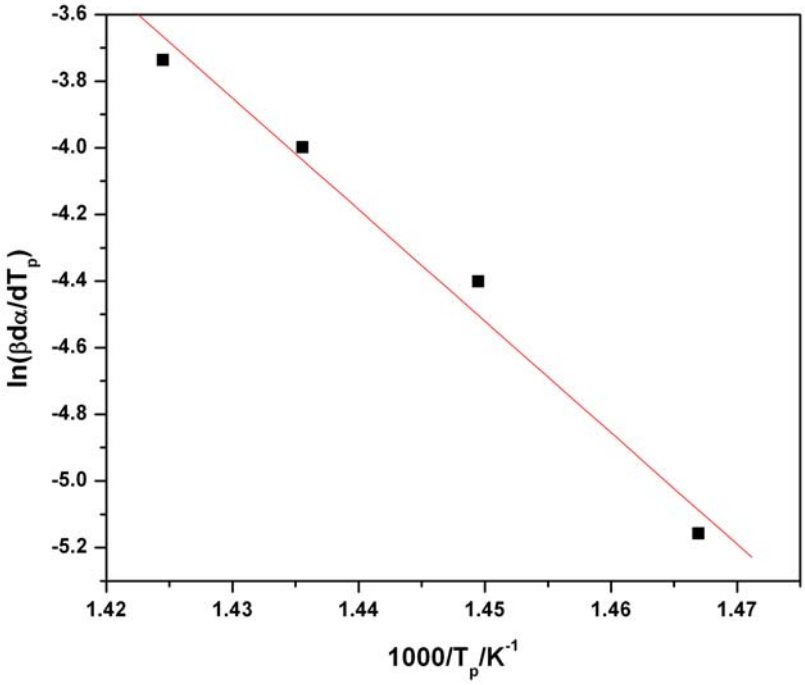

Fig. 4.22: Gao & Wang plot for $Zr_{52}Cu_{18}Ni_{14}Al_{10}Ti_6$

Table 4.7 Local Activation energy (E) at different conversion for different methods

α	E/kJ mol^{-1}		
	KAS	**OFW**	**Friedman**
0.1	264±2	256.4±2	245.5±9
0.2	272±2	269.5±2	317.3±7
0.3	278.8±2	276±2	303.9±7
0.4	279.1±2	276.3±2	298.2±3
0.5	280.7±2	277.9±2	295.7±5
0.6	282.7±3	279.7±3	324±5
0.7	285.7±3	282.6±3	320.7±4
0.8	294±3	290.5±3	371.1±4
0.9	303.8±2	299.9±2	360.5±2

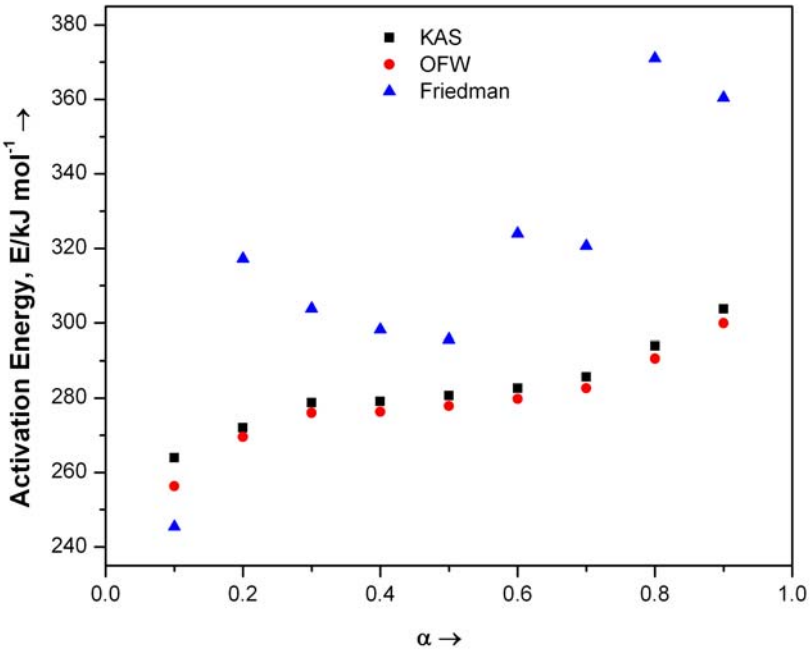

Fig. 4.23: Dependence of E on α from different methods for $Zr_{52}Cu_{18}Ni_{14}Al_{10}Ti_6$

4.5.2.3 Isokinetic Methods

The Matusita and Sakka plot for a constant temperature, the plot of $ln[-ln(1-\alpha)]$ versus $ln\beta$ gives a straight line [Fig. 4.24-(a)] and the slope gives the value of n. Here we have taken seven different constant temperatures and the average value of n comes out to be 2.66. The plot of $ln[-ln(1-\alpha)]$ versus $1/T$ at constant heating rate should be a straight line and the value of m is obtained from the slope [Fig. 4.24-(b)]. Different values of n are derived from these m values by using $n = (m+1)$ and are given in Table 4.8.

Table 4.8 Values of Avrami exponent (n) from different methods

Heating rate	Augis & Bennett	Matusita & Sakka
5	2.5	2.7
10	3.5	2.9
15	3.1	2.9
20	2.8	3.0

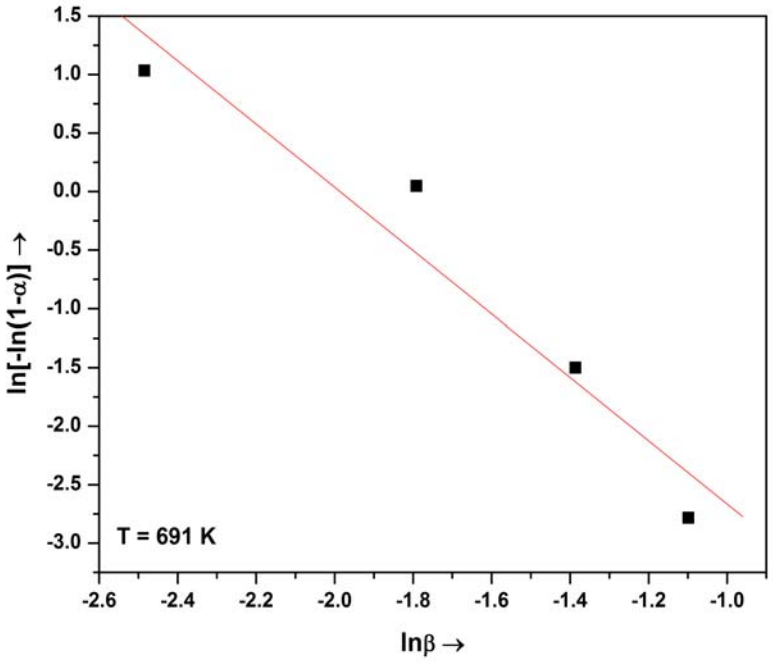

Fig. 4.24-(a): Matusita & Sakka plot of ln[-ln(1- α)] Vs. lnβ for T = 691 K

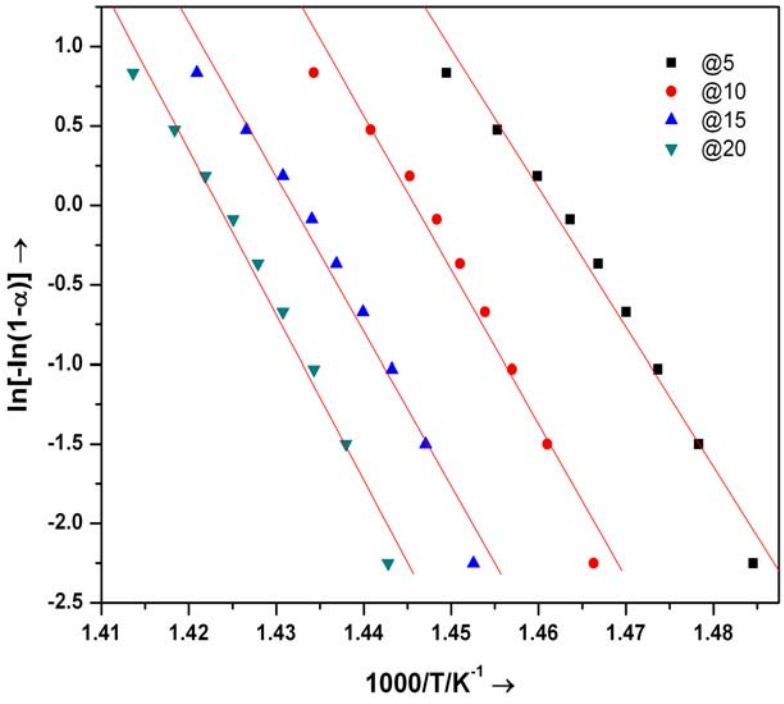

Fig. 4.24-(b): Matusita & Sakka plot of ln[-ln(1- α)] Vs. 1000/T for different heating rates

In order to derive *E* from Modified Kissinger equation, one must know the value of *n*. The *n* value can be obtained from the slope of the plot of $ln[-ln(1-\alpha)]$ Vs. $ln\beta$ at constant temperature. In order to evaluate *E*, the average value of $n = 2.66$ is substituted in Eq. (4.16). Then the plot of $\ln\left(\frac{\beta^n}{T_p^2}\right)$ Vs. $\frac{1}{T_p}$ (Fig. 4.25) gives the values of activation energy *E*, which is 428.12 kJ/mol.

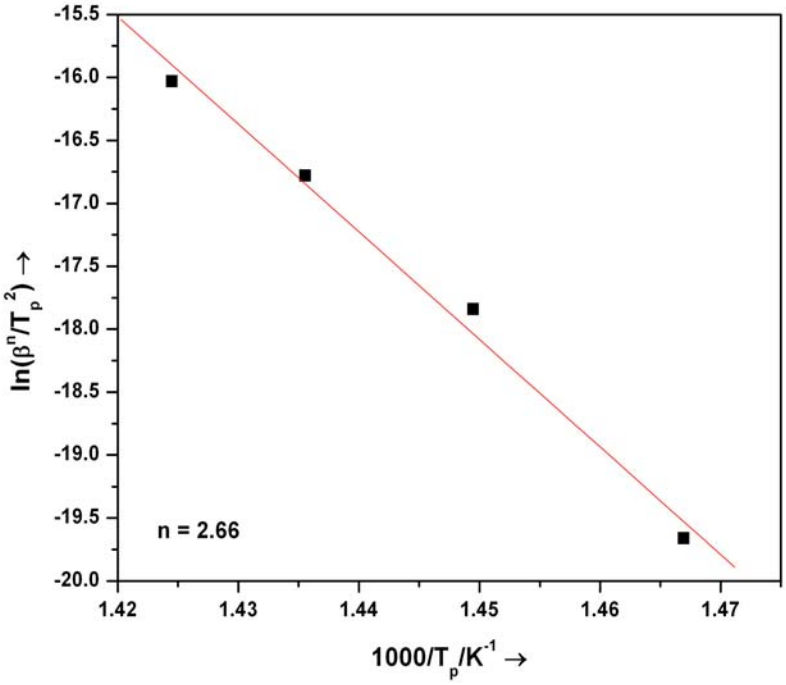

Fig. 4.25: Modified Kissinger plot for n = 2.66

4.6 Conclusions

Both model dependent isokinetic and model free isoconversional methods have been utilized to study the crystallization kinetics of the first peak of the crystallization process involved in the presently taken systems namely $Co_{66}Si_{12}B_{16}Fe_4Mo_2$ and $Zr_{52}Cu_{18}Ni_{14}Al_{10}Ti_6$ metallic glasses. The isokinetic methods, though model dependent, provide single value of activation energy. Besides, they also provide Avrami exponent n, which gives an idea about the dimensionality of the growth of crystals. Isoconversional techniques, on the other hand, provide quite accurate values of E_α as a function of α as these analytical methods are supposed to be model free.

For $Zr_{52}Cu_{18}Ni_{14}Al_{10}Ti_6$ metallic glass, it is obvious from the results obtained through KAS and OFW equations that activation energy initially increases with α. However, from α=0.4 to 0.5, there is an incremental increase in E_α. Thereafter, E_α increases again with α. This interesting result is an indication of the fact that even before first step of crystallization is completed, second step starts. The activation energy, E obtained using the Friedman method, on the other hand, show appreciable variation and there is no systematic trend. This is attributed to the signal noise involved [29]. It is also noteworthy that the activation energy values using various isoconversional methods and the special cases of isoconversional techniques namely Kissinger, Ozawa, Augis & Benett, Boswell and Gao & Wang are quite consistent, whereas modified Kissinger method overestimates it.

For Co-based metallic glass, the activation energy obtained through KAS and OFW methods, decreases initially, then increases upto α = 0.6 and then decreases again.

The activation energy, determined by Friedman method increases upto 0.5, then decreases and becomes very less for α = 0.8 & 0.9. The special cases of isoconversional methods namely Kissinger, Ozawa, Augis & Bennett & Boswell gives quite consistent results and modified Kissinger methods also incorporates with them. Isoconversional methods provide activation energy values, *E* as a function of conversion, α. The isokinetic methods, on the other hand, are used considering the crystallization mechanism to be the same throughout the entire conversion (crystallization) and give single constant value of activation energy. For metallic glasses, the thermally activated phase transformations are more physical than chemical. In fact, crystallization is a complex process involving nucleation and growth and on rigorous grounds, it cannot be considered to be a single-step process. The isokinetic analysis always leads to a single activation energy (rather say, apparent activation energy) giving an overall picture of the crystallization process. However, the difficulty (and hence uncertainty) in choosing the proper reaction model persists in isokinetic analysis. Therefore, the isoconversional methods are definitely superior to the isokinetic methods as far as the determination of *E* is concerned [4.56]. Nonetheless, accurate determination of E is not the only issue in the kinetic analysis of crystallization process in metallic glasses. The micro-structural evolution during the non-isothermal heating of the metallic glasses is also important. For the determination of the dimensionality of the growth and the grain size, one needs to know a precise reaction model that closely follows the crystallization process. A reaction model independently proposed by John-Mehl-Avrami-Kolmogorov (JMAK) is found to be the most suitable for describing the nucleation and growth process

during the non- isothermal crystallization of metallic glasses. This model does help to determine the kinetic parameters, like the dimensionality of growth (apart from *E* and *A*). The model-free isoconversional methods are definitely superior to the isokinetic methods for the accurate determination of kinetic parameters like E and A. However, the knowledge of accurate E and A is not sufficient for the detailed investigations of the dimensionality of the growth and the grain size using thermal analysis. A precise reaction model accounting for the phase transformations during the crystallization process is a prerequisite for deriving such micro-structural information. This could be a valid proposition if it is explicitly related to the phase transformations involving significant chemical changes. Therefore, isokinetic methods (despite its limited applicability) are important and useful for the analysis of non-isothermal crystallization data. So, as far as the study of thermally activated phase transformation in metallic glasses is concerned, both the types of methods are complementary and provide not only useful data, but also pave way into the insight of the crystallization process.

References

[4.1] M. Castro, *Physical Review B* **67**; 2003: pp. 035412.

[4.2] R.A. Ligero, J. Vazquez, P. Villares, and R. Jimenez-Garay, *Thermochim. Acta*, **162**; 1990: pp. 427.

[4.3] A.H. Moharram, M.A. El-Oyoun, and A.A. Abu-Sehly, *J. of Phys. D App. Phys.* **34**; 2001: pp. 2541.

[4.4] N. Rysava, T. Spasov and L. Tichy, *J. Therm. Anal.* **32**; 1987: pp. 1015.

[4.5] A. Giridhar, and S. Mahadevan, *J. Non-Cryst. Solids* **51**; 1982: pp. 305.

[4.6] S. Afify, *J. Non-Cryst. Solids* **128**; 1991: pp. 279.

[4.7] K.N. Lad, R.T. Savalia, Arun Pratap, G.K. Dey and S. Banerjee, *Thermochim. Acta* **473**; 2008: pp. 74.

[4.8] A.T. Patel and Arun Pratap, *J. Therm. Anal. and Calorim.* **107**; 2012: pp. 159.

[4.9] A.K. Galwey, *Thermochim. Acta* **399**; 2003: pp. 1.

[4.10] S. Vyazovkin, *Thermochim. Acta* **397**; 2003: pp. 269.

[4.11] S. Lesz, & D. Szewieczek, *Proceedings of the Worldwide Congress on Materials and Manufacturing Engineering and Technology COMMENT*, Poland, Gliwice-Wisla (CD-ROM), **637**; 2005: pp. 16.

[4.12] D. Szewieczek, & S. Lesz, *Proceedings of the 13th International Scientific Conference, Achievements in Mechanical & Materials Engineering AMME'05,* Gliwice-Wisla **637**; 2005: pp.

[4.13] D. Szewieczek, & S. Lesz, *J. Mater. Proces. Tech.* **157–158**; 2004: pp. 771.

[4.14] G.A. Jones, P. Bonnett & S.F.H. Parker, *J. Magnet. & Magnet. Mater.* **58**; 1986: pp. 216.

[4.15] D.M. Minic, & B. Adnadevic, *Thermochim. Acta* **474**; 2008: pp. 41.

[4.16] D.M. Minic, A. Gavrilovic, P. Angerer, D.G. Minic, & A. Mariclc, *J. Alloy Comp.* **482**; 2009: pp. 502.

[4.17] A. Hsiao, M.E. McHenry, D.E. Luaghlin, M.J. Kramer, C. Ashe, & T. Ohkubo, *IEEE Trans. Magnet.* **38**; 2002: pp. 3039.

[4.18] D.M. Minic, *Sci. Sint.* **38**; 2006: pp. 83.

[4.19] J. Bonastre, L. Escoda, J. Saurina, J.J. Sunol, J.D. Santos, M.L. Sanchez and B. Hernando, *J. Non-Cryst. Solids* **354**; 2008: pp. 5126.

[4.20] J.S. Blazquez, M. Millan and C.F. Conde, *Phil. Mag.* **87**; 2007: pp. 4151.

[4.21] J.J. Sunol, N. Clavaguera, M.T. Clavaguera-Mora, *J. Therm. Anal. Calorim.* **52**; 1998: pp. 853.

[4.22] M.J. Starink, *J. Mater. Sci.* **32**; 1997: pp. 6505.

[4.23] H.E. Kissinger, *Anal. Chem.* **29**; 1957: pp. 1702.

[4.24] T. Ozawa, *Bullet. Chem. Soc. Japan* **38**; 1965: pp. 1881.

[4.25] J.A. Augis, & J.E. Bennett, *J. Therm. Anal. Calorim.* **13**; 1978: pp. 283 (Print), 1572 (electronic version).

[4.26] P.G. Boswell, *J. Therm. Anal. Calorim.* **18**; 1980: pp. 353 (Print), 1572 (electronic version)

[4.27] J.H. Flynn and L.A. Wall, *Journal of Research of the National Bureau of Standards. Section- A. Physics and Chemistry,* **70A**, 1966: pp. 487.

[4.28] T. Akahira and T. Sunose, *Research Report, Chiba. Institute of Technology (Science and Technology)* **16**; 1971: pp. 22.

[4.29] C.R. Li and T.B. Tang, *Thermochimica Acta* **325**; 1999: pp. 43.

[4.30] A.K. Gupta, A.K. Jena and M.C. Chaturvedi, *Scripta Metal.* **22**; 1988: pp. 369.

[4.31] H.L. Friedman, *J. Polymer Sci.* ***Part C*** **6**; 1964: pp. 183.

[4.32] Y.Q. Gao and W. Wang, *J. Non-Cryst. Solids* **81**; 1986: pp. 129.

[4.33] S. Vyazovkin and C.A. Wight, *The J. Phys. Chem.y A* **101**; 1997: pp. 8279.

[4.34] F. Paulik, Ch. 10*, Special Trends in Thermal Analysis*, John Wiley & Sons, Chichester, UK: 1995.

[4.35] M.J. Starink, Thermochim. Acta **404**; 2003: pp. 163.

[4.36] P. Roura and J. Farjas, *J. Mater. Res.* **24**; 2009: pp. 3095.

[4.37] A. Rotaru and M. Gosa, *J. Therm. Anal. Calorim.* **97**; 2009: pp. 421.

[4.38] J.M. Cai and S.Y. Chen, *J. Comput. Chem.* **30**; 2009: pp. 1986.

[4.39] J.M. Criado, P.E. Sanchez-Jimenez and L.A. Perez-Maqueda, *J. Therm. Anal. and Calorim.* **92**; 2008: pp. 199.

[4.40] S. Vyazovkin, *Anal. Chem.* **82**; 2010: pp. 4936.

[4.41] C.D. Doyle, *J. App. Poly. Sci.* **5**; 1961: pp. 285.

[4.42] C.D. Doyle, *J. App. Poly. Sci.* **6**; 1962: pp. 693.

[4.43] C.D. Doyle, *Nature (London)* **207**; 1965: pp. 290.

[4.44] A.W.Coats and J.P. Redfern, *Nature (London)* **201**; 1964: pp. 68.

[4.45] H. Dhurandhar, A.T. Patel, T.L.S. Rao, K.N. Lad and A. Pratap, *J. ASTM International* **7**; 2010: pp. 1.

[4.46] K. Matusita, and S. Sakka, *Phys. Chem. Glass.***20**; 1979: pp. 81.

[4.47] K. Matusita, and Sakka, *J. Non-Cryst. Solids* **38-39**; 1980: pp. 741.

[4.48] I.C. Rho, C.S.Yoon, C.K.Kim, T.Y.Byun, and K.S. Hong, *J. Non-Cryst. Solids* **316**; 2003: pp. 289.

[4.49] G. Buttino, A. Cecchetti and M, Poppi, *J. Magn. Magn. Mater.* **241**; 2002: pp. 183.

[4.50] I.C. Rho, C.S. Yoon, C.K Kim, T.Y. Byun and K.S. Hong, *Mater. Sci. Engg.* B **96**; 2002: pp. 48.

[4.51] Z.Z. Yuan, X.D. Chen, B.X. Wang and Z.J. Chen, *J. Alloy. Comp.* **399**; 2005: pp. 166.

[4.52] G.Herzer, *IEEE Trans. Magn. Mag*. **26**; 1990: pp. 1397.

[4.53] H.K. Lachowicz, R. Zuberek, M. Kuzminski and A. Slawska-waniewska, *J. Magn. Magn. Mater.* **196**; 1999: pp. 151.

[4.54] P. Garcia-Tello, N. Murillo, J.Gonzatez, E. Amano, R. Valenzuela and J.M. Gonzalez, *J. Magn. Magn. Mater.* **203**; 1999: pp. 211.

[4.55] J.C.Martinez-Garcia, J.A.Garcia and M.Rivas, *J. Non-cryst. Solids* **354**; 2008: pp. 5132.

[4.56] S.C. Glade, R. Busch, D.S. Lee, W.L. Johnson, R.K. Wunderlich, H.J. Fecht, *J. App. Phy.* **87**; 2000: pp. 7242.

CHAPTER – 5

KINETICS OF GLASS TRANSITION OF METALLIC GLASSES

The most prominent feature of a metallic glass is that, before the crystallization takes place, it undergoes a glass transition which appears as a step transition in the DSC thermogram. Knowledge of the glass transition kinetics of metallic glasses is very much important as one can determine the useful range of operating temperature before the crystallization takes place. The kinetics of glass transition of $Ti_{50}Cu_{20}Ni_{30}$ and $Fe_{67}Co_{18}B_{14}Si_1$ metallic glasses are studied using DSC for four different heating rates and activation energies are calculated. The fragility index, *m*, is also calculated using glass transition temperature for both metallic glassy systems.

5.1 Introduction

The most prominent feature of a metallic glass is that it undergoes a glass transition, T_g, prior to crystallization [5.1]. Below T_g, a metallic glass can be thought of as an extremely viscous liquid. At T_g, the metallic glass undergoes a transformation into liquid like behavior manifested by a sudden increase in the heat capacity (C_p), and several orders of magnitude decrease in the viscosity (η). These reversible changes suggest that, metallic glasses can revert to the supercooled liquid state without crystallization. In the scientific community working with metallic glasses, this state is normally referred as the undercooled (or supercooled) liquid region. This reversibility also suggests that the structure i.e., the atomic arrangement of the glass is closely related to the atomic arrangements present in the liquid state. At a temperature T_x, which is higher than T_g, the undercooled liquid transforms into the crystalline phase. The temperature interval between T_x and T_g is known as the width of the undercooled liquid region, i.e. $\Delta T_x = T_x - T_g$. The value of ΔT_x is different for different glasses, and is usually taken as an indication of the thermal stability of the glass produced. In case of BMGs, this temperature interval is usually quite large and considered as thermal processing window [5.2].

The liquid-glass transition or glass transition is the reversible transition in amorphous materials from a hard and relatively brittle state into a molten or rubber-like state. The glass transition temperature (T_g) of an amorphous material is the critical temperature at which the material changes its behavior from being “glassy” to being “rubbery”. If the material is at a temperature below its T_g, large-scale molecular motion is not possible because the material is essentially frozen. If it is at a temperature above its

T_g, molecular motion takes place allowing it to be soft or rubbery. There is no unique value T_g for a given material (unlike the melting or freezing temperature which is thermodynamically defined and so it is fixed), but it is a kinetic parameter.

Understanding the glass transition kinetics of metallic alloys is of great importance in order to know its thermal stability and finally to determine the useful range of operating temperature for a specific technological application before the crystallization takes place [5.3]. In the present chapter, kinetics of glass transition of $Ti_{50}Cu_{20}Ni_{30}$ and $Fe_{67}Co_{18}B_{14}Si_1$ metallic glasses are reported using Differential Scanning Calorimetry (DSC) for four different heating rates and activation energies are calculated. The fragility index, m, is also calculated using T_g, for both the system taken up in the present study, which is a measure of glass forming ability of the given system.

5.2 Experimental Work

The amorphous ribbons of $Ti_{50}Cu_{20}Ni_{30}$ alloy were prepared by a single roller melt-spinning technique in an argon atmosphere at the Institute of Materials Research, Tohoku University, Sendai (Japan). The amorphicity of these ribbons were examined by X-ray diffractometry (XRD) and transmission electron microscopy (TEM).

Specimens of amorphous $Fe_{67}Co_{18}B_{14}Si_1$ (2605CO) ribbons were procured from Allied Corporation, USA prepared by single roller melt spinning technique. The amorphous nature of ribbons was confirmed by XRD and TEM.

DSC has become a convenient and widely used tool not only for studying the thermal stability of amorphous phase but also for investigating the kinetics of phase

transformations. The samples of $Ti_{50}Cu_{20}Ni_{30}$ and $Fe_{67}Co_{18}B_{14}Si_1$ are heated in DSC (Shimadzu, DSC-50) at four different heating rates (2, 4, 8 and 16 deg/min for $Ti_{50}Cu_{20}Ni_{30}$ and 5, 10, 15 and 20 deg/min for $Fe_{67}Co_{18}B_{14}Si_1$) from room temperature to 560˚C. The DSC scans are recorded by Thermal Analyzer (TA-50, WSI, Shimadzu, Japan) interfaced to computer. The curves of heat flux versus temperature are shown in Figure 5.1 and Figure 5.2 for $Ti_{50}Cu_{20}Ni_{30}$ and $Fe_{67}Co_{18}B_{14}Si_1$ metallic systems respectively.

In the present work, the kinetics of glass transition for a metallic glass $Ti_{50}Cu_{20}Ni_{30}$, which is a shape memory alloy, and for $Fe_{67}Co_{18}B_{14}Si_1$, whose commercial name is 2605CO, are studied. Using glass transition temperature (T_g), the activation energy (E) and fragility index (m) are determined.

DSC defines the glass transition as a change in the heat capacity as the amorphous matrix goes from the glassy state to the rubber state. This is a second order endothermic transition (requires heat to go through the transition). So in the DSC the transition appears as a step transition.

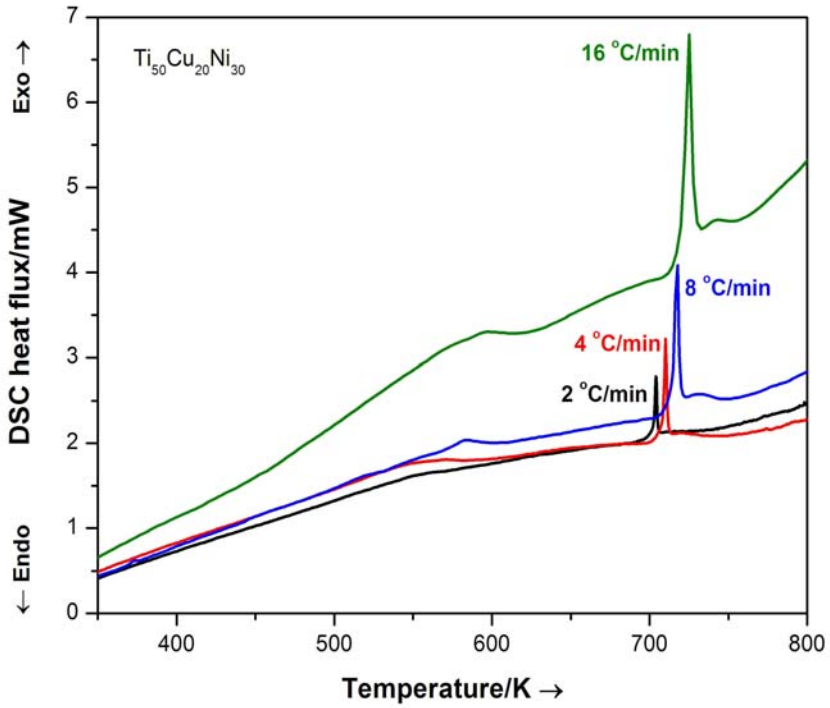

Fig. 5.1: DSC thermograms of the metallic glass $Ti_{50}Cu_{20}Ni_{30}$ at four different heating rates

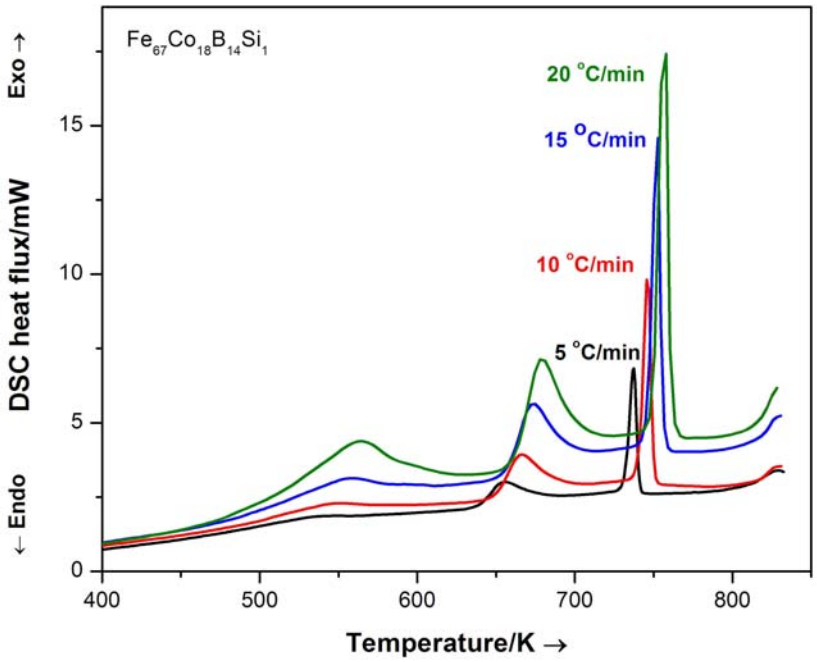

Fig. 5.2: DSC thermograms of the metallic glass $Fe_{67}Co_{18}B_{14}Si_1$ at four different heating rates

5.3 Different Methods to Study Kinetics of Glass Transition

The Activation Energy E is determined using the following glass transition methods [5.3].

(1) Moynihan method

(2) Kissinger method

The evaluation of E using the theory of glass transition kinetics and structural relaxation as developed by Moynihan and other workers [5.4-5.6] from the heating rate dependence of glass transition temperature is widely discussed in literature [5.7]. The most frequently used approach to evaluate the activation energy of glass transition is the Moynihan method [5.8].

$$\frac{d\ln\beta}{d\left(1/T_g\right)} = -\frac{E}{R} \tag{5.1}$$

where, β is the heating rate and R is the gas constant.

The Kissinger equation [5.9] is another approach which is extensively used to determine the glass transition activation energy [5.10, 5.11] and is given by

$$\frac{d\ln\left(\beta/T_g^{\,2}\right)}{d\left(1/T_g\right)} = -\frac{E}{R} \tag{5.2}$$

The plot of $ln\ (\beta/T_g^2)$ versus $1000/T_g$ should be linear in nature and will give value of E from the slope.

Fragility is defined as the increasing rate of viscosity of a supercooled liquid at a glass transition temperature in the cooling process. Glass-forming liquids can be

classified into strong liquids and fragile liquids, depending on their fragility [5.12-5.14]. The fragility of a given glass can be quantified by the fragility index '*m*' which is a measure of the rate at which the relaxation time decreases with increasing temperature around T_g and is given by [5.15]

$$m = \frac{E}{RT_g \ln 10} \tag{5.3}$$

Where, E is the glass transition activation energy.

5.4 Results & Discussions

One of the most interesting problems in the area of glasses is the understanding of glass transition kinetics which can be studied in terms of glass transition temperature (T_g) and activation energy of thermal relaxation (E). The glass transition temperature (T_g) of an amorphous material is the critical temperature at which the material changes its behavior from being "glassy" to being "rubbery" i.e. structure relaxes at this phase. For the systems taken up in the present study, the values of glass transition temperature were found to increase with increase in heating rates (Table 5.1). This may be attributed to the fact that when heating rate is high, the system doesn't get sufficient time for nucleation and crystallization. As heating rate increases, relaxation time, τ decreases. As relaxation time decreases, T_g increases due to the fact that the product of relaxation time and glass transition temperature is constant.

$$\tau T_g = Const.$$

So, T_g shifts to higher values with increase in heating rate.

Table 5.1 Glass transition temperature for $Ti_{50}Cu_{20}Ni_{30}$ and $Fe_{67}Co_{18}B_{14}Si_1$ metallic glass

$Ti_{50}Cu_{20}Ni_{30}$		$Fe_{67}Co_{18}B_{14}Si_1$	
Heating Rate, β/deg min^{-1}	**Glass Transition Temp., T_g/K**	**Heating Rate, β/deg min^{-1}**	**Glass Transition Temp., T_g/K**
2	554	5	539
4	568	10	547
8	583	15	560
16	596	20	566.5

5.4.1 Study of Kinetics of Glass Transition for $Ti_{50}Cu_{20}Ni_{30}$ and $Fe_{67}Co_{18}B_{14}Si_1$ Metallic Glasses

Titanium based alloys are lighter and less expensive, still maintaining their toughness and ductility. Due to absence of crystallinity, they have high tensile strength, high hardness, and excellent wear properties. They exhibit good corrosion resistance because they lack crystal structure. They are much more ductile than conventional glasses and have high fatigue resistance. They have high electrical resistivity than crystalline alloys of same composition.

Fe-based metallic glasses have been recognized to possess two important properties, i.e. slender magnetization loop and high resistivity. Also, Fe-based metallic glasses have attracted much attention as they possess soft ferromagnetic properties which made them very applicable in different devices, including transformers, sensors, magnetic tapes and heads of recorder [5.16].

For Moynihan method, the plot of $ln\ \beta$ versus $1000/T_g$ gives straight line (Figure 5.3 and Figure 5.4) and the activation energies, E of glass transition are calculated using the slope for both Ti-based and Fe-based metallic glasses.

The glass transition activation energies are calculated using Kissinger equation for both the systems taken up in present study. The plot of $ln\ (\beta/T_g^2)$ versus $1000/T_g$ is linear in nature and obtains activation energy value, E from slope. The Kissinger plots are shown in Fig. 5.5 & 5.6. The glass transition activation energy is the amount of energy which is absorbed by a group of atoms in the glassy region to jump from one metastable state to another [5.17]. Around the glass transition temperature, structure relaxes and rearrangement of the atoms starts. The activation energies determined by both the methods are compiled in Table 5.2.

Table 5.2 Activation energy for $Ti_{50}Cu_{20}Ni_{30}$ and $Fe_{67}Co_{18}B_{14}Si_1$ metallic glass

$Ti_{50}Cu_{20}Ni_{30}$		**$Fe_{67}Co_{18}B_{14}Si_1$**	
Method	**Activation Energy, E/kJ mol^{-1}**	**Method**	**Activation Energy, E/kJ mol^{-1}**
Moynihan method	134.74	Moynihan method	120.01
Kissinger equation	125.20	Kissinger equation	110.82

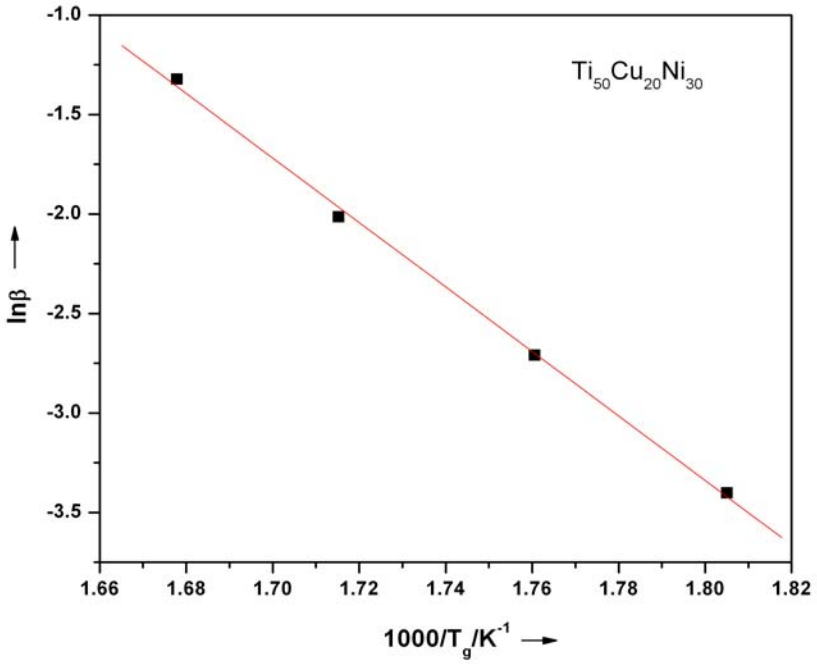

Fig. 5.3: A plot of ln β vs. $1/T_g$ for Moynihan method for $Ti_{50}Cu_{20}Ni_{30}$ metallic glass

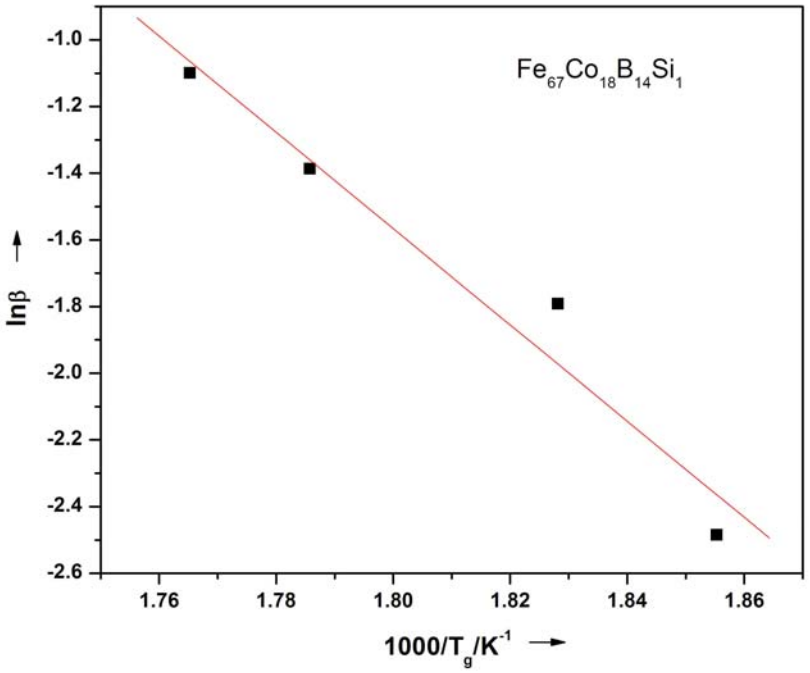

Fig. 5.4: A plot of ln β vs. $1/T_g$ for Moynihan method for $Fe_{67}Co_{18}B_{14}Si_1$ metallic glass

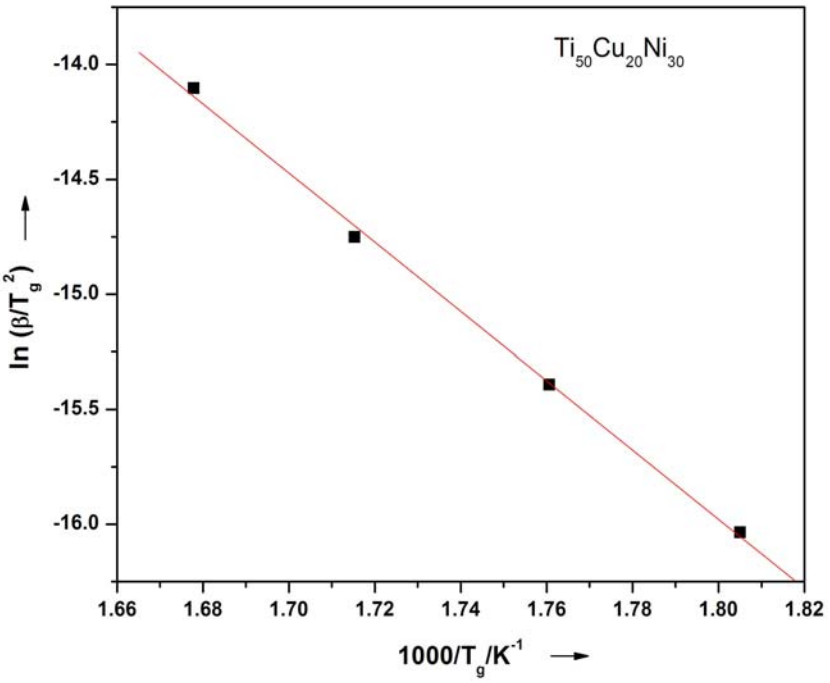

Fig. 5.5: A plot of ln (β/T_g^2) vs. $1/T_g$ for Kissinger equation for $Ti_{50}Cu_{20}Ni_{30}$ metallic glass

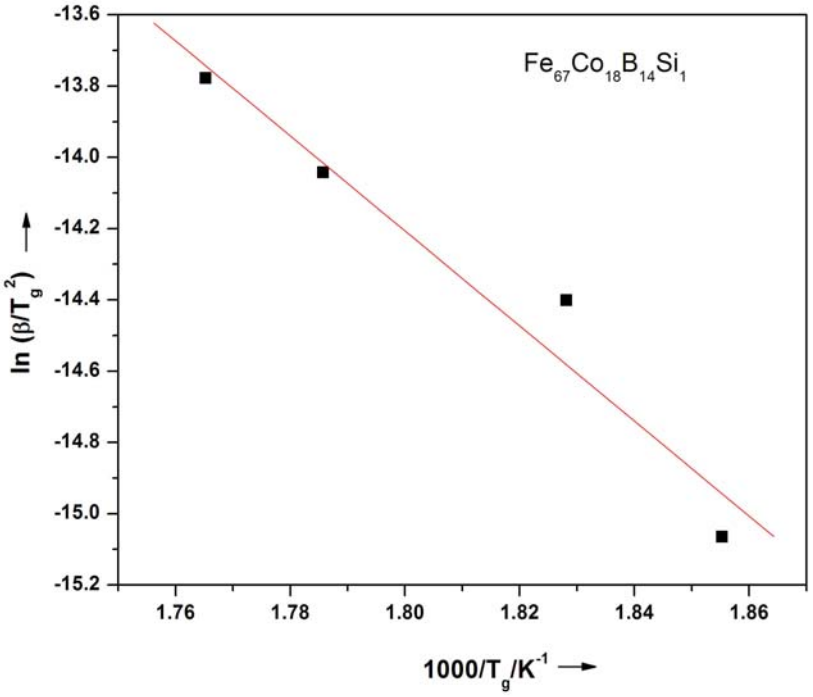

Fig. 5.6: A plot of ln (β/T_g^2) vs. $1/T_g$ for Kissinger equation for $Fe_{67}Co_{18}B_{14}Si_1$ metallic glass

If the fragility index, *m* is below 16 then the system falls in the category of 'strong' glass former. On the contrary, for the other class termed as 'fragile' this index lies above 16 but below 200. The fragility indices '*m*' are calculated for both the metallic glasses using activation energies obtained by Moynihan method and Kissinger method and listed in Table 5.3 and Table 5.4. It is clear that these values of *m* for $Ti_{50}Cu_{20}Ni_{30}$ and $Fe_{67}Co_{18}B_{14}Si_1$ metallic alloys are below 16 and hence they fall in the category of strong glass forming systems.

Table 5.3 Fragility Index, m for $Ti_{50}Cu_{20}Ni_{30}$ metallic glass

Heating Rate, β/deg min^{-1}	**Glass Transition Temp., T_g/K**	**Fragility Index, m by Moynihan method**	**Fragility Index, m by Kissinger equation**
2	554	12.70	11.80
4	568	12.39	11.51
8	583	12.07	11.22
16	596	11.81	10.97

Table 5.4 Fragility Index, m for $Fe_{67}Co_{18}B_{14}Si_1$ metallic glass

Heating Rate, β/deg min^{-1}	Glass Transition Temp., T_g/K	Fragility Index, m by Moynihan method	Fragility Index, m by Kissinger equation
5	539	11.63	10.74
10	547	11.46	10.58
15	560	11.49	10.34
20	566.5	11.06	10.22

5.5 Conclusions

The Kinetics of the glass transition of two different types of metallic glasses namely $Ti_{50}Cu_{20}Ni_{30}$ and $Fe_{67}Co_{18}B_{14}Si_1$ are studied using DSC with continuous heating of the sample at various heating rates. The glass transition activation energy is a good indicator of thermal stability. The glass transition activation energy is involved in the molecular motions and rearrangement of the atoms around the glass transition temperature.

The main advantage of using kinetics of glass transition is that one can determine activation energy at glass transition temperature which is lower than the crystallization peak temperature. By employing different models, the activation energy of the glass transition was determined. It is clear from the values of activation energy that despite different theoretical basis of the two methods, Moynihan and Kissinger equations lead to similar values of the activation energies.

The Moynihan and Kissinger equations are based on different theoretical methods.

The activation energy determined by Moynihan's method depends substantially on the thermal history because of the dependence of relaxation time on temperature as well as structure. Hence, activation energy determined from this relation must be taken as apparent activation energy.

On the contrary, activation energy evaluated from Kissinger's method has less dependence on thermal history. This method is most commonly used in analyzing crystallization data in DSC. Although originally derived for the crystallization process, which is a phase transformation from amorphous phase to crystalline phase, it may be valid for glass to amorphous transformation process also. Kissinger method was originally used for peak crystallization temperatures. When applied for glass transition process, the glass transition temperature T_g is obtained by the intersection of onset and endset of endothermic shift of base line.

The Fragility Index of a given system is determined using the activation energy E and the glass transition temperature T_g. The result shows that the fragility index 'm' of the given systems is less than 16. This indicates that the given systems are strong liquid with excellent Glass Forming Ability (GFA).

References

[5.1] C.A. Angell, *Science* **267**; 1995: pp. 1924.

[5.2] C. Suryanarayana and A. Inoue, *Bulk metallic Glass*, Chapter **1**, CRC Press Taylor & Francis Group, 2011.

[5.3] S.X. Wang, S.G. Quan and C. Dong, *Thermochim. Acta.* 2011; doi:10.1016/j.tca.2010.12.2005

[5.4] S.O. Kasap and C. Juhasz, *J. Mater. Sci.* **21**; 1986: pp.1329.

[5.5] J.P. Larmagnac, J. Grenet and P. Michon, *J. Non-Cryst Solids.* **45**; 1981: pp. 157.

[5.6] C.T. Moynihan, A.J. Easteal, J. Wilder and J. Tucker, *J. Phys Chem.* **78**; 1974: pp. 2673.

[5.7] N. Mehta and A. Kumar, *J. Optoelect. Adv. Mater.* **7**; 2005: pp.1473.

[5.8] C.T. Moynihan, *J. Am. Ceram. Soc.***76**; 1993: pp. 1081.

[5.9] H.E. Kissinger, *Anal. Chem.* **29**; 1957: pp.1702.

[5.10] H.A. Abd El Ghani, M.M. Abd El Rahim, K.K. Wakkad, A. Abo Sehli and N. Assraan, *Physica B* **381**; 2006: pp. 156.

[5.11] M.M.A. Imran, N.S. Saxena, D. Bhandari and M. Husain, P*hys. Status Solidi (A)* **181**; 2000: pp. 357.

[5.12] W.M. Wang, A. Gebert, S. Roth, U. Kuehn and L. Schultz, *Intermetallics* **16**; 2008: pp. 267.

[5.13] C.A. Angell, *J. Non-Cryst. Solids* **102**; 1988: pp. 205.

[5.14] C.A. Angell, *J. Non-Cryst. Solids.***131**; 1991: pp. 13.

[5.15] O.A. Lafi and M.M.A. Imran, *J. Alloys. Compd.* 2011; doi:10.1016/j.jallcom.2011.01.150

[5.16] D.M. Minic and B. Adnadevic, *Thermochim. Acta.* **474**; 2008: pp. 41.

[5.17] M. Saxena, S. Gupta and A. Agarwal, *Pelagia Res. Lib.* **2**; 2011: pp. 109.

CHAPTER – 6

NANOCRYSTALLINE GRAIN SIZE LIMIT FOR BULK METALLIC GLASSES

It will be interesting to study properties of metallic glass in their nanocrystalline phase. By controlling the crystallization of bulk metallic glasses nanocrystalline composites can be obtained. This is achieved by optimizing the heat treatment conditions (annealing temperature and time, heating rate etc.) so that the amorphous phase crystallizes completely into a polycrystalline material with ultrafine crystallites. It has been observed that minimum grain size of nanocrystallites has an inverse relation with the ΔG value. Owing to this, thermodynamic investigation has been carried out for a number of BMG alloys through Gibbs free energy to explore the possible lower limit of grain size that can be achieved by annealing amorphous system.

6.1 Introduction

The amorphous solids are in thermodynamically metastable state. Crystallization is such a transformation during which amorphous phase crystallizes into one or more stable or metastable polycrystalline phases. The driving force for crystallization is Gibbs free energy difference between the amorphous and crystalline state (ΔG). The dimension of the crystallite ranges from a few micrometers to few nanometers, and is strongly dependent on the chemical composition of the amorphous phase and annealing conditions.

In recent years, there has been growing interest in bulk metallic glass (BMG) alloys since these alloys exhibit an excellent glass forming ability, wide supercooled liquid region and some unique properties which are much different from those of conventional materials. Crystallization of metallic glasses usually involves nucleation and growth processes. To obtain nanoscale structure the crystallization should proceed with largest nucleation rate and the slowest crystal growth. By controlling the crystallization of the BMG alloys bulk nanocrystalline composites can also be obtained.

The basic principle for synthesis of nanocrystalline materials by crystallization of amorphous solids is to control the crystallization kinetics. This is achieved by optimising the heat treatment conditions (annealing temperature and time, heating rate etc.) so that the amorphous phase crystallizes completely into a polycrystalline material with ultrafine crystallites. Various routes have been used to prepare amorphous solids like melt spinning, splat quenching, mechanical alloying, vapour

deposition or electrodeposition etc. [6.1]. Crystallization of amorphous solids has not only been applied to alloy systems e.g. in Fe, Co and Ni – based alloys [6.2-6.5], but also to few elements (Se, Si) [6.6 - 6.8]. Crystallization of amorphous structure has emerged as an efficient way to produce porosity-free dense nanocrystalline products in large quantities. However, grain sizes in the nanocrystallization products are strongly influenced by annealing conditions of the amorphous solids. The choice of annealing temperature is one of the most important factors dominating the grain-size while using isothermal annealing. Various results indicate that the annealing temperature dependence of grain size is quite different in different alloy systems. However, it has been observed that minimum grain sizes frequently appear when the annealing temperature is close to about $0.5T_m$, where T_m is the melting temperature of the alloy. This has been inferred in terms of kinetics of phase transition, that at $T_m/2$ the nucleation rate I is the largest whereas the growth rate u is relatively low [6.9]. This phenomenon certainly seems to have a consequence of nanocrystallization mechanism which needs further careful attention and investigation. Owing to this, thermodynamic investigation has been carried out for a number of BMG alloys through Gibbs free energy to explore the possible lower limit of grain size that can be achieved by annealing amorphous system.

6.2 Theoretical Formulation for Estimation of Minimum Grain Size

The Gibbs free energy balance for the transition of the glass to the nanocrystalline state with grain size *D* when 1 mol of amorphous material is crystallized is given by [6.10]

$$\Delta g(T_x) = -\Delta G(T_x) + 3v_g\gamma_{GB} \big/ D \tag{6.1}$$

Where, ΔG is the change in the Gibbs free energy, γ_{GB} is the specific excess free energy of grain boundary and v_g is the molar volume.

At $\Delta g = 0$ the temperature dependent lower limit of the grain size $D_{min}(T_x)$ can be given as

$$D_{\min}(T_x) = 3v_g\gamma_{GB} \big/ \Delta G(T_x) \tag{6.2}$$

From this it is clear that $D_{min}(T_x)$ reaches the minimum value at the temperature where ΔG is maximum.

Here, $$\gamma_{GB} = 4h\Delta S_m \Delta H_m \big/ (3v_g R) \tag{6.3}$$

ΔS_m and ΔH_m are the change in entropy and enthalpy at melting temperature respectively and *h* is the atomic diameter.

Substituting Eq.(6.3) in Eq.(6.2) it reduces to

$$D_{\min} = 4h\Delta S_m \Delta H_m \big/ \Delta G(T_x) R \tag{6.4}$$

The difference in Gibbs free energy between the liquid and crystalline phases (discussed in Chapter-2) is given by

$$\Delta G = \frac{\Delta H_m}{T_m}\Delta T - \int_T^{T_m} \Delta C_p dT + T\int_T^{T_m} \Delta C_p \frac{dT}{T} \tag{6.5}$$

where, ΔC_p is the difference in specific heats of under cooled liquid and the corresponding crystalline phase.

Experimental ΔG can be calculated through Eq. (6.5) if we know the values of ΔC_p, but due to metastable nature of the metallic glasses, it is difficult to measure ΔC_p and experimental data are lacking. Hence, to calculate ΔG several expressions are available in the literature [6.11 – 6.20] which assume ΔC_p to be constant.

Hence, assuming ΔC_p to be constant in Eq. (6.5) and integrating the terms it reduces to

$$\Delta G = \frac{\Delta H_m \Delta T}{T_m} + \Delta C_p \left[T \ln\left(\frac{T_m}{T}\right) - \Delta T \right] \tag{6.6}$$

In the present work the maximum value of ΔG has been calculated using the expressions given by Lad et al [6.18, 6.20]

$$\Delta G = \frac{\Delta H_m}{T_m}\left(1 - \frac{\Delta T}{2T}\right) \tag{6.7}$$

$$\Delta G = \frac{\Delta H_m \Delta T}{T_m}\left(\frac{4T^2}{T + T_m}\right) \tag{6.8}$$

Both these expressions are derived by approximating the logarithmic term in Eq. (6.6) using Taylor series expansion. In derivation of Eq. (6.7) the logarithmic term is

expanded upto the 1st term while in case of Eq.(6.8) expansion of logarithmic term is considered upto the 2nd term of Taylor series. So in most of the bulk metallic glasses the ΔG values calculated using these expressions lie close to the experimental values in the entire under cooled region.

6.3 Results and Discussions

The maximum value of ΔG has been calculated for different bulk metallic systems using the Eqs. (6.7) & (6.8). Using these values the grain size has been calculated through Eq. (6.4) for different bulk metallic glass systems and the obtained results are shown in Table 6.3. The parameters required for calculation of ΔG and D_{min} are given in Table 6.1 and Table 6.2. The grain size is also calculated using the experimental ΔG for all the systems and are given in Table 6.3. It is obvious from Eq. (6.4) that the limiting value of grain size has an inverse relation with the maximum value of ΔG i.e. $\Delta G(T_x)$. The temperature at which ΔG reaches its maximum corresponds to *'Kauzmann temperature',* T_K. Hence, to get minimum grain size, the sample of metallic glass should be annealed at T_K, instead of $0.5T_m$.

6.4 Conclusions

One can see from the Eq. (6.4) that minimum grain size is inversely proportional to the maximum value of Gibbs free energy difference between amorphous metallic alloy and its crystalline counterpart, i.e. $\Delta G(T_x)$. The temperature at which ΔG reaches its maximum corresponds to *'Kauzmann temperature',* T_K. Kauzmann

temperature, also known as the ideal glass transition temperature, is the temperature at which ΔS goes to zero. Practically, it is difficult to find this temperature as it is lower than the glass transition temperature. Therefore, in principle, it is this value of temperature at which the amorphous sample should be annealed to obtain smallest possible grain size. The T_K values do not always fall to be ~ $(T_m/2)$ as observed by many workers.

It can be observed from the Table 6.3 that if annealing is carried out at T_K, to obtain nanocrystalline products with limiting value of grain size, the theoretically calculated values of grain size are larger as compared to experimental grain size limits for most of the metallic glassy systems. This is due to the fact that ΔC_p is assumed to be constant in the entire theoretical calculations (both Lad-1 & Lad-2). In the experimental evaluation of ΔG, polynomial form of variation for ΔC_p has been incorporated in Eq. (6.5) using experimentally determined $\Delta C_{p.}$ Another point that may be noted down is the closeness of the limiting value of grain size calculated from Lad-1 expression with that of the experimentally obtained minimum grain size as compared to the one derived through Lad-2 approach. The exact reason for this proximity of data given by Eq. (6.7) [Lad-1] may not be very clear. However, possibility of improving the present results can be expected if one uses recently proposed expression [6.21] of ΔG which does not approximate the logarithmic term and assumes ΔC_p to be either constant for few glass forming systems and incorporates hyperbolic behavior for few other bulk glass formers with extremely good glass forming ability (GFA).

Table 6.1 Parameters used for calculations of ΔG and D_{min}

System	T_m(K)	T_K(K)	ΔH_m (kJ/mol)
$La_{55}Al_{25}Ni_{20}$	711.6	337	7.48
$La_{55}Al_{25}Ni_{15}Cu_5$	659.7	318	7.50
$La_{55}Al_{25}Ni_{10}Cu_{10}$	662.1	332	6.837
$La_{55}Al_{25}Ni_5Cu_{15}$	663.4	304	7.208
$La_{55}Al_{25}Ni_5Cu_{10}Co_5$	660.9	363	6.094
$Pd_{40}Cu_{30}Ni_{10}P_{20}$	804	563	4.84
$Pd_{40}Ni_{40}P_{20}$	884	500	9.39
$Cu_{47}Ti_{34}Zr_{11}Ni_8$	1120	537	11.3
$Zr_{52.5}Cu_{17.9}Ni_{14.6}Al_{10}Ti_5$	1085	638	8.2
$Zr_{57}Cu_{15.4}Ni_{12.6}Al_{10}Nb_5$	1105	664	9.4

Table 6.2 Theoretical and experimental ΔG_{max} values at T_x used for calculating D_{min}

System	Experimental		Ref: Lad et al - 1		Ref: Lad et al – 2	
	T_x(K)	ΔG_{max} at T_x	T_x(K)	ΔG_{max} at T_x	T_x(K)	ΔG_{max} at T_x
$La_{55}Al_{25}Ni_{20}$	350	2.29	410	2.0	400	1.7
$La_{55}Al_{25}Ni_{15}Cu_5$	331	2.20	385	2.01	395	1.7
$La_{55}Al_{25}Ni_{10}Cu_{10}$	330	2.18	390	1.83	380	1.55
$La_{55}Al_{25}Ni_5Cu_{15}$	330	2.089	390	1.93	390	1.63
$La_{55}Al_{25}Ni_5Cu_{10}Co_5$	356	1.644	390	1.63	390	1.38
$Pd_{40}Cu_{30}Ni_{10}P_{20}$	562	0.817	560	1.15	560	0.99
$Pd_{40}Ni_{40}P_{20}$	587	2.40	510	2.52	510	2.13
$Cu_{47}Ti_{34}Zr_{11}Ni_8$	530	3.45	637	3.03	637	2.56
$Zr_{52.5}Cu_{17.9}Ni_{14.6}Al_{10}Ti_5$	648	2.12	640	2.2	630	1.86
$Zr_{57}Cu_{15.4}Ni_{12.6}Al_{10}Nb_5$	685	2.18	670	2.51	650	2.13

Table 6.3 Values of minimum grain size for different bulk metallic systems

System	D_{min}(nm)		
	Ref: Lad et al-1	**Ref: Lad et al-2**	**Expt.**
$La_{55}Al_{25}Ni_{20}$	4.72	5.57	4.12
$La_{55}Al_{25}Ni_{15}Cu_5$	5.12	6.08	4.67
$La_{55}Al_{25}Ni_{10}Cu_{10}$	4.64	5.48	3.89
$La_{55}Al_{25}Ni_5Cu_{15}$	4.88	5.78	4.51
$La_{55}Al_{25}Ni_5Cu_{10}Co_5$	4.14	4.91	4.11
$Pd_{40}Cu_{30}Ni_{10}P_{20}$	3.05	3.46	4.29
$Pd_{40}Ni_{40}P_{20}$	4.76	5.63	4.99
$Cu_{47}Ti_{34}Zr_{11}Ni_8$	5.10	5.55	3.97
$Zr_{52.5}Cu_{17.9}Ni_{14.6}Al_{10}Ti_5$	3.40	4.02	3.51
$Zr_{57}Cu_{15.4}Ni_{12.6}Al_{10}Nb_5$	3.85	4.53	4.41

References

[6.1] H.H. Liebermann, in Amorphous Metallic Alloys, edited by F. E. Luborsky, London: Butterworths, 1988, pp. 26.

[6.2] K. Lu, J.T. Wang and W.D. Wei, *J. Appl. Phys.* **69**; 1991: pp. 522.

[6.3] H.Y. Tong, J.T. Wang, B.Z. Ding, H.G. Jiang and K. Lu, *J. Non-Cryst Solids* **150**; 1992: pp. 444.

[6.4] X.D. Liu, J.T. Wang and B.Z. Ding, *Scr. Metall. Mater.* **28**; 1993: pp. 59.

[6.5] M.M. Nicolaus, H.R. Sinning and F. Haessner, *Mater. Sci. Eng. A* **150**; 1992: pp. 101.

[6.6] Y.L. He and X.N. Liu, *Acta Electron Sinica* **4**; 1982: pp. 70.

[6.7] H.Y. Zhang, Z.Q. Hu and K. Lu, *Nanostruct. Mater.* **5**; 1995: pp. 41.

[6.8] H. Y. Zhang, K. Lu and Z. Q. Hu, *Acta Phys. Sinica* **44**, 109 (1994).

[6.9] K. Lu, *Mater. Sci. Eng. R* **16**; 1996: pp. 161.

[6.10] Q. Jiang, Z. Wen and T. Wang, *J. Phys.: Condens. Matter* **13**; 2001: pp. 5503.

[6.11] D. Turnbull, *J. Appl. Phys.* **21**; 1950: pp. 1022.

[6.12] J.D. Hoffman, *J. Chem. Phys.* **29**; 1958: pp. 1192.

[6.13] D.R.H. Jones and G.A. Chadwick, *Phil. Mag.* **24**; 1971: pp. 995.

[6.14] C.V. Thompson and F. Spaepen, *Acta Metall.* **27**; 1979: pp. 1855.

[6.15] H.B. Singh and A. Holz, *Solid State Commun.* **45**; 1983: pp. 985.

[6.16] K.S. Dubey and P. Ramchandrarao, *Acta Metall.* **32**; 1984: pp. 91.

[6.17] L. Battezzati and E. Garrone, *Z. Metallkunde* **75**; 1984: pp. 305.

[6.18] K.N. Lad, A. Pratap and K.G. Raval, *J. Mater Sci. Lett.* **21**; 2002: pp. 1419.

[6.19] K. Mondal, U.K. Chatterjee and B.S. Murthy, *Appl. Phys. Lett.* **83**; 2003: pp. 671.

[6.20] K.N. Lad, K.G. Raval and A. Pratap, J. *Non-Cryst Solids* **334 & 335**; 2004: pp. 259.

[6.21] H. Dhurandhar, T.L.S. Rao, K.N. Lad and A. Pratap, *Phil. Mag. Letts.* **88**; 2008: pp. 239.

CHAPTER – 7

CONCLUSIONS & SCOPE FOR FUTURE WORK

CHAPTER - 7
Conclusions and Scope for Future Work

The thesis entitled "*ATOMIC MOTION, AMORPHOUS PHASE FORMATION AND NANOCRYSTALLIZATION STUDY IN LIQUID METALS AND THEIR ALLOYS*" encompasses theoretical as well as experimental study of metallic glass forming alloys. Theoretical investigations include study of thermodynamic aspects of metallic glasses, gauges different GFA parameters and estimation of minimum grain size for formation of nanocrystals. Experimental study is mainly divided in two parts:

(i) understanding the crystallization kinetics of metallic glasses namely $Co_{66}Si_{12}B_{16}Fe_4Mo_2$ and $Zr_{52}Cu_{18}Ni_{14}Al_{10}Ti_6$

(ii) study of kinetics of glass transition of $Ti_{50}Cu_{20}Ni_{30}$ and $Fe_{67}Co_{18}B_{14}Si_1$ metallic glasses

At the theoretical front different thermodynamic parameters i.e. Gibbs free energy difference ΔG, Entropy difference ΔS and Enthalpy difference ΔH are evaluated for different metallic glassy systems. Gibbs free energy change for crystallization of an undercooled liquid exponentially depends on nucleation rate. Gibbs free energy difference is the driving force for the crystallization; therefore, lower the value of ΔG, higher is the glass forming ability (GFA) of metallic glasses. Hence, correct prediction of ΔG is important from designing point of view of new glassy materials. The ΔG values can be estimated if one knows the experimental specific heat difference (ΔC_p).

But there is a lack of experimental data of ΔC_p, due to the metastable nature of undercooled liquids. Therefore, in deriving expression for ΔG, linear and hyperbolic

variations of ΔC_p are assumed. These expressions excellently account for ΔG in multicomponent metallic glass forming alloys in the entire undercooled region.

Up till now no such method was available from which one can find out a priori whether the nature of ΔC_p is constant or varying. This could be possible if one had the estimate of Kauzmann temperature T_K and the other two parameters viz. ΔC_p^m at melting temperature T_m. As explained in Chapter 3, for a particular metallic glass if values of α_1 and α_2 are nearly equal then ΔC_p can be taken as constant for that particular system and if two α values are different then ΔC_p is not constant and it is varying with temperature in the undercooled region for that system.

Glass forming ability (GFA) of metallic glassy systems is very much important from theoretical and practical point of view. There are so many different criteria available in literature for the estimation of glass forming ability.

ΔG has played an important role in predicting the GFA of multicomponent metallic alloys. Lesser the value of ΔG, easier is the formation of BMGs. From the results, ΔG emerges out as the best GFA criterion.

Apart from the thermodynamic properties, magnetic properties of metallic glasses can be studied and electrical conductivity measurement can be done using four probe method.

Using Gibbs free energy difference ΔG, in the undercooled regime one can plot Time-Temperature-Transformation curve. From nose temperature T_n and nose time t_n of the T-T-T diagram, critical cooling rate, R_c can be estimated.

Metallic glasses can be transformed to crystalline state by continuous heating in DSC. The transformation from amorphous to fully crystalline state can proceed in one step

(polymorphous and eutectic crystallization) or in several steps (primary crystallization). Crystallization of metallic glasses involves nucleation and growth processes. DSC technique is used to study crystallization kinetics of $Co_{66}Si_{12}B_{16}Fe_4Mo_2$ and $Zr_{52}Cu_{18}Ni_{14}Al_{10}Ti_6$ metallic glasses. The activation energies have been found using isokinetic and isoconvertional approaches. The most prominent feature of a metallic glass is that it undergoes a glass transition T_g, prior to crystallization. Understanding the glass transition kinetics of metallic alloys is of great importance in order to know its thermal stability and finally to determine the useful range of operating temperature for a specific technological application before the crystallization takes place. Kinetics of glass transition has been studied for shape memory alloy $Ti_{50}Cu_{20}Ni_{30}$ and $Fe_{67}Co_{18}B_{14}Si_1$ which is a soft magnetic amorphous alloy. Using two different approaches namely Moynihan method and Kissinger method, activation energies are found out. One can explore new methods to find out the glass transition activation energies of metallic glasses.

It will be interesting to see properties of metallic glass in their nanophase. To obtain nanoscale structure the crystallization should proceed with largest nucleation rate and the slowest crystal growth. By controlling the crystallization of the BMG alloys bulk nanocrystalline composites can be obtained. This is achieved by optimising the heat treatment conditions (annealing temperature and time, heating rate etc.) so that the amorphous phase crystallizes completely into a polycrystalline material with ultrafine crystallites. It has been observed that minimum grain size of nanocrystallites has an inverse relation with the ΔG value. Owing to this, thermodynamic investigation has been carried out for a number of BMG alloys through Gibbs free energy to explore

the possible lower limit of grain size that can be achieved by annealing amorphous system.

However, possibility of improving the present results can be expected if one uses recently proposed expression of ΔG which assumes variation of ΔC_p to be either linear or hyperbolic.

The hysteresis curve can also be traced for systems having various grain sizes of nanocrystals. The nano-crystalline form may be useful to study the oxidative stability as well as the corrosion resistance behavior of these systems in nano-structured form.

Study of kinetics of glass transition of metallic glasses

Ashmi T. Patel & Arun Pratap

Journal of Thermal Analysis and Calorimetry
An International Forum for Thermal Studies

ISSN 1388-6150
Volume 110
Number 2

J Therm Anal Calorim (2012)
110:567-571
DOI 10.1007/s10973-012-2527-8

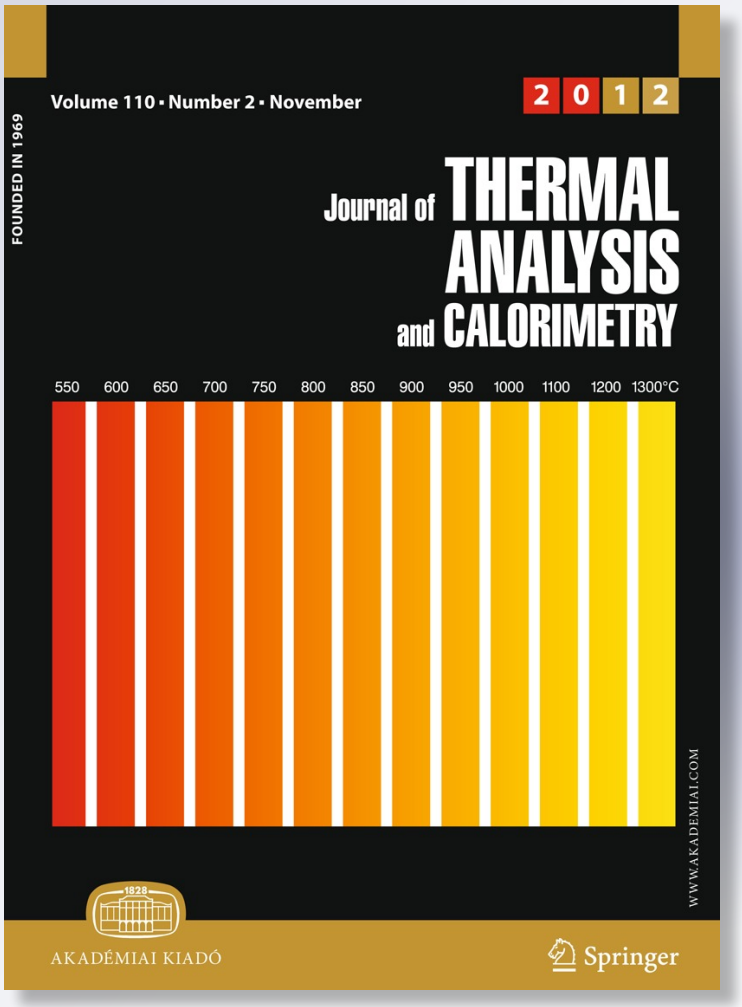

Springer

J Therm Anal Calorim (2012) 110:567–571
DOI 10.1007/s10973-012-2527-8

Study of kinetics of glass transition of metallic glasses

Ashmi T. Patel · Arun Pratap

SATAC-ACT2011 Conference Special Chapter

Abstract In this study, the kinetics of glass transitions of $Ti_{50}Cu_{20}Ni_{30}$ and $Fe_{67}Co_{18}B_{14}Si_1$ metallic glasses are studied using thermal analysis technique, i.e., differential scanning calorimetry, by means of continuous heating of the sample at various heating rates. In the present study, based on the heating rate dependence of glass transition temperature (T_g), the activation energy (E) of the glass transition region is determined by two most frequently used approaches, i.e., Moynihan's method and Kissinger's equation. The fragility index, m, is also calculated using T_g, which is a measure of glass-forming ability of the given system. The result shows that the fragility index, m, of the given systems is <16. This indicates that the given systems are strong liquids with excellent glass-forming ability.

Keywords Glass transition · Metallic glass · Activation energy · Fragility index

Introduction

Metallic glass has a combination of amorphous structure and metallic bond. Metallic glasses have been regarded as potential structural and functional materials with unique disordered atomic configuration [1, 2]. They are used in sky equipment, cell phone casings, in USB Memory Stick, baseball bats, golf sticks, as well as in jewelry making.

Titanium-based alloys are lighter and less expensive, yet maintaining their toughness and ductility. Owing to the absence of crystallinity, they have high tensile strength, high hardness, and excellent wear properties. They exhibit good corrosion resistance because they lack crystal structure. They are much more ductile than conventional glasses and have high fatigue resistance. They have high electrical resistivity than crystalline alloys of same composition.

Fe-based metallic glasses have been recognized to possess two important properties, i.e., slender magnetization loop and high resistivity. Also, Fe-based metallic glasses have attracted much attention as they possess soft ferromagnetic properties which make them widely applicable in different devices, including transformers, sensors, magnetic tapes, and heads of recorder [3].

Understanding the glass transition kinetics of metallic alloys is of great importance to know its thermal stability, and finally to determine the useful range of operating temperatures for a specific technological application before the crystallization takes place [4]. In the present study, kinetics of glass transitions of $Ti_{50}Cu_{20}Ni_{30}$ and $Fe_{67}Co_{18}B_{14}Si_1$ metallic glasses are studied using differential scanning calorimetry (DSC) for four different heating rates and activation energies are calculated.

Experimental methods

The amorphous ribbons of $Ti_{50}Cu_{20}Ni_{30}$ alloy were prepared by a single roller melt-spinning technique in an argon atmosphere at the institute of materials research, Tohoku university, Sendai (Japan). The amorphicity of these ribbons were examined using X-ray diffractometry (XRD) and transmission electron microscopy (TEM).

Specimens of amorphous $Fe_{67}Co_{18}B_{14}Si_1$ (2605CO) ribbons were procured from Allied Corporation, USA prepared by single roller melt-spinning technique. The

A. T. Patel · A. Pratap (✉)
Condensed Matter Physics Laboratory, Applied Physics Department, Faculty of Technology & Engineering, The M. S. University of Baroda, Vadodara 390 001, India
e-mail: apratapmsu@yahoo.com

amorphous nature of ribbons was confirmed by XRD and TEM.

The DSC has become a convenient and widely used tool not only for studying the thermal stability of amorphous phase but also for investigating the kinetics of phase transformations. The samples of $Ti_{50}Cu_{20}Ni_{30}$ and $Fe_{67}Co_{18}B_{14}Si_1$ are heated in DSC (Shimadzu, DSC-50) at four different heating rates (2, 4, 8, and 16 °C min^{-1} for $Ti_{50}Cu_{20}Ni_{30}$ and 5, 10, 15, and 20 °C min^{-1} for $Fe_{67}Co_{18}B_{14}Si_1$) with temperatures ranging from room temperature to 560 °C. The DSC scans are recorded by Thermal Analyzer (TA-50, WSI, Shimadzu, Japan) interfaced to computer. The curves of heat flux versus temperature are shown in Figs. 1 and 2 for $Ti_{50}Cu_{20}Ni_{30}$ and $Fe_{67}Co_{18}B_{14}Si_1$ metallic systems, respectively.

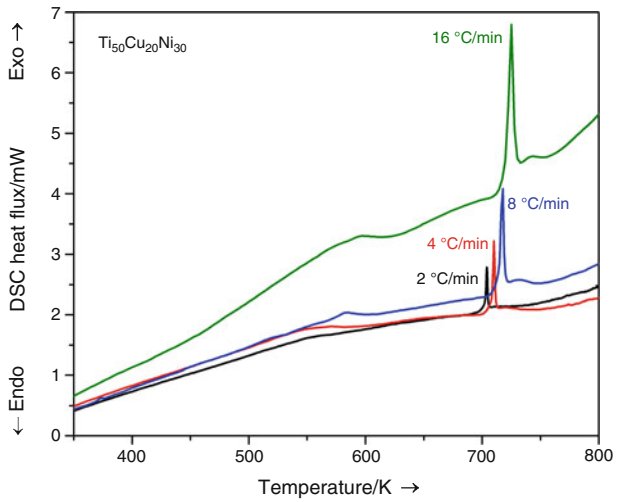

Fig. 1 DSC thermograms of the metallic glass $Ti_{50}Cu_{20}Ni_{30}$ at four different heating rates

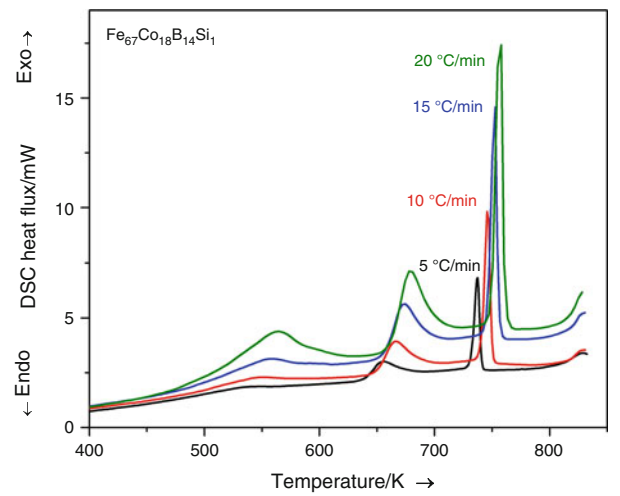

Fig. 2 DSC thermograms of the metallic glass $Fe_{67}Co_{18}B_{14}Si_1$ at four different heating rates

In the present study, the kinetics of glass transition for a metallic glass $Ti_{50}Cu_{20}Ni_{30}$, which is a shape memory alloy, and for $Fe_{67}Co_{18}B_{14}Si_1$, commercial name of which is 2605CO, are studied. Using glass transition temperature (T_g), the activation energy (E), and fragility index (m) are determined.

The DSC defines the glass transition as a change in the heat capacity as the amorphous matrix goes from the glassy state to the rubber state. This is a second-order endothermic transition (requires heat to go through the transition). Hence, in the DSC, the transition appears as a step transition.

Results and discussion

One of the most interesting problems in the area of glasses is the understanding of glass transition kinetics which can be studied in terms of glass transition temperature (T_g) and activation energy of thermal relaxation (E). The T_g of an amorphous material is the critical temperature at which the material changes its behavior from being "glassy" to being "rubbery". For the systems taken up in the present study, the values of glass transition temperature were found to increase with the increasing heating rates (Table 1). This may be attributed to the fact that when heating rate is high, the system does not get sufficient time for nucleation and crystallization. As heating rate increases, relaxation time, τ decreases. As relaxation time decreases, T_g increases because the product of relaxation time and glass transition temperature is constant.

$$\tau T_g = Const.$$

Hence, T_g shifts to higher values with increasing heating rates.

The activation energy, E, is determined using the following glass transition methods [4].

(1) Moynihan's method; and
(2) Kissinger's method

The evaluation of E using the theory of glass transition kinetics and structural relaxation as developed by

Table 1 Glass transition temperatures for $Ti_{50}Cu_{20}Ni_{30}$ and $Fe_{67}Co_{18}B_{14}Si_1$ metallic glasses

$Ti_{50}Cu_{20}Ni_{30}$		$Fe_{67}Co_{18}B_{14}Si_1$	
Heating rate, β/deg min^{-1}	Glass transition Temp., T_g/K	Heating rate, β/deg min^{-1}	Glass transition Temp., T_g/K
2	554	5	539
4	568	10	547
8	583	15	560
16	596	20	566.5

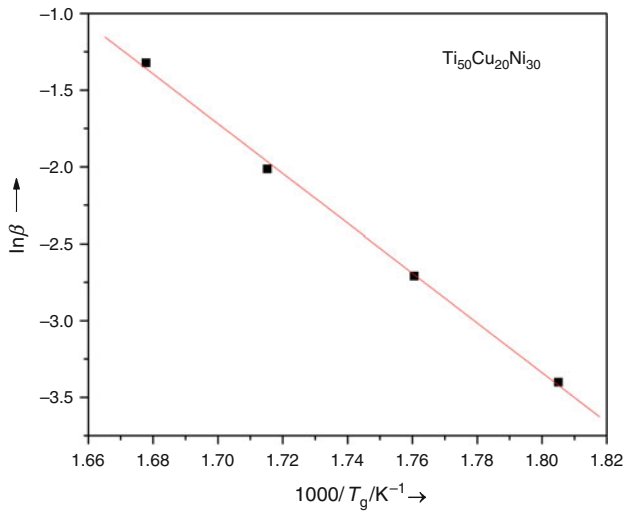

Fig. 3 A plot of ln β versus $1/T_g$ for Moynihan's method for $Ti_{50}Cu_{20}Ni_{30}$ metallic glass

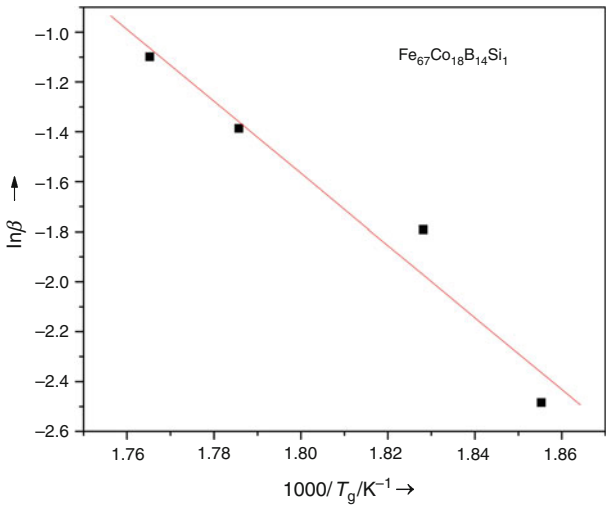

Fig. 4 A plot of ln β versus $1/T_g$ for Moynihan's method for $Fe_{67}Co_{18}B_{14}Si_1$ metallic glass

Moynihan and other workers [5–7], based on the heating rate dependence of glass transition temperature, is widely discussed in the literature [8]. The most frequently used approach to evaluate the activation energy of glass transition is the Moynihan's method [9].

$$\frac{d\ln\beta}{d(1/T_g)} = -\frac{E}{R} \quad (1)$$

where, β is the heating rate, and R is the gas constant. The plot of ln β versus $1{,}000/T_g$ gives straight line (Fig. 3 and Fig. 4), and the activation energies, E, of glass transition are calculated using the slope for both Ti- and Fe-based metallic glasses (Table 2).

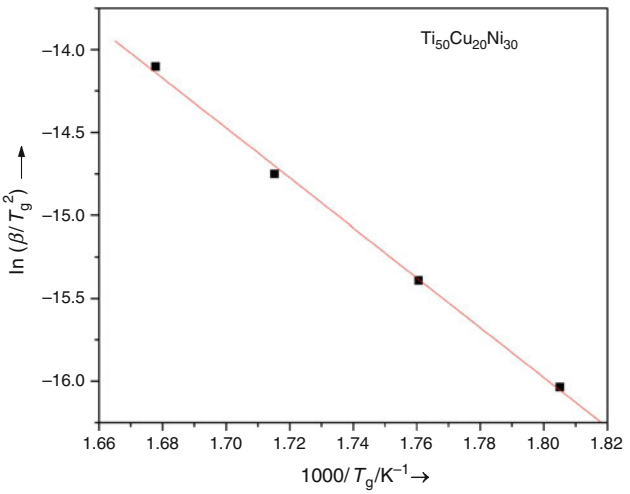

Fig. 5 A plot of ln (β/T_g^2) versus $1/T_g$ for Kissinger's equation for $Ti_{50}Cu_{20}Ni_{30}$ metallic glass

Table 2 Activation energy for $Ti_{50}Cu_{20}Ni_{30}$ and $Fe_{67}Co_{18}B_{14}Si_1$ metallic glass

$Ti_{50}Cu_{20}Ni_{30}$		$Fe_{67}Co_{18}B_{14}Si_1$	
Method	Activation energy, E/kJ mol^{-1}	Method	Activation energy, E/kJ mol^{-1}
Moynihan's method	134.74	Moynihan's method	120.01
Kissinger's equation	125.20	Kissinger's equation	110.82

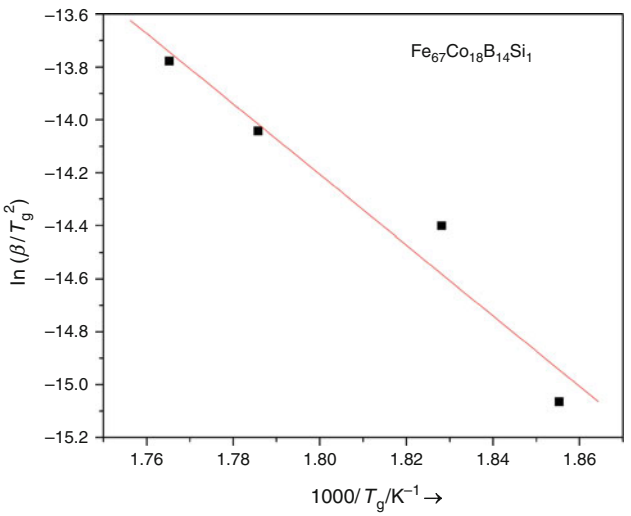

Fig. 6 A plot of ln (β/T_g^2) versus $1/T_g$ for Kissinger's equation for $Fe_{67}Co_{18}B_{14}Si_1$ metallic glass

The Kissinger's equation [10] is another approach which is extensively used to determine the glass transition activation energy [11, 12] and is given by

Table 3 Fragility Index, m, for $Ti_{50}Cu_{20}Ni_{30}$ metallic glass

Heating Rate, β/deg min^{-1}	Glass Transition Temp., T_g/K	Fragility Index, m by Moynihan's method	Fragility Index, m by Kissinger's equation
2	554	12.70	11.80
4	568	12.39	11.51
8	583	12.07	11.22
16	596	11.81	10.97

Table 4 Fragility Index, m, for $Fe_{67}Co_{18}B_{14}Si_1$ metallic glass

Heating Rate, β/deg min^{-1}	Glass Transition Temp., T_g/K	Fragility Index, m by Moynihan's method	Fragility Index, m by Kissinger's equation
5	539	11.63	10.74
10	547	11.46	10.58
15	560	11.49	10.34
20	566.5	11.06	10.22

$$\frac{d\ln\left(\beta/T_g^2\right)}{d\left(1/T_g\right)} = -\frac{E}{R} \tag{2}$$

The plot of ln (β/T_g^2) versus 1,000/T_g is linear (Figs. 5 and 6) in nature and obtains the value of E from the slope. The glass transition activation energies are calculated using Kissinger's equation for both the systems taken up in the present study (Table 2). The glass transition activation energy is the amount of energy which is absorbed by a group of atoms in the glassy region to jump from one metastable state to another [13]. Around the T_g, the structure undergoes relaxation, and rearrangement of the atoms starts.

Fragility is defined as the increasing rate of viscosity of a supercooled liquid at a glass transition temperature in the cooling process. Glass-forming liquids can be classified into strong liquids and fragile liquids, depending on their fragility [14–16]. The fragility of a given glass can be quantified by the fragility index, m, which is a measure of the rate at which the relaxation time decreases with increasing temperature around T_g and is given by [17]

$$m = \frac{E}{RT_g \ln 10} \tag{3}$$

where, E is the glass transition activation energy.

If the fragility index, m, is below 16, then the system falls in the category of "strong" glass former. On the contrary, for the other class termed as "fragile," this index lies between 16 and 200. The fragility indices, m, are calculated for both the metallic glasses using activation energies obtained by Moynihan's method and Kissinger's method and listed in Table 3 and Table 4. It is clear that these values of m for $Ti_{50}Cu_{20}Ni_{30}$ and $Fe_{67}Co_{18}B_{14}Si_1$ metallic alloys are below 16, and hence they fall in the category of strong glass-forming systems.

Conclusions

The Kinetics of the glass transition of two types of metallic glasses, namely, $Ti_{50}Cu_{20}Ni_{30}$ and $Fe_{67}Co_{18}B_{14}Si_1$ are studied using DSC with continuous heating of the sample at various heating rates. The glass transition activation energy is a good indicator of thermal stability. The glass transition activation energy is involved in the molecular motions and rearrangement of the atoms around the glass transition temperature.

The main advantage of using kinetics of glass transition is that one can determine activation energy at glass transition temperature which is lower than the crystallization peak temperature. By employing different models, the activation energy of the glass transition was determined. It is clear from the values of activation energy that despite different theoretical basis of the two methods, Moynihan and Kissinger's equations lead to similar values for the activation energies.

The Moynihan and Kissinger's equations are based on different theoretical methods. The activation energy determined by Moynihan's method depends substantially on the thermal history because of the dependence of relaxation time on temperature as well as structure. Hence, activation energy determined from this relation must be taken as apparent activation energy.

On the contrary, activation energy evaluated from Kissinger's method has less dependence on thermal history. This method is most commonly used in analyzing crystallization data in DSC. Although originally derived for the crystallization process, which is a phase transformation from amorphous phase to crystalline phase, it may be valid for glass-to-amorphous transformation process also. Kissinger's method was originally used for peak crystallization temperatures. When applied for glass transition process, the glass transition temperature, T_g, is obtained by the intersection of the onset and the endset of endothermic shift of base line.

The fragility Index of a given system is determined using the activation energy, E, and the glass transition temperature, T_g. The result shows that the fragility index, m. of the given systems is <16. This indicates that the given systems are strong liquids with excellent glass-forming ability.

References

1. Jiang QK, Wang XD, Nie XP, Zhang GQ, Ma H, Fecht HJ, Bendnarcik J, Franz H, Liu YG, Cao QP, Jiang JZ. Zr–(Cu, Ag)–Al bulk metallic glasses. Acta Mater. 2008;56:1785–96.
2. Yu ZH, Ding D, Lu T, Xia L, Dong YD. Effect of minor Al addition on glass-forming ability and thermal stability of Zr–Cu binary alloy. Mod Phys Lett B. 2010;24(20):2143–50.
3. Minic DM, Adnadevic B. Mechanism and kinetics of crystallization of α-Fe in amorphous $Fe_{81}B_{13}Si4C_2$ alloy. Thermochim Acta. 2008;474:41–6.
4. Wang SX, Quan SG, Dong C. Kinetic of glass transition of $Zr_{57.2}Al_{21.4}Ni_{21.4}$ bulk metallic glass. Thermochim Acta. 2011; doi:10.1016/j.tca.2010.12.2005.
5. Kasap SO, Juhasz C. Kintematical transformations in amorphous selenium alloys used in xerography. J Mater Sci. 1986;21: 1329–40.
6. Larmagnac JP, Grenet J, Michon P. Glass transition temperature dependence on heating rate and on ageing for amorphous selenium films. J Non Cryst Solids. 1981;45:157–68.
7. Moynihan CT, Easteal AJ, Wilder J, Tucker J. Dependence of the glass transition temperature on heating and cooling rate. J Phys Chem. 1974;78:2673–7.
8. Mehta N, Kumar A. Applicability of Kissinger's relation in the determination of activation energy of glass transition process. J Optoelect Adv Mater. 2005;7:1473–8.
9. Moynihan CT. Correlation between the width of the glass transition region and the temperature dependence of the viscosity of high-T_g glasses. J Am Ceram Soc. 1993;76:1081–7.
10. Kissinger HE. Reaction kinetics in differential thermal analysis. Anal Chem. 1957;29:1702–6.
11. Abd El Ghani HA, Abd El Rahim MM, Wakkad KK, Abo Sehli A, Assraan N. Crystallization kinetics and thermal stability of some composition of Ge–In–Se chalcogenide system. Phys B. 2006;381:156–63.
12. Imran MMA, Saxena NS, Bhandari D, Husain M. Glass transition phenomena, Crystallization kinetics and enthalpy released in binary $Se_{100-x}In_x$ ($x = 2$, 4 and 10) semiconducting glasses. Phys Status Solidi (A). 2000;181:357–68.
13. Saxena M, Gupta S, Agarwal A. Kinetic investigation of glass transition in bulk $Te_x(Bi_2Se_3)_{1-x}$ chalcogenide glasses. Pelagia Res Lib. 2011;2:109–16.
14. Wang WM, Gebert A, Roth S, Kuehn U, Schultz L. Glass formability and fragility of $Fe_{61}Co_{9-x}Zr_8Mo_5W_xB_{17}$ ($x = 0$ and 2) bulk metallic glassy alloys. Intermetallics. 2008;16:267–72.
15. Angell CA. Structural instability and relaxation in liquid and glassy phases near the fragile liquid limit. J Non Cryst Solids. 1988;102:205–11.
16. Angell CA. Relaxation in liquids, polymers and plastic crystals–strong/fragile patterns and problems. J Non Cryst Solids. 1991; 131:13–31.
17. Lafi OA, Imran MMA. Compositional dependence of thermal stability, glass-forming ability and fragility index in some Se–Te–Sn glasses. J Alloys Compd. 2011. doi:10.1016/j.jallcom.2011.01.150.

Kinetics of crystallization of $Zr_{52}Cu_{18}Ni_{14}Al_{10}Ti_6$ metallic glass

Ashmi T. Patel & Arun Pratap

Journal of Thermal Analysis and Calorimetry
An International Forum for Thermal Studies

ISSN 1388-6150
Volume 107
Number 1

J Therm Anal Calorim (2012)
107:159-165
DOI 10.1007/s10973-011-1549-y

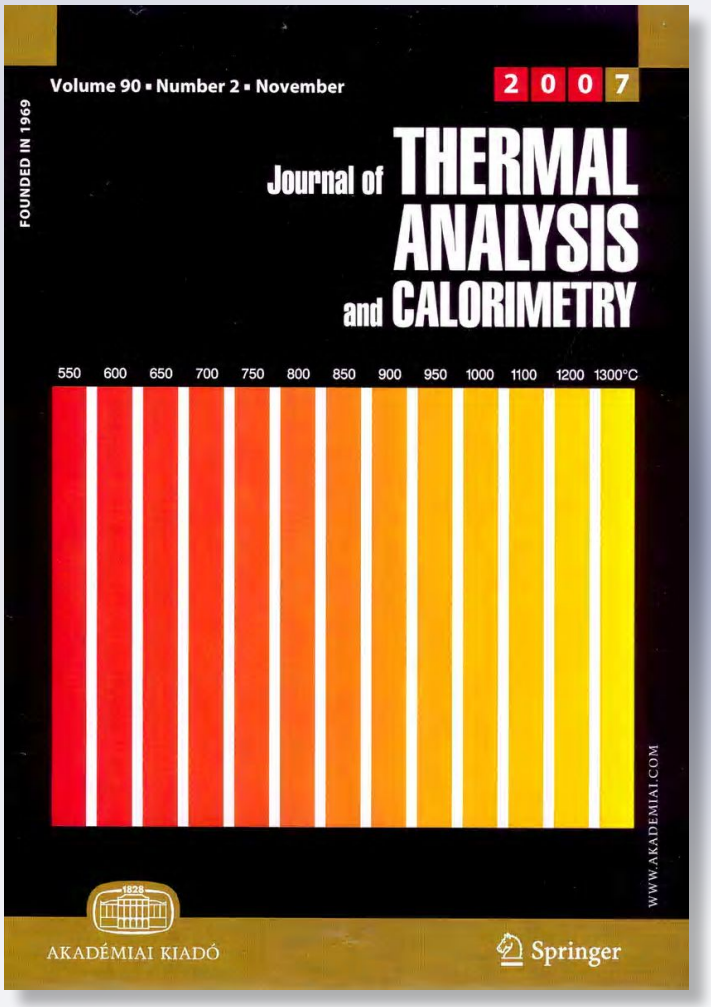

Springer

J Therm Anal Calorim (2012) 107:159–165
DOI 10.1007/s10973-011-1549-y

Kinetics of crystallization of $Zr_{52}Cu_{18}Ni_{14}Al_{10}Ti_6$ metallic glass

Ashmi T. Patel · Arun Pratap

29th STAC-ICC Conference Special Chapter

Abstract Metallic glasses have received considerable attention in comparison to normal metallic materials due to their superior physical and mechanical properties. These systems possess large under cooled region, ΔT ($\Delta T = T_x - T_g$ where, T_x is crystallization temperature and T_g is glass transition temperature) and hence increased thermal stability against crystallization. Due to this, the study of their crystallization kinetics is important and interesting. It is interesting because of the fact that, crystallization becomes multi-step process due to several components present in these systems. In this paper, we report the experimental investigations of crystallization of $Zr_{52}Cu_{18}Ni_{14}Al_{10}Ti_6$ glassy alloy system, which is among the best non-beryllium containing glasses, using differential scanning calorimetry (DSC). The crystallization, as expected, consists of multiple steps. Interestingly, the peak heights of these steps vary with heating rate. At lower heating rates, first peak is most prominent and subsequently diminishes with increase in heating rate with last peak prominence visible at highest heating rate. Both, iso-kinetic and isoconversional methods of analysis of kinetics of crystallization have been used to evaluate the activation energy and Avrami exponents and consistent results are obtained.

A. T. Patel · A. Pratap (✉)
Condensed Matter Physics Laboratory, Applied Physics Department, Faculty of Technology & Engineering, The M. S. University of Baroda, Vadodara 390001, India
e-mail: apratapmsu@yahoo.com

Keywords Crystallization kinetics · Isoconversional · Isokinetic · Metallic glass · Activation energy

Introduction

Metallic glasses are presently among the most actively studied metallic materials. A large number of multi-component systems with excellent glass forming ability (GFA), e.g., Pd- and Zr-based metallic glasses with critical diameters larger than 1 cm have been developed. In this work, the kinetics of the crystallization of $Zr_{52}Cu_{18}Ni_{14}Al_{10}Ti_6$ glass forming alloy have been studied, which is among the best nonberyllium containing glasses, making them easier to process and to handle [1]. The crystallization kinetics can be studied with the help of thermo-analytical techniques, e.g., differential scanning calorimetry (DSC) and differential thermal analyzer (DTA). These DSC/DTA experiments can be carried out in isothermal as well as non-isothermal [2–6] environment. To analyze the data obtained from DSC and hence to obtain kinetic parameters of the crystallization processes (such as activation energy, rate constant, etc.), there are several methods available in literature. These methods are generally based on either the isokinetic hypothesis or the isoconversional principle and they can be accordingly classified as (1) isokinetic methods where rate of reaction is considered to be the same throughout the temperature/time range; and (2) isoconversional methods, which are generally used for non-isothermal (linear heating) analysis, assume that the reaction rate at a constant degree of transformation is only a function of temperature. Therefore, in the isokinetic analysis, the kinetic parameters are assumed to be constant with respect to time and temperature; while in case of isoconversional study, the kinetic parameters are considered to be

dependent on the degree of transformation at different temperature and time [7].

Experimental methods

Specimens of amorphous $Zr_{52}Cu_{18}Ni_{14}Al_{10}Ti_6$ alloy were prepared by a melt spinning technique. The linear heating experiments were carried out on the as-quenched samples at four different linear heating rates (5, 10, 15, and 20 °C/min) in a DSC (DSC-50, Shimadzu, Japan) from room temperature to 833 K in air. The DSC has a minimum detection sensitivity of 10 μW. The samples of the metallic glass (5–6 mg) under consideration and the reference material α-Al_2O_3 were crimped in aluminum pans.

Theory

To study the phase transformation, which involves nucleation and growth, many methods are developed. Most of the methods depend on the transformation rate equation given by Kolmogorov, Johnson, Mehl, and Avrami [8–12], popularly known as KJMA equation, basically derived from experiments carried out under isothermal conditions. The KJMA rate equation is given by

$$\frac{d\alpha}{dt} = nk(1-\alpha)[-\ln(1-\alpha)]^{(n-1)/n} \quad (1)$$

where, α is degree of transformation at a given time t, n Avrami (growth) exponent, k the rate constant.

The Arrhenius form of the rate constant is given by

$$k(T) = k_0 \exp\left(-\frac{E}{RT}\right) \quad (2)$$

where, k_0 is pre-exponential factor, E activation energy, and R universal gas constant.

KJMA rate equation is based on some important assumptions and it has been suggested that the KJMA kinetic equation is accurate for reactions with linear growth subject to several conditions [13].

The isoconversional methods are also known as model-free methods. Therefore, the kinetic analysis using these methods is more deterministic and gives reliable values of activation energy E, which depend on degree of transformation, α. However, only activation energy will not give a perfect picture of crystallization kinetics. The microstructural information (e.g., dimensionality of the growth) of the precipitating phase during the transformation is also very important for understanding the whole kinetics of crystallization. Microstructural information would be known to us when we take the isokinetic methods into account. Therefore, the complementary use of both the methods is more useful for understanding the kinetics of crystallization.

Results and discussion

The DSC thermograms at four different heating rates (5, 10, 15, 20 deg/min) are shown in Fig. 1. The thermograms show three-stage crystallization process. The peak height of these steps varies with the heating rate. At lower heating rates, first peak is much distinct and diminishes as we go for higher heating rates and last peak visibility increases with increasing heating rate. Second peak is not much prominent in the 5, 10, and 15 deg/min heating rates. In this paper, the first peak is taken into consideration for the kinetic analysis. Glass transition temperature is not very evident in all four thermograms. The analysis of DSC data to evaluate the kinetic parameters can be obtained from non-isothermal rate laws by both isokinetic also known as model fitting methods and isoconversional methods.

Isoconversional analysis

Isoconversional methods evaluate the activation energy values at progressive degrees of conversion E_α without modelistic assumptions. The isoconversional methods can be broadly classified into two categories: (1) isothermal methods and (2) non-isothermal methods. The latter can further be classified as differential and integral methods. The isoconversional methods are based on the basic kinetic equation:

$$\frac{d\alpha}{dt} = k(T)f(\alpha) \quad (3)$$

$k(T)$ is the rate constant as given by Eq. 2 and $f(\alpha)$ is the reaction model which in case of KJMA formalism gives Eq. 1. The integral form of the above Eq. 3 can be given by

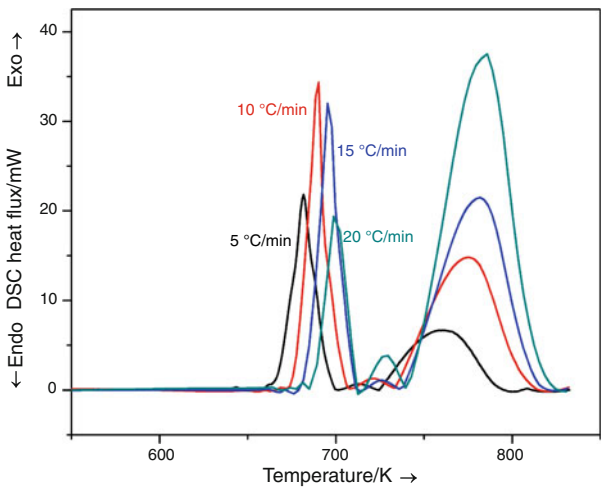

Fig. 1 DSC thermograms of the metallic glass $Zr_{52}Cu_{18}Ni_{14}Al_{10}Ti_6$ at different heating rates

$$g(\alpha) = \int_0^{\alpha} [f(\alpha)]^{-1} d\alpha = \frac{k_0}{\beta} \int_0^{T} \exp\left(-\frac{E}{RT}\right) dT \quad (4)$$

As mentioned earlier, exact solution of the temperature integral is not available and various approximations made for this has resulted into different methods. We have discussed a few most commonly used methods and kinetic parameters are calculated with the help of them. Different isoconversional methods are analyzed and discussed in detail by Starink [14].

Linear integral isoconversional methods

Kissinger–Akahira–Sunose (KAS) method Kissinger, Akahira, and Sunose [15, 16] used the approximation given by Coats and Redfern [17] to evaluate the integral in the rate Eq. 4. KAS method is based on the expression

$$\ln\left(\frac{\beta}{T^2}\right) = \ln\left(\frac{k_0 R}{E g(\alpha)}\right) - \frac{E}{RT} \quad (5)$$

The activation energy can be evaluated from the slope of plot $\ln(\beta/T^2)$ vs. $1000/T$ for constant conversion, α (Fig. 2) Values of E are given in Table 1. The discussion given ahead describes some of the methods available in the literature which are basically special cases of the KAS Eq. 5.

(i) Kissinger method: This well-known method assumes that the reaction rate is maximum at the peak temperature (T_p). This assumption also implies a constant degree of conversion (α) at T_p. The equation used by Kissinger is

$$\ln\left(\frac{\beta}{T_p^2}\right) = -\frac{E}{RT_p} + \ln\left(\frac{k_0 R}{E}\right) \quad (6)$$

Table 1 Local activation energy (E) at different conversion for different methods

α	E/kJ mol^{-1}		
	KAS	OFW	Friedman
0.1	264 ± 2	256.4 ± 2	245.5 ± 9
0.2	272 ± 2	269.5 ± 2	317.3 ± 7
0.3	278.8 ± 2	276 ± 2	303.9 ± 7
0.4	279.1 ± 2	276.3 ± 2	298.2 ± 3
0.5	280.7 ± 2	277.9 ± 2	295.7 ± 5
0.6	282.7 ± 3	279.7 ± 3	324 ± 5
0.7	285.7 ± 3	282.6 ± 3	320.7 ± 4
0.8	294 ± 3	290.5 ± 3	371.1 ± 4
0.9	303.8 ± 2	299.9 ± 2	360.5 ± 2

A plot of $\ln(\beta/T_p^2)$ vs. $1000/T_p$ (Fig. 3) gives an approximate straight line and the activation energy E and pre-exponential factor k_0 is calculated using the slope and the intercept (Table 2).

(ii) Augis and Bennett's method: This method was suggested by Augis and Bennett [18] and is an extension of Kissinger method showing its applicability to heterogeneous reaction described by Avrami expression. Apart from the peak crystallization temperature it also incorporates the onset temperature of crystallization, T_o and it is supposed to be a very accurate method of determining E through the equation

$$\ln\left(\frac{\beta}{(T_p - T_o)}\right) = -\frac{E}{RT_p} + \ln k_0 \quad (7)$$

where T_p and T_o are the peak and the onset temperatures of crystallization, respectively. The values of E and k_0 obtained from the plot ($\ln(\beta/(T_p - T_o))$ vs. $1000/T_p$ (Fig. 4) are given in Table 2.

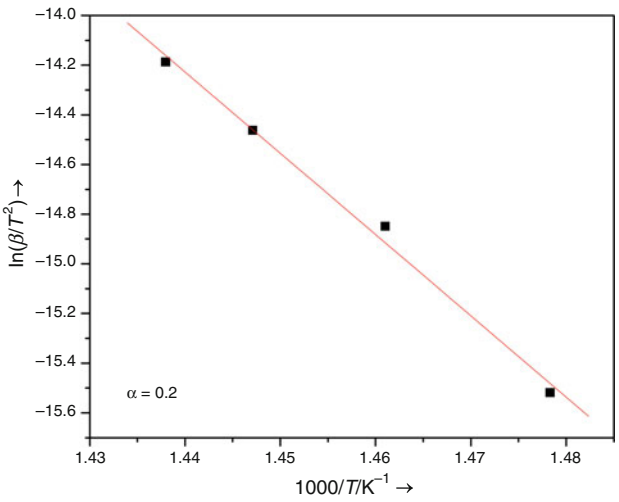

Fig. 2 KAS plot at $\alpha = 0.2$

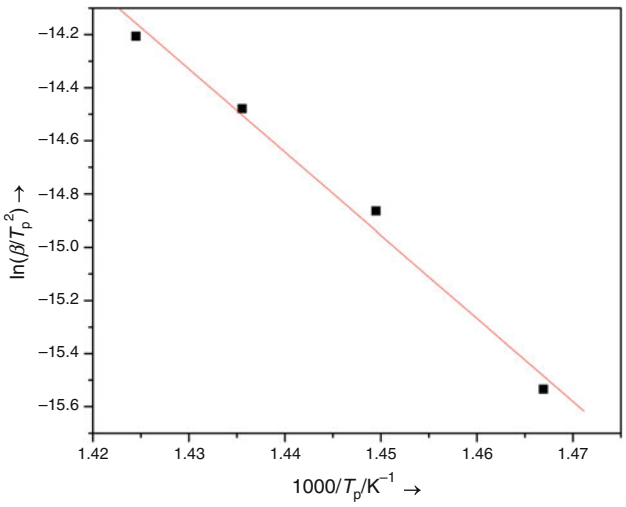

Fig. 3 Kissinger plot

Table 2 Activation energy (E) and pre-exponential factor (k_0) derived using various methods

Method	E/kJ mol^{-1}	k_0/s^{-1}
Kissinger	259.9 ± 2	4.86×10^{17}
Ozawa	258.1 ± 2	–
Augis and Bennett	271.7 ± 1	3.33×10^{18}
Boswell	256.4 ± 2	–
Gao and Wang	278.4 ± 3	–

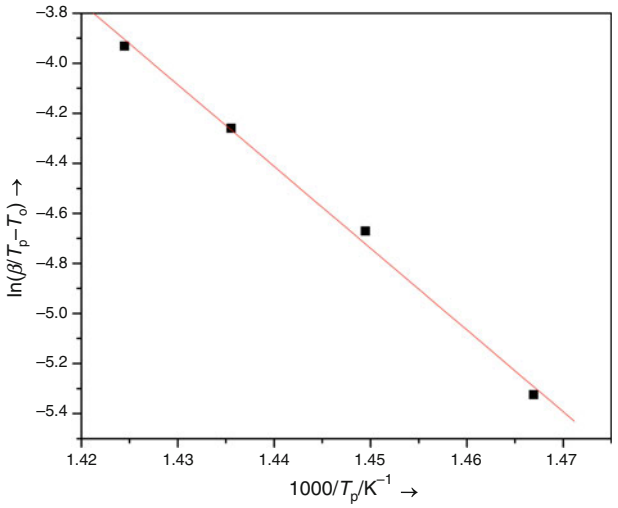

Fig. 4 Augis and Benett plot

Table 3 Values of Avrami exponent (n) from different methods

Heating rate	Augis and Bennett	Matusita and Sakka
4	2.5	2.7
6	3.5	2.9
8	3.1	2.9
10	2.8	3.0

Further,

$$n = 2.5\frac{T_p^2}{\Delta T\left(\frac{E}{R}\right)} \tag{8}$$

where ΔT is the full width at half maximum of the DSC curve. n derived using Eq. 8 is given in Table 3.

(iii) Boswell method: Boswell method [19] determines the activation energy at peak temperature (Table 2) using the following equation

$$\ln\left(\frac{\beta}{T_p}\right) = -\frac{E}{RT_p} + \text{const} \tag{9}$$

Plot of $\ln(\beta/T_p)$ vs. $1000/T_p$ (Fig. 5) gives the activation energy E listed in Table 2.

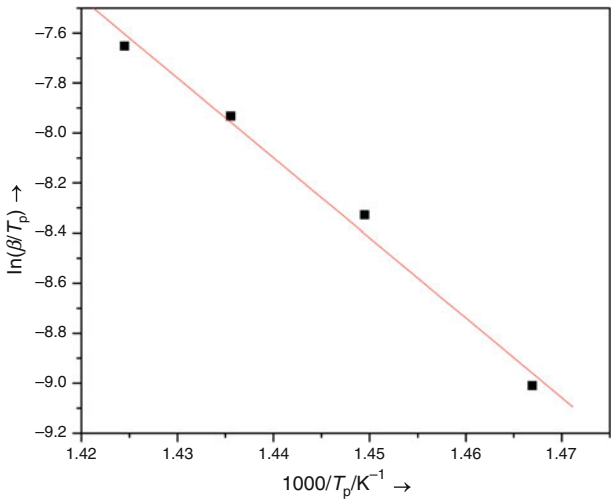

Fig. 5 Boswell plot

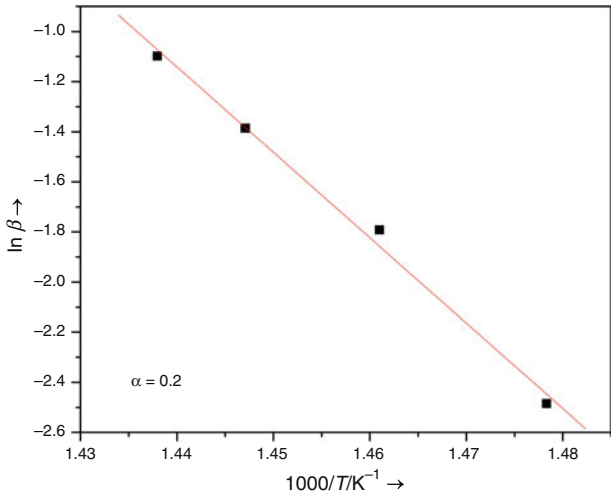

Fig. 6 OFW plot $\alpha = 0.2$

Ozawa–Flynn–Wall (OFW) method In this method [20, 21] the temperature integral in Eq. 4 is simplified by using the Doyle's approximation [22–24] and hence we obtain the following equation:

$$\ln\beta = -1.0516\frac{E(\alpha)}{RT_\alpha} + \text{const} \tag{10}$$

The plot of ln β vs. $1/T_\alpha$ (Fig. 6) gives the slope -1.0516 $E(\alpha)/R$ from which the activation energy has been evaluated (Table 1). At $T_\alpha = T_p$, (Ozawa method) the value of E determined (from Fig. 7) using Eq. 10 is given in Table 2.

Linear differential isoconversional method

The method suggested by Friedman [25] sometimes known as transformation rate-isoconversional method, utilizes the differential of the transformed fraction and hence it is

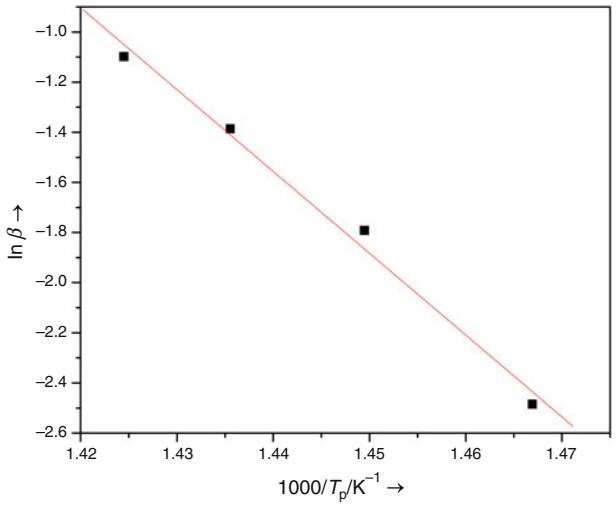

Fig. 7 Ozawa plot

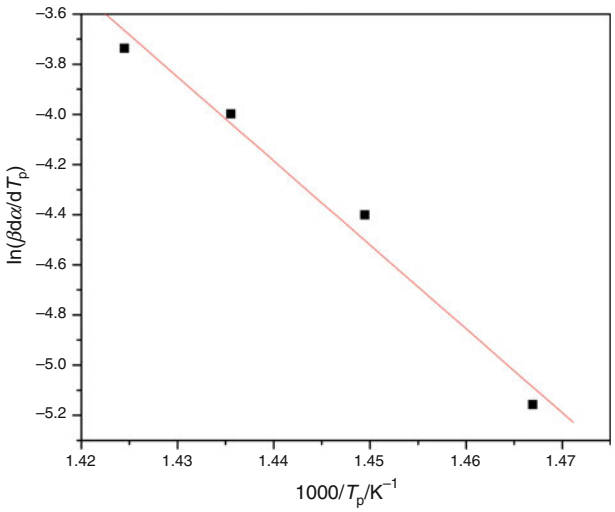

Fig. 9 Gao and Wang plot

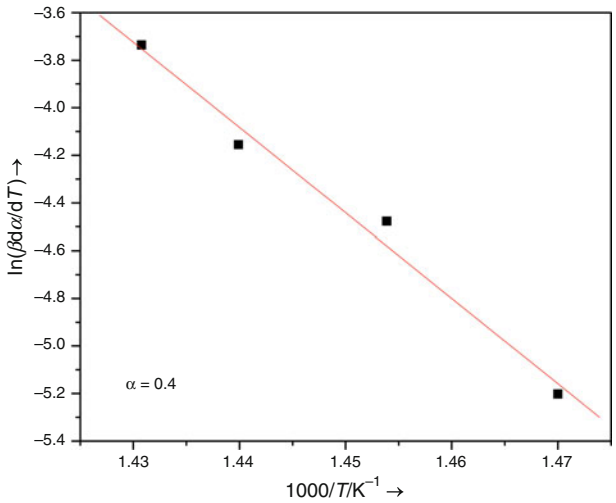

Fig. 8 Friedman plot $\alpha = 0.4$

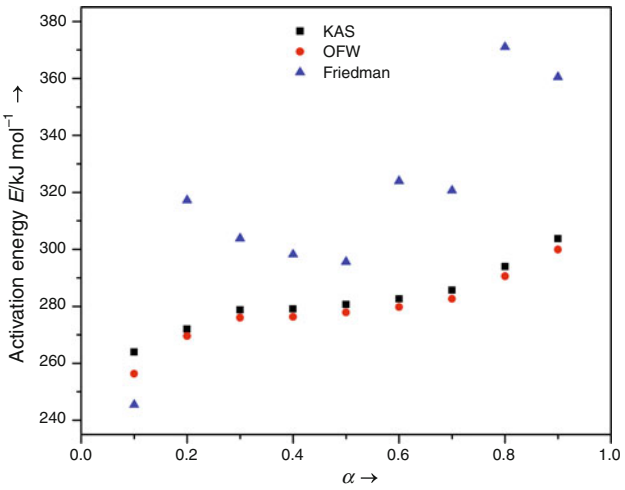

Fig. 10 Local activation energy E at different α from different methods

called differential isoconversional method. Substituting value of $k(T)$ in Eq. 3 Friedman derived a linear differential isoconversional expression as

$$\ln\left(\frac{\mathrm{d}\alpha}{\mathrm{d}t}\right)_\alpha = \ln\beta\left(\frac{\mathrm{d}\alpha}{\mathrm{d}T}\right)_\alpha = \ln(Af(\alpha)) - \frac{E_\alpha}{RT_\alpha} \tag{11}$$

by taking logarithm on both sides of Eq. 3. For a constant α, the plot of $\ln\left(\beta\frac{\mathrm{d}\alpha}{\mathrm{d}T}\right)$ vs $\left(\frac{1}{T}\right)$ should be a straight line (Fig. 8) whose slope gives us the value of E.

Since this method does not take any mathematical approximation for the temperature integral, it is considered to give accurate estimate of E. Thus the method does not require any assumption on $f(\alpha)$, i.e., it is a so-called model-free method. However, being a differential method, its accuracy is limited by the signal noise.

A method suggested by Gao and Wang [26] is a special case of the Friedman method. This method uses the following expression to determine the activation energy. The value of activation energy obtained is given in Table 2.

$$\ln\left(\beta\frac{\mathrm{d}\alpha}{\mathrm{d}T_\mathrm{p}}\right) = -\frac{E}{RT_\mathrm{p}} + \text{const} \tag{12}$$

A plot of $\ln\left(\beta\frac{\mathrm{d}\alpha}{\mathrm{d}T_\mathrm{p}}\right)$ vs. $\left(\frac{1}{T_\mathrm{p}}\right)$ is given in Fig. 9.

The values of local activation energy E_α as a function of α has been given in Table 1 using three different isoconversional methods namely, KAS, OFW, and Friedman. This result has also been shown graphically in Fig. 10. It appears from this graph that results obtained using KAS and OFW methods lie quite close to each other while Friedman points are quite scattered.

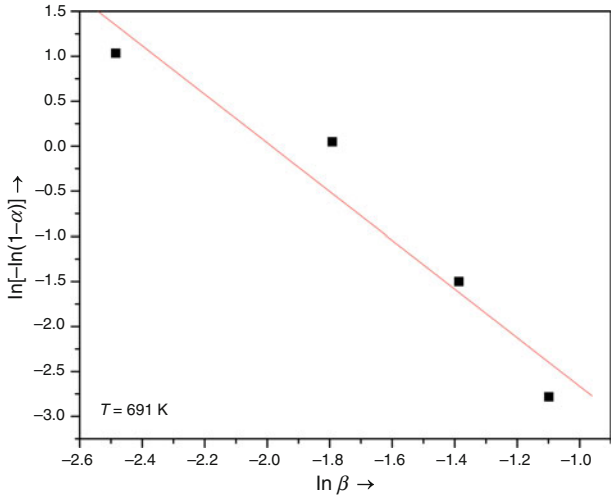

Fig. 11 Plot of $\ln[-\ln(1-\alpha)]$ vs. $\ln \beta$ at $T = 691$ K

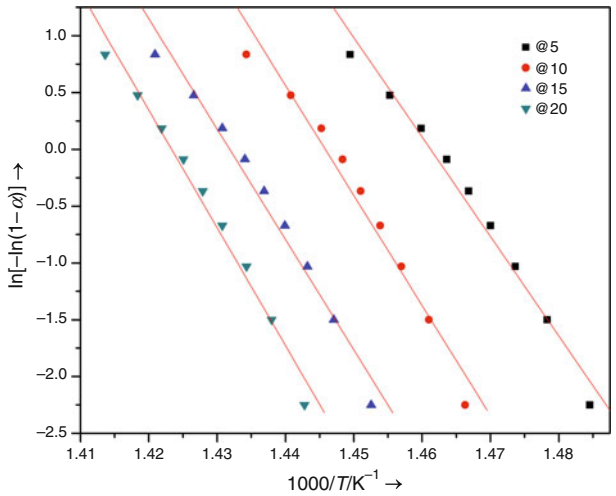

Fig. 12 Plot of $\ln[-\ln(1-\alpha)]$ vs. $1000/T$ for different heating rates

Isokinetic methods

Matusita and Sakka method

Matusita and Sakkka [27] suggested the following equation specifically for the non-isothermal data

$$\ln[-\ln(1-\alpha)] = -n \ln \beta - \frac{mE}{RT} + \text{const.} \quad (13)$$

where m is an integer depends on the dimensionality of the crystal and the Avarami exponent n depends on the nucleation process. For a constant temperature, the plot of $\ln[-\ln(1-\alpha)]$ vs. $\ln \beta$ gives a straight line (Fig. 11) and the slope gives the value of n. Here we have taken seven different constant temperatures and the average value of n comes out to be 2.66. The plot of $\ln[-\ln(1-\alpha)]$ vs. $1/T$ at constant heating rate should be a straight line and the value

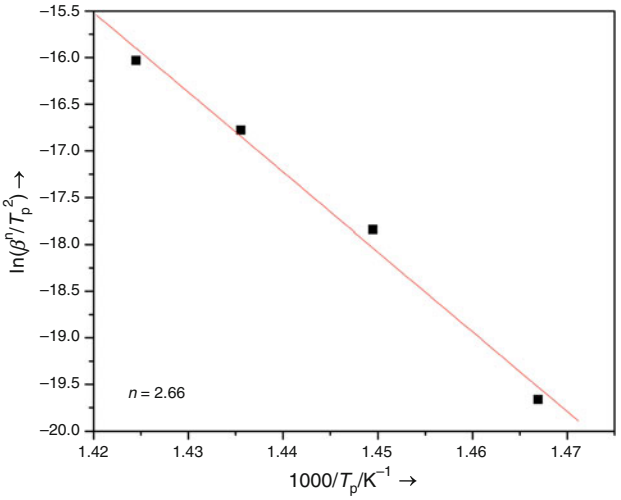

Fig. 13 Modified Kissinger plot for $n = 2.66$

of m is obtained from the slope (Fig. 12). Different values of n are derived from these m values by using $n = (m + 1)$ and are given in Table 3.

Modified Kissinger method

The modified Kissinger equation [28] given below can be utilized to derive the activation energy (E).

$$\ln\left(\frac{\beta^n}{T_p^2}\right) = -\frac{mE}{RT_p} + \text{const} \quad (14)$$

where E is the activation energy for crystallization, T_p is the peak temperature, and R is the universal gas constant. m is known as the dimensionality of growth and for the sample without preannealing treatment, $m = (n - 1)$. In order to derive E from this equation, one must know the value of n. The n value can be obtained from the slope of the plot of $\ln[-\ln(1-\alpha)]$ vs. $\ln \beta$ at constant temperature. In order to evaluate E, the average value of $n = 2.66$ is substituted in Eq. 14. Then the plot of $\ln\left(\frac{\beta^n}{T_p^2}\right)$ vs. $\frac{1}{T_p}$ (Fig. 13) gives the values of activation energy E, which is 428.12 kJ/mol.

Conclusions

Both model dependent isokinetic and model-free isoconversional methods have been utilized to study the crystallization kinetics of the first peak of the crystallization process involved in the presently taken system namely $Zr_{52}Cu_{18}Ni_{14}Al_{10}Ti_6$ metallic glass. The isokinetic methods, though model dependent, provide single value of activation energy. Besides, they also provide Avrami exponent n, which gives an idea about the dimensionality

of the growth of crystals. Isoconversional techniques, on the other hand, provide quite accurate values of E_α as a function of α as these analytical methods are supposed to be model free. It is obvious from the results obtained through KAS and OFW equations that activation energy initially increases with α. However, from $\alpha = 0.4$ to 0.5, there is an incremental increase in E_α. Thereafter, E_α increases again with α. This interesting result is an indication of the fact that even before first step of crystallization is completed, second step starts. The activation energy, E obtained using the Friedman method, on the other hand, show appreciable variation and there is no systematic trend. This is attributed to the signal noise involved [29]. It is also noteworthy that the activation energy values using various isoconversional methods and the special cases of isoconversional techniques namely Kissinger, Ozawa, Augis and Benett, Boswell, and Gao and Wang are quite consistent, whereas modified Kissinger method overestimates it. The isoconversional approach has been utilized to obtain the dependence of activation energy on transformed fraction for few Fe-based multicomponent amorphous alloys [30]. Various forms of the conversion function have been used and Sestak–Berggren function in temperature-programmed reduction has been recently reported [31].

References

1. Glade SC, Busch R, Lee DS, Johnson WL, Wunderlich RK, Fecht HJ. Thermodynamics of $Cu_{47}Ti_{34}Zr_{11}Ni_8$, $Zr_{52.5}Cu_{17.9}Ni_{14.6}Al_{10}Ti_5$ and $Zr_{57}Cu_{15.4}Ni_{12.6}Al_{10}Nb_5$ bulk metallic glass forming alloys. J Appl Phys. 2000;87:7242–8.
2. Ligero RA, Vazquez J, Villares P, Jimenez-Garay R. Crystallli-zation kinetics in the As–Se–Te system. Thermochim Acta. 1990;162:427–34.
3. Moharram AH, El-Oyoun MA, Abu-Sehly AA. Calorimetric study of the chalcogenide $Se_{72.5}Te_{20}Sb_{7.5}$ glass. J Phys D Appl Phys. 2001;34:2541–6.
4. Rysava N, Spasov T, Tichy L. Isothermal DSC methods for evaluation of the kinetics of crystallization in the Ge–Sb–S glassy system. J Therm Anal. 1987;32:1015–21.
5. Giridhar A, Mahadevan S. Studies on the As–Sb–Se glass system. J Non Cryst Solids. 1982;51:305–15.
6. Afify S. Differential scanning calorimetric study of chalcogenide glass $Se_{0.7}Te_{0.3}$. J Non Cryst Solids. 1991;128:279–84.
7. Lad KN, Savalia RT, Pratap A, Dey GK, Banerjee S. Isokinetic and isoconversional study of crystallization kinetics of a Zr-based metallic glass. Thermochim Acta. 2008;473:74–80.
8. Kolmogorov AN. On the statistical theory of the crystallization of metals. Bull Acad Sci USSR Phys Ser. 1937;3:555.
9. Johnson WA, Mehl PA. Reaction kinetics of nucleation and growth. Trans Am Inst Min Metall Eng. 1939;135:416–32.
10. Avrami M. Kinetics of phase change. I General theory. J Chem Phys. 1939;7:1103–12.
11. Avrami M. Kinetics of phase change. II Transformations-time relations for random distribution of nuclei. J Chem Phys. 1940; 8:212–24.
12. Avrami M. Granulation, phase change, and microstructure kinetics of phase change. III. J Chem Phys. 1941;9:177–84.
13. Starink MJ. On the meaning of the impingement parameter in kinetic equations for nucleation and growth reactions. J Mater Sci. 2001;36:4433–41.
14. Starink MJ. The determination of activation energy from linear heating rate experiments: a comparison of the accuracy of isoconversion methods. Thermochim Acta. 2003;404:163–76.
15. Kissinger HE. Reaction kinetics in differential thermal analysis. Anal Chem. 1957;29:1702–6.
16. Akahira T, Sunose T. Joint convention of four electrical institutes. Res Report Chiba Inst Technol. 1971;16:22–31.
17. Coats AW, Redfern JP. Kinetic parameters from thermogravimetric data. Nature. 1964;201:68–9.
18. Augis JA, Bennett JE. Calculation of the Avrami parameters for heterogeneous solid state reactions using a modification of the Kissinger method. J Therm Anal. 1978;13:283–92.
19. Boswell PG. On the calculation of activation energies using modified Kissinger method. J Therm Anal. 1980;18:353–8.
20. Ozawa T. A new method of analyzing thermogravimetric data. Bull Chem Soc Jpn. 1965;38:1881–6.
21. Flynn JH, Wall LA. General treatment of the thermogravimetry of polymers. J Res Natl Bur Stand A Phys Chem. 1966;70A: 487–523.
22. Doyle CD. Kinetic analysis of thermogravimetric data. J Appl Polym Sci. 1961;5:285–92.
23. Doyle CD. Estimating isothermal life from thermogravimetric data. J Appl Polym Sci. 1962;6:642–93.
24. Doyle CD. Series approximations to the equation of thermogravimetric data. Nature. 1965;207:290–1.
25. Friedman HL. Kinetics of thermal degradation of char-forming plastics from thermogravimetry. Application to phenolic plastic. J Polym Sci. 1964;C6:183–95.
26. Gao YQ, Wang W. On the activation energy of crystallization in metallic glasses. J Non Cryst Solids. 1986;81:129–34.
27. Matusita K, Sakka S. Kinetic study of crystallization of glass by differential scanning calorimetry. Phys Chem Glasses. 1979;20: 81–4.
28. Matusita K, Sakka S. Kinetic study on crystallization of glass by differential thermal analysis—criterion on application of Kissinger plot. J Non Cryst Solids. 1980;38–39:741–6.
29. Dhurandhar H, Patel AT, Shanker Rao TL, Lad KN, Pratap A. Kinetics of crystalllization of co-based multi-component amorphous alloy. J ASTM Int. 2010;7:1–15.
30. Sunol JJ, Bonastre J. Crystallization kinetics of metallic glasses. J Therm Anal Calorim. 2010;102:447–50.
31. Munteanu G, Segal E. Sestak–Berggren function in temperature-programmed reduction. J Therm Anal Calorim. 2010;101:89–95.

Thermodynamics of $Zr_{52.5}Cu_{17.9}Ni_{14.6}Al_{10}Ti_5$ bulk metallic glass forming alloy

Ashmi T. Patel, Heena R. Shevde & Arun Pratap

Journal of Thermal Analysis and Calorimetry
An International Forum for Thermal Studies

ISSN 1388-6150
Volume 107
Number 1

J Therm Anal Calorim (2012)
107:167-170
DOI 10.1007/s10973-011-1591-9

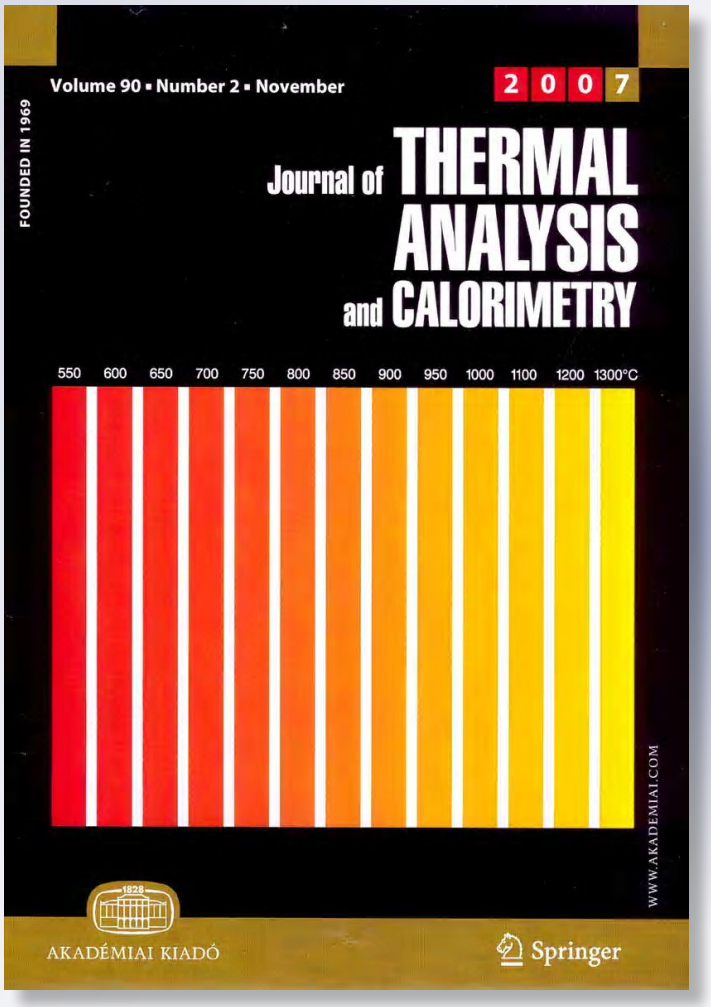

Springer

J Therm Anal Calorim (2012) 107:167–170
DOI 10.1007/s10973-011-1591-9

Thermodynamics of $Zr_{52.5}Cu_{17.9}Ni_{14.6}Al_{10}Ti_5$ bulk metallic glass forming alloy

Ashmi T. Patel · Heena R. Shevde · Arun Pratap

29th STAC-ICC Conference Special Chapter

Abstract Recently, multicomponent glass forming alloys have been found which exhibit extraordinary glass forming ability and cooling rates of less than 100 K/s are sufficient to suppress nucleation of crystalline phases and consequently bulk metallic glass (BMG) is formed. The undercooled melts of BMG systems have high thermal stability in the undercooled region. Therefore, it is interesting to study the thermodynamics of such materials. This article investigates the thermodynamic behavior of a BMG system namely $Zr_{52.5}Cu_{17.9}Ni_{14.6}Al_{10}Ti_5$ by estimating the Gibbs free energy difference ΔG, entropy difference ΔS, enthalpy difference ΔH between the undercooled liquid and corresponding equilibrium crystalline solid phase, in the entire temperature range from T_m to T_K. Glass forming ability (GFA) of this system has been investigated through various GFA parameters indicating the degree of ease of glass formation.

Keywords Bulk metallic glass · Thermodynamic properties · Undercooling · Glass forming ability

A. T. Patel · A. Pratap (✉)
Condensed Matter Physics Laboratory, Applied Physics Department, Faculty of Technology & Engineering, The M. S. University of Baroda, Vadodara 390 001, India
e-mail: apratapmsu@yahoo.com

H. R. Shevde
Department of Electronics, Mukesh Patel School of Technology Management and Engineering, SVKM's NMIMS Deemed University, Vile Parle West, Mumbai 400 056, India

Introduction

In this modern era of new technology, a number of new bulk metallic glass (BMG) forming alloys have been developed. These alloys may solidify as a glass when cooled at sufficient rates, known as critical cooling rates. They possess excellent corrosion resistance, extremely high mechanical strength and have fairly good thermal stability. The thermodynamic functions of metallic glass forming alloys in the undercooled liquid phase provide information about their glass forming ability. It is normally accepted that the stability of the undercooled melt exponentially depends on nucleation rate of a crystalline phase, which is a good indicator of the glass forming ability (GFA) [1–3]. The classical nucleation theory suggests that the nucleation rate is known by thermodynamic and kinetic factors. The thermodynamic contribution is mainly given by the Gibbs free energy difference, ΔG, between the undercooled liquid and corresponding crystalline phase, entropy difference, ΔS and enthalpy difference, ΔH. Gibbs free energy difference, ΔG between undercooled melt and corresponding crystalline solid acts as the driving force of crystallization. In an amorphous alloy system, lower value of ΔG indicates less driving force of crystallization, which enhances stability of metallic supercooled liquid and leads to better glass forming ability. In fact, ΔG is the best glass forming ability indicator compared to other glass forming ability criteria. The Gibbs free energy difference, ΔG gives a qualitative measure of the stability of the glass compared to the crystalline state.

In this article, we investigate the thermodynamic behavior of $Zr_{52.5}Cu_{17.9}Ni_{14.6}Al_{10}Ti_5$ by calculating ΔG in the entire temperature range from T_m to T_K. This amorphous mulitcomponent alloy is one of the best nonberyllium containing glasses, making it easier to process and

manage [4]. In order to find out the thermodynamic properties of BMG, knowledge of specific heat difference, ΔC_p is required. However, in most of the cases, the specific heat capacity data of undercooled liquid is not available because of its metastable nature. Due to the nonavailability of specific heat data in the undercooled region, the temperature dependence of ΔG, ΔS, and ΔH must be estimated with the help of theoretical formulation.

Formulation of theoretical expressions

In this article, the expression for ΔG is based on linear and hyperbolic variations of ΔC_p with temperature and does not consider limited undercooling region to take care of large undercooled region of this alloy. The results obtained show excellent agreement with ΔG obtained using experimental data [4]. There are number of expressions available for calculations of ΔG in the literature [5–11], in which the assumption of $\Delta C_p =$ constant has been taken. Values of ΔG are obtained using these equations and compared with the present calculations.

Now, the Gibbs free energy difference between undercooled melt and corresponding crystalline phase is given by

$$\Delta G = \Delta H - T\Delta S \tag{1}$$

where

$$\Delta H = \Delta H_{\mathrm{m}} - \int_{T}^{T_{\mathrm{m}}} \Delta C_p \mathrm{d}T \tag{2}$$

and

$$\Delta S = \Delta S_{\mathrm{m}} - \int_{T}^{T_{\mathrm{m}}} \Delta C_p \frac{\mathrm{d}T}{T} \tag{3}$$

where T_{m} is the melting temperature, ΔS_{m} is the entropy of fusion, and ΔH_{m} is the enthalpy of fusion. They are related to each other by the following relation:

$$\Delta S_{\mathrm{m}} = \frac{\Delta H_{\mathrm{m}}}{T_{\mathrm{m}}} \tag{4}$$

ΔC_p, defined as $C_p^{\mathrm{l}} - C_p^{x}$, is the difference in specific heats of the liquid and corresponding crystalline phases of metallic alloy. Therefore, experimental ΔG can be calculated using Eqs. 1–3, if the experimental specific heat data is available for the undercooled and the crystal phases of a material. However, metallic liquids are generally not stable over an extended temperature range in the supercooled liquid, making it difficult to determine the specific heat capacity; one has to switch to suitable expression of ΔC_p that effectively represents the temperature dependence of ΔC_p.

In this study, the difference in specific heat capacity is determined using linear and hyperbolic variations with temperature, which involves coefficients A & B for linear trend and C & D for hyperbolic trend. These four coefficients are easily evaluated with the help of ΔC_p^{m} and T_{K}, where ΔC_p^{m} is specific heat difference at melting temperature and T_{K} is Kauzmann temperature also known as isentropic temperature because at T_{K} the entropy difference, ΔS becomes zero.

Considering the most common linear expression which is given by

$$\Delta C_p = AT + B \tag{5}$$

Inserting Eq. 5, in Eqs. 2 and 3, Eq. 1 can be simplified to

$$\Delta G = \frac{\Delta H_{\mathrm{m}} \Delta T}{T_{\mathrm{m}}} - \frac{1}{2} A (\Delta T)^2 + B\left(T \ln \frac{T_{\mathrm{m}}}{T} - \Delta T\right) \tag{6}$$

where the undercooling $\Delta T = T_{\mathrm{m}} - T$.

Now, taking the hyperbolic variation of ΔC_p, which is given by

$$\Delta C_p = \frac{C}{T} + D \tag{7}$$

Substituting ΔC_p from the above equation in Eqs. 2 and 3 and simplifying Eq. 1, one can get the following expression

$$\Delta G = \frac{\Delta H_{\mathrm{m}} \Delta T}{T_{\mathrm{m}}} + \ln \frac{T_{\mathrm{m}}}{T}(DT - C) - \Delta T\left(D - \frac{C}{T_{\mathrm{m}}}\right) \tag{8}$$

There are four unknown constants A & B and C & D in the ΔG expressions (6) and (8), respectively. Since there are two unknowns in both linear and hyperbolic case, one needs another expression for evaluation of the constants. By deriving an expression for ΔS from that of ΔG given by Eqs. 6 and 8 using the following relation

$$\Delta S = -\frac{\partial \Delta G}{\partial T} \tag{9}$$

one can easily find out the required constants.

In the case of linear dependence of ΔC_p on T, one gets the following expression for ΔS through Eq. 9

$$\Delta S = \frac{\Delta H_{\mathrm{m}}}{T_{\mathrm{m}}} - A\Delta T - B \ln \frac{T_{\mathrm{m}}}{T} \tag{10}$$

Utilizing the condition that ΔS becomes zero at isentropic temperatures, T_{K} also known as Kauzmann temperature one easily gets the unknown constants A and B in terms of known experimental parameters

$$A = \frac{\frac{\Delta H_{\mathrm{m}}}{T_{\mathrm{m}}} - \Delta C_p^{\mathrm{m}} \ln \frac{T_{\mathrm{m}}}{T_{\mathrm{K}}}}{T_{\mathrm{m}} - T_{\mathrm{K}} - T_{\mathrm{m}} \ln \frac{T_{\mathrm{m}}}{T_{\mathrm{K}}}} \tag{11}$$

and

$$B = \Delta C_p^{\mathrm{m}} - AT_{\mathrm{m}} \tag{12}$$

Similarly, the expression for ΔS in case of hyperbolic dependence of ΔC_p on T obtained from Eq. 9 by partial differentiation of Eq. 8 provides

$$\Delta S = \frac{\Delta H_{\mathrm{m}}}{T_{\mathrm{m}}} - D\ln\frac{T_{\mathrm{m}}}{T} - C\left(\frac{T_{\mathrm{m}} - T}{T_{\mathrm{m}}T}\right) \tag{13}$$

One gets the expressions for constants C and D from Eq. 13 after solving it for $\Delta S = 0$ at Kauzmann temperature, $T = T_{\mathrm{K}}$

$$C = \frac{\Delta H_{\mathrm{m}} - T_{\mathrm{m}}\Delta C_p^{\mathrm{m}}\ln\frac{T_{\mathrm{m}}}{T_{\mathrm{K}}}}{\frac{T_{\mathrm{m}}-T_{\mathrm{K}}}{T_{\mathrm{K}}} - \ln\frac{T_{\mathrm{m}}}{T_{\mathrm{K}}}} \tag{14}$$

and

$$D = \Delta C_p^{\mathrm{m}} - \frac{C}{T_{\mathrm{m}}} \tag{15}$$

Either of the Eqs. 6 and 8 can be used to evaluate ΔG in the entire undercooled region, when the constants A & B for linear nature and C & D for hyperbolic trend are known through Eqs. 11 & 12 and 14 & 15, respectively.

Results and discussion

Figure 1 shows the Gibbs free energy difference between undercooled liquid and corresponding crystalline solid for $Zr_{52.5}Cu_{17.9}Ni_{14.6}Al_{10}Ti_5$. It is obvious from the figure that plots of ΔG estimated using linear and hyperbolic variation of ΔC_p almost coincide with the experimental points in the entire undercooled region and hence are in excellent agreement with the experiment. The parameters used [4] for calculations of ΔG are given in Table 1. Surprisingly, expression given by Lad et al. [9] abbreviated as Lad-1 provides results somewhat closer to the experimental ones, even though ΔC_p = constant assumption has been taken in this approach. Other expressions given by various workers either underestimate or overestimate ΔG particularly in large undercooled region. Since ΔG is the driving force for crystallization, its accurate evaluation is important from the view point of alloy design for various applications.

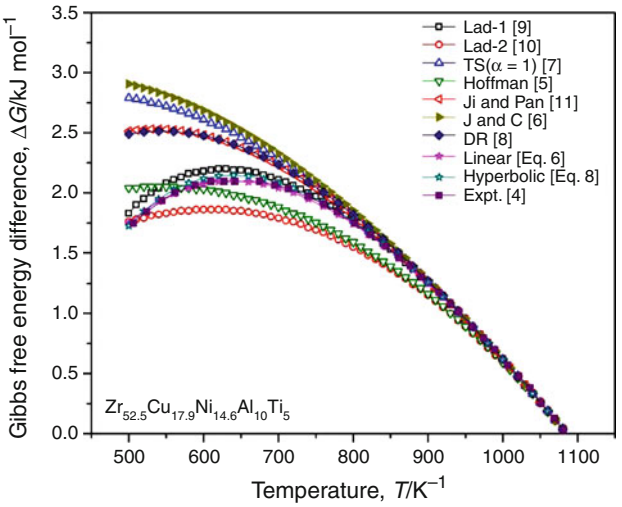

Fig. 1 Gibbs free energy difference, ΔG as a function of temperature, T for $Zr_{52.5}Cu_{17.9}Ni_{14.6}Al_{10}Ti_5$

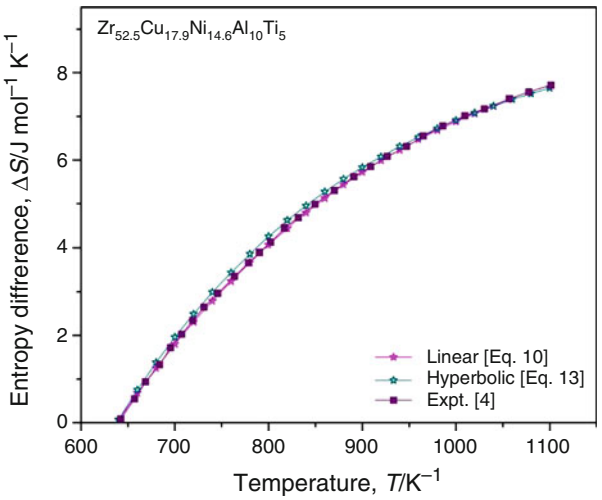

Fig. 2 Entropy difference, ΔS as a function of temperature, T for $Zr_{52.5}Cu_{17.9}Ni_{14.6}Al_{10}Ti_5$

The entropy difference, ΔS between the undercooled liquid and corresponding crystalline solid has been obtained from the derivative of the plotted ΔG using Eqs. 10 and 13 and the same has been shown in Fig. 2 along with experimental results of Glade et al. [4]. It can be seen from the figure that the present approach accounts for accurate ΔS values in the entire temperature range and is matching excellently with the experimental points. Calculations using other theoretical expressions have not been shown as they are expected to show large variation from experiment. This has already been indicated in the ΔG plot and ΔS have been derived using the derivative of ΔG only. ΔH, the enthalpy difference between undercooled liquid and corresponding crystalline solid has been also evaluated from the known values of ΔG and ΔS using Eq. 1. The

Table 1 Parameters used for calculation of thermodynamic quantities ΔG, ΔS, and ΔH and different GFA criteria

System	T_g/K	T_x/K	T_m/K	T_l/K	T_K/K	ΔH_m/kJ mol^{-1}	ΔC_p^m/J mol^{-1}K^{-1}	ΔS_m/J mol^{-1}K^{-1}	Ref.
$Zr_{52.5}Cu_{17.9}Ni_{14.6}Al_{10}Ti_5$	675	727	1085	1091	638	8.2	7.02	7.6	[4]

Table 2 Different GFA criteria

System	$\delta = \frac{T_K}{T_m}$	$T_{rg} = \frac{T_g}{T_m}$	$\gamma_m = \frac{(2T_x - T_g)}{T_l}$	$\gamma = \frac{T_x}{T_g + T_l}$	$\frac{T_x}{T_l}$	$\frac{\Delta C_p^m}{\Delta S_m}$	$\Delta G(T_K)$/kJ mol^{-1}
$Zr_{52.5}Cu_{17.9}Ni_{14.6}Al_{10}Ti_5$	0.588	0.622	0.714	0.412	0.666	0.923	2.11
$Zr_{57}Cu_{15.4}Ni_{12.6}Al_{10}Nb_5$	0.601	0.617	0.719	0.413	0.665	1.514	2.18

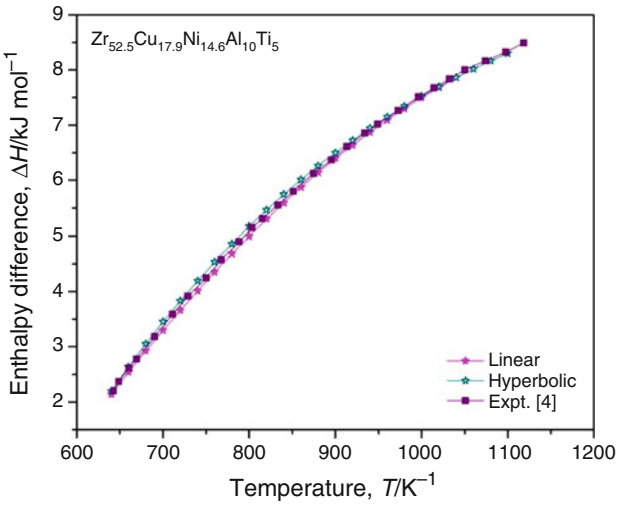

Fig. 3 Enthalpy difference, ΔH as a function of temperature, T for $Zr_{52.5}Cu_{17.9}Ni_{14.6}Al_{10}Ti_5$

difference in the enthalpy between the liquid and the crystalline states at the glass transition, should in principle, provide the amount of enthalpy frozen into the liquid at T_g. The changing thermodynamics between the phases has also been recently investigated [12].

Besides the evaluation of ΔG in the undercooled region, various other GFA parameters [13] indicating the tendency of glass formation in this system have been derived and are given in Table 2. For getting an idea of relative glass forming tendency of this system, GFA indicating parameters of another system [3] having Nb in place of Ti have also been listed in the same Table. From the Table, it appears that glass forming ability of both these systems is nearly identical. Addition of an extra element like Nb or Ti does not seem to affect the GFA of Zr–Cu–Ni–Al system [14] reported to have super high glass forming ability (Figure 3).

Conclusions

The theoretical formulations used in this study provide excellent results for thermodynamic parameters ΔG, ΔS, and ΔH in the entire undercooled region of BMG forming alloy, $Zr_{52.5}Cu_{17.9}Ni_{14.6}Al_{10}Ti_5$. Among these three parameters, accurate evaluation of ΔG is very important as its value is an indicator of GFA of BMG's. It is obvious from the ΔG values obtained for this system that it has fairly good glass forming tendency owing to smaller value of ΔG. ΔG is a signature of driving force for crystallization. Other two parameters, ΔS and ΔH follow from ΔG and hence these two also show one to one correspondence with the experiment. Further, the present system exhibits good glass forming tendency as indicated by various GFA parameters.

References

1. Wunderlich RK, Fecht H. Thermophysical properties of bulk metallic forming alloys in the stable and undercooled liquid—a microgravity investigation. Mater Trans. 2001;42:565–78.
2. Legg BA, Schrores J, Busch R. Thermodynamics, kinetics, and crystallization of $Pt_{57.3}Cu_{14.6}Ni_{5.3}P_{22.8}$ bulk metallic glass. Acta Mater. 2007;55:1109–16.
3. Patel AT, Shevde HR, Pratap A. Thermodynamic study of bulk metallic glass: $Zr_{57}Cu_{15.4}Ni_{12.6}Al_{10}Nb_5$. J Sci Technol Manag. 2011;3(1):9–12.
4. Glade SC, Busch R, Lee DS, Johnson WL, Wunderlich RK, Fecht HJ. Thermodynamics of $Cu_{47}Ti_{34}Zr_{11}Ni_8$, $Zr_{52.5}Cu_{17.9}Ni_{14.6}Al_{10}Ti_5$ and $Zr_{57}Cu_{15.4}Ni_{12.6}Al_{10}Nb_5$ bulk metallic glass forming alloys. J Appl Phys. 2000;87:7242–8.
5. Hoffman JD. Thermodynamic driving force in nucleation and growth processes. J Chem Phys. 1958;29:1192–3.
6. Jones DRH, Chadwick GA. An expression for the free energy of fusion in the homogeneous of solid from pure melts. Phil Mag. 1971;24:995–8.
7. Thompson CV, Spaepen F. On the approximation of free energy change on crystallization. Acta Metall. 1979;27:1855–9.
8. Dubey KS, Ramachandrarao P. On the free energy change accompanying crystallization of undercooled melts. Acta Metall. 1984;32:91–6.
9. Lad KN, Pratap A, Raval KG. Estimation of the free energy change on crystallization of multicomponent glass forming alloys. J Mater Sci Lett. 2002;21:1419–22.
10. Lad KN, Raval KG, Pratap A. Estimation of Gibbs free energy difference in bulk metallic glass forming alloys. J Non-Cryst Solids. 2004;334–335:259–62.
11. Ji X, Pan Y. Gibbs free energy difference in metallic glass forming liquids. J Non-Cryst Solids. 2007;353:2443–6.
12. Wunderlich B. Thermodynamic description of condensed phases. J Therm Anal Calorim. 2010;102:413–24.
13. Singh PK, Dubey KS. Analysis of thermodynamic behaviour of bulk metallic glass forming melts and glass forming ability. J Therm Anal Calorim. 2010;100:347–53.
14. Sun YJ, Qu DD, Huang YJ, Liss KD, Wei XS, Xing DW, Shen J. Zr–Cu–Ni–Al bulk metallic glasses with superhigh glass forming ability. Acta Mater. 2009;57:1290–9.

Solid State Phenomena Vol. 171 (2011) pp 121-126
Online available since 2011/May/17 at www.scientific.net

doi:10.4028/www.scientific.net/SSP.171.121

Glass forming ability of Ca-based bulk metallic glasses

Ashmi T. Patel [a], Kirit N. Lad [b] and Arun Pratap [c]

Condensed Matter Physics Laboratory, Applied Physics Department, Faculty of Technology and Engineering, The M. S. University of Baroda, Vadodara – 390 001, India

[a] ashmi0707@yahoo.co.in, [b] kiritlad@yahoo.com, [c] apratapmsu@yahoo.com

Key words: Glass forming ability, Gibbs free energy, Bulk metallic glasses

Abstract. Knowledge of glass forming ability (GFA) of amorphous metallic alloys is very important from both theoretical and practical point of view. Thermodynamically, the Gibbs free energy difference, ΔG between the undercooled liquid and the corresponding crystalline state is driving force for crystallization. As a consequence, it is a good indicator for glass forming ability of metallic glasses. A novel expression for ΔG has been used to estimate the GFA of recently developed Ca-based bulk metallic glasses viz. $Ca_{53}Mg_{23}Cu_{24}$,$Ca_{65}Mg_{15}Cu_{20}$,$Ca_{40}Mg_{25}Cu_{35}$, $Ca_{50}Mg_{22.5}Cu_{27.5}$ and $Ca_{55}Mg_{15}Cu_{30}$. Different GFA criteria are also evaluated for systems taken up in the study and effect of addition of variation in composition of Ca-Mg-Cu system is also investigated. Present work suggests that among different GFA criteria, ΔG is the best criterion for the prediction of GFA for Ca-based bulk metallic glasses.

Introduction

Bulk metallic glasses (BMGs) have been discovered in many multicomponent alloy systems after the first successful formation of metallic glasses by rapid solidification of liquid alloy. The critical thickness of these alloy systems has been increased from 1mm to several centimeters in the past decades. From the physical metallurgy point of view, critical thickness is directly related to critical cooling rate, R_c, above which the multicomponent BMG forming systems are supposed to be fully amorphous as no crystallization occurs. R_c, in turn, is a measure of glass forming ability (GFA) of these BMGs. In fact, lower R_c corresponds to higher GFA [1] and vice versa. Although R_c is a parameter which provides a way to evaluate and compare the GFA of various alloy systems, a number of solidification trials with different cooling rates are required [2]. In order to simplify the experiments, many theoretical approaches have been proposed [3-10] to explore the possibility of designing new glasses with improved GFA [11-13], large supercooled liquid region and high thermal stability. The most extensively used GFA criteria are the reduced glass transition temperature, T_{rg}, the parameter, γ and the supercooled liquid range, ΔT_x [3,5,6]. Actually, quite a large number of good glass forming systems obey these criteria barring few exceptions [14-15]. Recently, Suo et al [16] have proposed a new criterion for the evaluation of GFA of Ca-based BMGs. This approach combines the liquid phase stability, resistance to crystallization and the glass transition enthalpy. Ca-based bulk metallic glasses are a relatively new class of light weight amorphous alloys and have been formed with simple alkaline earth metals (Ca and Mg) and late transition metals (e.g. Ag, Cu, Zn and Ni). They have some unique properties such as low characteristic temperatures, low density, low moduli and good biocompatibility.

Present work reports the estimation of GFA of Ca-based bulk metallic glasses at five compositions viz. $Ca_{53}Mg_{23}Cu_{24}$,$Ca_{65}Mg_{15}Cu_{20}$,$Ca_{40}Mg_{25}Cu_{35}$, $Ca_{50}Mg_{22.5}Cu_{27.5}$ and $Ca_{55}Mg_{15}Cu_{30}$ through ΔG. Besides, a comparative study of the present investigation of GFA of these BMGs has also been done with other existing GFA parameters.

Theoretical formulations

I. Thermodynamics of Amorphous alloys. Knowledge of the thermodynamic properties i.e, Gibbs free energy difference (ΔG), entropy difference (ΔS), enthalpy difference (ΔH) and specific

heat differece (ΔC_p), plays an important role in order to find out the glass forming ability and thermal stability of metallic amorphous alloys.The Gibbs free energy differece gives a qualitative measure of the stability of the glass compared to the crystalline state.

The difference in Gibbs free energy between the liquid and crystalline phases is given by

$$\Delta G = \Delta H - T\Delta S \tag{1}$$

where

$$\Delta H = \Delta H_m - \int_T^{T_m} \Delta C_p dT \tag{2}$$

and

$$\Delta S = \Delta S_m - \int_T^{T_m} \Delta C_p \frac{dT}{T} \tag{3}$$

where, T_m is the melting temperature, ΔS_m is the entropy of fusion and ΔH_m is the enthalpy of fusion. They are related to each other by the following relation:

$$\Delta S_m = \frac{\Delta H_m}{T_m} \tag{4}$$

ΔC_p, defined as $C_p^l - C_p^x$, is the difference in specific heats of the liquid and corresponding crystalline phases of metallic alloy. Therefore, experimental ΔG can be calculated using Eq. (1) - (3), if the experimental specific heat data is available for the undercooled and the crystal phases of a material. However, due to the metastable nature of amorphous metallic materials experimental ΔC_p data is unavailable; therefore one has to switch to suitable expression of ΔC_p that adequately represents the temperature dependence of ΔC_p. The most common is the linear expression given by

$$\Delta C_p = AT + B \tag{5}$$

Substituting Eq. (5) in Eqs. (2) and (3), Eq. (1) can be simplified to

$$\Delta G = \frac{\Delta H_m \Delta T}{T_m} - \frac{1}{2} A(\Delta T)^2 + B\left(T \ln \frac{T_m}{T} - \Delta T \right) \tag{6}$$

where $\Delta T = T_m - T$.

To simplify Eq. (6), TS [17] used the following approximation:

$$\ln\left(\frac{T_m}{T}\right) = \ln\left(1 + \frac{\Delta T}{(T_m + T)/2}\right) \cong \frac{2\Delta T}{T_m + T} \tag{7}$$

and derived the expression

$$\Delta G = \frac{\Delta H_m \Delta T}{T_m}\left(\frac{2T}{T_m + T}\right) \tag{8}$$

The approximation given in Eq. (7) is strictly valid only for small undercooled region, ΔT. But, for the multicomponent metalllic glass forming alloys, which exhibit a large undercooled regime.

Therefore, to account for the wide undercooled region of the multicomponent metallic alloys Lad et al [18] obtained the following expression.

$$\Delta G = \frac{\Delta H_m \Delta T}{T_m}\left(1 - \frac{\Delta T}{2T}\right) \tag{9}$$

Different approximations for the logarithmic term given in Eq. (6) are used by Eq. (8) and Eq. (9) and it has been found that neither Eq. (8) nor Eq. (9) works for many multicomponent amrphous alloys.
Now, considering the Taylor series expansion of Eq. (7) up to second order gives the following approximation:

$$\ln\left(\frac{T_m}{T}\right) \cong \frac{4T\Delta T}{\left(T_m + T\right)^2} \tag{10}$$

Substituting Eq. (10) in Eq. (6) Lad et al [19] obtained the following equation for the Gibbs free energy difference

$$\Delta G = \frac{\Delta H_m \Delta T}{T_m}\left(\frac{4T^2}{\left(T + T_m\right)^2}\right) \tag{11}$$

II. Glass forming ability. It is well known since the pioneering work of Turnbull [3] that melting enthlpy (ΔH) is an important parameter for influencing the Gibbs free energy difference (ΔG) between undercooled liquid and the corresponding crystalline solid. The expression relating ΔG and ΔH, proposed by Turnbull in the undercooled region is given by

$$\Delta G = \Delta H_m \frac{\Delta T}{T_m} \tag{12}$$

ΔG has played an important role in predicting the glass forming ability of multicomponent metallic alloys. Lesser the value of ΔG, smaller is the driving force for crystallization and easier is the formation of BMGs. It can be seen from Eq. (12) that ΔG increases linearly with ΔH. This clearly indicates that a relationship between ΔH and GFA is expected. Turnbull's linear expression between ΔG and ΔH provides good results in smaller undercooled region, but fails to account for non-linearity in large undercooled region in BMGs, since ΔG does not increase rapidly and shows saturation at large ΔT, when the temperature approaches T_K. To avoid Kauzmann paradox, the undercooled liquid is transformed into glass much before T_K at its corresponding glass transition temperature, T_g. However, study of ΔG in large undercooled region is very interesting to guage the GFA of these alloys. Here, it may be noted that the expression proposed by Lad et al [19] is able to account for non-linearity in ΔG particularly at large ΔT and it clearly shows the improvement of the proposed expression given by Eq.11 over that of rather simple Turnbull equation expressed by Eq.12. Nevertheless, the present study of Ca-based metallic glasses at five different composition reiterates the linear relationship between ΔH and GFA.

Results and Discussion

The prime requirement for the formation of amorphous phase from a liquid state is essentially suppression of competing nucleation and growth of the crystalline phases in the supercooled region. Turnbull [3] divelged a ratio, widely adapted as reduced glass transition temperature, T_{rg}; a ratio

between glass transition temperature T_g and liquidus temperature T_l of an alloy, often used as a criterion to determine the GFA of an alloy.

There are so many different criteria available in literature [13, 20] for the estimation of GFA, such as $\gamma_m(=2T_x - T_g/T_l)$, $\gamma(=T_x/T_g+T_l)$ and T_x/T_l . These criteria are mainly based on melting temperature (T_m), crystallization temperature (T_x), glass transition temperature (T_g), liquidus Temperature (T_l),.The systems which are taken up in this study, different GFA criteria are calculated for them and they are compiled in table – 1.

It can be seen from the evaluated parameters given in Table-1 that different GFA criteria laid down by different workers do not show any systematic variation in the glass forming tendency at various compositions of these Ca-based ternary alloys. The parameters namely T_{rg} , γ_m and γ are almost constant with values of 0.6, 0.7 and 0.4 respectively and even T_x/T_l does not vary appreciably. Only recently proposed parameter Q by Suo et al [16] seems to be a sensitive parameter showing variation with change in composition. However, it may be noted that the evaluation of Q essentially requires the knowledge of crystalline enthalpy ΔE. Another interesting point may be observed from the expression of Q that this parameter also indicated the inverse relation of GFA with ΔH_m . As ΔH_m decreases, glass forming tendency increases. This can be seen from Table-2.

Table 1. Different GFA criteria

System	$T_{rg}=\frac{T_g}{T_l}$	$\gamma_m=\frac{(2T_x-T_g)}{T_l}$	$\gamma=\frac{T_x}{T_g+T_l}$	$\frac{T_x}{T_l}$	$Q=\left(\left(T_g+T_x\right)/T_l\right)\left(\Delta E/\Delta H_m\right)$ Ref. [16]
$Ca_{53}Mg_{23}Cu_{24}$	0.62	0.72	0.41	0.67	0.886
$Ca_{65}Mg_{15}Cu_{20}$	0.56	0.64	0.38	0.60	0.683
$Ca_{40}Mg_{25}Cu_{35}$	0.59	0.69	0.40	0.64	0.558
$Ca_{50}Mg_{22.5}Cu_{27.5}$	0.60	0.73	0.41	0.67	0.916
$Ca_{55}Mg_{15}Cu_{30}$	0.56	0.67	0.39	0.62	0.744

Table 2. $\Delta G\ (T_g)$ as an indicator of glass forming ability parameter

System	T_g (K) [16]	T_x (K) [16]	T_m (K) [16]	T_l (K) [16]	ΔH_m [kJ/mol] [16]	$\Delta G\ (T_g)$ [kJ/mol]	$\Delta G(T_g)/\Delta H_m$
$Ca_{53}Mg_{23}Cu_{24}$	406	439	627	655	8.25	1.8	0.218
$Ca_{65}Mg_{15}Cu_{20}$	383	409	630	682	8.27	1.85	0.223
$Ca_{40}Mg_{25}Cu_{35}$	399	436	650	680	8.69	1.94	0.223
$Ca_{50}Mg_{22.5}Cu_{27.5}$	400	442	625	663	8.94	1.96	0.219
$Ca_{55}Mg_{15}Cu_{30}$	397	437	626	706	9.85	2.17	0.220

We evaluated the GFA of this ternary alloy at five different composition in the entire undercooled region and could see a clear cut trend in increase of GFA with decreasing ΔG values at T_g of the respective alloys. This is quite logical as the lower values of ΔG is a signature of lower driving force for crystallization. Thus, $Ca_{53}Mg_{23}Cu_{24}$ appears to have highest glass forming tendency having lowest ΔG value of 1.8 at T_g and $Ca_{55}Mg_{15}Cu_{30}$ having high value (2.17)of ΔG at T_g. ΔG has been evaluated through Eq.11 and the plots for five composions of this alloy system are shown in Fig.1. The ΔG at T_g and $\Delta G(T_g)/\Delta H_m$ are given in Table-2 along with other parameters used in evaluation of ΔG and other GFA parameters provided in Table-1. It can be guaged from the $\Delta G(T_g)/\Delta H_m$ values of the alloys of different compositions that all the values for five compositions lie ~ 0.22. This constant value of 0.22 of the ratio indicates that lower the value of $\Delta G(T_g)$, lower the value of the corresponding ΔH_m and better is the glass forming ability. This underlines the fact that ΔH_m is also an important parameter, which speaks apriori about the tendency of an alloy to form amorphous phase.

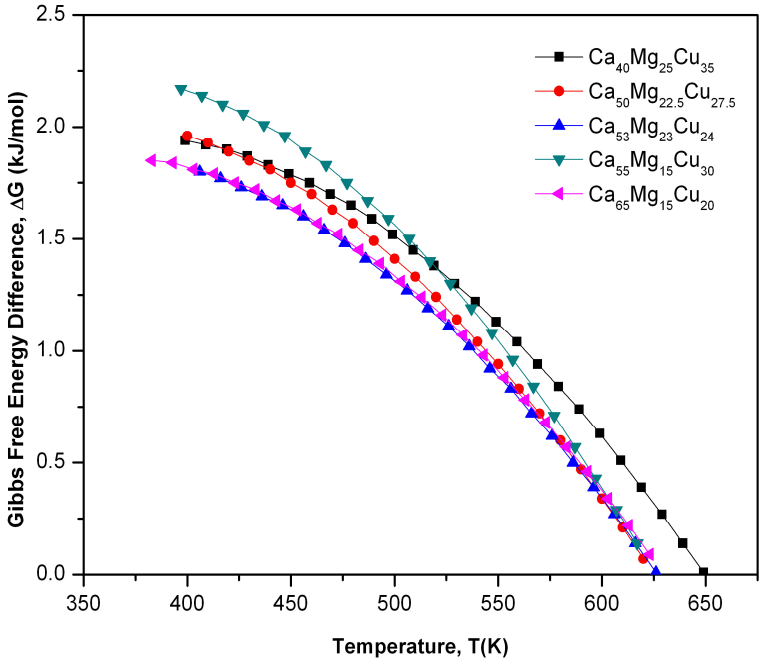

Fig. 1. Gibbs free energy difference, ΔG as a function of temperature, using Lad *et al*. [18,19] expression for different five Ca-based multicomponent metallic alloys.

Conclusion

Based on the results obtained using Eq.11 proposed by us, one can say that ΔG is an important parameter and its theoretical estimation provides quite a fair idea about the GFA of multi-component alloys.Moreover, it does not need many parameters for calculation except for T_m and ΔH_m. The other GFA parameters not only need many parameters but also lack consistency. Besides,
ΔG at T_g shows appreciable variation for different compositions of the alloy which is a signature of variable GFA of these systems.

References

[1] A. Inoue: Acta Mater. Vol. 48 (2000), p. 279

[2] O. N. Senkov: Phys. Rev. B Vol. 76 (2007), p. 104202

[3] D. Turnbull: Contem. Phys. Vol. 10 (1969), p. 473

[4] Z. P. Lu, H. Tan, Y. Li, S. C. Ng: Scripta Mater. Vol. 42 (2000), p. 667

[5] A. Inoue, T. Zhang, T. Masumoto: J. Non-Cryst. Solids: Vol. 473 (1993), p. 156

[6] O. N. Senkov, J. M. Scott: Scripta Mater. Vol. 50 (2004), p. 449

[7] D. Ma, H. Tan, D. Wang, Y. Li, E. Ma: Appl. Phys. Lett. Vol. 86 (2005), p. 191905

[8] G. H. Fan, H. Choo, P. K. Liaw: J. Non-Cryst. Solids Vol. 353 (2007), p. 102

[9] X. D. Du, J. C. Huang, C. T. Liu, Z. P. Lu: J. Appl. Phys. Vol. 101 (2007), p. 086108

[10] X. L. Ji, Y. Pan, F. S. Ni: Mater. Des. Vol. 30 (2009), p. 842

[11] Z. L. Long, H. Q. Wei, Y. H. Ding, P. Zhang, G. Q. Xie, A. Inoue: J. Alloys Compds. Vol. 475 (2009), p. 207

[12] C. Suryanarayana, J. Seki, A. Inoue: J. Non-Cryst. Solids Vol. 355 (2009), p. 355

[13] S. Guo, C. T. Liu: Intermetallics Vol. 18 (2010), p. 2065

[14] A. Takeuchi, A. Inoue: Mater. Sci. Engg. A Vol. 304-306 (2009), p. 446

[15] Z. P. Lu, C. T. Liu: Acta Mater. Vol. 50 (2002), p. 3501

[16] Z. Y. Suo, K. Q. Qiu, Q. F. Li, J. H. You, Y. L. Ren, Z. Q. Hu: Mater. Sci. Engg. A Vol. 528 (2010), p. 429

[17] C. V. Thompson, F. Spaepen: Acta Metall. Vol. 27 (1979), p. 1855

[18] K. N. Lad, A. Pratap, K. G. Raval: J. Mater. Sci. Lett. Vol. 21 (2002), p. 1419

[19] K. N. Lad, K. G. Raval, A. Pratap: J. Non-Cryst. Solids Vol. 334&335 (2004), p. 259

[20] S. Guo S, Lu ZP, Liu CT, Intermetallics Vol. 18 (2010) p.883.

Latest Trends in Condensed Matter Physics
doi:10.4028/www.scientific.net/SSP.171

Glass Forming Ability of Ca-Based Bulk Metallic Glasses
doi:10.4028/www.scientific.net/SSP.171.121

Study of Thermodynamic Properties of Pt57.3Cu14.6Ni5.3P22.8 Bulk Metallic Glass

Ashmi T. Patel and Arun Pratap

Citation: AIP Conf. Proc. **1249**, 161 (2010); doi: 10.1063/1.3466547
View online: http://dx.doi.org/10.1063/1.3466547
View Table of Contents: http://proceedings.aip.org/dbt/dbt.jsp?KEY=APCPCS&Volume=1249&Issue=1
Published by the American Institute of Physics.

Study of Thermodynamic Properties of $Pt_{57.3}Cu_{14.6}Ni_{5.3}P_{22.8}$ Bulk Metallic Glass

Ashmi T. Patel and Arun Pratap

Condensed Matter Physics Laboratory, Applied Physics Department, Faculty of Technology & Engineering, The Maharaja Sayajirao University of Baroda, Vadodara – 390 001.

Abstract. Improving the capability of predicting the glass forming ability (GFA) of metallic glasses is of theoretical and practical significance. Thermodynamically, the Gibbs free energy difference, ΔG between the undercooled melts and the corresponding crystalline solids is exponentially related to nucleation rates. If ΔG is small the critical nucleation work for the formation of a crystal becomes large and therefore the nucleation rates are greatly reduced. ΔG is the driving force for crystallization and as a consequence, it is a good measurement for glass forming ability. Lesser the value of ΔG, higher is the GFA. In the present paper, ΔG is calculated using linear and hyperbolic variations of specific heat difference, ΔC_p in the undercooled region for $Pt_{57.3}Cu_{14.6}Ni_{5.3}P_{22.8}$ bulk metallic glass, which shows an extraordinary ability to resist crystallization. Different thermodynamic properties like ΔS and ΔH also have been evaluated using linear and hyperbolic variations. Theoretical results show very good agreement with experimental values.

Keywords: Glass forming ability, thermodynamic properties, bulk metallic glass, platinum

PACS: 65.60.+a

INTRODUCTION

Bulk metallic glasses (BMG) have drawn a lot of interest because of their superior physical and chemical properties than their crystal counterpart. Bulk glass formation in multi component metallic alloys has also widened the area of possible technological applications of metallic glasses. These alloys show an extraordinary ability to resist crystallization and may solidify as a glass when cooled at sufficiently high rates.

The $Pt_{57.3}Cu_{14.6}Ni_{5.3}P_{22.8}$ alloy has been developed, with a critical cooling rate of the order of ~20 K/s. Its low liquidus temperature and large supercooled region expresses remarkable processing advantages over conventional platinum alloys [1].

Thermodynamically, the knowledge of Gibbs free energy difference ΔG between the crystalline and corresponding amorphous phase, entropy difference ΔS and enthalpy difference ΔH plays an important role to investigate nucleation and growth phenomena and to predict glass forming ability (GFA). The tendency for the glass formation is high if the Gibbs free energy difference between the undercooled melts and the corresponding crystalline solids is small. In this case, the critical nucleation work for the formation of a crystal becomes large and therefore the nucleation rates are greatly reduced. In fact, nucleation rate has an exponential dependence on Gibbs free energy difference, ΔG. ΔG is the driving force for crystallization and as a result, it is a good measurement for GFA. In general, lesser the value of ΔG, higher is the GFA. The values of ΔG, ΔS &ΔH can be calculated if the specific heat capacities, ΔC_p of the liquid and crystalline phase are known as a function of temperature.

THEORETICAL FORMULATION

With the knowledge of the specific heat of the undercooled liquid, the thermodynamic functions can be determined. Therefore, it is very important for further research on the mechanism of solidification and formation of

CP1249, *5th National Conference of Thermophysical Properties (NCTP-09),* edited by A. Pratap and N. S. Saxena

metastable materials [1]. However, in most of the cases, the specific heat data of undercooled liquid is not available due to its metastable nature. A simple extrapolation of the data of the liquid state for the undercooled region is only a crude approximation because in that case we get very few experimental points. In absence of specific heat data in undercooled region the functional dependence of ΔG, ΔS and ΔH on undercooling are estimated theoretically. Many expressions are available for ΔG calculations in literature [2-5]. All these expressions depend on some kind of assumption for temperature dependence of heat capacity.

ΔC_p defined as C_p^l - C_p^s is the difference in specific heats of the two phases. We may choose an expression which satisfactorily explains the temperature dependence of ΔC_p. It is observed that ΔC_p shows linear and hyperbolic variation with temperature. So in the present case we have opted for these two linear and hyperbolic variations of ΔC_p, which involves A & B coefficients for linear variation and C & D coefficients for hyperbolic variation. These coefficients can be evaluated with the knowledge of ΔC_p^m and T_K. Where, ΔC_p^m is specific heat difference and T_K is Kauzmann temperature where entropy difference, $\Delta S = 0$.

Considering these two types of ΔC_p variations, expressions for ΔG are derived. The most common is the linear expression is given by

$$\Delta C_p = AT + B \tag{1}$$

And the hyperbolic expression for ΔC_p is given by

$$\Delta C_p = \frac{C}{T} + D \tag{2}$$

Now, the difference in the Gibbs free energy between undercooled liquid and the corresponding crystalline phase is given by

$$\Delta G = \Delta H - T\Delta S \tag{3}$$

Where,

$$\Delta H = \Delta H_m - \int_T^{T_m} \Delta C_p dT \tag{4}$$

and

$$\Delta S = \Delta S_m - \int_T^{T_m} \Delta C_p \frac{dT}{T} \tag{5}$$

Where, T_m is the melting temperature, ΔS_m is the entropy of fusion and ΔH_m is the enthalpy of fusion. They are related to each other by the following relation.

$$\Delta S_m = \frac{\Delta H_m}{T_m} \tag{6}$$

Hence, the expression for ΔG becomes

$$\Delta G = \frac{\Delta H_m \Delta T}{T_m} - \int_T^{T_m} \Delta C_p dT + T\int_T^{T_m} \Delta C_p \frac{dT}{T} \tag{7}$$

Considering linear variation of ΔC_p given by equation (1), the expression for ΔG (7) becomes

$$\Delta G = \frac{\Delta H_m \Delta T}{T_m} - \frac{1}{2} A(\Delta T)^2 + B\left[T \ln\left(\frac{Tm}{T}\right) - \Delta T \right] \tag{8}$$

Similarly, considering linear variation of ΔC_p, equation (5) becomes

$$\Delta S = \frac{\Delta H_m}{T_m} - A\Delta T - B\ln\frac{T_m}{T} \tag{9}$$

At $T = T_K$, $\Delta S = 0$, therefore equation (9) becomes,

$$0 = \frac{\Delta H_m}{T_m} - A\Delta T - B\ln\frac{T_m}{T_K}$$

or,

$$\frac{\Delta H_m}{T_m} = A\left[T_m - T_K\right] + B\ln\left(\frac{T_m}{T_K}\right) \tag{10}$$

Now, taking into account linear variation of ΔC_p, B can be written as,

$$B = \Delta C_p^m - AT_m \tag{11}$$

Using the above expression of B in equation (10), we get the expression for A as follows,

$$A = \frac{\Delta H_m / T_m - \Delta C_p^m \ln\left(T_m / T_K\right)}{T_m - T_K - T_m \ln\left(T_m / T_K\right)} \tag{12}$$

On the other hand, hyperbolic variation of ΔC_p given by equation (2), considering that ΔG and ΔS equations become,

$$\Delta G = \frac{\Delta H_m \Delta T}{T_m} + \ln\left(\frac{T_m}{T}\right)\left[DT - C\right] - \Delta T\left[D - \frac{C}{T_m}\right] \tag{13}$$

$$\Delta S = \frac{\Delta H_m}{T_m} - D\ln\left(\frac{T_m}{T}\right) - C\left[\frac{1}{T} - \frac{1}{T_m}\right] \tag{14}$$

At $T=T_K$, $\Delta S = 0$, therefore equation (14) becomes,

$$0 = \frac{\Delta H_m}{T_m} - D\ln\left(\frac{T_m}{T_K}\right) - C\left[\frac{1}{T_K} - \frac{1}{T_m}\right]$$

or,

$$\frac{\Delta H_m}{T_m} = D\ln\left(\frac{T_m}{T_K}\right) + C\frac{\left(T_m - T_K\right)}{T_m - T_K} \tag{15}$$

Considering hyperbolic variation of ΔC_p, D can be written as,

$$D = \Delta C_p^m - \frac{C}{T_m} \tag{16}$$

Using the above expression of D in equation (15), we get the expression for C as follows,

$$C = \frac{\Delta H_m - T_m \Delta C_p^m \ln\left(T_m / T_K\right)}{\left(T_m - T_K\right)/T_K - \ln\left(T_m / T_K\right)} \tag{17}$$

RESULTS & DISCUSSION

The coefficients A, B, C & D required for evaluation of ΔC_p assuming linear trend and hyperbolic variation respectively have been evaluated using equations (11), (12) and (16) & (17). For the evaluation of these coefficients using parameters given in TABLE-1 have been utilized. These coefficients, in turn, have been incorporated in the expressions for Gibbs free energy difference ΔG, entropy difference ΔS, and enthalpy difference ΔH considering linear and hyperbolic variation of specific heat difference $\Delta C_p{}^m$.

TABLE 1. Parameters used for the calcualtions

System	T_m (K)	T_k (K)	ΔH_m (kJ/mol)	$\Delta C_p{}^m$ (J/mol-K)	Reference
$Pt_{57.3}Cu_{14.6}Ni_{5.3}P_{22.8}$	775	396	11.4	10.22	1

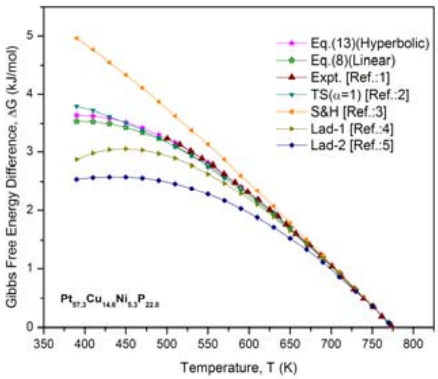

FIGURE 1. Gibbs free energy difference, ΔG of $Pt_{57.3}Cu_{14.6}Ni_{5.3}P_{22.8}$ in the undercooled melt as a function of temperature.

Fig. 1 shows the Gibbs free energy difference, ΔG between undercooled liquid and corresponding crystalline solid as a function of temperature. Values of ΔG calculated using Linear and hyperbolic variations of heat capacity from Eqs. (8) and (13) are shown along with results obtained through other theoretical approaches and the experimental data. One can see that they are in excellent agreement with each other and also with the experimental points. The results obtained through other theoretical approaches, on the other hand, show large deviation (except TS-1) [2] in almost entire temperature range. The ΔG values evaluated using Lad-1 & Lad-2 equation [4,5] fall much below the experimental data while that using S&H equation [3] overestimate ΔG, even though, ΔG plot evaluated using TS-1 equation [2] is close to the experimental data. The closeness of our results with the experimental data in comparison to other theoretical curves may be attributed to the fact that all the earlier workers have assumed constancy of ΔC_p and have not considered it as a variable with respect to temperature in the entire undercooled region.

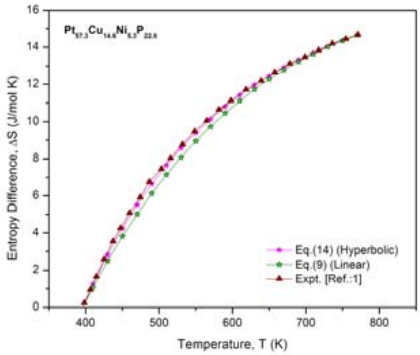

FIGURE 2. Entropy difference, ΔS of $Pt_{57.3}Cu_{14.6}Ni_{5.3}P_{22.8}$ in the undercooled melt as a function of temperature.

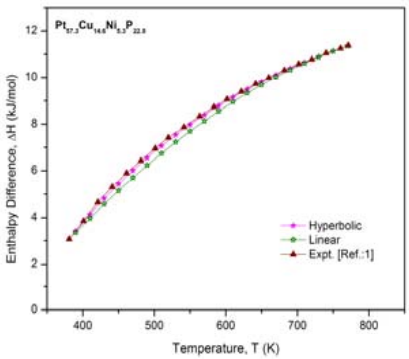

FIGURE 3. Enthalpy difference, ΔH of $Pt_{57.3}Cu_{14.6}Ni_{5.3}P_{22.8}$ in the undercooled melt as a function of temperature.

The entropy difference ΔS for $Pt_{57.3}Cu_{14.6}Ni_{5.3}P_{22.8}$ system calculated from Eqs. (9) and (14) is shown in Fig. 2. The results from the other approaches [S&H, Lad-1 and Lad-2] [3-5] are not shown because of their large deviation from the experimental ΔG values as seen from Fig. 1. The calculated values show similar variation as seen for the experimental data. Once ΔG and ΔS values are known one can evaluate values of enthalpy difference, ΔH using Eq. (1). The results obtained for ΔH for $Pt_{57.3}Cu_{14.6}Ni_{5.3}P_{22.8}$, using both linear and hyperbolic variation of ΔC_p are plotted in Fig. 3. The experimental values of ΔH are also shown in the figure and it can be seen that the calculated values lie quiet close to the experimental values.

So far, no one has taken ΔC_p variation with temperature for evaluation of thermodynamic properties, ΔG, ΔS, & ΔH.. Most of the expressions which are available in literature consider ΔC_p is to be constant. An attempt has been made by Mondal *et al*. [6] to evaluate the constants *a* and *b*. Their results for few bulk metallic systems are in good agreement with experimental data. However, it may be pointed out that there is an inconsistency in their derivation of the expressions for ΔC_p^{α} at T_{α} (isenthalpic temperature) and ΔC_p^{m} at T_m. The expressions have been obtained by treating ΔC_p as constant in the entire undercooling range. Further, Mondal *et al.* [6] utilize the above expressions for ΔC_p^{α} and ΔC_p^{m} to derive the constants *a* and *b* taking ΔC_p occurring in the expression which assumes ΔCp to be a linear function of temperature. These two simultaneous assumptions:

1. treating ΔC_p to be a constant; and
2. putting back the so-obtained ΔC_p^{α} at T_{α} to get the constants *a* & *b*,

are contradictory making the whole exercise futile.

CONCLUSIONS

The expressions for ΔG which are proposed in the present paper assuming linear and hyperbolic variation for ΔC_p gives excellent results in the entire undercooled region of $Pt_{57.3}Cu_{14.6}Ni_{5.3}P_{22.8}$ BMG. The linear and hyperbolic values of ΔG appear to be almost superimposed on the experimental data. Values of ΔS and ΔH derived from so obtained ΔG values also lie very close to each other. The hyperbolic values superimposed the experimental one while linear values have slight deviation with experimental one.

One can say that presently proposed expressions for ΔG assuming linear and hyperbolic variation of heat capacity, ΔC_p with temperature offer quite accurate results for $Pt_{57.3}Cu_{14.6}Ni_{5.3}P_{22.8}$ BMG. The results assuming ΔC_p to be constant with temperature does show large variation and can not be applied in the present system. Therefore, to find out accurate values of thermodynamic properties one has to take into account variation of heat capacity difference, ΔC_p with temperature as considered in the present work. The accuracy in the estimation of Gibbs free energy difference, ΔG is often critically important when used in the analysis of nucleation phenomena, since the nucleation frequency has an exponential dependence on ΔG.

REFERENCE

1. Benjamin A. Legg, Jan Schroers and Ralf Busch, *Acta Materialia* **55**, 1109-1116 (2007).
2. C. V. Thompson and F. Spaepen, *Acta Metall.* **27**, 1855 (1979).
3. H. B. Singh and A. Holz, *Solid State Commu.,* **45**, 985 (1983).
4. K. N.Lad, Arun Pratap and K. G. Raval, J. Mater. Sci. Lett. **21**, 1419 (2002).
5. K. N. Lad, K. G. Raval and Arun Pratap, *J. Non-Cryst. Solids* **259**, 334 & 335 (2004).
6. K. Mondal, U. K. Chatterjee and B. S. Murthy, Appl. Phys. Lett. **83**, 671 (2003).

5

Crystallization Kinetics of Metallic Glasses

Arun Pratap and Ashmi T. Patel
Condensed Matter Physics Laboratory, Applied Physics Department,
Faculty of Technology & Engineering, The Maharaja Sayajirao University of Baroda,
Vadodara,
India

"Crystallization is still in many ways, more an art than a science."
–David Oxtoby, Nature, August 3, 2000.

1. Introduction

Metallic glasses are kinetically metastable materials. Metallic glass is defined as "A liquid, which has been cooled into a state of rigidity without crystallizing". Properties of metallic glasses differ form non metallic glasses. Ordinary glasses are made up of silica while metallic glasses are made of alloy metals. Ordinary glasses are transparent whereas metallic glasses are opaque. In ordinary glasses, covalent bond is observed while in metallic glasses metallic bond is observed. On the basis of internal arrangement of atoms or molecules and type of force acting between them, the material can be classified into the following two categories:

i. Crystalline solid: Those materials in which the constituent ions or atoms and molecules are arranged in regular pattern are called crystalline solids. Besides, crystalline solids have a definite external geometrical form.
   e.g. Quartz, Calcite, Diamond, Sugar, and Mica
ii. Amorphous or glassy solid: Those materials do not have definite geometric pattern are called amorphous solids. In amorphous solid atoms, ions or molecules are not arranged in definite pattern.
   e.g. Rubber, Glass, Plastic and Cement

Also, an amorphous solid is a solid in which there is no long range order of the positions of the atoms. Solids in which there is long-range atomic order are called crystalline solids.

At high cooling rate, any liquid can be made into an amorphous solid. Cooling reduces molecular mobility. If the cooling rate is faster, then molecules can not organize into a more thermodynamically favourable crystalline state and an amorphous solid will be formed. Materials in which such a disordered structure is produced directly from the liquid state during cooling are called "Glasses" and such amorphous metals are commonly referred to as "Metallic Glasses" or "Glassy Metals". The metallic glasses have a combination of amorphous structure and metallic bond. This combination provides a metallic glass a new and unique quality, which cannot be found in either pure metals or regular glass.

In the past, small batches of amorphous metals have been produced through a variety of quick-cooling methods. For instance, amorphous metal wires have been produced by sputtering molten metal onto a spinning metal disk. The rapid cooling, of the order of millions of degrees a second, is too fast for crystals to form and the material is "locked in" a glassy state. Now-a-days number of alloys with critical cooling rates low enough to allow formation of amorphous structure in thick layers (over 1 millimetre) have been produced; these are known as bulk metallic glasses (BMG).

However, there are various methods in which amorphous metals can be produced, preventing the crystallization. Sputtering, glow discharge sputtering, chemical vapour deposition (CVD), gel desiccation, electrolyte deposition, reaction amorphization, pressure–induced amorphization, solid state diffusion amorphization, laser glazing, ion implantation, thin-film deposition, melt quenching and melt spinning are some of them.

The study of the thermally-activated phase transformations is of great significance in the field of materials science as the properties of materials change due to the change in the composition and/or microstructure. The properties of fully or partly crystalline materials are usually different from their amorphous counterparts. From the viewpoint of a materials scientist, the crystallization of amorphous or non-crystalline materials involves the nucleation and growth processes. The processes driven by nucleation and growth have attracted a lot of interest for tailoring technological applications. For example, the recrystallization of the deformed metals, controlling the nucleation and growth of islands on terraces in order to get large scale arrays of nanostructures in the manufacturing of thin-film transistors (Castro, 2003). Thus, the knowledge of the kinetics of crystallization would help to attain products with the required crystallized fraction and microstructure (e.g. nanocrystalline or quasicrystalline) or to avoid the degradation of materials at high processing (& operating) temperatures.

The kinetics of the crystallization process can be studied with the help of thermo-analytical techniques namely, differential scanning calorimetry (DSC) and differential thermal analyzer (DTA). The DSC/DTA experiments can be carried out in isothermal as well as non-isothermal (linear heating) conditions (Ligero et al., 1990; Moharram et al., 2001; Rysava et al., 1987; Giridhar & Mahadevan, 1982; Afify, 1991). Efforts made by the researchers in this field so far, to analyze the data obtained from DSC and hence to determine the kinetic parameters of the crystallization processes (say, activation energy, rate constant etc.), raise two important issues: (i) the selection of the mode of experiment (isothermal or non-isothermal) and, (ii) the choice of a sound method for the analysis of the experimental data. However, we are more concerned with the later issue due to the fact that several methods for the kinetic analysis are available in the literature. These methods are generally based on either the isokinetic hypothesis or the isoconversional principle and they can be accordingly categorized as: (1) isokinetic methods where the transformation mechanism is assumed to be the same throughout the temperature/time range of interest and, the kinetic parameters are assumed to be constant with respect to time and temperature; (2) isoconversional methods, which are generally used for non-isothermal analysis, assume that the reaction (transformation) rate at a constant extent of conversion (degree of transformation) is only a function of temperature (Lad et al, 2008; Patel & Pratap, 2012). The kinetic parameters, in this case, are considered to be dependent on the degree of transformation at different temperature and time. The use of isoconversional methods is widespread in the physical

chemistry for the determination of the kinetics of the thermally activated solid-state reactions. The physicochemical changes during an exothermic or endothermic event in DSC (or DTA) are complex and involve multi-step (serial or parallel) processes occurring simultaneously at different rates. Therefore, the activation energies for such processes can logically not be same and it may vary with the degree of conversion. This is contrary to the isokinetic view assuming all the constituents of the material to react simultaneously at the same rate. The activation energy, in the isokinetic case, is thus constant and independent of the degree of conversion. A strong difference of opinion persists among the researchers in the field of thermal analysis about the concept of variable activation energy (Galwey, 2003; Vyazovkin, 2003). In the metallurgical branch of materials science, most of the thermal phase transformations (like crystallization, recovery) are morphological and are considered to be governed by the nucleation and growth processes. The transformation mechanisms in these processes are also complex e.g. interface-controlled, diffusion-controlled growth. Notwithstanding this, the kinetic analysis of the transformation process like crystallization is done according to isokinetic hypothesis. The isoconversional methods are scarcely used for the study of the crystallization kinetics of metallic glasses.

2. Theory

To study the phase transformation, which involves nucleation and growth, many methods are developed. Most of the methods depend on the transformation rate equation given by Kolmogorov, Johnson, Mehl and Avrami (Lesz & Szewieczek, 2005; Szewieczek & Lesz, 2005; Szewieczek & Lesz, 2004; Jones et al., 1986; Minic & Adnadevic, 2008), popularly known as KJMA equation, basically derived from experiments carried out under isothermal conditions. The KJMA rate equation is given by

$$\frac{d\alpha}{dt} = nk(1-\alpha)[-ln(1-\alpha)]^{(n-1)/n} \tag{1}$$

where, $a \rightarrow$ degree of transformation at a given time t,
$n \rightarrow$ Avrami (growth) exponent
$k \rightarrow$ the rate constant

The Arrhenius form of the rate constant is given by

$$k(T) = k_0 \, exp\left(-\frac{E}{RT}\right) \tag{2}$$

where, $k_0 \rightarrow$ pre-exponential factor
E $\rightarrow$ activation energy, and
R $\rightarrow$ universal gas constant

KJMA rate equation is based on some important assumptions and it has been suggested that the KJMA kinetic equation is accurate for reactions with linear growth subject to several conditions (Minic et al., 2009).

The isoconversional methods are also known as model-free methods. Therefore, the kinetic analysis using these methods is more deterministic and gives reliable values of activation energy E, which depends on degree of transformation, *a*. However, only activation energy

will not give a perfect picture of crystallization kinetics. The microstructural information (e.g. dimensionality of the growth) of the precipitating phase during the transformation is also very important for understanding the whole kinetics of crystallization. Microstructural information would be known to us when we take the isokinetic methods into account. Therefore, the complementary use of both the methods is more useful for understanding the kinetics of crystallization.

Differential Scanning Calorimetry (DSC) has become a convenient and widely used tool for studying the kinetics of phase transformations. The volume fraction (x) of the sample transformed in crystalline phase during the crystallization event has been obtained from the DSC curve as a function of temperature (T). The volume fraction of precipitated crystal can be obtained from the DSC curve by using

$$x = S/S_0$$

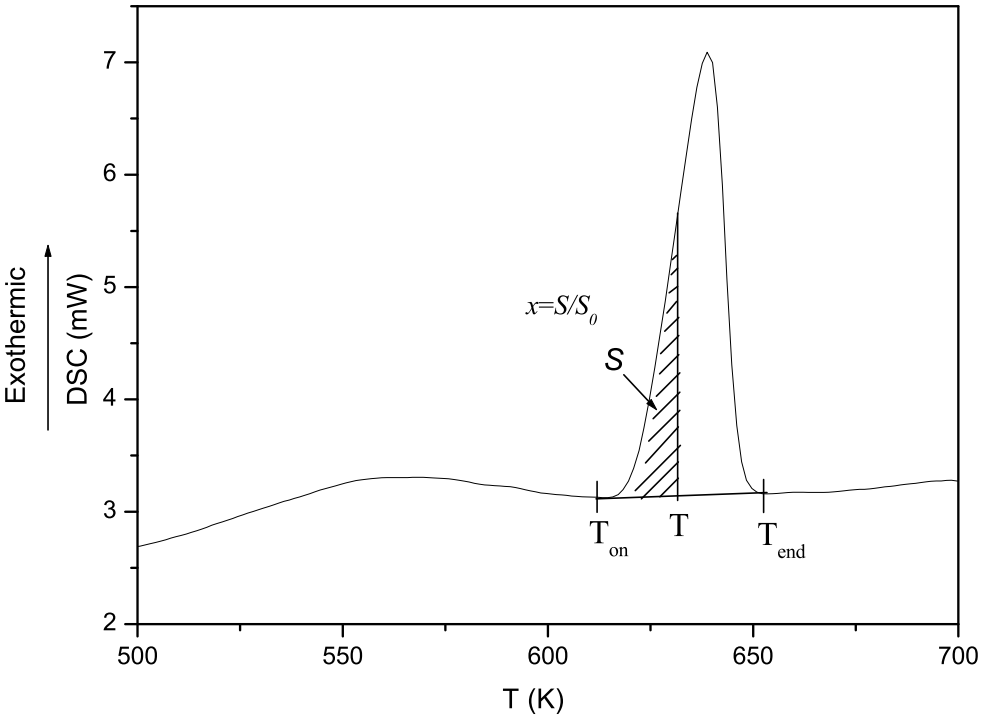

Where S_0 is the total area under the crystallization curve i.e. the area under the curve between the temperature at the onset of crystallization T_{on} and the end-set temperature T_{end} when the crystallization is completed. S is the area at any temperature T between T_{on} and T at which the fractional crystallization is required to be known.

There are three important modes of crystallization involving nucleation and growth processes, depending on the composition of a particular alloy: primary crystallization, polymorphous

crystallization and eutectic crystallization (Hsiao et al., 2002). In primary crystallization the primary phase of the alloy constituents crystallizes first. The dispersed primary crystallized phase coexists with the amorphous matrix and may serve as the nucleation site for secondary or tertiary crystallization. In Fe-based alloys α-Fe crystallizes first, which is a kind of primary crystallization. Polymorphous crystallization is a transition of the amorphous phase to a crystalline one without any change in the composition of that phase. There is no concentration difference across the reaction front because the concentration does not change. Eutectic crystallization is simultaneous crystallization of two crystalline phases by a discontinuous reaction. This reaction takes longer than polymorphous crystallization to proceed because the two components have to separate by diffusion into two separate phases within the crystallized region (Minic, 2006).

3. Results and discussion

The DSC thermograms at four different heating rates are shown in Fig.1. The thermograms show three-stage crystallization. The first crystallization peak is evaluated for heating rates 4, 6, 8 and 10 deg/min. Glass transition becomes clear as we go for the higher heating rates, but the third crystallization peak becomes less prominent as we go to the higher heating rates. The onset and endset of first crystallization exotherms exhibit different levels of heat flow i.e. the crystallization ends at slightly higher level followed by the second and third crystallization peak. This difference of the level indicates that the phases at the start of crystallization and at the end of it are not same. The analysis of DSC data to evaluate the kinetic parameters can be obtained from non-isothermal rate laws by both isokinetic also known as model fitting methods and isoconversional methods.

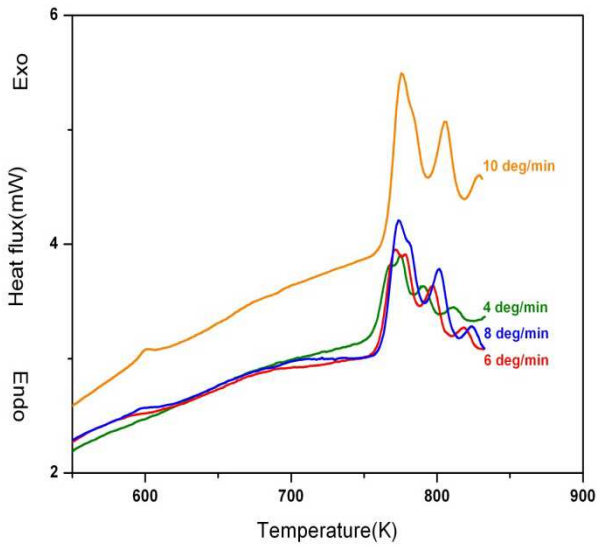

Fig. 1. DSC thermograms of the metallic glass $Co_{66}Si_{12}B_{16}Fe_4Mo_2$ at different heating rates

3.1 Isoconversional analysis

The isoconversional methods require the knowledge of temperatures $T_\alpha(\beta)$ at which an equivalent stage of reaction occurs for various heating rates. The equivalent stage is defined as the stage at which a fixed amount is transformed or at which a fixed fraction, α of the total amount is transformed (Starink, 1997). These methods are further categorized as linear and non-linear isoconversional methods. The linear integral isoconversional methods (Kissinger, 1957; Ozawa, 1965; Augis & Bennett, 1978; Boswell, 1980; Flynn & Wall, 1966; Akahira & Sunose, 1971; Li & Tang, 1999) depend on the approximation of the temperature integral and require the data on $T_\alpha(\beta)$. The differential isoconversional methods depend on the rate of transformation at $T_\alpha(\beta)$ and the data on $T_\alpha(\beta)$ (Gupta et al., 1988; Friedman, 1964; Gao & Wang, 1986). Vyazovkin (Vyazovkin & Wight, 1997) introduced a non-linear isoconversional method to increase the accuracy of evaluating the activation energy. The isoconversional methods are based on the basic kinetic equation (Paulik, 1995)

$$\frac{d\alpha}{dT} = \frac{1}{\beta} k(T) f(\alpha) = \frac{A}{\beta} exp\left(-\frac{E}{RT}\right) f(\alpha) \tag{3}$$

where $k(T)$ is the rate constant, β is the heating rate, α is the conversion fraction and $f(\alpha)$ is the reaction model which in case of KJMA formalism gives the Eq. (1). Eq. (3) can also be expressed in the integral form as

$$g(\alpha) = \int_0^\alpha [f(\alpha)]^{-1} d\alpha = \frac{A}{\beta} \int_0^T exp\left(-\frac{E}{RT}\right) dT \tag{4}$$

As mentioned earlier, exact solution of the temperature integral is not available and various approximations made for this has resulted into different methods. We have selected a few most commonly used methods. The accuracy of various isoconversional methods and, the experimental and analytical errors associated with these methods are discussed in detail by Starink (Starink, 2003). Roura and Farjas (Roura & Farjas, 2009) have proposed an analytical solution for the Kissinger equation. Rotaru and Gosa (Rotaru & Gosa, 2009) describe their recently developed software that implements a number of known techniques such as various isoconversional methods, a method of invariant kinetic parameters, master plots methods, etc. Cai and Chen (Cai & Chen, 2009) have proposed a new numerical routine for a linear integral isoconversional method that allows one to obtain accurate values of the activation energy in the cases when the latter varies strongly with the extent of conversion. Criado et al. (Criado et al., 2008) provide a critical overview of isoconversional methods, putting the focus on establishing whether the observed variations in the activation energy are real or apparent (Vyazovkin, 2010).

Linear integral isoconversional methods

a. Ozawa-Flynn-Wall (OFW) method

In this method (Ozawa, 1965; Augis & Bennett, 1978; Boswell, 1980; Flynn & Wall, 1966) the temperature integral in Eq. (4) is simplified by using the Doyle's approximation (Doyle, 1961, 1962, 1965) and hence we obtain the following equation:

$$ln\,\beta = -1.0516\frac{E(\alpha)}{RT_{\alpha}} + const \tag{5}$$

The plot of $ln\beta$ vs $1000/T_{\alpha}$ (Fig.2) gives the slope $-1.0516\ E(a)/R$ from which the activation energy has been evaluated (Table 1). At $T_{\alpha} = T_p$, (Ozawa method) the value of E determined using Eq. (5) is given in Table 2.

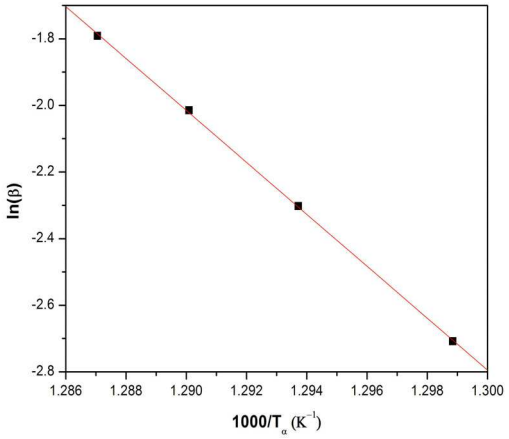

Fig. 2. OFW plot for peak-1

b. Kissinger-Akahira-Sunose (KAS) method

Kissinger, Akahira and Sunose (Kissinger, 1957; Ozawa, 1965; Augis & Bennett, 1978; Boswell, 1980; Flynn & Wall, 1966; Akahira & Sunose, 1971) used the approximation given by Coats & Redfern (Coats & Redfern, 1964) to evaluate the integral in the rate Eq. (4). KAS method is based on the expression

$$ln\left(\frac{\beta}{T^2}\right) = ln\left(\frac{AR}{Eg(\alpha)}\right) - \frac{E}{RT} \tag{6}$$

The activation energy can be evaluated from the slope of plot $ln(\beta/T^2)$ vs $1000/T$ for constant conversion, α (Fig. 3) Values of E are given in Table 1. The discussion given ahead describes some of the methods available in the literature which are basically special cases of the KAS equation (6).

i) Kissinger method: This well-known method assumes that the reaction rate is maximum at the peak temperature (T_p). This assumption also implies a constant degree of conversion (α) at T_p. The equation used by Kissinger is

$$ln\left(\frac{\beta}{T_p^2}\right) = -\frac{E}{RT_p} + ln\left(\frac{AR}{E}\right) \tag{7}$$

A plot of $ln(\beta/T_p^2)$ vs $1000/T_p$ gives an approximate straight line and the activation energy E is calculated using the slope (Table 2).

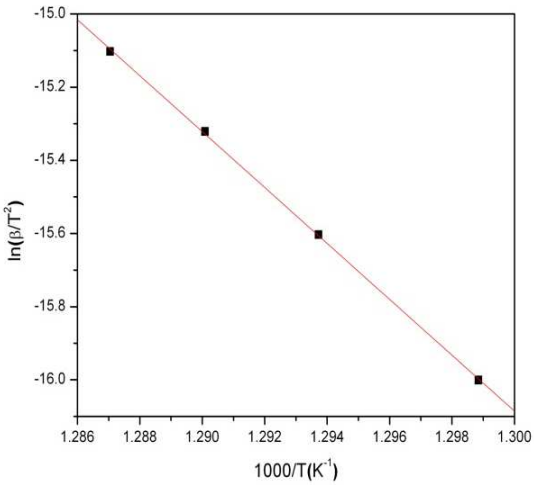

Fig. 3. KAS plot for peak-1

ii) Augis & Bennett's method: This method was suggested by Augis and Bennett (Augis & Bennett, 1978) and is an extension of Kissinger method showing its applicability to heterogeneous reaction described by Avrami expression. Apart from the peak crystallization temperature it also incorporates the onset temperature of crystallization, T_o and it is supposed to be a very accurate method of determining E through the equation

$$ln\left(\frac{\beta}{\left(T_p - T_o\right)}\right) = -\frac{E}{RT_p} + ln\,A \tag{8}$$

where T_p and T_o are the peak and the onset temperatures of crystallization respectively. The values of E obtained from the plot $(ln(\beta/(T_p-T_o))$ vs $1000/T_p$ is given in Table 2.

Further,

$$n = 2.5\frac{T_p^2}{\Delta T\left(\frac{E}{R}\right)} \tag{9}$$

where ΔT is the full width at half maximum of the DSC curve. n can be derived using Eq. (9).

iii) Boswell method: Boswell (Boswell, 1980) has found a limitation in the Augis & Bennett method that if

$$\frac{T_p - T_o}{T_p} \approx 1$$

then Augis & Bennett gives crude results. However, it may be noted that this condition may not apply to the present case.

Boswell method determines the activation energy at peak temperature (Table 2) using the following equation

$$ln\left(\frac{\beta}{T_p}\right) = -\frac{E}{RT_p} + const \tag{10}$$

c. Li-Tang Method

Li and Tang (Li & Tang, 1999) have developed an isoconversional integral method which does not make any assumption about the kinetic model and involves no approximation in the Eq. (3) as

$$\int_0^\alpha \left(ln\frac{d\alpha}{dt}\right)d\alpha \;\; = G(\alpha) - \frac{E_\alpha}{R}\int_0^\alpha \left(\frac{1}{T}\right)d\alpha \tag{11}$$

Where $G(\alpha) = \alpha ln A + \int_0^\alpha (ln f(\alpha))d\alpha$ has the same value for a given reaction under study and a given α irrespective of β. A plot of $\int_0^\alpha ln\left(\frac{d\alpha}{dt}\right)d\alpha$ vs $\int_0^\alpha \left(\frac{1}{T}\right)d\alpha$, for a set of β's at constant conversion α will have the slope $-E/R$.

Linear differential isoconversional method

The method suggested by Friedman (Friedman, 1964) sometimes known as transformation rate-isoconversional method, utilizes the differential of the transformed fraction and hence it is called differential isoconversional method. Substituting value of *k(T)* in Eq. (3) and taking logarithm, Friedman derived a linear differential isoconversional expression as

$$ln\left(\frac{d\alpha}{dt}\right)_\alpha = ln\beta\left(\frac{d\alpha}{dT}\right)_\alpha = ln\left(A\, f(\alpha)\right) - \frac{E_\alpha}{RT_\alpha} \tag{12}$$

by taking logarithm on both sides of Eq.(3). For a constant α, the plot of $ln\left(\beta\frac{d\alpha}{dT}\right) vs \left(\frac{1}{T}\right)$ should be a straight line (Fig. 4) whose slope gives us the value of *E* (Table 1).

Since this method does not take any mathematical approximation for the temperature integral, it is considered to give accurate estimate of *E*. Thus the method does not require any assumption on $f(\alpha)$, i.e. it is a so-called model-free method. However, being a differential method, its accuracy is limited by the signal noise (Dhurandhar et al, 2010).

A method suggested by Gao and Wang (Gao & Wang, 1986) is a special case of the Friedman method. This method uses the following expression to determine the activation energy.

$$ln\left(\beta\frac{d\alpha}{dT_p}\right) = -\frac{E}{RT_p} + const \tag{13}$$

$$K_p = \frac{\beta E}{RT_p^2} \tag{14}$$

where,

$$K_p = A\,exp\left(\frac{-E}{RT_p}\right) and \left(\frac{d\alpha}{dt}\right)_p = 0.37nK_p$$

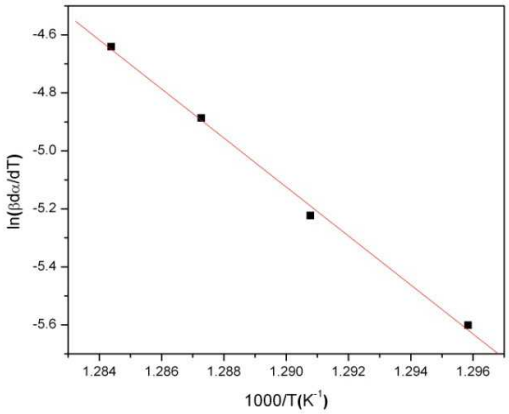

Fig. 4. Friedman plot for peak-1

α	E (kJ/mol)		
	KAS	OFW	Friedman
0.1	602 ± 2	584 ± 2	555 ± 1
0.2	597 ± 1	580 ± 1	626 ± 1
0.3	603 ± 1	586 ± 2	648 ± 1
0.4	615 ± 1	597 ± 1	687 ± 1
0.5	635 ± 1	616 ± 1	725 ± 1
0.6	654 ± 1	634 ± 1	702 ± 3
0.7	648 ± 1	629 ± 1	522 ± 5
0.8	606 ± 1	589 ± 1	398 ± 5
0.9	549 ± 1	534 ± 1	318 ± 2

Table 1. Local Activation energy (E) at different conversion for different methods.

Method	E (kJ/mol)
Kissinger	553 ± 2
Ozawa	546 ± 2
Augis & Bennett	532 ± 2
Boswell	443 ± 7

Table 2. Activation energy (E) using various methods.

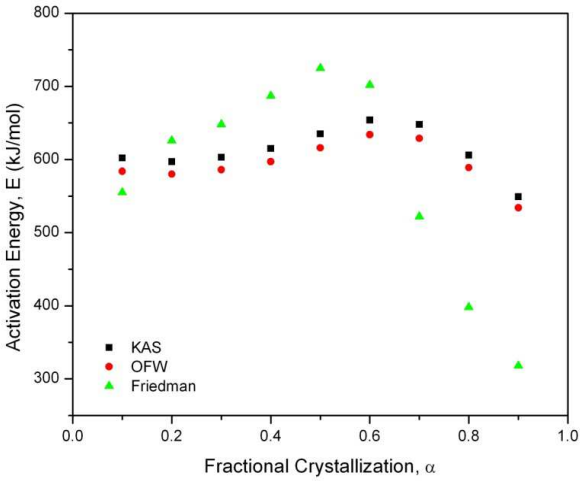

Fig. 5. Local Activation energy E at different α from different methods

Non-linear isoconversional method

Vyazovkin and Wight (Vyazovkin & Wight, 1997) described an advanced isoconversional method. Similar to other isoconversional methods, this method is also based on the assumption that the reaction model, $g(\alpha)$ is independent of the heating program. So, for any two experiments conducted at different heating rates the ratio of the temperature integral I (E, T_α) to the heating rate β is a constant. For a given conversion and a set of n experiments performed under different heating rates, the activation energy can be determined at any particular value of α by finding the value of E_α for which the function

$$\sum_{i\neq j}^{n}\sum^{n}\frac{\left[I(E_\alpha,T_{\alpha i})\beta_j\right]}{\left[I(E_\alpha,T_{\alpha j})\beta_i\right]} \tag{15}$$

is a minimum. The minimization procedure is repeated for each value of α to find the dependence of activation energy on the extent of conversion.

3.2 Isokinetic methods

a. Matusita and Sakka method

Matusita and Sakkka (Matusita & Sakka, 1979) suggested the following equation specifically for the non-isothermal data

$$\ln[-\ln(1-\alpha)] = -n\ln\beta - \frac{mE}{RT} + Const \tag{16}$$

where m is an integer depends on the dimensionality of the crystal and the Avarami exponent n depends on the nucleation process. For a constant temperature, the plot of ln[-

ln(1-α)] versus lnβ gives a straight line (Fig.6) and the slope gives the value of *n*, which come out to be n = 1.33 and *n* = 1.36 for temperatures T = 775 K and *T* = 778 K respectively. The plot of ln[-ln(1-α)] versus 1/T at constant heating rate should be a straight line and the value of mE is obtained from the slope (Fig.7).

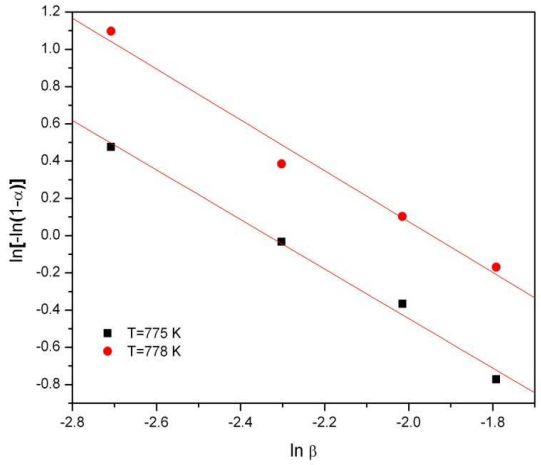

Fig. 6. Plot of ln[-ln(1- α)] Vs. lnβ for diff. Temp.

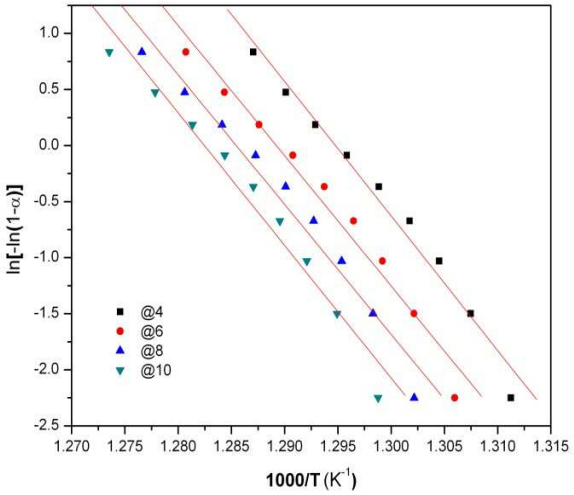

Fig. 7. Plot of ln[-ln(1- α)] Vs. 1000/T for diff. heating rates.

a) Modified Kissinger method

The modified Kissinger equation (Matusita & Sakka, 1980) given below can be utilized to derive the activation energy (*E*).

$$ln\left(\frac{\beta^n}{T_p^2}\right) = -\frac{mE}{RT_p} + Const \tag{17}$$

Where E is the activation energy for crystallization, T_p is the peak temperature and R is the universal gas constant. m is known as the dimensionality of growth and here $m = n$. In order to derive E from this equation, one must know the value of n. The n value can be obtained from the slope of the plot of ln[-ln(1-α)] Vs. lnβ at constant temperature. In order to evaluate E, the values of n are substituted in Eq. (17). Then plots of $ln\left(\frac{\beta^n}{T_p^2}\right)$ Vs. $\frac{1}{T_p}$ (Fig. 8) gives the values of activation energy E, and the average E obtained is 549.80 kJ/mol.

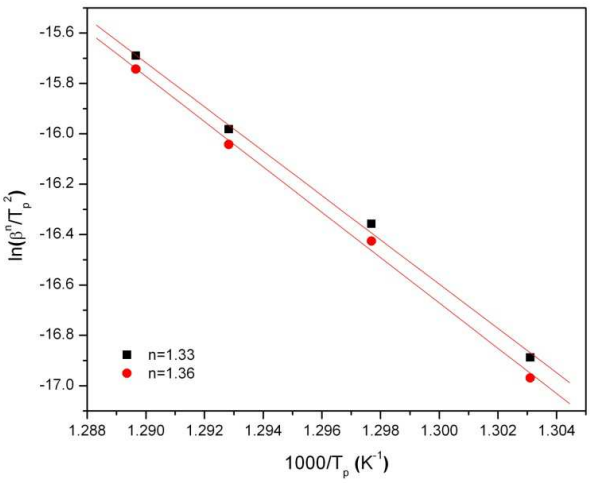

Fig. 8. Mod. Kissinger plot for n = 1.33 and n = 1.36

A general trend of decrease in the values of n with increasing heating rate can be observed. Such trend has been also seen by Matusita and Sakka (Matusita & Sakka, 1979) and in other Fe-based (Raval et al., 2005) metallic glasses.

Heating rate	*Matusita & Sakka*
4	*1.81*
6	*1.76*
8	*1.75*
10	*1.79*

Table 3. Values of Avrami exponent (n)

b. Coats & Redfern method

One of the most popular model-fitting methods is the Coats and Redfern method (Coats & Redfern, 1964). This method is based on the equation

$$ln\frac{g_i(\alpha)}{T^2} = ln\left[\frac{A_iR}{\beta E_i}\left(1-\frac{2RT}{E_i}\right)\right]-\frac{E_i}{RT} \tag{18}$$

$$\cong ln\frac{A_iR}{\beta E_i}-\frac{E_i}{RT}$$

The graph of $ln\frac{g_i(\alpha)}{T^2}$ Vs. $\frac{1}{T}$ gives a straight line whose slope and intercept allow us to calculate E and A for a particular reaction model. For the different kinetic models and for $0.1 \leq \alpha \leq 0.9$, the straight lines corresponding to CR method are characterized by correlation coefficients (r). The general practice in this method to determine E is to look for the model corresponding to maximum r. In some cases, the so-obtained value of E is significantly different from those obtained from other methods.

c. The invariant kinetic parameter (IKP) method

It has been observed that the same experimental curve $\alpha=\alpha(T)$ can be described by different function of conversion $(f(\alpha))$. Further, the values of the activation energy obtained for various $f(\alpha)$ for single non-isothermal curve are correlated through the compensation effect (Galwey, 2003). These observations form the basis of the IKP method. In order to apply this method, $\alpha = \alpha(T)$ curves are obtained at different heating rates (β_v = 4, 6, 8, 10) using DSC. For each heating rate the pairs (A_{vj}, E_{vj}), where j corresponds to a particular degree of conversion, are determined using the following equation:

$$ln\frac{g(\alpha)}{T^2} = ln\frac{AR}{\beta E}-\frac{E}{RT} \tag{19}$$

For constant β, a plot of $ln\frac{g(\alpha)}{T^2}$ Vs. $\frac{1}{T}$ is a straight line whose slope allows the evaluation of activation energy E_v and intercept, pre-exponential factor, A_v for different reaction models $g(\alpha)$. The same procedure is repeated to obtain the pairs (E_v, A_v) for different heating rates. Now, the calculation of invariant activation parameters is done using the compensation relation (Budrugeac, 2007)

$$ln\,A_v = \alpha^* + \beta^* E_v \tag{20}$$

The Eq. (20) represents a linear relationship between lnA and E; any increase in the magnitude of one parameter is offset, or compensated, by appropriate increase of the other. Plotting lnA_v Vs. E_v for different heating rates, the compensation effect parameters α^* and β^* are obtained. These parameters follow an equation

$$\alpha^* = \ln \boldsymbol{A} - \beta^* \boldsymbol{E} \tag{21}$$

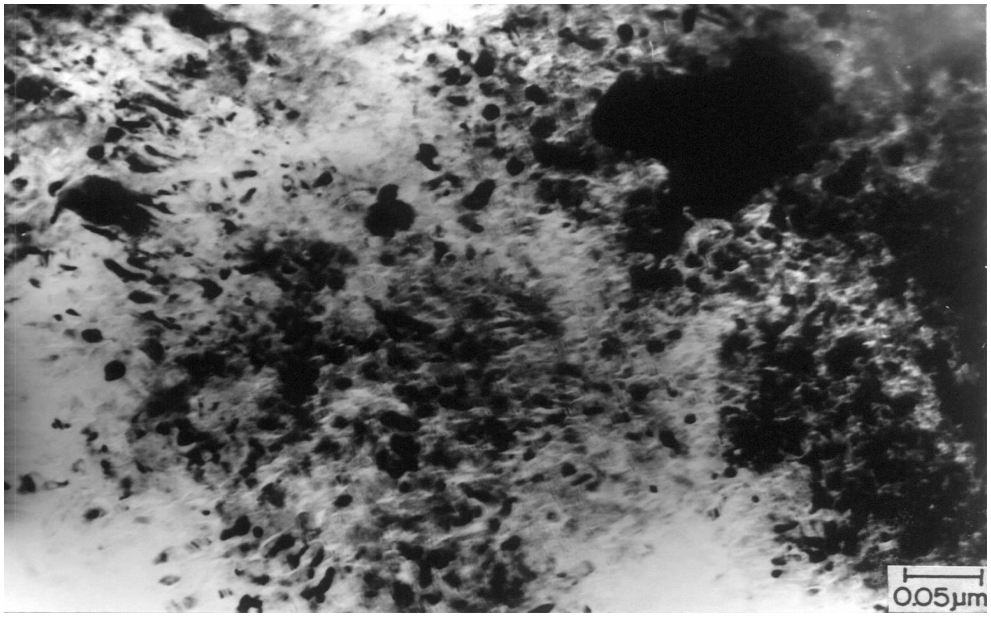

Fig. 9. Bright field TEM image of $Ti_{20}Zr_{20}Cu_{60}$ metallic glass after annealing at 673 K for 4 hours

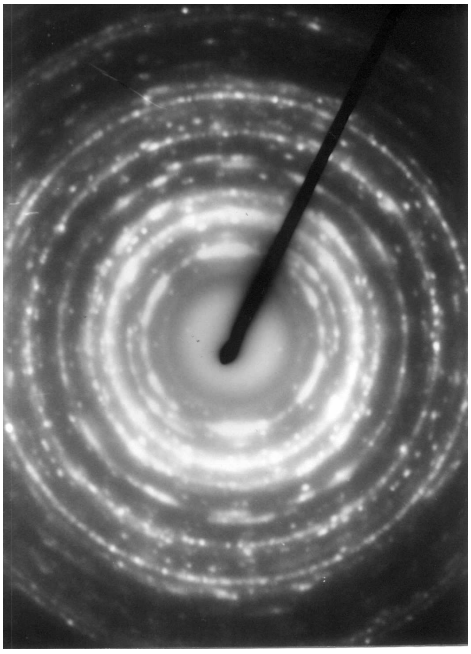

Fig. 10. SAD pattern of $Ti_{20}Zr_{20}Cu_{60}$ metallic glass after annealing at 673 K for 4 hours

The plot of α^* and β^* gives the true values of E and A.

Nano-structures can be synthesized by controlled crystallization of metallic glasses also known as de-vitrification method.

The selected area diffraction (SAD) pattern shows characteristic rings with discontinuity. The phases can also be idetified as seen from fig.11.

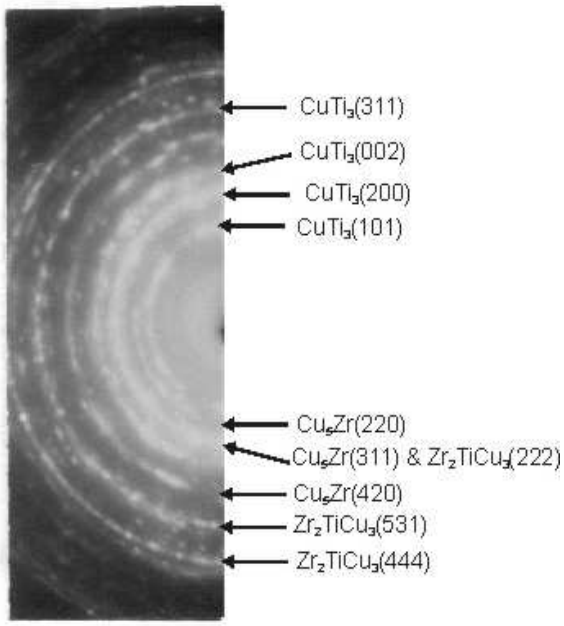

Fig. 11. Nano-phases present in $Ti_{20}Zr_{20}Cu_{60}$ metallic glass after annealing at 673 K for 4 hours

4. Conclusion

Based on the analysis of thermo-analytical data, the very obvious and straight forward question is: which is better, iso-conversional or iso-kinetic?

Iso-conversional methods provide activation energy values, E as a function of conversion, α. The iso-kinetic methods, on the other hand, are used considering the crystallization mechanism to be the same throughout the entire conversion (crystallization) and give single constant value of activation energy. For metallic glasses, the thermally activated phase transformations are more physical than chemical. In fact, crystallization is a complex process involving nucleation and growth and on rigorous grounds, it can not be considered to be a single-step process. The iso-kinetic analysis always leads to a single activation energy (rather say, apparent activation energy) giving an overall picture of the crystallization process. However, the difficulty (and hence uncertainty) in choosing the proper reaction model persists in isokinetic analysis. Therefore, the isoconversional methods are definitely

superior to the isokinetic methods as far as the determination of *E* is concerned (Pratap et al, 2007). Nonetheless, accurate determination of E is not the only issue in the kinetic analysis of crystallization process in metallic glasses. The micro-structural evolution during the non-isothermal heating of the metallic glasses is also important. For the determination of the dimensionality of the growth and the grain size, one needs to know a precise reaction model that closely follows the crystallization process. A reaction model independently proposed by John-Mehl- Avrami-Kolmogorov (JMAK) is found to be the most suitable for describing the nucleation and growth process during the non- isothermal crystallization of metallic glasses. This model does help to determine of the kinetic parameters, like the dimensionality of growth (apart from *E* and *A*). The model-free isoconversional methods are definitely superior to the isokinetic methods for the accurate determination of kinetic parameters like E and A. However, the knowledge of accurate E and A is not sufficient for the detailed investigations of the dimensionality of the growth and the grain size using thermal analysis. A precise reaction model accounting for the phase transformations during the crystallization process is a prerequisite for deriving such micro-structural information. This could be a valid proposition if it is explicitly related to the phase transformations involving significant chemical changes. One can find numerous publications where JMAK formalism has been found to be the most appropriate for the description of kinetics of nucleation and growth processes in metallic glasses. Therefore, in our opinion, isokinetic methods (despite its limited applicability) are important and useful for the analysis of non-isothermal crystallization data. So, as far as the study of thermally activated phase transformation in metallic glasses is concerned, both the types of methods are complementary and provide not only useful data, but also pave way into the insight of the crystallization process.

5. References

Afify, S. (1991). Differential scanning calorimetric study of chalcogenide glass $Se_{0.7}Te_{0.3}$, *Journal of Non Crystalline Solids,* Vol. 128, pp. 279-284; ISSN: 0022-3093

Akahira, T. & Sunose, T. (1971). Joint convention of four electrical institutes, *Research Report, Chiba. Institute of Technology (Science and Technology)*, Vol. 16, pp. 22-31

Augis, J.A. & Bennett, J.E. (1978). Calculation of the Avrami parameters for heterogeneous solid state reactions using a modification of the Kissinger method, *Journal of Thermal Analysis and Calorimetry*, Vol. 13, pp. 283-292; ISSN:1388-6150 (Print), 1572-894 (electronic version)

Boswell, P.G. (1980). On the calculation of activation energies using modified Kissinger method, *Journal of Thermal Analysis and Calorimetry*, Vol. 18, pp. 353-358 ISSN:1388-6150 (Print), 1572-894 (electronic version)

Budrugeac, P. (2007). The Kissinger law and the IKP method for evaluating the non-isothermal kinetic parameters, *Journal of Thermal Analysis and Calorimetry*, Vol. 89, pp. 143-151 ISSN:1388-6150 (Print), 1572-894 (electronic version)

Cai, J.M. & Chen, S.Y. (2009).A new iterative linear integral isoconversional method for the determination of the activation energy varying with the conversion degree *Journal of Computational Chemistry*, Vol. 30, pp. 1986-1991; Online ISSN: 1096-987X

Castro, M. (2003). Phae-field approach to heterogeneous nucleation, *Physical Review B*, Vol. 67, pp. 035412-035419; ISSN: 0163-1829 (Print), 1095-3795 (electronic version)

Coats, A.W. & Redfern J.P. (1964). Kinetic Parameters from Thermogravimetric Data, *Nature (London)*, Vol. 201, pp. 68-69; ISSN: 0028-0836 (Print), EISSN: 1476-4687

Criado, J.M.; Sanchez-Jimenez, P.E. & Perez-Maqueda, L.A. (2008). *Journal of Thermal Analysis and Calorimetry,* Vol. 92, pp. 199-203; ISSN:1388-6150 (Print), 1572-894 (electronic version)

Dhurandhar, H.; Patel, A.T.; Shanker-Rao, T.L.; Lad, K.N. & Pratap, A. (2010). Kinetics of crystallization of Co-based multi-component amorphous alloy, *Journal of ASTM International*, Vol. 7, pp. 1-15; 978-0-8031-7516-7

Doyle, C.D. (1961). Kinetic Analysis of Thermogravimetric Data, *Journal of Applied Polymer Science*, Vol. 5, pp. 285–292; ISSN: 1097-4628

Doyle, C.D. (1962). Estimating Isothermal Life from Thermogravimetric Data, *Journal of Applied Polymer Science*, Vol. 6, pp. 693-642; ISSN:1097-4628

Doyle, C.D. (1965). Series Approximations to the Equation of Thermogravimetric Data, *Nature (London)*, Vol. 207, pp. 290-291; ISSN: 0028-0836 (Print), EISSN: 1476-4687

Flynn, J.H. & Wall, L.A. (1966). General Treatment of the Thermogravimetry of Polymers, *Journal of Research of the National Bureau of Standards. Section- A. Physics and Chemistry,* Vol. 70A, pp. 487-523; 0022-4332

Friedman, H.L. (1964). Kinetics of thermal degradation of char-forming plastics from thermogravimetry. Application to phenolic plastic, *Journal of Polymer Science Part C*, Vol. 6, pp. 183-195; ISSN: 0449-2994

Galwey, A.K. (2003). Eradicating erroneous Arrhenius arithmetic, *Thermochimica Acta*, Vol. 399, pp. 1-29; ISSN: 0040-6031

Gao, Y.Q. & Wang, W. (1986). On the activation energy of crystallization in metallic glasses, *Journal of Non-Crystalline Solids*, Vol. 81, pp. 129-134; ISSN: 0022-3093

Giridhar, A. & Mahadevan, S. (1982). Studies on the As-Sb-Se glass system, *Journal of Non Crystalline Solids,* Vol. 51, pp. 305-315; ISSN: 0022-3093

Gupta, A.K.; Jena, A.K. & Chaturvedi, M.C. (1988). A differential technique for the determination of the activation energy of precipitation reactions from Differential Scanning Calorimetric data, *Scripta Metallurgica*, Vol. 22, pp. 369-371; ISSN: 0036-9748

Hsiao, A.; McHenry, M.E.; Luaghlin, D.E.; Kramer, M.J.; Ashe, C. & Ohkubo, T. (2002). The Thermal, Magnetic, and Structural Characterization of the Crystallization Kinetics of $Fe_{88}Zr_7B_4Cu_1$, An Amorphous Soft Magnetic Ribbon, *IEEE Transactions on Magnetics*, Vol. 38, No. 5, pp. 3039-3044; ISSN:0018-9464

Jones, G.A.; Bonnett, P. & Parker, S.F.H. (1986). Crystallilzation kinetics of the amorphous magnetic material 2605 Co ($Fe_{67}Co_{18}B_{14}Si_1$), *Journal of Magnetism & Magnetic Materials*, Vol. 58, pp. 216-226; ISSN:0304-8843

Kissinger, H.E. (1957). Reaction kinetics in differential thermal analysis, *Analytical Chemistry*, Vol. 29, pp. 1702-1706; ISSN:0003-2700

Lad, K.N.; Savalia, R.T.; Pratap, A., Dey, G.K. & Banerjee, S. (2008). Isokinetic and isoconversional study of crystallization kinetics of a Zr-based metallic glass, *Thermochimica Acta,* Vol. 473, pp. 74-80; ISSN: 0040-6031

Lesz, S. & Szewieczek, D. (2005). *Proceedings of the Worldwide Congress on Materials and Manufacturing Engineering and Technology COMMENT'2005*, Poland, Gliwice-Wisla (CD-ROM), Vol. 637, May 16-19, 2005

Li, C.R. & Tang, T.B. (1999). A new method for analyzing non-isothermal thermoanalytical data from solid-state reactions, *Thermochimica Acta,* Vol. 325, pp. 43-46; ISSN:0040-6031

Ligero, R.A.; Vazquez, J.; Villares, P. & Jimenez-Garay, R. (1990). Crystallization kinetics in the As-Se-Te system, *Thermochimica Acta*, Vol. 162, pp. 427-434; ISSN: 0040-6031

Matusita, K. & Sakka, S. (1979). Kinetic study of crystallization of glass by differential scanning calorimetry, *Physical Chemistry of Glasses*, Vol. 20, pp. 81-84; 0031-9090

Matusita, K. & Sakka, S. (1980). Kinetic study on Crystallization of glass by differential thermal analysis – criterion on application of Kissinger plot, *Journal of Non-Crystlline Solids*, Vol. 38-39, pp. 741-746; ISSN: 0022-3093

Minic D.M. (2006). Synthesis, Characterization and Stability of Amorphous Alloys, *Science of Sintering*, Vol. 38, pp. 83-92; 0350-820x

Minic, D.M. & Adnadevic, B. (2008). Mechanism and kinetics of crystallization of α-Fe in amorphous $Fe_{81}B_{13}Si_4C_2$ alloy, *Thermochimica Acta.*, Vol. 474, pp. 41-46; ISSN: 0040-6031

Minic, D.M.; Gavrilovic, A.; Angerer, P.; Minic, D.G. & Mariclc, A. (2009). Thermal stability and crystallization of $Fe_{89.8}Ni_{1.5}Si_{5.2}B_3C_{0.5}$ amorphous alloy, *Journal of Alloys and Compound*, Vol. 482, pp. 502-507; ISSN: 0925-8388

Moharram, A.H.; El-Oyoun, M.A. & Abu-Sehly, A.A. (2001). Calorimetric study of the chalcogenide $Se_{72.5}Te_{20}Sb_{7.5}$ glass, *Journal of Physics D Applied Physics*, Vol. 34, pp. 2541-2546; ISSN 0022-3727 (Print) ISSN 1361-6463 (Online)

Ozawa, T. (1965). A New Method of Analyzing Thermogravimetric Data, *Bulletin of the Chemical Society of Japan*, Vol. 38, pp. 1881-1886; ISSN 0009-2673

Patel, A.T. & Pratap, A. (2012). Kinetics of crystallization of $Zr_{52}Cu_{18}Ni_{14}Al_{10}Ti_6$ glass, *Journal of Thermal Analysis and Calorimetry*, Vol. 107, pp. 159-165; ISSN:1388-6150 (Print), 1572-894 (electronic version)

Paulik, F. (1995). Ch. 10*, Special Trends in Thermal Analysis*, John Wiley & Sons, Chichester, UK

Pratap, A.; Shanker-Rao, T.L.; Lad, K.N. & Dhurandhar, H.D. (2007). Isoconversional vs. Model fitting methods A case study of crystallization kinetics of a Fe-based metallic glass, *Journal of Thermal Analysis and Calorimetry*, Vol. 89, pp. 399-405; ISSN:1388-6150 (Print), 1572-894 (electronic version)

Raval, K.G.; Lad, K.N.; Pratap, Arun; Awasthi, A.M. & Bhardwaj, S. (2005). Crystallization kinetics of a multicomponent Fe-based amorphous alloy using modulated differential scanning calorimetry, *Thermochimica Acta*, Vol. 425, pp. 47-57; ISSN: 0040-6031

Rotaru, A. & Gosa, M. (2009). Computational thermal and kinetic analysis Complete standard procedure to evaluate the kinetic triplet form non-isothermal data, *Journal of Thermal Analysis and Calorimetry*, Vol. 97, pp. 421-426; ISSN:1388-6150 (Print), 1572-894 (electronic version)

Roura, P. & Farjas, J. (2009).Analytical solution for the Kissinger equaton, *Journal of Materials Research,* Vol. 24, pp. 3095-3098;

Rysava, N.; Spasov, T. & Tichy, L. (1987). Isothermal DSC methods for evaluation of the kinetics of crystallization in the Ge-Sb-S glassy system, *Journal of Thermal Analysis*, Vol. 32, pp. 1015-1021; ISSN:1388-6150 (Print), 1572-894 (electronic version)

Starink, M.J. (2003). The determination of activation energy form linear heating rate Experiments: A comparison of the accuracy of isoconversion methods, *Thermochimica Acta*, Vol. 404, pp. 163-176; ISSN: 0040-6031

Starink, M.J. (1997). On the applicability of isoconversion methods for obtaining the activation energy of reactions within a temperature-dependent equilibrium state, *Journal of Materials Science*, Vol. 32, pp. 6505-6512; ISSN: 0022-2461

Szewieczek, D. & Lesz, S. (2004). The Structure and Selected Physical Properties of the Nanocrystalline $Fe_{92.4}Hf_{4.2}B_{3.4}$ Alloy, *Journal of Materials Processing Technology*, Vol. 157–158, pp. 771–775; ISSN:0924-0136

Szewieczek, D. & Lesz, S. (2005). Influence of Structure on Magnetic and Mechanical Properties ofAmorphous and Nanocrystalline $Fe_{85.4}$ $Hf_{1.4}B_{13.2}$ Alloy, *Proceedings of the 13th International Scientific Conference, Achievements in Mechanical & Materials Engineering AMME'05,* Gliwice-Wisla, Vol. 637

Vyazovkin, S. & Wight, C.A. (1997). Isothermal and Nonisothermal Reaction Kinetics in Solids: In Search of Ways toward consensus,*The Journal of Physical Chemistry A*, Vol. 101, pp. 8279-8284; ISSN: 1089-5639

Vyazovkin, S. (2003). Reply to "What is meant by the term 'variable activation energy when applied in the kinetics analyses of solid state decompositions (crystolysis reactions)?", *Themochimica Acta*, Vol. 397, pp. 269-271; ISSN:0040-6031

Vyazovkin, S. (2010). Thermal Analysis, *Analytical Chemistry*, Vol. 82, pp. 4936-4949; ISSN 0003-2700

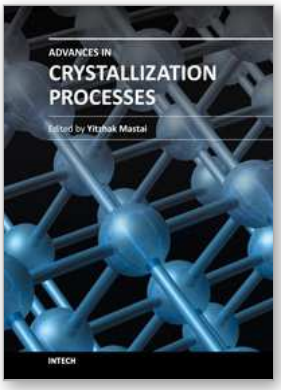

Advances in Crystallization Processes

Edited by Dr. Yitzhak Mastai

ISBN 978-953-51-0581-7
Hard cover, 648 pages
Publisher InTech
Published online 27, April, 2012
Published in print edition April, 2012

Crystallization is used at some stage in nearly all process industries as a method of production, purification or recovery of solid materials. In recent years, a number of new applications have also come to rely on crystallization processes such as the crystallization of nano and amorphous materials. The articles for this book have been contributed by the most respected researchers in this area and cover the frontier areas of research and developments in crystallization processes. Divided into five parts this book provides the latest research developments in many aspects of crystallization including: chiral crystallization, crystallization of nanomaterials and the crystallization of amorphous and glassy materials. This book is of interest to both fundamental research and also to practicing scientists and will prove invaluable to all chemical engineers and industrial chemists in the process industries as well as crystallization workers and students in industry and academia.

INTECH
open science | open minds

InTech Europe
University Campus STeP Ri
Slavka Krautzeka 83/A
51000 Rijeka, Croatia
Phone: +385 (51) 770 447
Fax: +385 (51) 686 166
www.intechopen.com

InTech China
Unit 405, Office Block, Hotel Equatorial Shanghai
No.65, Yan An Road (West), Shanghai, 200040, China
中国上海市延安西路65号上海国际贵都大饭店办公楼405单元
Phone: +86-21-62489820
Fax: +86-21-62489821